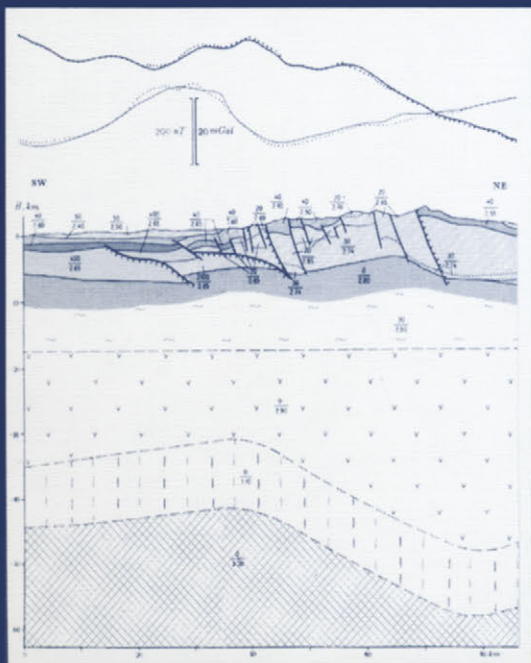


**MODERN APPROACHES IN GEOPHYSICS**

BORIS E. KHESIN, VYACHESLAV V. ALEXEYEV  
and LEV V. EPPELBAUM

# Interpretation of Geophysical Fields in Complicated Environments



**SPRINGER-SCIENCE+BUSINESS MEDIA, B.V.**

**INTERPRETATION OF GEOPHYSICAL FIELDS  
IN COMPLICATED ENVIRONMENTS**

# MODERN APPROACHES IN GEOPHYSICS

---

VOLUME 14

---

*Managing Editor*

G. Nolet, *Department of Geological and Geophysical Sciences,  
Princeton University, Princeton, N.J., U.S.A.*

*Editorial Advisory Board*

B. L. N. Kennett, *Research School of Earth Sciences,  
The Australian National University, Canberra, Australia*

R. Madariaga, *Institut Physique du Globe, Université Paris VI, France*

R. Marschall, *Geco-Prakla, Prakla-Seismos GMBH, Hannover,  
Germany*

R. Wortel, *Department of Theoretical Geophysics,  
University of Utrecht, The Netherlands*

*The titles published in this series are listed at the end of this volume.*

# INTERPRETATION OF GEOPHYSICAL FIELDS IN COMPLICATED ENVIRONMENTS

*by*

BORIS E. KHESIN

*Department of Geology,  
Ben Gurion University of the Negev,  
Be'er-Sheva, Israel*

VYACHESLAV V. ALEXEYEV

*"VNIIGeofizika" Association,  
Moscow Region, Russia*

and

LEV V. EPPELBAUM

*Department of Geophysics,  
Tel Aviv University, Tel Aviv, Israel*



SPRINGER-SCIENCE+BUSINESS MEDIA, B.V.

Library of Congress Cataloging-in-Publication Data

Khesin, Boris E. (Boris Emmanuel), 1932-

Interpretation of geophysical fields in complicated environments /  
by Boris E. Khesin, Vyacheslav V. Alexeyev and Lev V. Eppelbaum.

p. cm. -- (Modern approaches in geophysics ; v. 14)

Includes bibliographical references and index.

ISBN 978-90-481-4680-2 ISBN 978-94-015-8613-9 (eBook)

DOI 10.1007/978-94-015-8613-9

1. Geophysics--Methodology. I. Alexeyev, Vyacheslav  
V. (Vyacheslav Vasily), 1935-. II. Eppelbaum, Lev V. (Lev  
Vilen), 1959-. III. Title. IV. Series.

QC808.5.K47 1996

551'.028--dc20

96-196

ISBN 978-90-481-4680-2

---

*Printed on acid-free paper*

All Rights Reserved

© 1996 Springer Science+Business Media Dordrecht

Originally published by Kluwer Academic Publishers in 1996

No part of the material protected by this copyright notice may be reproduced or  
utilized in any form or by any means, electronic or mechanical,  
including photocopying, recording or by any information storage and  
retrieval system, without written permission from the copyright owner.

# Contents

<b>EDITOR'S PREFACE</b>	ix
<b>ACKNOWLEDGMENT</b>	xii
<b>INTRODUCTION</b>	1
<b>1 PECULIARITIES OF THE MEDIA UNDER STUDY AND THEIR GEOPHYSICAL INVESTIGATIONS</b>	6
1.1 General information . . . . .	6
1.2 Geophysical targets and noises in their study . . . . .	8
1.3 Integration of geophysical methods: Its necessity and routes to its optimization	23
<b>2 COMMON ASPECTS OF GEOPHYSICAL FIELDS IN QUESTION</b>	32
2.1 Common theoretical and model principles of anomaly interpretation . . . . .	32
2.2 Common techniques of correction for different observation heights . . . . .	43
<b>3 INFORMATIONAL CONTENT AND STRUCTURE OF THE INTERPRETATION PROCESS</b>	50
<b>4 DEVELOPMENT OF THE INITIAL MODEL OF THE MEDIUM</b>	56
4.1 Initial data sources; Petrophysical support of the interpretation . . . . .	57
4.2 Indicators of targets and interpretation criteria . . . . .	67
<b>5 INDICATOR SPACE GENERATION</b>	74
5.1 Elimination of field variations with time . . . . .	75
5.2 Terrain correction and utilization of topography for deriving geological information . . . . .	77
5.3 Execution of transformations . . . . .	119

<b>6 REVEALING AND LOCALIZATION OF TARGETS</b>	<b>144</b>
6.1 Regioning . . . . .	144
6.2 Delineation and determination of anomalous body axes; their representation with the results of regioning . . . . .	152
<b>7 DETERMINATION OF THE ANOMALOUS BODY PARAMETERS</b>	<b>161</b>
7.1 General issues of quantitative interpretation . . . . .	161
7.2 Techniques of magnetic anomaly interpretation under oblique magnetization	171
7.3 Quantitative interpretation of gravitational, electric, electromagnetic and thermal anomalies under inclined terrain relief and oblique polarization of objects . . . . .	197
7.4 Combinations of quantitative interpretation techniques . . . . .	218
<b>8 INTEGRATED INTERPRETATION</b>	<b>229</b>
8.1 Fundamental advantages of integration . . . . .	229
8.2 Variants of integrated interpretation . . . . .	231
8.3 Revealing of the desired objects by a set of indicators . . . . .	235
8.4 Stages of physico-geological modeling . . . . .	245
8.5 Examples of modeling . . . . .	256
<b>9 REVISION OF A MODEL OF A MEDIUM; REPRESENTATION AND EVALUATION OF INTERPRETATION RESULTS</b>	<b>263</b>
9.1 Developing a final model . . . . .	263
9.2 Graphic representation of the interpretation results and forming geological conclusions; Physico-geological models . . . . .	266
9.3 Interpretation examples for swamp and shoal waters . . . . .	275
9.4 Interpretation examples in detailed magnetic prospecting of archaeological objects in Israel . . . . .	285
9.5 Estimation of the interpretation reliability and its application for optimizing a system of geophysical investigation . . . . .	286
<b>10 CHARACTERISTIC FEATURES OF THE IMIGO PACKAGE</b>	<b>298</b>
10.1 General characteristics . . . . .	298
10.2 IMIGO-based interpretation: technological order of execution . . . . .	303
10.3 Peculiarities of interpretation technology at different stages of geophysical investigations . . . . .	307

**TABLE OF CONTENTS**

vii

<b>CONCLUSION</b>	<b>309</b>
<b>APPENDIX A Elimination of time variations in the VLF method and near-surface thermal prospecting</b>	<b>312</b>
<b>APPENDIX B Description of the GSFC program</b>	<b>317</b>
<b>REFERENCES</b>	<b>331</b>
<b>INDEX</b>	<b>349</b>

## **EDITOR'S PREFACE**

Books published during recent years in the field of applied geophysics can be, in general, divided into two main types. The first type covers such multiaspect books as "Introduction to Geophysics", while the second – special works on fundamental theoretical problems with an elaborate mathematical description. The books of the first type are mainly intended for beginner students and specialists in adjacent fields. The books of the second type may be useful for teachers and theorists. However, there are also books of another (third) type. These books describe the experience in geophysical investigation under specific conditions or propose solutions to concrete geological problems, being a methodological guide for geophysicists and concentrating ideas both for advanced students and researchers. Authors hope to give the readers a book of this kind.

Interpretation of geophysical fields is a complex consistent process. Its successful realization requires: (a) knowledge of geological regularities and geological situation; (b) availability of petrophysical support; (c) mathematical methods of solving direct and inverse problems of geophysics (i.e. computation of geophysical fields from a known source and determination of source characteristics from known fields); (d) application of statistical and logico-informational procedures to the analysis and synthesis of observation results for revealing desired objects and peculiarities of the geological structure.

Meanwhile, in many cases the interpretation conditions may be simplified. When geophysical investigations are conducted in simple environments (absence of a large number of anomalous bodies, vertical polarization of objects, flat earth's surface, where one can use any space observation systems with bulky equipment) the problem solution is simplified.

However, more complicated situations are rather widespread. For these situations the following is typical: rugged terrain relief, highly variable geological medium, oblique magnetization (polarization) and often an unknown level of the normal field. Besides

mountainous regions, difficult to traverse are also areas of woods, swamps and shoal waters. For these areas the influence of oblique magnetization is of paramount importance, since these regions are studied, first of all, by magnetic survey. Some geophysical investigations are conducted within small isolated areas (for instance, archaeological investigations), where it is difficult to determine the level of the normal field.

Combination of all mentioned conditions is typical of mountainous regions. Therefore the book deals mainly with characteristics and methods of investigation for these regions. Nevertheless, it is noteworthy that almost all methods and procedures of geophysical fields interpretation described in this book can be efficiently used in simpler geological situations.

Mountainous regions account for about 30 percent of the land. A number of mineral resources are concentrated there. Geophysical data on the geological structure of mountainous regions throw light on the basic principles of evolution of the Earth, distribution of minerals and seismic activity. However, geophysical surveys under complicated conditions are generally complicated by poor accessibility of some mountainous regions, by unevenness of observation surfaces, as well as by a great variety and frequent change of tectonic structures and geological bodies with variable physical properties. The above mentioned factors either restrain geophysical surveys in complicated environments or confine the scope of useful information drawn from the results obtained. This has led to the development of special techniques of geophysical surveys, data processing and interpretation with due account of the experience accumulated in specific conditions of mountainous regions.

This book is a practical guide to the integration of methods developed for the interpretation of potential and quasi-potential fields in complicated situations. The peculiarities of the investigated media and geophysical surveys are discussed. The possibility of a common approach to the analysis of geophysical fields, such as magnetic, gravitational, thermal, self-potential (*SP*), electromagnetic field of very low frequency (*VLF*) transmitters and field of induced polarization (*IP*) has been substantiated. The book introduces the reader to the informational content and the structure of interpretation process developed by the authors. Our methods of treating noise effects, especially those of rugged relief, are illustrated in the book. The advantage of the application of high field complexity for receiving additional geological information is described.

The book not only discusses the techniques recommended for geophysical fields transformation and rapid methods of interpretation of the anomalies observed under the conditions of inclined surface and arbitrary polarization of the objects. It also describes physico-geological modeling by means of interactive computer selection of gravitational and magnetic fields in a rugged relief for complex three-dimensional media. It gives an idea of different variants of integrated interpretation based on probabilistic or deterministic approaches, their reliability estimation and data presentation. And, finally, it presents the interpreting software, such as the *IMIGO* program package (gravimetric and magnetic investigations of mountainous regions).

The authors of this book had been working in the former USSR for many years. They perceive that geophysics had been developing in this country for many decades in a certain isolation. Different methods and technologies were simultaneously developed in the East and in the West. Therefore, References mainly include relevant works of Soviet authors. I hope that the acquaintance with this literature will interest Western readers which are conversant with Western investigators' contribution to geophysics.

Boris E. Khesin

*Geological Department  
Ben-Gurion University  
Be'er-Sheva, Israel  
August 1995*

A 5 1/4-inch diskette containing software for 3-D combined modeling of gravity and magnetic fields in complicated geological conditions, for this book is available from

Dr Lev Eppelbaum  
Dept. of Geophysics and Planetary Sciences  
Tel Aviv University  
Ramat Aviv 69978  
TEL AVIV  
ISRAEL  
Tel. 972-3 640 76 67  
Fax: 972-3 640 92 82  
E-mail: lev@jupiter1.tau.ac.il

The programmes are written in PASCAL (operating system DOS) and FORTRAN-77 (operating system UNIX).

## **ACKNOWLEDGMENT**

We are thankful to Prof. D.S.Parasnus (Luleå University, Sweden) and Prof. A.A.Kaufman (Colorado School of Mines, USA) for the support of our work. We are grateful to our colleagues in Dept. of Geology and Mineralogy (Ben-Gurion University of the Negev), Dept. of Geophysics and Planetary Sciences (Tel Aviv University) and State Association “VNIIGeofizika” (Moscow) for the discussion of some questions dealt with in this book. Finally, authors are obliged to Mrs. V.Khesin for preparing some figures.

**Prof. B.E.Khesin**  
*(Ben Gurion University)*

**Dr. V.V.Alexeyev**  
*(VNIIGeofizika)*

**Dr. L.V.Eppelbaum**  
*(Tel Aviv University)*

# INTRODUCTION

In many regions geophysicists meet two great difficulties: rugged topography and polarization vector inclination. Magnetization vector is seldom vertical in the central and low latitudes, i.e. in the zone around the equator extending from Texas (USA) to Queensland (Australia). The inclination of polarization distorts habitual field patterns. The relief effect not only impedes geophysical surveys under mountainous conditions, but also distorts the results of observations. First, the effect of attraction of the bodies forming the relief is considerable. Second, when the data are recorded on an uneven surface, the vertical distance to the hidden body under study varies differently and anomalous vertical field gradient arises. The combination of these environmental factors with a complex geological structure has motivated the development of adequate methodologies.

Several books deal with the problems of geophysical investigation under mountainous conditions. Among them are [131] which covers, on the whole, the peculiarities of field work, and [135], where the interpretation of the obtained results is discussed. This primarily concerns qualitative and integrated interpretation which has been better developed for such conditions. Their brief review is given in [138]. Efficient, prompt and noninvasive methods of investigation of natural geophysical (magnetic, gravitational and certain electric) fields are primarily used for areal survey (areal mapping). Geophysical and geochemical quadrangle surveys are based on integrated key intersections including more cumbersome methods, such as seismic exploration and electric sounding.

The most attractive techniques employed for the interpretation of the areal mapping data, especially those obtained from large-scale mapping (1:50,000 – 1:25,000), are the correlation and information-statistical (logico-statistical) methods of singling out features of

interest of the geological structure. They are based on the accumulation of information relevant to expected effects and elimination of all other effects considered to be random. The deterministic methods of solving inverse and direct problems of geophysics are of great importance for regional (1:1,000,000 – 100,000) and detail (1:10,000 – 1:1,000) prospecting. They make it possible to determine relatively extended reference boundaries and to study isolated objects of comparatively simple shape.

Growing requirements for the informativity (informative efficiency) of geophysical works, advances in theory and investigation methods, more precise instrumentation stimulated further development of mountainous relief correction techniques and quantitative interpretation. This is especially relevant to magnetic prospecting with widely applied  $T$ -magnetometers (atomic optically pumped and proton-resonance), which replaced  $Z$ -instruments. Due to aeromagnetic survey, the data obtained from magnetic prospecting are available everywhere, but their application is often far from being adequate for lack of both interpretation techniques intended for complex conditions and the knowledge of the sequence of interpretation. These problems are treated in [146], some points of which can be extended to other geophysical methods or used as a key to similar developments.

Apart from the foregoing, such interpretation developments are brought about by the following factors.

The universal means of the interpretation for the environments concerned are the methods of modeling geophysical fields under real relief conditions. This route to the solution of the inverse problem via solving a series of direct problems gives stable results. But their wide application for mountainous conditions is impeded by the difficulties arising when selecting the initial approximation from the anomalous field. It is also difficult to obtain ample heights data, to approximate them reasonably for solving direct problems and to use detailed petrophysical results. Well-known methods are often also inapplicable for refining the first approximation. The methods concerned with analytical continuation into the source vicinity and localization of the singular points can hardly be used because of the complicated form of observation line and the presence of non-target singular points. Moreover, due to a prohibitive decrease in the

amplitude of weak useful anomalies, the reduction of the observed data to a common horizontal level of the highest points is often inefficient.

Besides, numerous economic mineral resources are associated with mountainous regions. Here endogenic deposits of various metals are located. But without a systematic geophysical study of mountainous regions, it is impossible to form a complete idea of their deep structure determining the distribution of economic minerals, as well as the ideas of ore controls (such as intrusions, folded structures, fractures and their intersections, body's boundaries) and salient features of deposits with composite morphology. Corresponding geophysical data are necessary for solving general problems of mountainous region geology, including prediction of seismic activity and other important tasks. The most significant are the problems of detecting oil-and-gas controls and hydrocarbon pools in mountainous conditions, since respective commercial deposits were found by drilling in the Rocky Mountains and Appalachians (USA), Zagros (Iran), in the Carpathians and the Caucasus, and in some other regions of the world.

As a result of our investigation, all developed techniques of processing and interpretation of potential and quasi-potential fields under mountainous environments were combined into a unified system of interpretation. It includes: (a) probabilistic and deterministic methods of terrain correction; (b) methods of qualitative interpretation for singling out the desired features of geological structure; and (c) methods of quantitative interpretation for the development of a physico-geological model (*PGM*) of the media under study.

The system has been tested both on various theoretical models and in practice in mountainous areas of the former USSR – the Greater and Lesser Caucasus, Altai, Urals. It proved to be efficient for developing reliable models of complex media under mountainous conditions on a 1:2,000 to 1:200,000 scale. These techniques were mainly tested on the materials of the first two regions thoroughly investigated by the authors. The above mentioned areas are rather typical of the mountainous regions. They represent intricate mountainous systems with very rugged topography, linear folding, predominance of sedimentary formations (Greater Caucasus), or

less manifested terrain relief and tectonics, and dominant magmatic associations (Lesser Caucasus).

The process of interpretation described in the present book includes the following steps:

- (1) development of the initial model;
- (2) development of indicator space (including terrain correction and topography application for obtaining geological information);
- (3) detection and localization of objects of prospecting;
- (4) determination of quantitative parameters of anomalous bodies;
- (5) integrated interpretation using logico-statistical and deterministic approaches;
- (6) revision of the model of the medium, data representation and estimation of the interpretation reliability.

The sequence of interpretation procedures is basically the same for all geophysical methods, though sometimes the content is substantially different. The procedures of magnetic and gravimetric data interpretation are very close. They have much in common with the interpretation of the results of *VLF*, *IP*, *SP*<sup>1</sup> and thermal prospecting. The interpretation of any kind of geophysical observations inevitably includes a stage where the results of other investigations are employed. This allows to illustrate the sequence of interpretation on one of geophysical methods. In this book we usually choose magnetic prospecting method for illustration. It is widely used in all regions and at all stages of prospecting. Magnetic field is the most difficult to interpret due to its vector nature, variability of magnetic properties and the presence of remanent magnetization. Quite a number of techniques for processing and interpretation of the geophysical data were developed by analogy with the techniques used in magnetic prospecting. The peculiarities of their application to various geophysical fields is also considered in this book.

The described investigation procedure is suitable for complicated environments, such as complex media, inclined polarization, unknown level of the normal field and rugged relief, since these conditions restrict the application of conventional techniques of interpretation. Naturally, our system can be employed in other conditions providing no above mentioned restrictions, which adds

---

<sup>1</sup>in Russian literature it is called Natural Electric Field method

greatly to its applicability.

The book has been composed by the following authors:

**B.E.Khesin** (Introduction, Sections 1, 3, 4, 5, 6, 7.1, 7.2.2, 7.2.4, 7.2.6, 7.3, 7.4, 8, 9, 10.3, Conclusion and editing)

**V.V.Alexeyev** (Sections 1.2, 2, 3, 4, 5.2, 5.3.1, 5.3.2, 6, 7, 8.4, 9.1, 9.2, 10)

**L.V.Eppelbaum** (Sections 1.2, 1.3, 2.1, 5.1, 5.2.2, 7.2.4, 7.2.5, 7.3, 7.4, 8.2, 8.4, 9.1, 9.2, 9.3.3, 9.4, 10.3).

# **Chapter 1**

## **PECULIARITIES OF THE MEDIA UNDER STUDY AND THEIR GEOPHYSICAL INVESTIGATIONS**

A specific character of mining geophysics has been amply covered in the books [131,135]. Models of media, details and sequence of interpretation process including petrophysical study are discussed with reference to magnetic prospecting in a subsequent book [146]. A separate Chapter [143] in [36] deals with the optimization of interpretation for detailed prospecting under mountainous conditions. These works have formed the basis for the analytical review exposed below.

### **1.1 General information**

According to Solovov [157], open areas, where ore-bearing rocks outcrop onto the surface or are covered with eluvial and deluvial products of their weathering, can be divided into two groups. One of them, having a severe topography, is considered unfavorable for geophysical prospecting. This approach to typical orogens (mountainous folded areas) of open (one-stage) type can be easily explained. On the one hand, complex geophysical equipment can hardly be applied in hardly accessible mountainous regions, and anomalies caused by relief are pronounced and difficult to be taken into account. On the other hand, good outcropping favors the solution of prospecting problems by purely geological methods.

However, mountainous regions objectively call for systematic

application of geophysical methods of investigation. Moreover, only these methods can ensure a sequential, deep and sufficiently rapid study of the endogenic mineralization distribution and its relation to geological structure. The prospecting for large hidden deposits is carried out allowing for this relationship. Many valuable deposits of different types are located in mountainous regions over 2,000 m high, which account for about 12 per cent of the total continental area, and in those over 1,000 m high, which account for as much as 30 per cent of the total land. A large portion of this area consist of mountainous structures formed or rejuvenated during the Alpine epoch [127].

At the same time, mountainous conditions can hardly be treated only as an obstacle. Deep erosional truncation and lack or low thickness of loose deposits encourage the application of visual geological methods. They make it possible to obtain extensive geological evidence on the nature of anomaly sources, to correlate them with geophysical data, as well as to study physical properties of rocks and ores in natural and artificial exposures. Rugged relief allows to calculate effective physical parameters of a section part exposed to the erosion basing on the results of measuring the corresponding fields on an uneven surface. It also facilitates geological application of topography data. Outcropping of mountainous regions promotes integrated application of conventional geophysical methods along with not only visual geological, but also geochemical, petrophysical, physico-chemical and nuclear geophysical investigations (including areal study), which sharply reduces the ambiguity of geophysical interpretation.

The most specific conditions for geophysical study are those of alpine-type mountainous regions. In these regions solid heterogeneous associations approach to the earth's surface. These associations are multiply folded, with intensive rupture tectonics (including thrust tectonics). Rocks of various origin and composition with a broad range of physical properties rapidly change along both vertical and lateral directions. This predetermines the complexity of the image of physical fields. Due to the curvature of earth-to-air interface and rugged observation surface, the relief exerts a pronounced effect on the observations. Dissected relief, difficulties in transportation, orientation and observation, network tie-in affect the investigation procedure. They restrict the increase in efficiency

at the expense of more intricate and cumbersome equipment and survey systems.

The requirements to geophysical techniques specified for mountainous conditions are less stringent at the stages of regional and detailed prospecting. In the first case, in airborne survey the observation network may be tied-in with comparatively stable elements of the relief. In ground survey, it is tied with one or another communication route or river bed for geophysical observations with cumbersome equipment. In such way key intersections are performed which are used as reference sections for large-scale survey of the area (Fig.1.1). In the second case, a small area of the plots and their developed character facilitate the transportation and organization of geophysical work, allowing to use rather complex equipment.

As for the study of areas in the vicinity of wells and measurements in mines, in mountainous regions they are characterized by specific conditions of the equipment transportation and the separation of wells and mines. The latter, particularly, requires a study of isolated wells. It is noteworthy that extended adits and a rugged topography make it possible to deploy rather complicated spatial systems for earth's surface/mine geophysical surveying. As a rule, these operations are carried out at the exploration stages [36].

## 1.2 Geophysical targets and noises in their study

Due to the high heterogeneity of geological medium and secondary alterations in the section under study, comparatively stable marker interfaces are rarely traced, especially in large-scale surveying. Rather frequently the objects of geophysical investigation are specific areas (sections) or isolated geological bodies, which are markedly different from the host medium in their physical properties.

In typical mountainous regions the objects of direct prospecting occur in the upper, considerably exposed structural stage. The targets of direct prospecting are endogenic deposits. These valuable deposits are often represented by small objects of various shape. The targets of indirect prospecting, particularly ore-bearing (gold, cobalt, mercury, etc.) structures and some other ore controls,



Fig.1.1. Integrated geophysical observations along the reference profile at the Lesser Caucasus (NW Azerbaijan, from Novo-Ivanovka to Beyuk-Kishlak)

*Caption to Fig.1.1*

(I)  $\Delta g$  plot of local anomalies in incomplete Bouguer reduction ( $1 \text{ mGal} = 10^{-5} \text{ m/s}^2$ ); (II)  $\Delta T_{an}$  curve plotted by the map on a 1:50,000 scale; (III)  $Z_{an}$  curve plotted by the map on a 1:25,000 scale; (IV) plot of observed  $Z_{an}$  values; (V)  $\eta_a$  section; (VI)  $\rho_a$  section; (VII) velocity section obtained by refraction survey; (VIII) geological section; (IX) geological section with the account of geophysical data

(1) sandy-clay and gravel-pebble deposits ( $Q$ ); (2) predominantly clastic formations ( $Ng_2-Q$ ); (3) mudstones, tuffaceous sandstones, tuff gritstones ( $Pg_2$ ); (4) limestones ( $K_2cmp+maa$ ); (5) mudstones and tuffaceous clastic rocks ( $K_2con$ ); (6) tuffaceous clastic rocks and mudstones ( $J_3clv$ ); (7) porphyrite and tuffaceous rocks ( $J_2bth$ ); (8) quartzose plagioporphyrines ( $J_2baj_1$ ); (9) porphyrites and tuffs ( $J_2baj_1$ ); (10) basal conglomerates, sandstones and shales ( $J_1$ ); (11) metamorphic schists ( $Pz$ ); (12) gabbro-diorites ( $\gamma Pg_3$ ); (13) syenodiorites, monzodiorites ( $\varepsilon\delta Pg_3$ ); (14) subporphyritic quartz-syenodiorites; quartz-dioritic porphyrites ( $\varepsilon\delta K_1$ ); (15) plagiogranites ( $\gamma\pi J_2baj_2(?)$ ); (16) inferred zones of dikes; (17) fracture zones according to wave dynamic analysis; (18) disjunctive dislocations

are more often narrow-localized, as well. The above mentioned situation essentially differs from that characteristic of oil-and-gas and ore geophysics in platform regions. Here geophysical targets of prospecting were formerly reduced to tracing marker interfaces and horizons, and mapping bedrocks covered with thick sediments within a smoothed relief (Kursk Magnetic Anomaly, Krivoy Rog, Turgay and some other areas). On the contrary, in Alpine mountainous regions the major attention is focused on geophysical field regioning (to single out tectonic blocks) and location of objects with relatively stable geophysical features.

The small sizes of most of the objects dictate the predominance of large-scale and detailed prospecting. For example, in half of the cases the thickness of steeply dipping blocks does not exceed 0.5 km in the Dashkesan mining district of the Lesser Caucasus (Fig.1.2a). According to the data of the Institute of Exploration Geophysics, St.Petersburg, represented in Fig.1.2b, the thickness of geological bodies of a folded complex in half of the cases does not exceed 1 km (max. 4 km) for all one-stage regions.

Endogenic deposits and alpinotype structures which control them

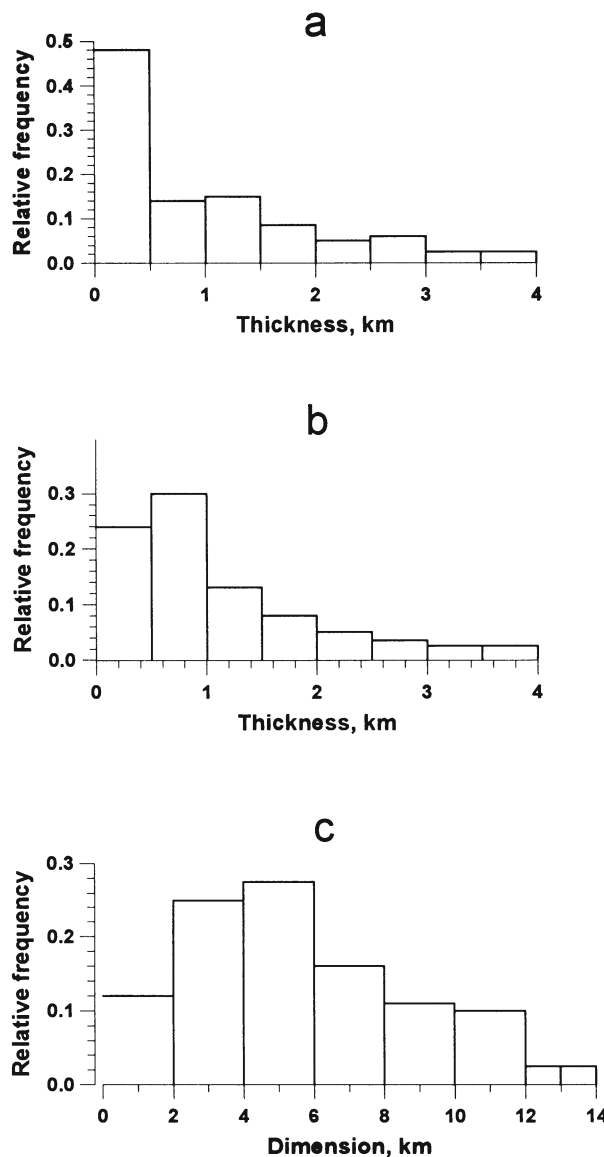


Fig.1.2. Histograms of relative frequency of geological block dimensions: (a) for block thickness from geological sections in the Dashkesan ore district (Lesser Caucasus); (b) for thickness and (c) extension of geological bodies on the folded complex maps in one-stage regions (histograms (b) and (c) after Stolpner [256])

most often have a clear strike. As a result, the observation network is usually rectangular, and the methods of solving two-dimensional problems are employed in quantitative interpretation of geophysical data. These considerations can be supported by the evidence on the size of the blocks under investigation both along and across the strike (Fig.1.2c).

To select networks, we have to take into account the laws of distribution of geophysical fields and objects of investigation, geometrical probabilities of the objects detection, field spectra on the basis of Kotelnikov's theorem (sampling theorem) [292], as well as all possible economical benefits and losses.

The evaluation of predominant strikes of anomalies or structures at the rectangular net points is rather important. The experience in the investigation of the Carpathians and some other regions has shown that a change in the direction of rectangular network profiles from the meridional to the latitudinal may cause a turn in the direction of anomaly axes from the latitudinal to the meridional in the isoline maps. The results of investigation of the Belokan-Zakatala ore district (southern slope of the Greater Caucasus) under the conditions of known strikes and the respective modeling prove that the superposition of anomalies from different strikes may produce false strikes in the rose diagram, which are intermediate between real ones.

In contrast to a large-scale survey, the regional prospecting, which is usually carried out on a medium scale (1:500,000 to 1:100,000), and detail prospecting, are affected to a lesser degree by mountainous conditions. The regional ore controls are larger ore-bearing and ore-distributing structures and, therefore, are related with corresponding regional boundaries of physical properties (Fig.1.3). This makes it possible to study the behavior of the Pre-Alpine basement in order to detect large metallogenic crust blocks. For regional prospecting, deep inhomogeneities may be approximated by simple deterministic models developed according to the level of available knowledge. It allows us to apply the deterministic methods of quantitative interpretation provided they are adapted to the complex observation surface and other complicating factors. Some lithologic and stratigraphic boundaries and tectonic lines, mineral deposit borders and intervals of hydrothermal alterations

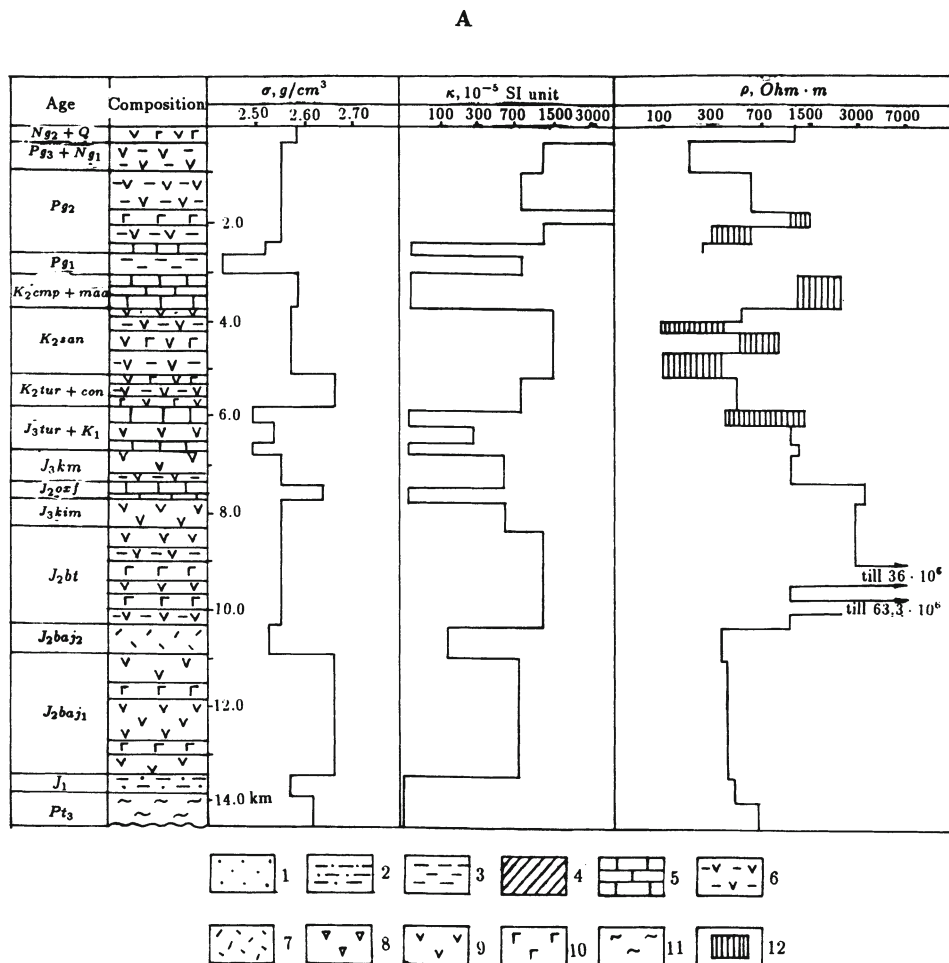
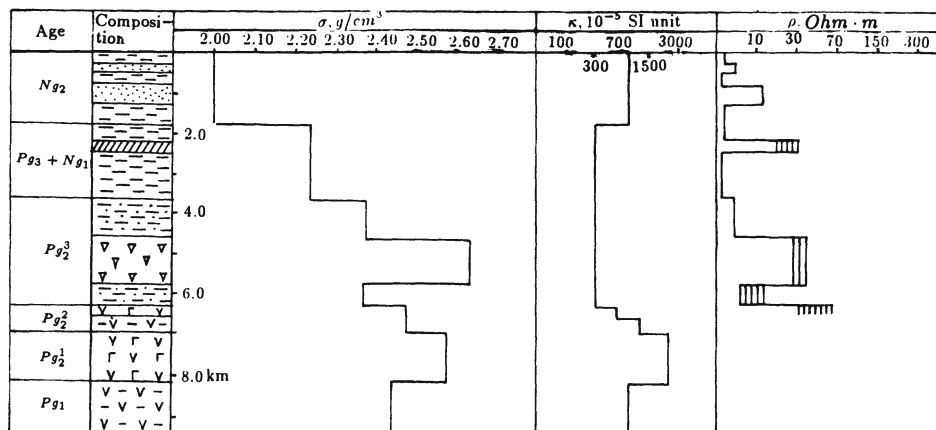
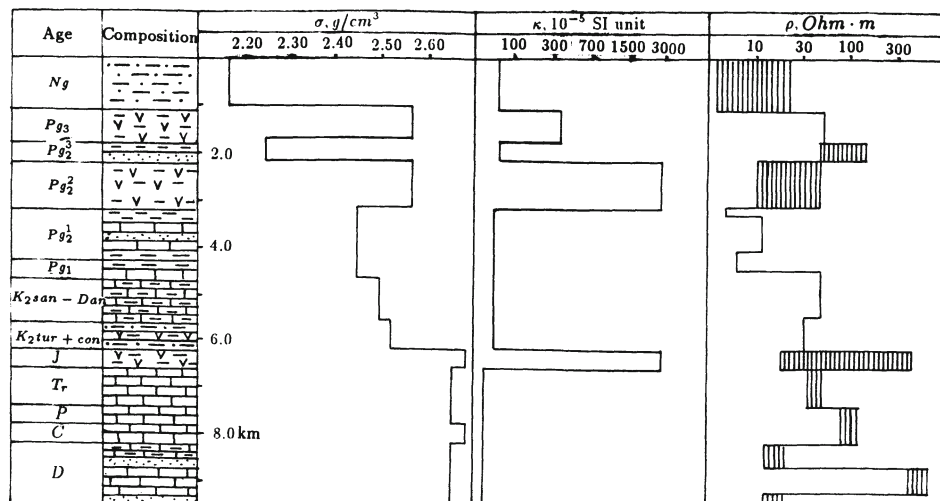


Fig.1.3. Petrophysical columns: (A) north-eastern part of the Lesser Caucasus, (B) Araks zone, (C) Talysh anticlinorium

(1) sands and sandstones; (2) sand and clay deposits; (3) clays; (4) marls; (5) limestones and dolomites; (6) volcanogeno-sedimentary rocks; (7) liparites and plagioliparites; (8) trachyandesites and trachybasalts; (9) andesites; (10) basalts, andesite-basalts, diabases; (11) metamorphic schists; (12) interval of resistivity mean values



may be also considered as reference marks within the areas under detailed investigation (Fig.1.4).

It should be emphasized that many peculiarities of geological structure (for example, plicative and disjunctive dislocations) control different mineral resources, including oil and gas [140] and underground water [243].

The analysis of the accumulated data has allowed us to establish that in most cases the types of geometrical approximations of the objects are confined to a comparatively small number of classes (Table 1.1).

**Table 1.1. Typical approximation of geological objects by bodies of the simplest shape**

GEOPHYSICAL TARGETS		APPROXIMATION
Objects outcropping onto earth's surface and under overburden	Buried or cropping out when surveying by aerial method	
Tectono-magmatic zones, sill-shaped intrusions and thick dikes, large fault zones, thick sheet-like ore deposits	Tectono-magmatic zones, thick sheet intrusives and zones of hydrothermal alterations	Thick bed
Thin dikes, zones of disjunctive dislocations and hydrothermal alterations, sheet-like ore deposits, veins	Sheet intrusives, dikes, disjunctive dislocations, sheet-like ore deposits	Thin bed
Lens- and string-like deposits	Folded structures, elongated morphostructures, large mineral lenses	Horizontal circular cylinder
Pipes, vents of eruption, ore shoots	Intrusions (isometric in plan), pipes, vents of volcanos, large ore shoots	Vertical (inclined) circular cylinder or pivot
Karst cavities, hysterogenetic ore bodies	Brachy-folds, isometric morphostructures, karst cavities, hysterogenetic ore bodies	Sphere

The pronounced gravitational and magnetic anomalies are typi-

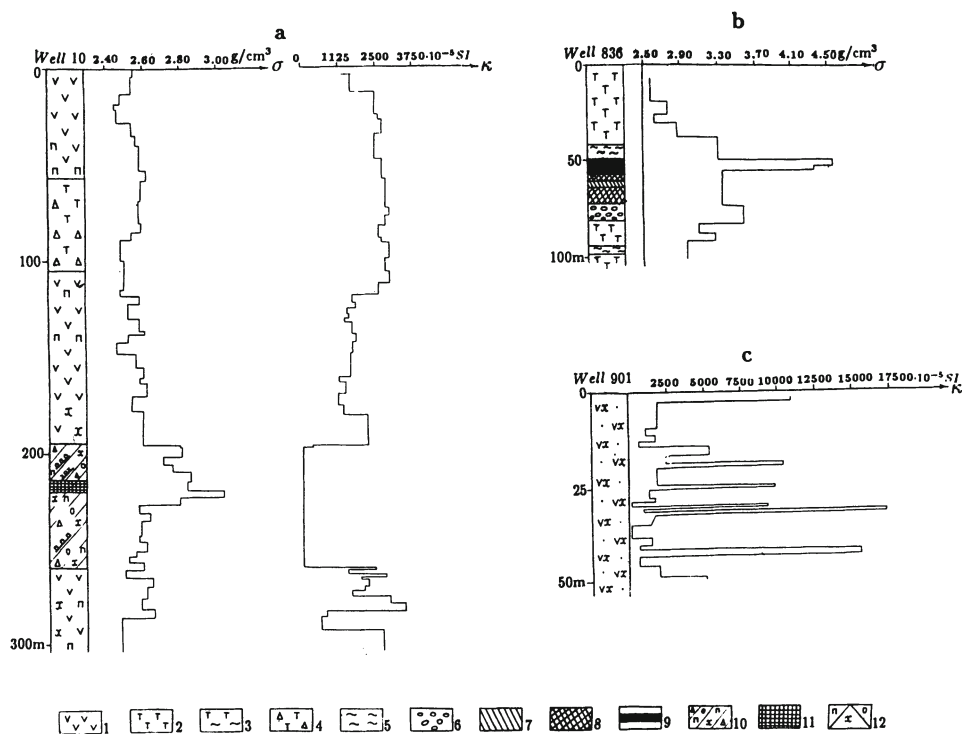


**Fig.1.4. Petrophysical variation in cores (north-eastern part of the Lesser Caucasus):** (a) Kyzylbulakh gold-pyrite deposit, (b) Dashkesan iron deposit, (c) Murut site

(1) porphyrites; (2) slightly altered tuffs; (3) hornfelsed tuffs; (4) tuff breccias; (5) hornfels; (6) garnet skarns; (7) magnetite-garnet skarns; (8) lean skarn-magnetite ore; (9) rich skarn-magnetite ore; (10) zone with phenocrysts, nests, and places of occurrence of pyrite and chalcopyrite massive ores; (12) pyritization, chloritization, silicification

cal bodies of the majority of the objects included in Table 1.1, while ore and the zones of hydrothermal alterations are also distinguished by the *SP* and *IP* anomalies. The objects of the two mentioned classes and disjunctives are often detected by the *VLF* and thermal methods. Most often, the objects are reflected by the anomalies recorded by several methods. This determines the common character of their models and the possibility of an integrated approach to their study.

Geophysical investigation of the orogens is complicated by rapidly changing media and a great number of near-surface anomaly sources. Even for medium-scale areal survey of the north-eastern part of the Lesser Caucasus, up to 5 or 6 petrophysical varieties (by the classification of the Institute of Geology, St.Petersburg) fall on a cell of  $4 \text{ km}^2$  [120]. The petrophysical survey of the Kedabeck ore district of the Lesser Caucasus showed that an area of  $700 \text{ km}^2$  prospected on a scale of 1:50,000 had 17 petromagnetic and 11 petrodensity gradations. A changeability of mountainous regions along the lateral is accompanied by their rapid change along the vertical (see Fig.1.4).

Characteristically, the petrophysical variability is typical of geologically identical rocks (Fig.1.5).

The range of variability of physical properties can be illustrated by Table 1.2.

The erosion of young mountainous structures causes a considerable change in near-surface associations. Physical properties of the rocks occurring close to the earth's surface may not, therefore, be the same as those of deep-seated rocks of the same composition and age (see Fig.1.5a). Consequently, the measurements of physical properties of the rocks located in the upper portion of a section should be treated with great care, especially when they are extrapolated to the depth. There is, however, a need for a shallow survey, since the majority of the deposits under study occur in the upper portion of a section. When investigating deeper horizons, the effect of this rapidly changing portion should be corrected taking into account its true parameters. All these factors attract a special attention to the physical properties of rocks and ores measured on samples taken from the surface, in their natural bedding, drill cores or mines. They make it expedient to carry out their determination on the basis of the

**Table 1.2. Physical properties of rocks and minerals (on the basis of [219], with supplements)**

Object	Electric resistivity $\text{Ohm} \cdot \text{m}$	Polarizability %	Magnetic susceptibility $10^{-6}$ (rationalized SI)	Thermal conductivity $W/(m \cdot {}^\circ C)$	Density $\text{g}/\text{cm}^3$	Compressional velocity $\text{km}/\text{s}$
<b>Rocks and sediments</b>						
Rock salt	$10^6 - 10^7$		-10.3	5.3 - 7.2	2.1 - 2.4	4.0 - 5.5
Gypsum	$10^5 - 10^6$		-12.6	0.5 - 1.5	2.1 - 2.5	3.4 - 4.6
Granite	$5000 - 10^6$	1.7	10 - 65 (without magnetite) 25 - 50 000 (with magnetite)	1.9 - 3.2	2.5 - 2.7	4.6 - 7.0
Basalt	$1000 - 10^8$	0.2 - 4.2	1500 - 25 000	1.5 - 2.2	2.7 - 3.3	2.5 - 6.4
Gabbro	$1000 - 10^8$	0.5 - 1.8	3800 - 90 000*)	2.0 - 2.3	2.7 - 3.5	6.0 - 7.2
Diabase (dykes)	1200 - 2500	0.9 - 1.0	1250 - 5000	2.1 - 2.3	2.5 - 3.2	
Gneiss	$1000 - 10^6$	0.8 - 1.1	0 - 3000	1.9 - 3.7	2.6 - 2.9	5.2 - 6.3
Sandstone	35 - 4000		25 - 5000	2.5 - 3.2	1.8 - 2.7	1.5 - 4.0
Limestone	120 - 4000	1.3	25 - 3000	2.0 - 3.0	2.6 - 2.7 (compact)	3.5 - 6.5
Sand	$1 - 10^6$		25 - 5000	0.3 - 2.95	1.3 - 2.0	0.3 - 1.5
Clay	1 - 120	2.0	25 - 1000	0.25 - 1.08	1.2 - 2.4	1.2 - 2.5
Graphite	$10^{-3} - 10^1$	32.3				
Shale						
<b>Ore and other minerals</b>						
Sulphide Ore	$10^{-4} - 10^{-3}$	5 - 20	10 - 40 $10^3 - 10^5$	3.3 - 4 3.5	4.6	5.0
Pyrrhotite	$10^{-5} - 10^{-3}$			10.7	4.2	4.85
Chalcopyrite	$10^{-4} - 10^{-1}$	10 - 25	35 - 60 (pure) $7 \cdot 10^4 - 14 \cdot 10^6$ (ore)	9.5 - 15 5.2	5.0 5.2	8.0 7.0
Pyrite	$10^{-4} - 10^1$					
Magnetite	$10^{-2} - 10^1$	10 - 40				
Galena	$10^{-2} - 300$			2.0	7.5	
Sphalerite	$> 10^4$			26.7	4.0	
Graphite	$10^{-4} - 10^{-2}$		-100	1.15 - 17	2.2	4.1
Water	$0.1 - 10^5$			0.59(25°C)	1.0	1.43 - 1.59
Oil	$10^9 - 10^{14}$			0.11 - 0.16	0.9	
Coal	$10^2 - 10^4$			0.13 - 2.2	1.2 - 1.5	2.4 - 2.7

\*) Leucocratic gabbro of low magnetization ( $\sim 100 \text{ mA/m}$ ) occurs in some regions (for instance, Caucasus, Sinai)

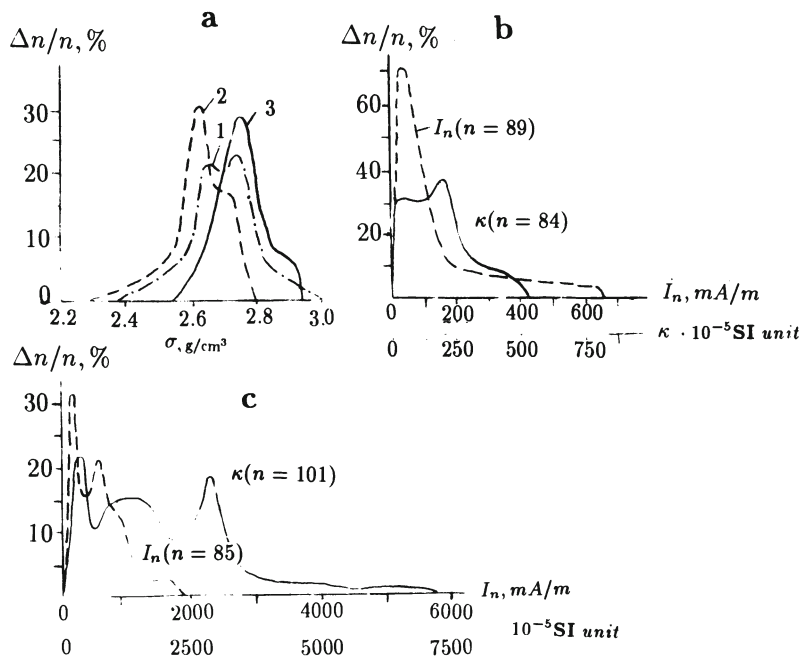


**Fig.1.5. Physical properties of crystalline schists from the Pre-Jurassic basement (a,b) and porphyritic tuffs from the Jurassic (c) in the north-eastern part of the Lesser Caucasus (1) for all samples ( $N = 159$ ); (2) for samples taken from the surface ( $N = 87$ ); (3) for core samples ( $N = 75$ )**

observed geophysical fields. The variability of physical properties makes it possible to derive additional information, to single out the specific ore quides by petrophysical investigations.

Geophysical field study is considerably complicated not only by the geological section inhomogeneity which, in principle, may be a target of investigation. The topography effect, rapid variation of composition and thickness of eluvial-deluvial, proluvial, colluvial and alluvial formations, moistening and weathering, instrument sitting and signal generation conditions may also interfere in such studies. For instance, poor grounding in the resistivity methods on stony mountain slopes limit its application. Therefore, it is expedient to use methods of inductive electric prospecting [91,274].

A detailed analysis of noises impeding geophysical prospecting under mountainous conditions was expounded by Khesin [131]. To

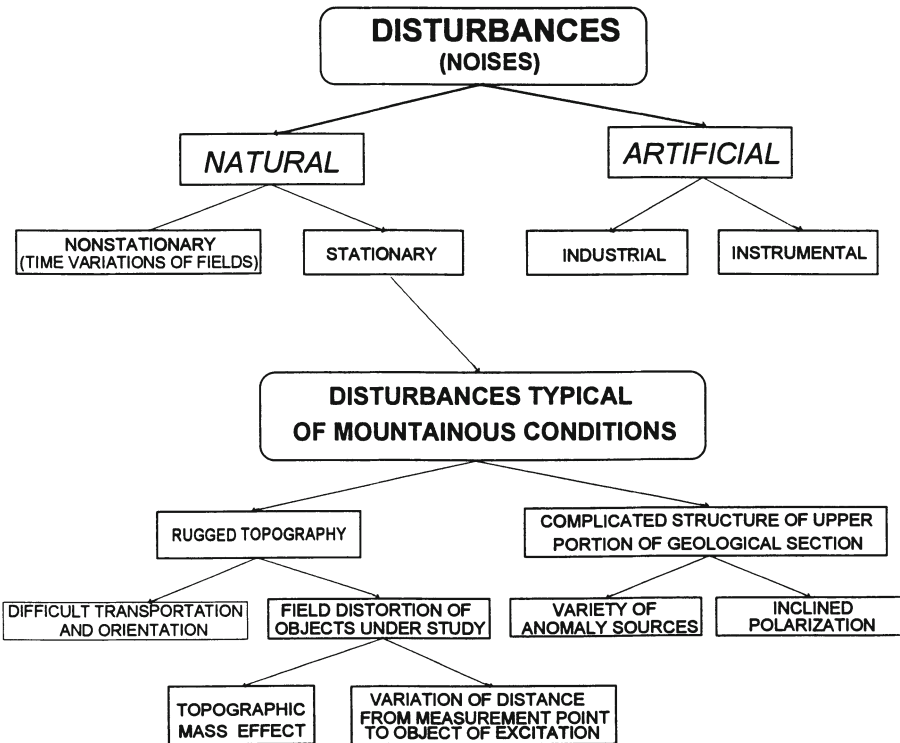


**Fig.1.6. Noises in geophysical investigations**

generate the obtained data, the main noises indicated in this book are summarized in Fig.1.6 [72].

Nonstationary noises – time variations of fields – are typical of natural (gravitational, magnetic, self-potential, thermal) and quasi-natural<sup>1</sup> (electromagnetic, due to VLF transmitters) fields. Several factors are responsible for these noises. In gravimetric prospecting they are lunar-solar and other gravity variations [1], in magnetic prospecting and VLF technique – changes in the ionosphere [100,299] and, finally, in SP method and near-surface thermal

<sup>1</sup> This term was introduced by Khesin [131] especially for the methods employing investigator-independent sources

prospecting – meteorological factors (diurnal and seasonal variations of temperature, pressure and humidity) [62,80,240].

Technogenic noises arise from industrial activities. Noises in the *VLF* and *SP* methods and magnetic prospecting are caused by power lines, stray currents and drill pipes.

Instrumental noises reflect the properties of geophysical instruments, such as the drift of gravimeters.

The main factors that complicate the geophysical prospecting under mountainous conditions are the rugged topography effect and the complexity of the upper part of geological sections.

As Fig.1.6 shows, a rugged relief is responsible for: (a) problems with transportation and orientation, which may result in erroneous determination of observation point heights and their plan coordinates; (b) geophysical field distortion due to the topographic effect of a mass with certain density and magnetization, electric and thermal properties; (c) change in the distance from the point of measurement to the anomalous object, which brings about a change both in the amplitude and in the anomaly extremum position.

The complex upper portion of geological section typical of mountainous regions determines a multitude of geophysical field anomaly sources. Besides, the anomalies are often distorted due to inclined polarization of the disturbing objects.

A great variety of anomaly sources and the superposition of fields of different origin require: (1) probabilistic-statistical or information-statistical methods for singling out the objects of prospecting; and (2) methods for quantitative interpretation of anomalies under the condition of an unknown level of the normal field. Additional problems of interpretation are due to the inclined polarization effect, since the major extremum is shifted from the projection of the upper edge of object on the plan, and an additional extremum may appear [4,5,72,131,143,146].

The methods of the account of the above mentioned noises and their interpretation techniques are covered in several Chapters of the present book.

What defines the importance of the statistical approach?

Human errors in geophysical observations are reduced by em-

ploying the equipment with simultaneous analog and digital recording. If the instrument is jerked, tares are eliminated by comparing different observations and making control measurements. The systematic noise effect including both the geological (regional background) and instrumental (gradual change in zero position) noises are corrected using special methods of observation and data processing.

However, it is impossible to take into account the majority of random noises (or those regarded as random, since they are practically indeterminable) by the above methods. Random noises may arise due to many causes. This is confirmed by a close-to-normal distribution of noise in the *SP* method applied to the obviously barren area in the Kedabeck ore district of the Lesser Caucasus. The hypothesis that noise distribution does not contradict the normal law was tested, in a similar way, by magnetic prospecting on the southern (presumably barren) part of the Filizchai ore area in the Belokan-Zakatala ore district of the Greater Caucasus. The investigation of this region showed that the distribution of absolute altitudes in the detailed work area does not contradict to the normal distribution, too. All mentioned above facilitates the application of the well-known statistical procedures for considering the noise effect employing the probability approach at the stage of detailed prospecting.

Thus, it is expedient to regard the geological media under study and geophysical fields representing them as multicomponent probabilistic systems. The effect of random components of such systems may be eliminated or smoothed out by statistical processing. Some components, the effect of which can be calculated (e.g., anomalies caused by morphostructures or known deep inhomogeneities), are eliminated by applying deterministic methods for solving the direct problem. As a result, we can reveal the target elements of a geological structure with stable geophysical features. They include most of pyrite and magnetite ore deposits, the most important ore controls – deep faults, intrusive magmatism and hydrothermal alteration zones and some others reflected in geophysical fields [131,135,138] and sometimes in a height field.<sup>2</sup>

---

<sup>2</sup> Large endogenic deposits of various types tend to occur in the corners of blocks with different strikes of earth's relief contour lines [135]

Intersections of faulted zones, highly dislocated crust areas and geologically non-trivial areas are rather important indicators of large endogenic deposits of various types. To single out these indicators, it was necessary to develop special procedures described in the book. Here we have revealed that some of the factors are common for control both ore and oil-and-gas deposits (Fig.1.7), and for control both ore and underground water deposits [243].

Moreover, such objects as nodes of large intersecting zones control the location of strong earthquake's focuses [126].

### **1.3 Integration of geophysical methods: Its necessity and routes to its optimization**

The complexity of current geological problems and the ambiguity of the interpretation of geophysical observations call for an integration of geophysical methods proper with geochemical and geological investigations. To select and optimize a set of methods means to find a combination of methods which would enable one to obtain the information required for solving geological problems at a low cost and minimal labor and time consumption [41,131,135].

This problem was discussed by different investigators in numerous publications. For example, Borovko [41] noted that the absence of a correct solution of the optimization problem permits one to obtain only approximate solutions based on the optimization of separate stages by some (as a rule, rather stringent) assumptions.

Exploration geophysicists share two standpoints as to the number of methods in a geophysical set. Some of them tend to expand the set, thus increasing the reliability of the solution of various geological problems. The others note that the expansion of a set is at variance with the economical efficiency of the operations and complicates the latter both from organizational and technical viewpoints. There is also a basic limitation imposed on the number of method. As noted in [66], a growing number of geophysical indicators of the objects under study increases the requirements to the amount of standard information. At the same time, a great number of standards of identical type tend to occur only in well explored provinces, where quantitative prediction is apparently less

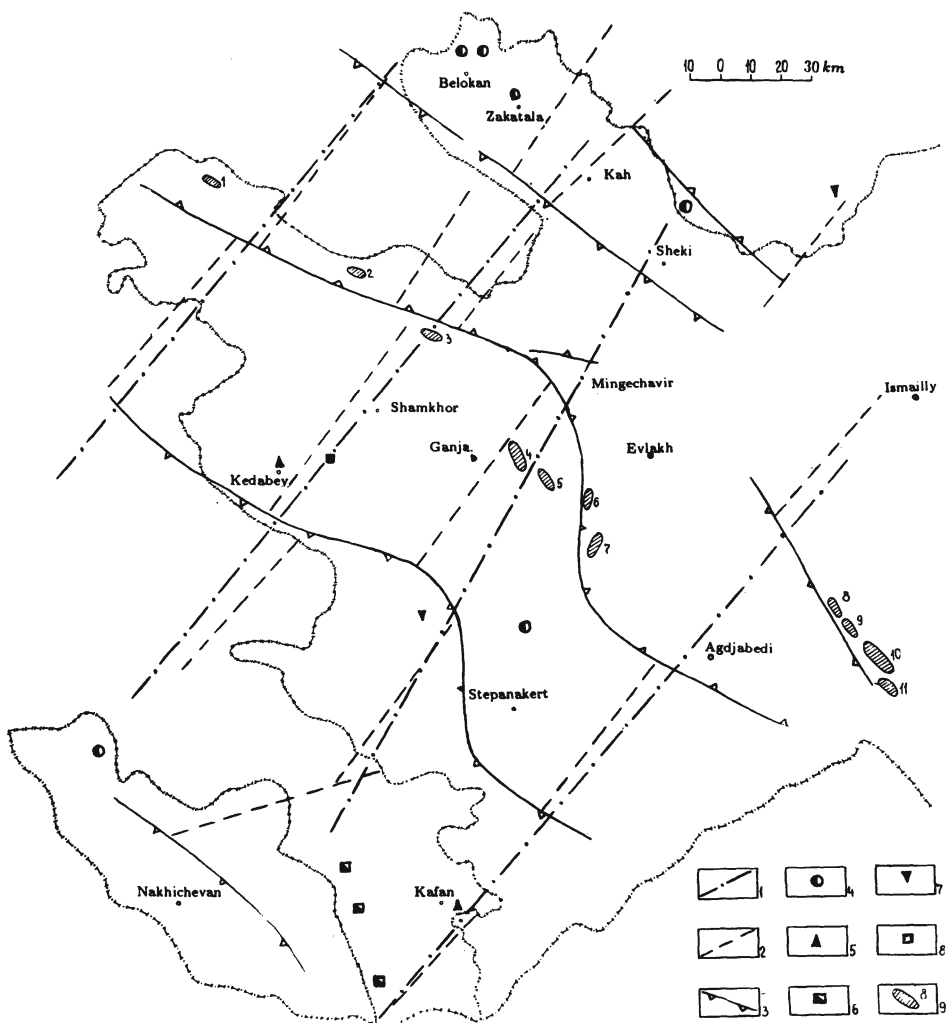


**Fig.1.7. Comparison of regional rupture dislocations and distribution of deposits in the East Caucasus**

(1) generalized transverse dislocations from [135]; (2) revised position of through transverse dislocations from [114]; (3) deep faults as geostructural zone boundaries from [114]; typical ore deposits from [135]: (4) polymetallic ore (lead, zinc, copper), (5) copper, (6) copper and molybdenum, (7) mercury, (8) aluminum; (9) oil and gas deposits from [190] ( 1 – Takhtatope, 2 – Gyurzundakh, 3 – Tarsdallar, 4 – Kazanbulakh, 5 – Adjidere, 6 – Naftalan, 7 – Mir-Bashir, 8 – Zardob, 9 – Shykhbagy, 10 – Muradkhanly, 11 – Jafarly)

urgent than in insufficiently well explored areas. This dictates the tendency of confining the survey set to a minimum of methods.

The number of geophysical methods for solving problems of geological mapping for various useful minerals in the former USSR [44,135] and in the West [219,246,277] does not generally exceed two or three.

The results of the application of two methods (e.g. gravimetric and magnetic survey) are shown in Table 1.3: 1 = negative field, 2 = positive field, 3 = approximately zero field, 4 = alternating field, and 5 = high-gradient field.

**Table 1.3. An example of integrated interpretation**

Typical field combination					Class of objects					
magnetic					gravitational					
1	2	3	4	5	1	2	3	4	5	
1						3				marl
	2					2				gabbroide
1					1					salt
		4						5		fracture zone

Four classes of desired objects can be represented by four combinations of two parameters, each ranging from 1 to 5. The number of combinations is 25. Many geological features under study can be characterized by one of 25 combinations.

The number of combinations can be increased at the expense of secondary parameters obtained via the transformation of fields.

Using quantitative estimations, it is necessary to remember that they are based on certain assumptions and simplifications. Thus, if the probabilities cannot be calculated (the probabilities can change from 0 to 1), they are usually equated to 0.5 (that is most plausible). It is also necessary to take into account concrete geological conditions. For example, in Table 1.3 the value 11 can be obtained for aqueous marls, and this may lead to an erroneous conclusion that other rocks are present at this point. A certain abundance of the set of methods is, therefore, very advisable.

The intuitive use of a small number of elements in practice can be theoretically substantiated by the solution of a well-known

mathematical and cartographic problem of four colors [14,15]. It allows to utilize this solution for regioning and prospecting of useful minerals by integration of geophysical methods [147].

Geophysical investigation is usually a multistage procedure beginning with areal studies and ending in the exploration. For the sake of simplicity, it will be assumed that the task of each stage is the selection of an area for more detailed operations at the next stage. The result of prospecting is primarily a substantiated evaluation of the areas under investigation and their classification into two groups: those worthy and unworthy of further exploration. In this case, the objective of prediction is determined by the general dilemma of a geological exploration processes, – that of obtaining maximum information for given expenditures.

Let us now examine the four color theorem from this stand-point. Using elementary notions of the theory of graphs, the problem can be formulated as follows: it is to be proved that all vertices of an arbitrary planar graph can be colored with four colors in such a way that no two vertices joined by a common edge are of the same color. It was proved as long ago as the middle of the 19th century that four colors suffice to color different counties on the map of England. However, a general solution of this theorem was obtained only recently [14,15]. The authors subdivided all possible maps into almost 2,000 types and developed a computer program for their investigation. For each type the same problem was solved, – whether a map which cannot be colored with four colors can be found among the variety of maps. After investigations of long standing, the answer “no” was obtained for all the types, and this fact confirms the above solution.

Any territory under study can be divided into separate geological areas according to certain indicators. The following system of subclassification according to their prospects has been adopted in the USA [265]: high (*H*), medium (*M*), low (*L*) and unknown (*U*). The objective of prediction is to single out promising areas (if any) from the whole set by means of an integrated geophysical survey. By colors we mean various combinations of geophysical methods. A positive conclusion made on the basis of the materials of a certain prospecting method will be labeled as (+), and a negative conclusion as (-). It is evident that a combination of at least

two independent geophysical methods is necessary for the first three gradations ( $H$ ,  $M$  and  $L$ ); the gradation  $U$  implies no application of the method set (on the necessary scale or not at all) on the territory under investigation (Table 1.4).

**Table 1.4. Subdivision of an area according to its prospects using integrated geophysical survey results**

Level of knowledge of the area	Geophysical method		Combination number (color)
	first	second	
High ( $H$ )	+	+	1
Medium ( $M$ )	+	-	2
Low ( $L$ )	-	-	3
Unknown ( $U$ )	no necessary data		4

The geophysical methods employed are *a priori* assumed as being of equal significance. The threshold field values (the borderline between plus and minus) and particular types of geophysical investigations are determined according to prospecting results for similar objects investigated previously and other geophysical preconditions. By area borderline we mean a certain line (surface) with specified physical characteristics passing over the threshold field values while intersecting it. These physical characteristics may, for example, include amplitudes of observed fields, field gradients or degrees of field variability.

For instance, in an area of copper-porphyry deposit in Kazakhstan marginal values have been selected for specific electric resistance of  $50 \text{ Ohm} \cdot \text{m}$ , for magnetic field of  $0 \text{ nT}$  (deposits of this type are characterized by low resistance ( $< 50 \text{ Ohm} \cdot \text{m}$ ) and negative magnetic field). Figure 1.8 shows: 4a – isoohms, 4b – isogams, 4c – coloring in four colors according to Table 1.4. The contour of the deposit is clearly revealed on the basis of the data of the two methods.

It can be concluded from the foregoing that an optimum geophysical set is that consisting of two independent geophysical methods. A map of geophysical results colored with four colors by the above technique serves as a basis for more detailed investigation.

It should, however, be kept in mind that the employed geophysi-

cal set is usually oriented to a particular problem and substantiated by a corresponding physico-geological model of the medium. A change in the problem (e.g., an increase of the required depth of investigation) or in geological and geophysical pattern of the area may bring about a change in the set of methods. This may, in its turn, affect the “coloring” of the area under study. In this connection, a certain redundancy of the set is needed. It is generally a good practice to use three geophysical methods which are effective under given conditions, the more so that the addition of, say, a radiometric channel to a combination of aerial magnetic and electric surveys results in a negligible increase of the cost.

An integration of geophysical methods is a subsystem of the prospecting set. From this stand-point, it is of interest to analyze geological exploration process as a whole [124]. According to [166], the optimization provides for the estimation of the opportunities of methods. It defines the methods allowing to reveal the indicators of the targets from several stages and to exclude “redundant” indicators and methods. Similar considerations form the basis for developing a general type of integration and the stages of geophysical investigation under mountainous conditions [131,138].

The core of the integration set consists of prompt, highly efficient and ecologically pure (noninvasive) methods of investigating natural fields. These methods are often called passive. Their main limitation is the impossibility to amplify a useful signal. However, these methods provide an increased depth of investigation: the objects under study are sources of gravitational, magnetic and other anomalies. Therefore, a distance to the point of field measurement is shorter than the range of the artificial signal generated on the terrain surface. Besides, magnetic, gravity, SP and VLF methods of exploration are very important, since they are applicable to solving typical problems of prospecting. The latter include revealing steeply dipping heterogeneities, tectonic blocks mapping when surveying and detecting separate objects in search of ores.

The subhorizontal boundaries may be selected best of all using seismic prospecting and electric or electromagnetic soundings. However, their application is limited by the conditions of accommodating space observation system. Such systems are well-known in modern 3-D seismics. Special systems of seismic observations (for instance,

“slalom-profile” [220]) in hardly accessible regions are often located along river valleys. These valleys frequently coincide with fracture zones, i.e. with the boundaries of tectonic blocks. Therefore, investigations along such profiles are insufficient to obtain a correct representation of the internal structure of tectonic blocks. It is by no means a refusal of seismic investigations: in the majority of cases only seismics allows to determine the depth of occurrence of studied horizons with high accuracy. However, when passing to more complex geological situations, the interpretation of seismic data becomes rather complicated. Therefore, even in submountain regions seismic prospecting is combined with the magnetic and gravimetric surveys to reveal tectonic blocks and faults [242]. Besides, to estimate the material composition of the studied geological bodies, it is necessary to use a set of geophysical methods. The methods of natural geophysical field investigation hold indispensable place among them, taking into account the above mentioned reasons.

Complicated conditions of prospecting generate a need for both quantitative estimation of the competitiveness of each method and quantitative substantiation of the network selection. The calculated cost of a unit of information testifies to the expediency of using natural fields. It can be easily visualized if we consider the Belokan-Zakatala ore district as an example [291]. Here, in particular, the ratio of the informational significance of indicators to the cost of 1  $km^2$  survey on a 1:25,000 scale (in monetary units) equals 11 for surface magnetic prospecting, 43 for *SP* method and 120 for spectrometallometry on the secondary dispersion halos.

When selecting a set of methods, the mobility and resolution of each method are considered. Resolution implies the capability to single out an anomaly caused by the object to be found at a minimal depth. It is determined by physico-geological modeling.

Optimization of a set of geophysical methods, their modifications and observation systems is determined by the necessity to solve geological problems with minimum expenditures. The expansion of the amount of geophysical work is acceptable if it optimizes the whole process of geological exploration. Thus, the quality and quantity of the end product of geophysical investigation, i.e. the results of geophysical data interpretation, define the optimum decision-making. Therefore, the optimization is closely connected

with the efficiency of geophysical field interpretation based on the analysis of its essence, on the consideration of specific conditions of its application, and on the development of special techniques satisfying these conditions.

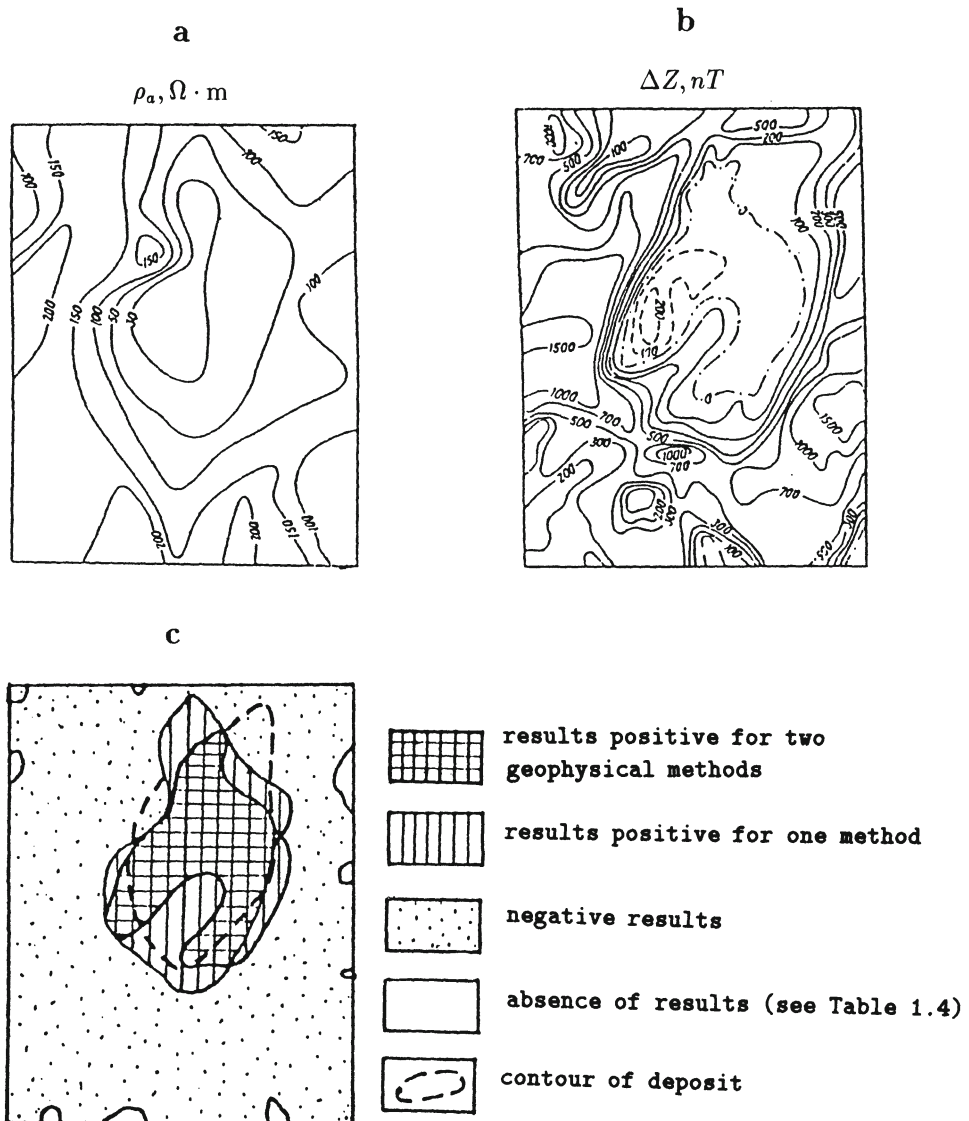


Fig.1.8. Electric (a) and magnetic (b) prospecting results at Benkaly copper-porphyry deposit and their processing according to "four color problem" solution (c)  
(a, b and contour of deposit after [209])

## Chapter 2

# COMMON ASPECTS OF GEOPHYSICAL FIELDS IN QUESTION

### 2.1 Common theoretical and model principles of anomaly interpretation

As mentioned above, magnetic prospecting is the best investigated method to be applied under mountainous conditions [146]. Alexeyev [5] has developed rapid methods for quantitative interpretation of anomalies observed under the conditions of oblique magnetization, rugged relief and unknown level of the normal field. Therefore, the possibility of adapting the techniques involved for other geophysical investigations and the analysis of the similarity of analytical expressions for the arising anomalies are note worthy. The comparative study of analytical expressions for some geophysical fields has been carried out earlier in [18,205].

#### 2.1.1 Natural (gravitational, magnetic, thermal, self-potential) fields

The potential character of a gravitational field, which follows from the law of gravitation, is expressed by differential equations:

$$\text{rot } \mathbf{F} = 0 \quad (2.1)$$

and

$$\mathbf{F} = \text{grad } W, \quad (2.2)$$

where  $\mathbf{F}$  is the gravitational field intensity and  $W$  is the gravity potential.

The proportionality between the gravitational field intensity and the substance density  $\sigma$  is determined by the expression:

$$\operatorname{div} \mathbf{F} = -4\pi G\sigma, \quad (2.3)$$

where  $G$  is the gravitation constant.

As follows from equations (2.2) and (2.3), the gravity potential must satisfy Poisson's equation [122]:

$$\nabla^2 W = -4\pi G\sigma, \quad (2.4)$$

while as for points where the mass is zero ( $\sigma = 0$ ), it should satisfy Laplace's equation:

$$\Delta W = \frac{\partial^2 W}{\partial x^2} + \frac{\partial^2 W}{\partial y^2} + \frac{\partial^2 W}{\partial z^2}. \quad (2.5)$$

The magnetic field (for  $\Delta T$  – when magnetic susceptibility is below 0.1 SI unit) is potential [109,146,270], viz.

$$\mathbf{U}_a = -\operatorname{grad} V, \quad (2.6)$$

where  $\mathbf{U}_a$  is the anomalous magnetic field,  $V$  represents the magnetic potential.

This field satisfies Poisson's equation.

In solids, heat flows according to Fourier's law [283]:

$$\mathbf{q} = -\lambda \operatorname{grad} T = -\lambda \frac{\partial T}{\partial n}, \quad (2.7)$$

where  $T$  is the temperature,  $\mathbf{q}$  is the heat flow density,  $\lambda$  is the thermal conductivity coefficient, and  $n$  is the outward normal to an isothermal surface.

If we assume that the heat transfer from the local sources is conductive and the temperature field is stationary, then the temperature distribution in a space without any sources satisfies Laplace's equation [283], being potential, too.

Self-potential (natural electric) polarization is brought about by spontaneous appearance of electric double layers on various

geological formation contacts. The electric fields  $\mathbf{E}$  of the electric double layer  $l$  caused by natural polarization are defined as the gradient of a scalar potential  $\Pi$ :

$$\mathbf{E} = -\text{grad } \Pi. \quad (2.8)$$

The potential  $\Pi$  satisfies Laplace's equation everywhere outside the layer  $l$  [303].

So, the analogy between (2.2), (2.6), (2.7), and (2.8) is evident. It basically substantiates the opportunity to employ the methods for interpreting one field in the investigation of other fields. We can, for example, extend the results obtained in the theory of magnetism to thermal prospecting [50].

The most common models in gravimetric, self-potential and thermal prospecting are dipping thin bed (*DTB*), horizontal circular cylinder (*HCC*) and sphere [18,172,195,300]. The comparison of analytical expressions for the fields of the above models for the methods under consideration and magnetic prospecting (two-dimensional case) is presented in Table 2.1.

**Table 2.1. Comparison of analytical expressions for natural geophysical fields**

Field	Analytical expression	
Magnetic	$DTB$ $Z_v = 2I2b \frac{z}{x^2+z^2}$	Point source (rod) $Z_v = \frac{mz}{(x^2+z^2)^{3/2}}$
Gravitational	$HCC$ $\Delta g = 2G\sigma \frac{z}{x^2+z^2}$	Sphere $\Delta g = GM \frac{z}{(x^2+z^2)^{3/2}}$
Self-potential	$HCC$ $\Delta U = \frac{2\rho_1}{\rho_1+\rho_2} U_o r_o \frac{z}{x^2+z^2}$	Sphere $\Delta U = \frac{2\rho_1}{2\rho_2+\rho_1} U_o R^2 \frac{z}{(x^2+z^2)^{3/2}}$
Temperature	—	Sphere $\Delta t = \frac{q}{\lambda_2} \frac{\mu-1}{\mu+2} \frac{R^3}{(x^2+z^2)^{3/2}}$

Here  $Z_v$  is the vertical magnetic field component at vertical magnetization;  $I$  is the magnetization;  $b$  is the horizontal semithickness of *DTB*;  $m$  is the magnetic mass;  $G$  is the gravitational constant;  $\sigma$  is the density;  $M$  is the mass of the sphere;  $\rho_1$  is the host medium resistivity;  $\rho_2$  is the anomalous object (*HCC* or sphere) resistivity;  $U_o$  is the potential jump at the *anomalous body/host medium* interface;  $r_o$  is the polarized cylinder radius;  $R$  is the sphere radius;

$q$  is the heat flow density;  $\lambda_2$  is the thermal conductivity of the anomalous object;  $\mu$  is the object-to-medium thermal conductivity ratio;  $x$  is the current coordinate;  $z$  is the depth of the upper *DTB* edge (*HCC* or sphere center) occurrence.

It is easy to prove that the analytical expressions are proportional for a *DTB* model in magnetic method and a *HCC* model in gravimetric and *SP* methods; for a point source in magnetic method and a sphere in gravimetric, thermal and *SP* methods.

## 2.1.2 Artificial (artificially-applied) fields

### 2.1.2.1 VLF method

The *VLF* method is based on the investigation of alternating electromagnetic fields from far transmitters. A long distance from transmitters, which is responsible for the uniformity of the field, allows us to assume the wavefront to be plane within the investigation area.

The main equations of the theory of alternating electromagnetic field are Maxwell's equations:

$$\text{rot } \mathbf{H} = \mathbf{j} + \frac{\partial \mathbf{D}}{\partial t}; \quad (2.9)$$

$$\text{rot } \mathbf{E} = -\frac{\partial \mathbf{B}}{\partial t}; \quad (2.10)$$

$$\text{div } \mathbf{B} = 0; \quad (2.11)$$

$$\text{div } \mathbf{D} = q. \quad (2.12)$$

Here  $\mathbf{H}$  and  $\mathbf{B}$  are magnetic field vector ( $\mathbf{H}$  stands for intensity and  $\mathbf{B}$  for induction);  $\mathbf{E}$  and  $\mathbf{D}$  are electric field vectors ( $\mathbf{E}$  stands for intensity and  $\mathbf{D}$  for induction);  $q$  is the charge density;  $\mathbf{j}$  is the conduction current density.

Equation (2.9) can be written as [173]:

$$\text{rot } \mathbf{H} = \mathbf{C} = \mathbf{j}_{\text{cond}} + \mathbf{j}_{\text{disp}},$$

where  $\mathbf{C}$  is the total current density;  $\mathbf{j}_{\text{cond}}$  and  $\mathbf{j}_{\text{disp}}$  are conduction and displacement current densities, respectively.

It has been found that at the frequencies of 10 to 25  $kH\text{z}$   $\mathbf{j}_{\text{disp}} \approx 0$  [300]. Therefore,

$$\operatorname{rot} \mathbf{H} = \mathbf{j}_{\text{cond}} \quad (2.14)$$

or

$$\mathbf{H} = \nu \mathbf{E}, \quad (2.15)$$

where  $\nu$  is the electric conductivity.

An *EM* field can be considered as quasi-stationary, if only it satisfies three conditions of quasi-stationarity. The physical meaning of these conditions was described by Landau and Lifshitz [173], and as applied to geophysics, they were formulated in [11]. These conditions are as follows:

(1) Slow field variation.

(2) Closed currents.

(3) To avoid an appreciable lag in the magnetic field variation, the region including magnetic field generating currents and observation points must not be too large.

Let us consider these conditions in more detail.

(1) The study of time variations of the *VLF* fields has shown that sharp changes in the intensity are not characteristic of these fields. Nonetheless, these variations should be eliminated by using a special procedure in the process of field work (see Appendix A).

(2) This condition follows from equation (2.14), since  $\operatorname{div} \operatorname{rot} \mathbf{H} = 0$  and, therefore,  $\operatorname{div} \mathbf{j} = 0$ . Almost closed currents do not violate this condition.

(3) This condition can be formulated in the following way: the length of electromagnetic wave in the ground should essentially surpass the length of the investigated objects. The condition, as a rule, is satisfied in the prospecting of ore deposits, study of faults and other objects of engineering geophysics, and in other detailed investigations.

It is well-known that the fundamental solution of Laplace's equation in 2-D case is the following function:

$$g_s(M, P) = \frac{1}{2\pi} \ln \frac{1}{R_{MP}}, \quad (2.16)$$

where  $R_{MP}$  is the distance between the points  $M$  and  $P$  ( $M$  is the observation point,  $P$  is the point of the body).

The fundamental solution of Helmholtz wave equation is Hankel function of the first kind of the zero order  $H_o^{(1)}$ :

$$g_o(M, P) = \frac{i}{4} H_o^{(1)}(kR_{MP}), \quad (2.17)$$

where  $k$  is the wave number,  $i$  is the imaginary unit.

The function (2.17) is the analogue of the function (2.16) for Laplace's equation.

Using the above correspondence, the authors of [57] and [107] established the analogy between Green's solutions of Laplace's and Helmholtz equations. This allowed them to prove the possibility of extending the results obtained in the potential theory to Helmholtz equation.

Dmitriev [58] indicates that the association of the singular points resulting from the VLF field anomaly plots with geometrical parameters of the bed is analogous to the well-known behavior of singular points in potential field anomalies.

Zhdanov [302] carried out a theoretical investigation of the application of a set of Cauchy-type integral analogues to the problems of electromagnetism. It was suggested that the methods developed in the potential theory for analytical continuation, separation and quantitative interpretation can be applied to the quasi-stationary electromagnetic anomaly investigation.

The quasi-stationarity of electromagnetic field follows from the condition (1).

The overview of publications [17, 100, 215, 237, 280] has shown that a conductive inclined thin bed is the most common model in the VLF technique. The analytical expression of the fields for the above mentioned model (two-dimensional case) are presented in Table 2.2.

Evidently,  $Z_v$  is proportional to  $H_x$ , while  $X_v$  is proportional to  $H_z$ . Similar results have been obtained for a HCC model [72].

Thus, the plots of magnetic fields of VLF transmitters can be interpreted by special methods elaborated in potential field theory (in particular, in magnetic prospecting). E-polarization vector, in the first approximation, is the analog of magnetization vector [72].

**Table 2.2. Comparison of analytical expressions for DTB in magnetic prospecting and VLF method**

Field	Analytical expression	
Magnetic	$Z_v = 2I2b \frac{z}{x^2+z^2}$	$X_v = -2I2b \frac{x}{x^2+z^2}$
VLF	$H_x = kH_o \frac{z}{x^2+z^2}$	$H_z = -kH_o \frac{x}{x^2+z^2}$

In this table  $Z_v$  and  $X_v$  are vertical and horizontal magnetic field components for vertical magnetization, respectively;  $H_x$  and  $H_z$  are horizontal and vertical VLF magnetic field components, respectively;  $H_o$  is the VLF primary field intensity;  $k$  is the coefficient involving geometry and conductivity of the bed.

#### 2.1.2.2 IP method

The active method is based on the investigation of secondary electric fields which are brought about in the ground by electric current. Its extensive application is due to its sensitivity to the presence of conductive minerals. Observations by the IP method are conducted both in the time and frequency domains. It should be noted that many authors, for example [65,108,115,161,277,306], underline the similarity between the results obtained in both domains. Here we will consider investigations in the time domain.

Based on [11,252] and taking also into account [18] IP field intensity can be written in the following form:

$$\mathbf{E}_{IP} = \frac{1}{2\pi\varepsilon_0} \int_s \frac{2(\mathbf{P}, \mathbf{r})\mathbf{r} - \mathbf{P}r^2}{r^4} ds, \quad (2.18)$$

where  $\varepsilon_0$  is the dielectric constant of free-space;  $S$  is the cross-section area of the body;  $\mathbf{P}$  is the polarization vector (dipole moment of a unit volume);  $r = \sqrt{(x_s - x)^2 + (z_s - z)^2}$  is the distance from the observation point  $M(x, z)$  to a certain point of the body  $P(x_s, z_s)$ ;  $\mathbf{r} = (x_s - x)\mathbf{i} + (z_s - z)\mathbf{k}$  is the radius-vector from the point  $M$  to the point  $P$ ,  $\mathbf{i}$  and  $\mathbf{k}$  are the unit vectors directed along  $Ox$ - and  $Oz$ -axis.

The projections of  $\mathbf{P}_{IP}$  on the coordinate axes are:

$$\begin{aligned} P_{IP,x} &= P_{IP} \cos \varphi_{IP}, \\ P_{IP,z} &= P_{IP} \sin \varphi_{IP}, \end{aligned} \quad (2.19)$$

where  $\varphi_{IP}$  is the inclination angle between the vector  $\mathbf{P}_{IP}$  and  $Ox$ -axis.

Then the components  $\mathbf{E}_{IP}$  may be written in the following forms:

$$E_{IP,x} = -\frac{1}{2\pi\varepsilon_0} \int_s P_{IP} \frac{(z_d^2 - x_d^2) \cos \varphi_{IP} - 2z_d x_d \sin \varphi_{IP}}{r^4} ds, \quad (2.20a)$$

$$E_{IP,z} = \frac{1}{2\pi\varepsilon_0} \int_s P_{IP} \frac{(z_d^2 - x_d^2) \sin \varphi_{IP} + 2z_d x_d \cos \varphi_{IP}}{r^4} ds, \quad (2.20b)$$

where  $z_d = z_s - z$  and  $x_d = x_s - x$ .

At the same time, the magnetic field components acquire the forms [5]:

$$X_{an} = \frac{\mu_o}{4\pi} \int_s I \frac{-(z_d^2 - x_d^2) \cos \varphi_m + 2z_d x_d \sin \varphi_m}{r^4} ds, \quad (2.21a)$$

$$Z_{an} = \frac{\mu_o}{4\pi} \int_s I \frac{(z_d^2 - x_d^2) \sin \varphi_m + 2z_d x_d \cos \varphi_m}{r^4} ds, \quad (2.21b)$$

where  $\mu_o$  is the absolute permeability of free-space,  $\varphi_m$  is the inclination angle between the vector  $\mathbf{I}$  and  $Oxx$ -axis.

Obviously, the expressions (2.20a) and (2.21a), (2.20b) and (2.21b) are proportional, respectively, to each other.

Taking into account that  $E_{IP,z}$  is not measurable and  $X_{an}$  is measured but rarely, it is necessary to establish other relations. If we denote

$$\varphi_{IP} = \varphi_m + 90^\circ, \quad P_{IP} = 4\pi k \varepsilon_0 I \quad (2.22)$$

(coefficient  $k = 1 \text{ V/A}$ ),

then we obtain  $E_{IP,z} = Z_{an}$ , since the right-hand sides of expressions (2.20a) (after some transformations) and (2.21b) are the same. This fact has been observed earlier for both vertical magnetization and horizontal induced polarization [24,161].

Equalities (2.22) show that the vector  $\mathbf{P}_{IP}$  deviates by  $90^\circ$  in the clockwise direction from the vector  $\mathbf{I}$ .

To calculate the *IP* anomaly from equation (2.20a), it is necessary to express the vector  $\mathbf{P}_{IP}$  in terms of the internal polarizing field and parameters of the medium and the anomalous object. A well-known technique [162,239] was used for the purpose; the effect of space-charge polarization was formally reduced to a decrease in the conductivity of the medium ( $\gamma_1$ ) and the body ( $\gamma_2$ )

$$\gamma_1^* = \gamma_1(1-\eta_1), \quad \gamma_2^* = \gamma_2(1-\eta_2),$$

where  $\eta_1$  and  $\eta_2$  are polarizabilities of the medium and the body, respectively.

We proceed from the expression [18]:

$$\frac{1}{\varepsilon_o} \mathbf{P}_{IP} = \frac{1}{\varepsilon_o} \mathbf{P}_e^* - \frac{1}{\varepsilon_o} \mathbf{P}_e = C_e^* \mathbf{E}_{int}^* - C_e \mathbf{E}_{int}, \quad (2.23)$$

where  $C_e$  and  $C_e^*$  are the values of electric polarization susceptibility (analogue of magnetic susceptibility) in the absence or presence of *IP*, respectively:

$$C_e = (\gamma_2 - \gamma_1)/\gamma_1 = \gamma_2/\gamma_1 - 1 = q - 1,$$

$$C_e^* = (\gamma_2^* - \gamma_1^*)/\gamma_1^* = \frac{q(1-\eta_2)}{1-\eta_1} - 1,$$

$\mathbf{E}_{int}$  and  $\mathbf{E}_{int}^*$  represent the internal field in the body in the absence and in the presence of the *IP*, respectively.

If we express the internal field in terms of the uniform primary polarizing field  $\mathbf{E}_o$  [18,146], we obtain

$$\begin{aligned} \frac{1}{\varepsilon_o} \mathbf{P}_{IP} &= \mathbf{i} \left( \frac{C_e^*}{1+N_x C_e^*} - \frac{C_e}{1+N_x C_e} \right) E_{Ox} + \\ &+ \mathbf{k} \left( \frac{C_e^*}{1+N_z C_e^*} - \frac{C_e}{1+N_z C_e} \right) E_{Oz}, \end{aligned}$$

where  $N_x, N_z$  are coefficients of the body's shape along the axes  $Ox$  and  $Oz$ , respectively.

After several manipulations, we obtain

$$\frac{1}{\varepsilon_o} \mathbf{P}_{IP} = -\frac{q\eta_{red}E_o}{1-\eta_1} \left[ \mathbf{i} \frac{\cos \varphi_o}{(1+N_x C_e^*)(1+N_x C_e)} + \mathbf{k} \frac{\sin \varphi_o}{(1+N_z C_e^*)(1+N_z C_e)} \right], \quad (2.24)$$

where  $\eta_{red} = \eta_2 - \eta_1$  is a redundant polarizability of the anomalous body;  $\varphi_o$  is the inclination angle between the vector  $\mathbf{E}_o$  and  $Ox$ -axis.

The absolute value of the vector  $\mathbf{P}_{IP}$  is defined from the formula:

$$\frac{1}{\varepsilon_o} P_{IP} = \frac{q\eta_{red}E_o}{1 - \eta_1} p, \quad (2.25)$$

where

$$p = \left[ \frac{\cos^2 \varphi_o}{(1+N_x C_e^*)^2 (1+N_x C_e)^2} + \frac{\sin^2 \varphi_o}{(1+N_z C_e^*)^2 (1+N_z C_e)^2} \right]^{1/2}$$

Substituting the value of  $P_{IP}$  into the equation (2.20a) we obtain

$$E_{IP,x} = \frac{1}{4\pi} \frac{q\eta_{red}}{1 - \eta_1} p E_o F(x, z), \quad (2.26)$$

where the function  $F(x, z)$  is equal to the right-hand side of the formula (2.21b) when  $I = 1$ ,  $\varphi_m = \varphi_{IP} - 90^\circ$ .

Let us consider specific cases of the equations (2.24) and (2.25).

If an anomalous object has a form of a steeply inclined bed, which may be approximated by an elliptical cylinder with a long axis directed along  $Oz$ -axis, then the coefficient  $N_z$  is very small along this axis. Assuming that the coefficient  $N_x = 1 - N_z \approx 1$  along the  $Ox$ -axis,

$$\frac{1}{\varepsilon_o} \mathbf{P}_{IP} = -\frac{\eta_{red} E_o}{1 - \eta_2} \left[ \mathbf{i} \frac{\cos \varphi_o}{q} + \mathbf{k} q \frac{1 - \eta_2}{1 - \eta_1} \sin \varphi_o \right]. \quad (2.27)$$

Formula (2.27) demonstrates that the vector  $\mathbf{P}_{IP}$  of the bed (elliptical cylinder) is not parallel to the vector  $\mathbf{E}_o$ .

In this case the absolute value of the vector  $\mathbf{P}_{IP}$  can be defined from the formula

$$\frac{1}{\varepsilon_o} P_{IP} = \frac{\eta_{red} E_o}{1 - \eta_2} \left[ \frac{\cos^2 \varphi_o}{q^2} + \frac{q^2 (1 - \eta_2)^2}{(1 - \eta_1)} \sin^2 \varphi_o \right]^{1/2}. \quad (2.28)$$

If the polarized bed does not differ from the host medium in conductivity, then  $q = 1$ . Since the value  $(1 - \eta_2)/(1 - \eta_1)$  differs only slightly from 1, it follows that

$$\frac{1}{\varepsilon_o} P_{IP} \approx \frac{\eta_{red}}{1 - \eta_2} E_o.$$

For a circular cylinder,  $N_x = N_z = 0.5$  and the formula (2.24) acquires the following form

$$\frac{1}{\varepsilon_o} P_{IP} = \frac{-4q\eta_{red}E_o}{[1-\eta_1+q(1-\eta_2)](1+q)} [\mathbf{i} \cos \varphi_o + \mathbf{k} \sin \varphi_o]. \quad (2.29)$$

In this case vectors  $\mathbf{P}_{IP}$  and  $\mathbf{E}_o$  are parallel. The absolute value of the vector  $\mathbf{P}_{IP}$  for a circular cylinder is equal to

$$\frac{1}{\varepsilon_o} P_{IP} = \frac{4q\eta_{red}E_o}{(1+q)[1-\eta_1+q(1-\eta_2)]}. \quad (2.30)$$

When  $q = 1$ , we have

$$\frac{1}{\varepsilon_o} P_{IP} = \frac{\eta_{red}E_o}{1 - 0.5(\eta_1+\eta_2)}.$$

Based upon the works [161,274] the anomaly  $\eta_{an}$  of apparent polarizability  $\eta_a$  can be determined from the formula:

$$\eta_{an} = \eta_a - \eta_1 = \frac{E_{IP}}{E_o + E_{IP}}. \quad (2.31)$$

Since, as a rule, the *IP* anomalies are small in comparison with the primary field, we can roughly write that

$$\eta_{an} \approx \frac{E_{IP}}{E_o}. \quad (2.32)$$

Substituting expressions  $E_{IP}$  from (2.31) into this formula for the models of an inclined thick bed (*ITB*), dipping (inclined) thin bed (*DTB*), and horizontal circular cylinder (*HCC*) and taking into account, in the first approximation, the ground-air interface effect, we obtain

$$\left. \begin{aligned} \eta_{an,ITB} &= \frac{1}{2\pi} \frac{q\eta_{red}}{1-\eta_1} p F_1(x), \\ \eta_{an,DTB} &= \frac{1}{2\pi} \frac{q\eta_{red}}{1-\eta_1} p 2b F_2(x), \\ \eta_{an,HCC} &= \frac{1}{2\pi} \frac{q\eta_{red}}{1-\eta_1} p S F_3(x). \end{aligned} \right\} \quad (2.33)$$

Here  $F_1(x)$ ,  $F_2(x)$  and  $F_3(x)$  are the analytical expressions obtained, respectively, for the above models in magnetic prospecting [143,146]:

$$\left. \begin{aligned} F_1(x) &= 2 \sin \varphi_2 \left[ \left( \arctan \frac{x+b}{h} - \arctan \frac{x-b}{h} \right) \cos \theta - \right. \\ &\quad \left. - \left( \ln \frac{\sqrt{(x+b)^2 + h^2}}{\sqrt{(x-b)^2 + h^2}} \right) \sin \theta \right], \\ F_2(x) &= 2 \frac{h \cos \theta - \sin \theta}{x^2 + h^2}, \\ F_3 &= 2 \frac{(h^2 - x^2) \cos \theta - 2x h \sin \theta}{(x^2 + h^2)^2}, \end{aligned} \right\} \quad (2.34)$$

where  $x$  is the running coordinate with respect to the anomalous object epicenter (projections on the plan of the upper edge of the bed or HCC center);  $h$  is the depth of upper edge of the bed or the center of the dipole axis (cylinder);  $\varphi_2$  is the dip angle of the bed ( $\varphi_2 = 90^\circ$  for cylinder);  $2b$  is the bed thickness;  $S$  is the cylinder cross-section area;  $\theta = \varphi_2 - \varphi_m$ ,  $\varphi_m$  is the angle of inclination of magnetization vector to the horizon.

The value  $\varphi_{IP}$  can be found making use of the first formula from equations (2.22).

All foregoing substantiate the possibility and expediency of applying the interpretation techniques developed for magnetic prospecting under complicated physical and geological conditions, to quantitative interpretation of natural and artificial geophysical fields discussed here. This possibility was noted previously for specified cases of *IP* prospecting in [161,227].

## 2.2 Common techniques of correction for different observation heights

The effect of different heights of observation points and the techniques of its correction were first discussed by Alexeyev [5] for magnetic prospecting. The problem was further developed in the book [146]. Similar techniques were discussed for the interpretation of gravity anomalies [7]. The theoretical analysis conducted in [4,5,72,143,149] has shown that all geophysical methods under

discussion admit common techniques of the correction for inclined relief.

In essence, there are only two types of general analytical expressions applicable to the description of these geophysical fields. They are

$$U_1(x, z) = P \int_s \frac{(z_s - z) \cos \gamma_p + (x_s - x) \sin \gamma_p}{r^2} dx_s dz_s, \quad (2.35)$$

$$U_2(x, z) = P \int_s \frac{[(z_s - z)^2 - (x_s - x)^2] \cos \gamma_p + 2(x_s - x)(z_s - z) \sin \gamma_p}{r^4} dx_s dz_s, \quad (2.36)$$

where  $\gamma_p = 90^\circ - \varphi_p$ ,  $\varphi_p$  is the inclination angle of the polarization vector to the horizon,  $P$  is its value (being a scalar in a particular case); the rest of the symbols are explained in the formula (2.18).

Therefore, it seems sufficient to illustrate the manipulations taking as an example expressions (2.35) and (2.36).

The peculiarity of an inclined profile is that the height of the observation point is a linear function of the horizontal distance, namely

$$z = x \tan \omega_o, \quad (2.37)$$

where  $\omega_o$  is the inclination angle of the observation profile (Fig.2.1).

The transformations are carried out in the following sequence. The inclined coordinate system  $x' Oz'$  is introduced in such a way that

$$\begin{aligned} x &= x' \cos \omega_o - z' \sin \omega_o, \\ z &= x' \sin \omega_o - z' \cos \omega_o. \end{aligned} \quad \left. \right\} \quad (2.38)$$

The formulas for  $x_s$  and  $z_s$  are similar. The  $Ox'$ -axis in this system coincides with the inclined profile, which gives  $z' = 0$  and results in formula (2.37). In the  $x' Oz'$  system, formulas (2.35) and (2.36) are transformed to the following forms:

$$U_1(x, z) = P \int_s \frac{z'_s \cos(\gamma_p + \omega_o) + (x'_s - x') \sin(\gamma_p + \omega_o)}{r'^2} dx'_s dz'_s, \quad (2.39)$$

$$U_2(x, z) = P \int_s \frac{[z'^2_s - (x'_s - x')^2] \cos \hat{\gamma}_p + 2(x'_s - x') z'_s \sin \hat{\gamma}_p}{r'^4} dx'_s dz'_s, \quad (2.40)$$

where  $r' = [(x'_s - x')^2 + (z'_s - z')^2]^{1/2}$  and  $\hat{\gamma}_p = \gamma_p + 2\omega_o$ .

It is obvious that the right-hand sides of expressions (2.39) and (2.40) correspond to the functions  $U'_1(x', 0), U'_2(x', 0)$  in the inclined system, but for a different inclination angle of the polarization vector. If a body in the initial system was vertically polarized, it turns out to be obliquely polarized (angles  $\omega_o$  or  $2\omega_o$  respectively) in the inclined system, since the polarization vector does not intersect the  $Ox'$ -axis at a right angle.

Expressions (2.39) and (2.40) can be essentially interpreted in the inclined coordinate system making use of the techniques developed for the horizontal profile, since the changing heights of observation points are not included there. To interpret in the initial system, we have to continue our manipulations in the following sequence.

The entire space with the anomalous object and the polarization vector is turned by the angle  $\omega_o$  and compressed at the compressibility coefficient of  $\cos \omega_o$ . In addition, when manipulating with formula (2.39),  $P$  is multiplied by  $\sec \omega_o$ . This done, the inclined profile  $Ox'$  coincides with the horizontal straight line, and the observation points on the profile pass along the vertical into the corresponding points on the horizontal straight line. An anomaly plot, constructed by these points (in horizontal projection) is a standard plot used routinely, although observations are made on an inclined relief. However, after the space rotation and compression the anomalous object occupies a different position with respect to the initial one. Its cross-section is smaller than the initial one, but the outline is similar.

After this transformation, formulas (2.39) and (2.40) acquire the following forms:

$$U_1(x, z) = U_{1f}(x, 0) = \\ = P_f \int_{sf} \frac{z_{sf} \cos(\gamma_p + \omega_o)(x_{sf} - x) \sin(\gamma_p + \omega_o)}{r_f^2} dx_{sf} dz_{sf}, \quad (2.41)$$

$$U_2(x, z) = U_{2f}(x, 0) = \\ = P_f \int_{sf} \frac{[z_{sf}^2 - (x_{sf} - x)^2] \cos \hat{\gamma}_p + 2(x_{sf} - x) z_{sf} \sin \hat{\gamma}_p}{r_f^4} dx_{sf} dz_{sf}. \quad (2.42)$$

Here, the subscript “*f*” stands for the parameters of a fictitious body. When used with symbols  $U_1$  and  $U_2$ , it denotes that they refer to a fictitious body.

The interpretation of the curves  $U_{1f}$  and  $U_{2f}$  results in obtaining parameters of a fictitious body, which are used to reconstruct those of a real body (denoted by “*s*” subscript) with the help of the following formulas of transition:

$$\left. \begin{array}{l} z_s = z_{sf} + x_{sf} \tan \omega_o; \\ x_s = -x_{sf} \tan \omega_o + x_{sf}; \\ S = S_{sf} \sec^2 \omega_o; \\ P = P_f \cos \omega_o \text{ (in the interpretation of } U_1); \\ P = P_f \text{ (in the interpretation of } U_2); \\ \gamma_p = \gamma_{pf} - \omega_o \text{ (in the interpretation of } U_1); \\ \gamma_p = \gamma_{pf} - 2\omega_o \text{ (in the interpretation of } U_2). \end{array} \right\} \quad (2.43)$$

Let us consider the analytical expression of the gravity anomaly caused by a certain anomalous body:

$$\Delta g = 2G\sigma \int_s \frac{(z_s - z) \cos \gamma_g + (x_s - x) \sin \gamma_g}{r^2} ds, \quad (2.44)$$

where the value  $\gamma_g$  is an analogue of the value  $\gamma_p$  in the equation (2.35).

This formula does not differ from the expression (2.35) by its structure. After the above manipulations it has the following form:

$$\Delta g_f = 2G\sigma_f \int_{sf} \frac{r_{gf} \cos \gamma_{gf} + (x_{sf} - x) \sin \gamma_{gf}}{r_f^2} ds_f, \quad (2.45)$$

such that

$$\gamma_{gf} = \gamma_g + \omega_o. \quad (2.46)$$

Taking into account that  $\gamma_g = 0$ , we obtain  $\gamma_{gf} = \omega_o$ . Hence, the anomaly of  $\Delta g$  observed on the inclined relief corresponds to that caused by a fictitious obliquely polarized body observed on the horizontal relief. The latter is affected both by vertical and horizontal gravity components. This is equivalent to the manifestation of “vectorial properties” of density on the inclined relief (see Fig.2.1).

On the whole, the effect of the profile inclination is equivalent to an increased effect of oblique polarization, if the vector  $\mathbf{P}$  and the

relief have the same sense of slope, and to a weakened effect, if the relief and the vector  $\mathbf{P}$  are inclined in opposite senses, up to their mutual neutralization. This fact determines the unified techniques for interpreting obliquely polarized bodies observed on the inclined relief. It facilitates the analysis of the distortions due to the effect of sloping relief, which can be completely attributed to the oblique polarization effect.

Thus, formulas (2.41) and (2.42) reduce the problem of interpretation of the potential fields observed on the inclined profile to the same problem for the horizontal profile. Formulas (2.43) describe the transition from the parameters obtained while interpreting a fictitious body to those of a real body.

The above data substantiate the conversion in the inclined semi-space, since a field observed on the complex relief can be expressed using a certain inclined system of coordinates, the reduction being accomplished as in the normal system. The field in the observation points of the relief is converted to an inclined straight line along the normal to the latter.

The advantage of such reduction consists in that the inclined plane of the reduction may be selected as close as possible not only to the highest points, but also to many points of the relief (Fig.2.2). As a result, the amplitude decreases appreciably less than when converting to the horizontal level of the highest relief points.

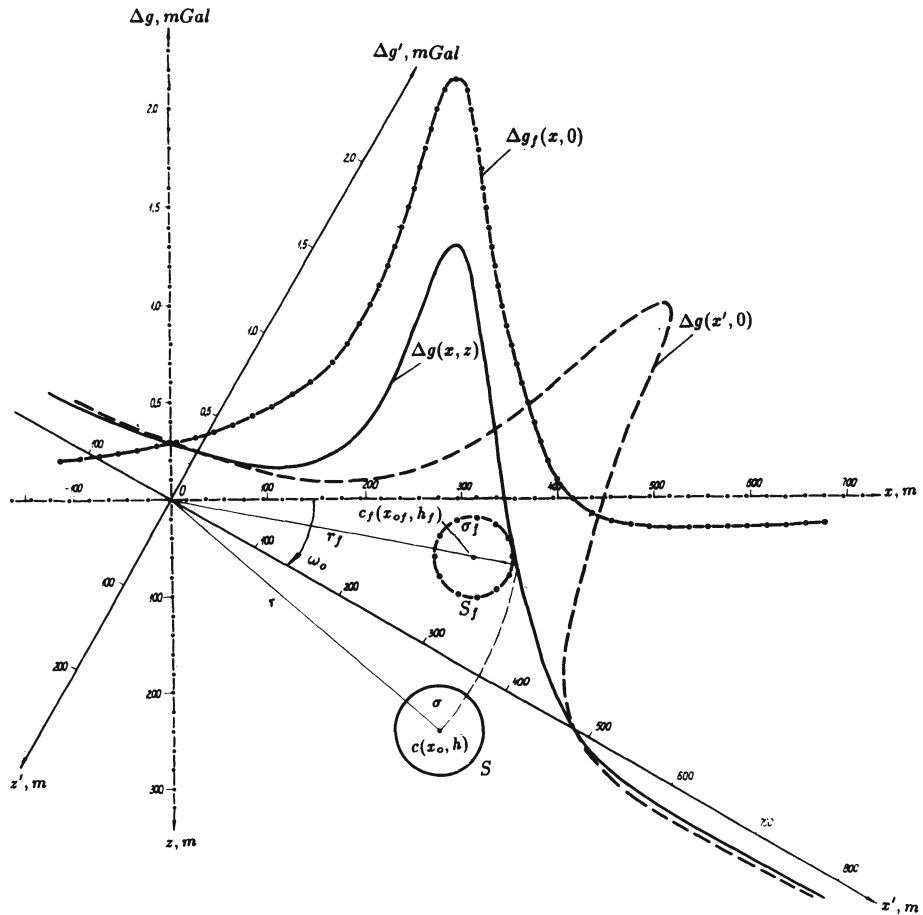
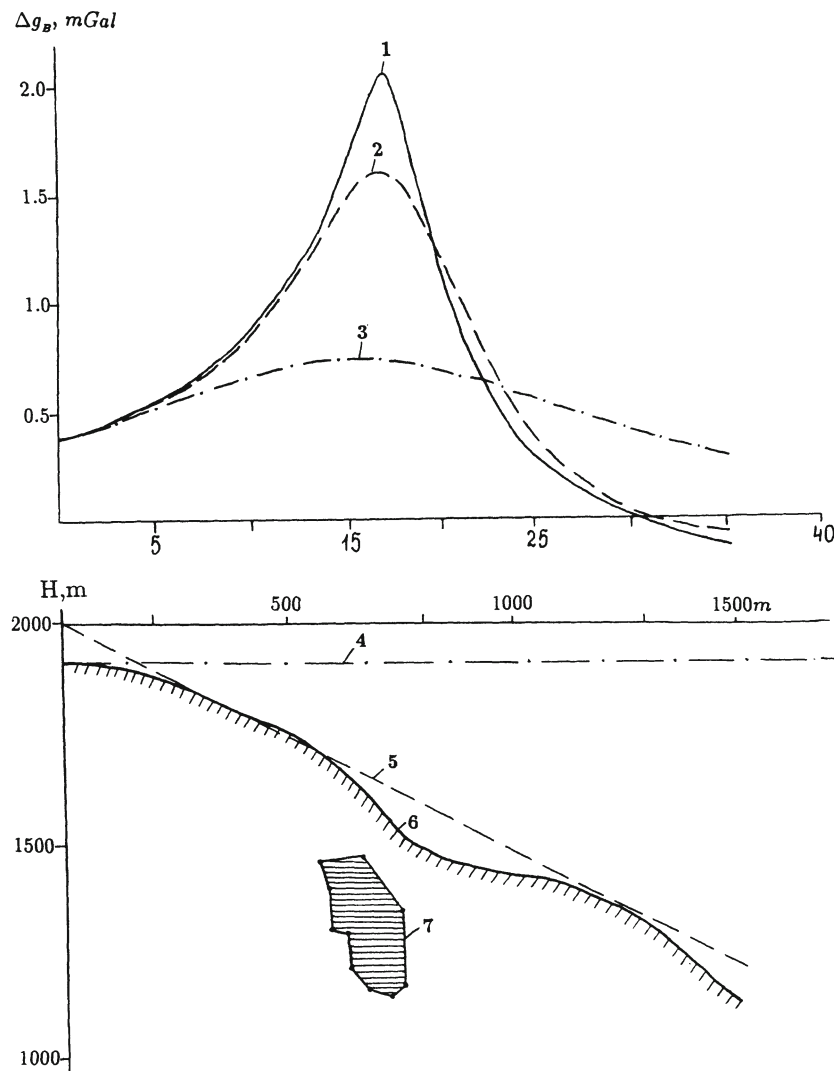


Fig. 2.1. On the interpretation of gravimetric observations for an inclined profile



**Fig. 2.2. Reduction of geophysical fields in the inclined semispace**

(1) effect of anomalous body 7 on uneven observation surface 6; (2) effect of anomalous body after reducing to inclined line 5; (3) effect of anomalous body after reducing to the horizontal level 4 of the highest relief points

## **Chapter 3**

### **INFORMATIONAL CONTENT AND STRUCTURE OF THE INTERPRETATION PROCESS**

The most important stage of interpretation is to formulate what kind of new information has to be derived from experimental data. However, geological interpretation of the observed field is not always possible, since either it does not contain the necessary information for solving a particular geological problem, or there are no methods (at least for the present) for extracting this information. Therefore, a geological problem should comply with: (1) measuring capabilities of the geophysical method selected, its applicability for measuring the field containing the information required; (2) properties of the medium under study, its capability to generate detectable signals (anomalies); (3) methods for data processing and interpretation, namely, their ability to extract information from the measured field containing the effects of the sought-for geological objects. A geological problem is considered to be well defined and solvable, when all the three conditions are satisfied.

Since the solution of geological problems calls for integration of different geophysical methods, the said aspects (measuring, petrophysical-morphological and interpretation) should be expressed in terms of the entire set. Only after that particular problems solvable by each method can be formulated.

At a specified accuracy of geophysical methods and characteristics of the objects, technique of integrated interpretation is of primary importance for developing a set of methods. The same refers to obtaining particular information from the separate method

results and to the formulation of requirements to this particular information. The particular information can be obtained in terms of physical sources corresponding to various classes of geological objects. The integrated interpretation providing intersection of classes, makes it possible to single out one or several geological targets, which form a solution of the geological objective sought for. In some cases only the comparison of fields measured by various geophysical methods of a set leads to an informational jump [64], which results in singling out the objects of search.

The presence of an object of the desired class may be substantiated by estimating the amount of the corresponding information contained in observations [267]. These estimations are especially convenient for integrated interpretation, as they provide a means for operating on the data obtained by various methods and expressed in common (informational) unit. The target is singled out by maximum information obtained making use of a set of methods.

The language of the information theory [245] is the best to express the essence of geological and geophysical investigations, i.e. of the process of acquisition and processing the information. The informational approach to geophysical data interpretation was suggested by Khalfin [128]. It had been developed in Moscow Geological Prospecting Institute [276], St.Petersburg Mining Institute (I.G.Klushin) and Institute of Exploration Geophysics (N.N.Borovko). Informational units were used by Khesin [131,133] for developing the methods of detecting ore controls and orebodies by one or several geophysical fields distorted by noises. Shannon's information unit ( $1bit = \log_2$ ) gives a well-defined "yes – no" answer as to the presence of one or another indicator (geophysical field anomaly), or its gradation. Therefore, in spite of the probabilistic calculus of the amount of information, the informational approach to the said problem introduces deterministic features. Here, the logical character of a number of interpretation methods based on information-statistical (logical-statistical) approach, becomes apparent. Besides, this approach includes such probabilistic methods as correlation, filtering and statistical decision-making, which are widely accepted for data processing and interpretation.

Geophysical data processing is mainly intended to reduce and eliminate noises. The main task of the qualitative interpretation

is to single out an object of the desired class, while that of the quantitative interpretation is to determine and refine parameters of the object. The solutions of these problems are closely interwoven and based on model conceptions of the interpreter (Fig. 3.1).

The classifying character of a number of problems may be demonstrated. Their solution is based on the image identification (pattern recognition) methods developed in cybernetics. The optimization of identification by statistical criterion of the minimum average risk and that of maximum information yields similar results under certain conditions [222]. Apart from the generality of statistical and informational treatments, the equivalence of the methods of maximum posteriori probability and Tikhonov's regularization [282] has been observed for certain conditions [179]. Thus, numerous methods set forth below are specific expressions of unified logical-statistical approach to the processing and interpretation of geophysical data.

The majority of specialists mention a conventional character of the notions of qualitative and quantitative interpretation. From the standpoint of the analogy and modeling theory [23,163], there are different levels of inference by analogy. The intuitive analogy is predominantly used in qualitative interpretation when a body of empirical facts is considered from the point of view of qualitative relations. The use of the *empirical field/geological object* relationship, obtained by summarizing the previous experience, makes it possible to relate the experimental field to the geological structure of the area under study and to come to new conclusions concerning its structural features. The new information thus obtained is immediately described in geological terms. When the amount of prior information is sufficient, qualitative relations can be expressed in the quantitative (statistical) form. In quantitative interpretation a model analogy is usually employed, i.e. the information obtained from a model study is carried over to the area under investigation.

The most complete description of the interpretative process structure is given by Strakhov [261]. An interpretation process may be roughly subdivided into the following stages: (1) summarizing prior information; (2) sequential analysis and (3) geological synthesis.

The contents of each stage depend on the objective, geological,

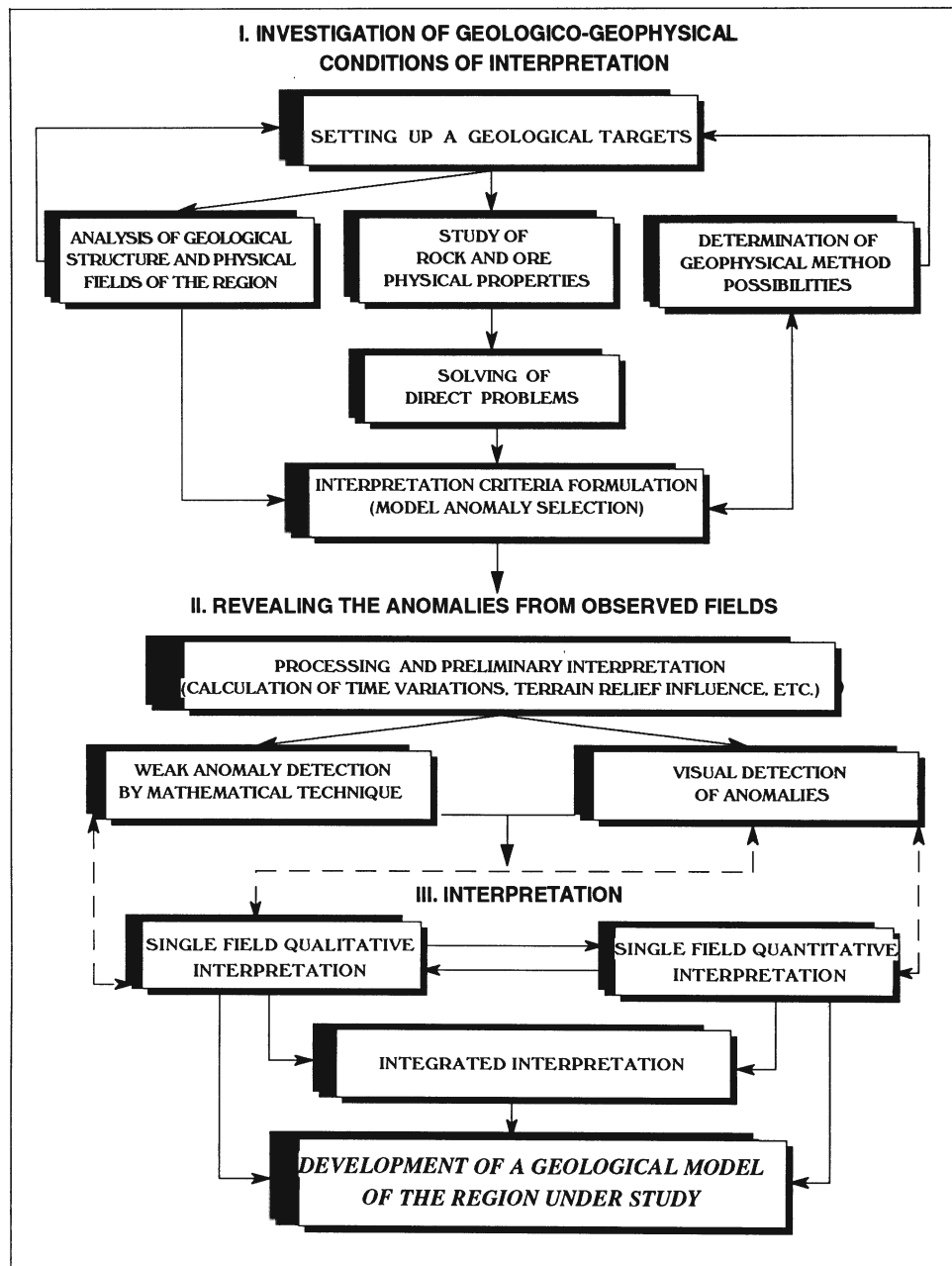


Fig.3.1. Processing and interpretation of geophysical data.  
Schematic diagram

geographical and other conditions of the area under study, state of its exploration, level of the development of the techniques applied for extracting information from experimental observations. All these factors are interrelated; as a result, interpretation is accomplished according to the *problem – model – procedure (interpretation)* principle. But it is impossible to provide an interpreter with a definite set of actions for each stage of interpretation suitable for any combination of the above factors in different regions. However, it is possible to classify these factors for typical conditions and, as a result, to work out a common approach to the interpretation sequence.

Obviously, there are no exhaustive receipts of synthesis available, since it involves nonformalized practice. Nevertheless, we can single out some major elements which are of the same type under similar conditions. For each geophysical method, the procedure used for interpreting the materials of integrated geophysical investigations (interpretation system) includes the following steps or stages:

- (1) development of the initial model of the medium;
- (2) indicator space generation by the results of observations;
- (3) revealing and localization of the sought-for objects;
- (4) determination of quantitative parameters of anomalous objects;
- (5) graphic representation of the interpretation results; revision of the model of the medium;
- (6) drawing up a geological report on the basis of interpretation results;
- (7) general estimation of the interpretation reliability.

Estimation of the interpretation reliability is very important and is carried out at several stages. Here we highlight only the final stage of the general reliability assessment. All steps of the procedure are of primary importance and interrelated. Steps 2 to 5 are partially automated.

There is a feedback between the steps. For example, after obtaining quantitative parameters of the object under study, there often appears a need to revise the initial model of the medium using additional prior information or application of other methods

to interpret the data available. Then steps 2 to 4 are repeated on the basis of revised model. Thus, in fact, step 5 is repeated many times.

Prior to the interpretation, it is necessary to make sure that the accuracy of measurements of field, Cartesian coordinates and heights of the observation points, quantity and quality of accompanying observations (geological routes, physical properties determination) correspond to the requirements of the geophysical project. It should be noted that under different conditions the successiveness of interpretation procedures may be changed.

## **Chapter 4**

### **DEVELOPMENT OF THE INITIAL MODEL OF THE MEDIUM**

An initial model is devised in one or another form to solve the geological objective when preparing a geophysical project for the given area. Otherwise, it is impossible to select a set of methods and interpretation procedure. The latter is revised before interpreting, if necessary. The initial development of a model of the medium is the most important stage, since the results of interpretation and of the investigation at large depend to a considerable degree upon its quality.

Any model must comply with two conflicting requirements, i.e. (a) reflect the essential features (indicators) of the object for modeling and (b) be sufficiently simple to use.

By a model of the medium we mean integrated and, as far as possible, formalized geological and geophysical data concerning the target and host rocks [164,197]. Hence, a model of the medium is classified among informational symbolic models. The background of the object's manifestation is no less important than the object itself and should be also considered in the model in detail. The model detail should correspond to the scale of investigation. Besides, various noise effects should be taken into account in the model.

In many cases characteristics of geological media for open (one-stage) regions testifies to the expediency of employing their stochastic models. However, when analyzing the observed geophysical fields as random functions, it is necessary to take into account that they may contain regular components of impulse or periodic nature. If we discard the tasks involving area mapping by statistical character-

istics of the field, which, as a whole, is considered as random, then a large group of the most important geological problems remains. They are based on the extraction of a regular component from its mixture with noises. This component may correspond to magnetized gabbroid or low-magnetic acid intrusions, a zone of hydrothermal alterations, skarn-magnetite or pyrrhotite containing lens, etc.

The desired regular component can not be revealed without certain model ideas. Such targets as large ore bodies are usually rare, and it is always a problem to obtain their statistical characteristics. This has generated a need for developing a special system of processing and interpretation of the results of geophysical investigations. Such a system makes it possible to extract the desired anomalies from a mixture of anomalies and noises on the basis of a deterministic approach to the object under study (desired anomaly) and probabilistic approach to all the rest of salient features of the medium and geophysical observations regarded as noises.

The deterministic study of geophysical targets, as follows from section 1.2, is facilitated by the possibility of confining geometrical approximations of the objects belonging to the main classes under investigation (see Table 1.1).

#### **4.1 Initial data sources; Petrophysical support of the interpretation**

The sources used for devising a model of the medium include geological data, materials of the physical property study, geophysical observations obtained in adjacent areas and results of solving problems of the same type under similar conditions.

When studying geological descriptions and graphic materials obtained in the region under examination and in other areas containing the objects of the desired class, it is necessary to single out the key geological factors, which define the geological pattern. The model must take account of all these factors. Any well-explored geological object related to the target (structure-facies zone, tectonic block, structure, ore field, orebody, etc.) may serve as a model for the object under investigation. As a result of geological data examination, we get a concrete idea of the possible classes of objects

occurring in the area under study, their geometry, composition and relation with host rocks.

Due to the integrated approach to the conducted investigation and interpretation, the materials of physical properties study are used for developing an integrated petrophysical model of the medium. As an example, it is sufficient to describe a process of compiling a petromagnetic model, which is analogous with the use of data on other physical properties for a similar purpose.

If in open areas the petromagnetic study is conducted parallel to the magnetic survey on the same scale, and petromagnetic map is drawn up, the latter represents a petromagnetic model of the surface area under investigation [111]. A need for constructing several petromagnetic sections presents no problems in this case. Of great importance are petromagnetic data obtained from core samples and deep mines, since they are not distorted by near-surface alterations. Determination of magnetic properties by correlating the observed field with the known geological section deserves special attention.

When no petromagnetic data are available for the area under investigation (which has to be an exception to the rule in future), one can use the data on magnetic properties of similar rocks in adjacent areas, and on objects analogous with the target, including those obtained from interpretation results. Naturally, the quality of a petromagnetic model in this case will be markedly lower. This may affect the quality of interpretation and the progress in solving the problem at large.

A petromagnetic model of a medium must yield the magnetic characteristic of all the rocks and their varieties occurring in the region. All stratified rock masses and compact geological bodies (including mineral deposits) should have corresponding average values of magnetic parameters with confidence limits. The same applies to the zones of altered rocks. Magnetic characteristics of the geological objects which do not outcrop onto the area under exploration, but are possible at a certain depth and known as occurring in adjacent areas, should not be ignored as well. When geophysical data obtained in neighboring or similar areas are employed, a model of the medium used for defining deeper portions of the section in the area under investigation (even on a smaller scale), and the intensity and shape of magnetic anomalies over the objects similar to those

sought for.

To develop a petromagnetic model, it is expedient to compute the total magnetization of the individual structural-material associations by the available geological classification. However, if the classification does not conform to the results of the analysis of petro- and paleomagnetic data on the section, it is necessary to devise a model according to petromagnetic features. In this case, the weighted average magnetization is calculated for certain rock complexes united by the magnetic property values or by the magnetization direction (within the same paleomagnetic zone). The explosive index of magmatic rocks, i.e. pyroclast percentage, may be of use when computing the weighted average values of their total magnetization, since pyroclastic rocks are characterized by lower magnetic susceptibility  $\kappa$  and natural remanent magnetization  $I_n$ , as compared to the lavas.

When dealing with oblique magnetization, it is mostly important to determine the direction of magnetization: the intensity and, especially, type of anomaly depend critically on the inclination angle of the object's redundant magnetization.

Alexeyev [5] examined magnetization of an arbitrary triaxial ellipsoid in the Earth's magnetic field  $T_o$ . Under certain simplifications, the limiting cases for this body are vertical bed, thick horizontal bed and horizontal circular cylinder. The above bodies having sufficiently high magnetic susceptibility are magnetized almost in parallel to the active field. The angular error is less than  $1.5^\circ$  at  $\kappa = 0.05 \text{ SI unit}$  and less than  $3^\circ$  at  $\kappa = 0.1 \text{ SI unit}$ .

Therefore, we can assume that for all examined values and any shape of a body, a vector equality for induced magnetization ( $I_i$ ) is valid:

$$I_i = \kappa T_o. \quad (4.1)$$

Note that for higher values of magnetic susceptibility ( $\kappa > 0.08 - 0.10 \text{ SI unit}$ ) the vector  $I_i$  is not parallel to the vector  $T_o$ . As generally known, a sphere is magnetized in parallel with the active field independently of the magnetic susceptibility value.

When analyzing magnetic properties, it is a common practice to admit only the induced magnetization  $I_i$ , whereas the remanent one  $I_n$  is assumed to be comparatively small. In this case it is sufficient

to have information on magnetic susceptibility of host rocks and desired objects. However, in contrast to the current opinion, the presence of remanent magnetization is often a general rule, rather than exception to the rule [2,120,146], especially for volcanogenic and intrusive rocks. Here it may take on a higher value and a direction different from that of the modern geomagnetic field. The remanent magnetization is added to the induced magnetization.

With the advent of induction susceptibility meters (kappameters), magnetic susceptibility became easy to measure. These measurements were introduced into the common practice. Remanent magnetization became the subject of paleomagnetic investigations. The aims, objects and character of presenting the results of these investigations do not comply with the requirements of magnetic prospecting involving the value and the direction of the total vector

$$\mathbf{I} = \mathbf{I}_i + \mathbf{I}_n. \quad (4.2)$$

Here  $\mathbf{I}_n$  is the natural remanent magnetization (*NRM*). Interestingly, many papers describing the results of paleomagnetic investigations do not present any data on *NRM*.

As paleomagnetic experience has shown, scattering is typical of the initial directions of  $\mathbf{I}_n$ , i.e. directions of *NRM* on a stereoprojection. They are often scattered over the whole field of stereoprojection, and sometimes reverse orientations occur. After eliminating unstable components of remanent magnetization by various ways (such as demagnetization, thermomagnetic cleaning) the directions came together to certain rather narrow area of the stereoprojection. The average direction defines the orientation of the ancient magnetic field in the rock formation period, which is different from the modern field  $\mathbf{T}_o$ .

However, the chaotic behavior of the initial directions of  $\mathbf{I}_n$  allows us to expect that the average total magnetization defined from formula (4.2), will not appreciably deviate from the direction of  $\mathbf{T}_o$  by virtue of direction averaging. This supposition was confirmed by the paleomagnetic investigation in the Kedabek district of the Lesser Caucasus [146]. In the course of this study, the initial materials were processed using formula (4.2) for 600 samples of volcanogenic and intrusive rocks of acid to basic composition from the Middle and Upper Jurassic, which are the primary sources of

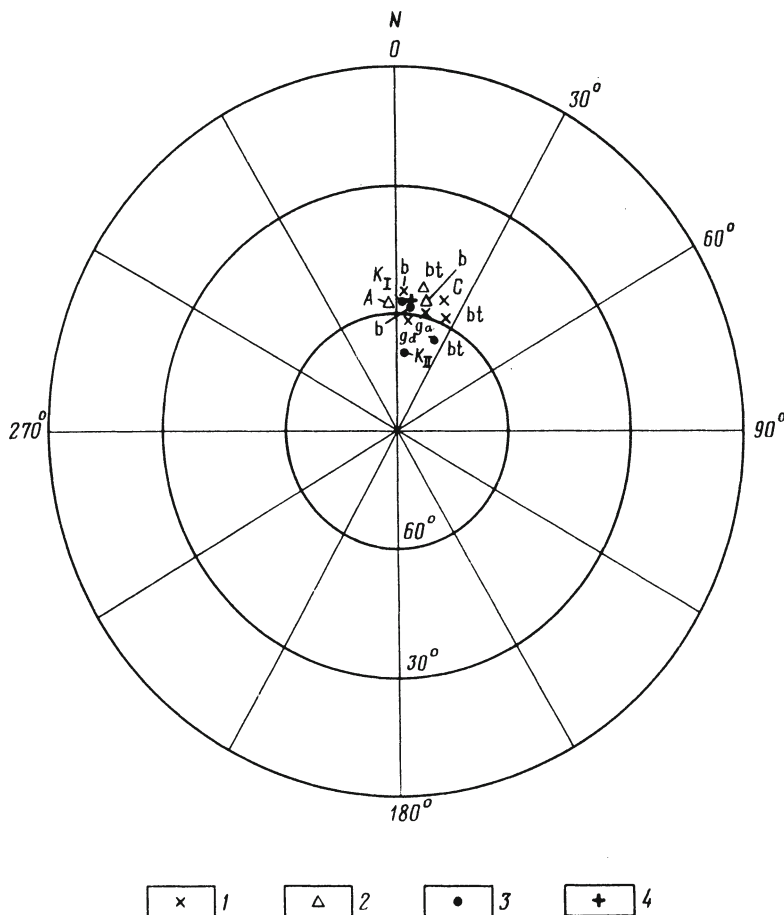


**Fig. 4.1. Stereoprojections of average directions of magnetization  $\mathbf{I} = \mathbf{I}_i + \mathbf{I}_n$  for volcaniclastic and intrusive rocks of the Kedabek district of the Lesser Caucasus**

Directions of rocks magnetization at the following values of  $I$ , A/m: (1)  $< 0.2$  ( $< 200 \cdot 10^{-6} \text{ cgs}$ ), (2)  $0.2 \div 1.0$  ( $200 \div 1000 \cdot 10^{-6} \text{ cgs}$ ), (3)  $> 1.0$  ( $> 1000 \cdot 10^{-6} \text{ cgs}$ ) (4) direction of the modern geomagnetic field.  $b$  and  $bt$  are effusive and pyroclastic rocks of the Bajocian and Bathonian ages, respectively;  $C$  are the plagiogranites of Slavyansky intrusion;  $K_I$  are the gabbro and gabbro-diorites of I phase of Kedabek intrusion;  $K_{II}$  are the diorites and quartz-diorites of II phase;  $A$  are the quartz-diorites and diorites of Aitaly intrusion;  $g_d$  and  $g_a$  are granodiorites and grano-aplites of sheet intrusions, respectively

anomalies in the region (Fig.4.1). The total vector of magnetization  $\mathbf{I}$ , in spite of chaotic character and the presence of reverse directions of  $\mathbf{I}_n$ , lies nearly in parallel with the modern geomagnetic field  $\mathbf{T}_o$  (average deviation being  $5^\circ$  for declination, and  $1^\circ$  for inclination). Similar calculations employing paleomagnetic data for magmatic rocks of the Mesozoic and Paleogene within the area of the whole Somkhit-Agdam region (Lesser Caucasus), Kedabek district being a part of it, give similar results. The magnetization of acid and basic intrusives along the field  $\mathbf{T}_o$  is confirmed in literature [67]. This is probably a general postulate. It is confirmed by the experience of many years obtained from the magnetite deposits study in the Krasnoyarsk area of the Altai-Sayan orogen (B.M.Afanasiev, private communication). Then the inclination angle of magnetization may be regarded as a fixed parameter for the interpretation under the condition of oblique magnetization.

Investigators should make sure that the condition

$$\mathbf{I} \parallel \mathbf{T}_o \quad (4.3)$$

is met for typical rocks in each region subjected to magnetic survey. If the condition is not fulfilled, it is necessary to study not only the magnetic susceptibility, but also the *NRM* vector.

The total magnetization direction can be estimated if we know the factor  $Q = \mathbf{I}_n / \mathbf{I}_i$  and rough direction of  $\mathbf{I}_n$ . Next, making use of formula (4.2), it is easy to obtain the expression:

$$\tau = \arctan [(Q \sin \nu) / (1 + Q \cos \nu)], \quad (4.4)$$

where  $\nu$  is the angle between the vector  $\mathbf{I}_n$  and the vector  $\mathbf{T}_o$ ,  $\tau$  is the angle between the vector  $\mathbf{I}$  and the vector  $\mathbf{T}_o$ .

To determine the angle  $\tau$ , we have plotted a nomograph (Fig.4.2) for values  $\nu = 0 \div 30^\circ$  ( $\mathbf{I}_n$  and  $\mathbf{T}_o$  being roughly parallel) and for  $\nu = 150 \div 180^\circ$  ( $\mathbf{I}_n$  and  $\mathbf{T}_o$  being roughly antiparallel). In this situation, the direction of  $\mathbf{I}_n$  does not fall outside the cone around  $\mathbf{T}_o$  with the angle of  $30^\circ$ . From the nomograph it follows that in the first case the direction of the total vector ( $\mathbf{I}$ ) is within the cone with a more acute angle ( $\tau < \nu$ ) for any values of  $Q$ ; the lower is the  $Q$  factor, the smaller is the angle. In the second case antiparallelism holds for higher values of  $Q$ , whereas for smaller ones  $\mathbf{I}$  is roughly parallel to the vector  $\mathbf{T}_o$ . The most unfavorable situation is at

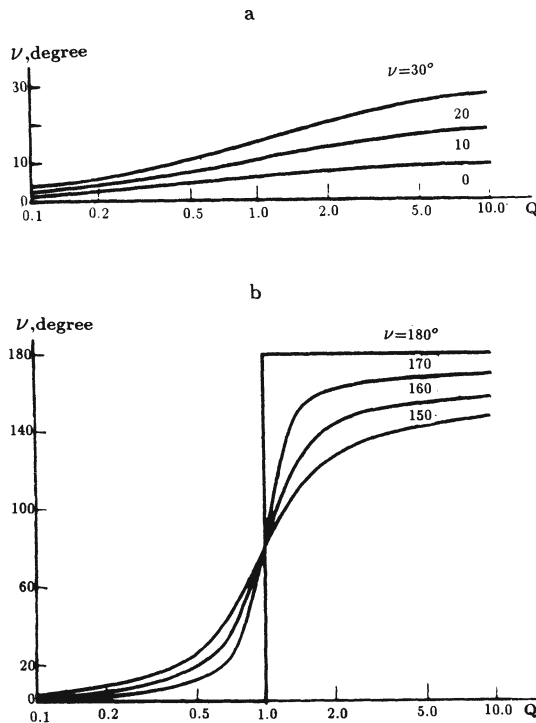


Fig.4.2. Nomograph for determining the deflection angle  $\tau$  of the magnetization vector  $\mathbf{I}$  from the geomagnetic field vector  $\mathbf{T}_0$  by a known angle  $\nu$  between  $\mathbf{I}_n$  and  $\mathbf{T}_0$  vectors, and the  $Q$  factor: (a)  $0^\circ \leq \nu \leq 30^\circ$ ; (b)  $150^\circ \leq \nu \leq 180^\circ$

$Q = 0.7 \div 1.5$ , when the direction of vector  $\mathbf{I}$  is markedly different from the  $\mathbf{T}_0$  direction. For the rocks characterized by such  $Q$  values and a reversed polarity of vector  $\mathbf{I}_n$ , the total vector is calculated by formula (4.2). For the first and second cases, it can be computed using a simple approximate formula

$$\mathbf{I} = \mathbf{I}_i(1 \pm Q) = \kappa \mathbf{T}_0(1 \pm Q). \quad (4.5)$$

Positive sign is taken for parallel vectors  $\mathbf{I}_n$  and  $\mathbf{T}_0$ , and negative sign when they are antiparallel.

Analysis of magnetic survey results and computation of direct magnetic effects call for operating on the local anomalous object's redundant magnetization with respect to host medium. In contrast

to excess density, redundant magnetization is a vector quantity, and in order to find it the investigator has to know all the components of magnetization vectors for both the local bodies and the host medium. If magnetization vectors of the body and the medium (of two adjacent objects) are parallel, in particular, if the condition (4.3) is fulfilled, then the redundant magnetization modulus is a simple difference in absolute values of these vectors, and its direction is parallel to the direction of initial vectors. When magnetization vectors for the body and the medium are not parallel, it is necessary to compute the redundant magnetization components.

The *NRM* direction in rocks depends on the influence of quite a number of components, which were formed during different geological time intervals. They can be altered as a result of some physical and chemical processes. Therefore, one should be rather careful when selecting the magnetization direction as a fixed parameter for the interpretation, and substantiate it on a statistically significant sampling. Constancy of the magnetization direction (accurate up to  $20^\circ$ ) must be satisfied not only for the objects of search, but also for the host rocks. The above selection is easy due to the fact that induced magnetization has a constant direction, and *NRM*, when measured on rock samples, varies randomly with respect to a certain average value. Therefore, the direction of their average sum, especially if  $Q < 1$ , will be close to that of the present geomagnetic field in the area under investigation.

The procedures of determining the density  $\sigma$ , resistivity  $\rho$ , polarizability  $\eta$  and other physical properties of non-vector nature are generally analogous with the above mentioned procedures of obtaining petromagnetic data, but they are simpler. Note once more that the complexity of terrain relief may be of use for determining such an important feature as effective density of the medium under study. This forms the basis for a well-known method of Nettleton [206], in which the Bouguer anomalies are calculated for different intermediate layer densities. The curve which is the least correlated with the relief profile corresponds to the mean density of rocks in the upper portion of the section. Various methods for determining the density with due regard to mountainous conditions are described by Parasnis [218], Berezkin [28], Varlamov [290], and as for other physical properties, they are described in [131] and other works, including reference books [212,274]. Density can be also determined

making use of the gravimetric measurements multiplication method. It involves a group of additional measurement points located around a point of the network [8].

The possibility of determining the density by the results of measurements at different levels of horizontal mines (adits, drifts) and by borehole gravimetric measurements is also worth mentioning [293].

As to electric parameters, the results of parametric measurements at outcrops (*in situ*) and electric sounding in the investigated sections are the most useful for their estimation.

In many cases, it is advisable not to estimate physical properties by their correlation with others. When dealing with rapidly changing rocks of various composition in mountainous regions, the correlation coefficient, say, between the velocity and density for intrusive and volcanogenic rocks on the Lesser Caucasus varies from  $0.1 \div 0.2$  to 0.5, i.e. the correlation is negligible [55]. This is connected with a pronounced porosity of igneous associations.

The correlation between physical properties of metamorphic rocks also breaks. For instance, ultrabasic rocks serpentinization leads to a sharp increase in their magnetization and to a simultaneous decrease in their density. Generally, it is not worthwhile to compute the density according to the density/velocity correlation for regions abundant with igneous and metamorphic rocks. The computation of gravitational field by such a density model will be effective in case of sediment section, where this correlation is reliable enough.

To determine physical properties, it is necessary to take into consideration the position of the sampling interval (see Fig.1.5), sufficient representability of the sample and of the number of measurements for statistical processing and obtaining stable results. For instance, according to Kotlyarevsky, who investigated 20 intrusive massifs in Uzbekistan, the effective magnetization obtained by aeromagnetic prospecting is in agreement with the magnetization determined by at least 200 samples [132].

Statistical processing makes it possible to determine the uniformity of data sample; to conduct, if necessary, additional petrophysical differentiation or, on the contrary, to unite certain sub-

associations and associations according to their physical properties [86,87,111,112]. The average characteristics (arithmetic average for a normal distribution and geometric average for a lognormal one) and their confidence intervals are selected on the basis of testing the hypotheses concerning distribution laws. The weighted values of physical properties thus obtained can be attributed to the corresponding geological associations or structural-material complexes, their distribution being refined later by physico-geological modeling [288]. Table 4.1 exemplifies this type of a model.

**Table 4.1. Summarized physico-geological model  
of iron deposits of Angara-Ilim type [22,288]**

OBJECTS	GEOMETRY OF PARTICULAR MODELS (OBJECTS OF MODELING)	PHYSICAL PARAMETERS			
		$\bar{\kappa} \cdot \varepsilon$ , SI units	$\bar{I} \cdot \varepsilon$ , A/m	$\bar{\sigma} \pm S$ , g/cm <sup>3</sup>	$\bar{\rho} \cdot \varepsilon$ , Ohm · m
Main economic deposits	Vertical elliptical cylinder (diatreme filled with breccia, tuffs, skarns and various ores)	$0.05 \cdot 3.5^{\pm 1}$	$200 \cdot 1.7^{\pm 1}$	$2.60 \pm 0.15$	$150 \cdot 1.7^{\pm 1}$
	Massive steeply dipping magnetite beds	$0.75 \cdot 1.5^{\pm 1}$	$1000 \cdot 1.6^{\pm 1}$	$4.00 \pm 0.10$	$40 \cdot 1.3^{\pm 1}$
	Four-layer model of horizontal beds (from the top): (1) tuffaceous-sedimentary rocks; (2) trapps; (3) subhorizontal orebodies; (4) tuffaceous-sedimentary rocks	$\kappa_1 < \kappa_2 \leq \kappa_3 \geq \kappa_4$ , $\kappa_1 = \kappa_4 \approx 0$	data absent	$\sigma_1 < \sigma_2 < \sigma_3 \geq \sigma_4$ , $\sigma_1 = \sigma_4$	$\rho_1 < \rho_2 < \rho_3 \geq \rho_4$ , $\rho_1 = \rho_4$
Host rocks	Tuffaceous-sedimentary rocks of platform cover	0	0	$2.30 \pm 0.07$	$200 \cdot 5^{\pm 1}$
	Trapps	$0.05 \cdot 3^{\pm 1}$	$20 \cdot 2^{\pm 1}$	$2.90 \pm 0.10$	$2000 \cdot 1.5^{\pm 1}$
Note: $\varepsilon$ is a standard multiplier; $S$ is standard deviation					

## 4.2 Indicators of targets and interpretation criteria

When developing a model of a medium, the most important thing is to compute anomalous effects from the objects of various classes against the background of a host medium field (or to apply suitable data available in literature) and to compare them with observed anomalies from similar objects. Comparison of the results allows to correct a model and to determine the criteria of singling out the targets. The criterion is a certain quantitative indicator (such as field value, dissection, gradient, etc.) exceeding the critical level only in presence of the target.

Effects caused by the targets are often weak under complicated conditions and, therefore, one has to use feeble criteria. Hence, the probability of misinterpretation (i.e., missing the target or erroneous conclusion as to its presence) increases. Due to the integrated approach to geophysical study, the risk of making a wrong decision can be considerably reduced. For example, if a weak anomaly<sup>1</sup> is detected using three points, and the mean square of the anomaly in each method is equal to the noise dispersion, then the interpretation reliability for separate methods amounts to 0.61 and for the set of three methods it reaches 0.87 [135].

The use of indirect indicators, i.e. the effects caused not by the objects proper (for example, ore bodies), but by larger geologic bodies (ore-controlling structures, etc.) which are spatially or genetically related to them (see Table 1.1), also reduces the interpretation error. And, finally, of major importance are secondary indicators, i.e. derived quantities [41], such as various initial field transforms, and their combinations (smoothed values of a field, its variability, predominant strike of isolines, etc.). If many cases the secondary indicators are far more important than the initial observed field. It is a common knowledge, in particular, that a rare combination of many features is a salient characteristic of large deposits and their significant secondary indicator.

However, too large amount of indicators is a negative factor

---

<sup>1</sup>Weak anomaly is a relative notion. Under very strong noises typical of open areas the desired anomaly may have a large amplitude, but is considered to be weak, since it has to be separated from the noise field background of the same intensity.

which affects both labor input and effectiveness of interpretation. As noted by Duda and Hart [66], the increased number of indicators adds to the requirements to the volume of standard information, while a great number of standards of the same type is available only in well-explored provinces where quantitative prediction is, apparently, less urgent than in insufficiently studied areas. Minor and non-economic objects may dominate among standard ones, and therefore, the prediction may result in revealing only similar deposits [40]. Indicators of large and unique deposits, which are the main goal of prospecting, in this case, may differ from standards.

At the same time, there are cases where the number of indicators or standards reaches one hundred or over. This is the reason why the selection of the most essential features is a very important stage of developing a model of the medium. In this situation, after critical analysis, the geophysical experience in solving similar problems under similar conditions is mainly employed. It is worth mentioning that, as a rule, only few methods are integrated in practice; nevertheless, positive results of the integration are well-known [30,44,132,219]. As shown in Section 1.3, a simple analysis testifies to great interpretative capabilities of a set consisting of three relatively simple methods.

In regional investigation, one and the same set of methods can, in principle, be employed to study the objects of various classes which control different types of mineral resources. Of special interest is a common approach to the prediction of ore and oil-and-gas presence on the basis of geophysical data, taking into consideration the discoveries of non-conventional oil-and-gas deposits in mountainous regions in connection to igneous and metamorphic associations [140]. Table 4.2 illustrates these fundamental potentialities.

Secondary indicators are usually obtained as a result of initial field transformations. Therefore, when developing a model of medium, not only secondary indicators should be selected. Methods of their obtaining, types and, especially, transformation parameters should be specified, as well. Experience and theoretical calculations show that the results of transformation depend on parameters, rather than on the type of transformation. Generally, the parameter selection must comply with the requirement of maximum efficiency of the final solution of the interpretation problem. But since con-

**Table 4.2. Revealing common controls of ore and oil-and-gas deposits by geophysical methods**

GEOLOGICAL CONTROLS (FLUID CONDUCTORS AND HOSTS OF MINERAL DEPOSITS)	PREDOMINANT LOCATION		TYPICAL GEOPHYSICAL METHODS AND THEIR RESULTS	
	mineralization	hydrocarbons	methods	field patterns and geometry of sources
Deep faults	pinnate jointing	fault zones to neighborhood	gravity and magnetic prospecting	gradient zones, local anomaly chains, linearly elongated anomalies
Overlap-overthrust structures	volcanogenic and sedimentary rock masses	sedimentary rock masses	seismic exploration  gravity prospecting	gently sloping reflecting boundaries  extremums on cover edges
Intersections of longitudinal and transcurrent fractures	local structures	regional structures	gravity and magnetic prospecting	interference pattern
Igneous rock concealed highs, their contacts with sedimentary rocks	exomorphic and endomorphic zones of intrusives	eroded volcanic structures, sedimentary rock pinching-out zones	magnetic and gravity prospecting  seismic exploration	anomalies of circular and ring shapes  zones of zero reflection
Porous and fractured metamorphites (secondary quartzites, serpentinites, shales)	scattered bodies	continuous filling	magnetic and gravity prospecting  electric prospecting	field decreasing (excluding magnetic maximums over serpentinites)  conductivity anomalies
Hydrothermal alteration and pyritization zones	pyritization zones	below pyritization zone	magnetic prospecting  electric prospecting	linear field decrease  increased polarizations
Brachy-anticlines in terrigenous-carbonate deposits	north-eastern flanks of structures	eastern and north-eastern flanks of structures	electric prospecting, seismic exploration	contact flexures of mediums with various physical properties

crete requirements entail certain difficulties, the parameter selection is usually confined to the analysis of changes in the model signal during transformation, and to evaluation of the corresponding expenses. The choice is determined by the increase in the signal/noise ratio and preservation of as much accumulated information as possible.

Of prime importance are indicators that are strongly correlated in the presence of the target and weakly (up to negligible) in its absence. It is the difference in correlation of indicators that is, in essence, the major source of information about its presence or absence.

Therefore, when selecting standards, we are interested in the objects which are well-explored not only by geological, but also by geophysical methods involving various transformations, and the study of the relations between indicators, which allow to develop a standard indicator space. As a rule, the amount of these objects is not large, but they should be found and used for devising a model of medium. This fact attaches great significance to the accumulation and analysis of priori geological and geophysical information for developing a model of medium. Another approach is the computer modeling of these objects (geological situations) and of respective indicator spaces, i.e. creation of imitation models.

We will not dwell on the quantitative criteria of the integrated interpretation set forth below. Note only that routine qualitative criteria are also integrated, since geological problems solvable using one geophysical method are very rare, whereas the combination of only two methods considerably expands the possibilities of geophysical data interpretation. This is well-known due to a number of papers dealing, for the most part, with the principles of joint interpretation of gravity and magnetic fields. For instance, it is expedient to consider qualitative criteria of singling out and tracing faults, which are among the main targets of geophysical investigation. It has been established that it is possible not only to isolate and trace the zones of fracture by some typical indicators in magnetic and gravity fields, but also to judge about their types. The main indicators of various faults reflected in magnetic and gravity fields are summarized in Table 4.3.

Therefore, the results obtained using the developed model of the medium should be as follows:

**Table 4.3. Magnetic and gravity fields over faults**

TYPES OF FRACTURES	GEOLOGICAL CHARACTERISTICS	REFLECTIONS IN FIELDS
Faults – channels for magma flow	Fractured zones filled with basic rocks	Linearly elongated positive anomalies
	Intrusions or volcanic centers localized along fractured zone	Chain of near-isometric maximums, or sometimes minimums
Contemporaneous (growth) faults	Abrupt change in lithological composition, facies and deposit thickness on both sides of a fault	Change of sign or behavior of the same sign field at the fault
Faults fixing vertical displacement of blocks	Abrupt change of boundary positions separating a section into individual structural facial complexes	Zone of high field gradients (additional criterion is abrupt change of occurrence depth for upper or lower anomalous mass edges)
	Crush zone due to differentiated movement of conjugated blocks along the fault	Chain of linearly elongated magnetic and gravity minimums coincident in plan
Faults fixing horizontal displacement of blocks	Horizontal rock displacement determined by comparing age, and structural and facies features of rocks on both sides of a fault	Rupture and echelon displacement of zones with linearly elongated anomalies, abruptly inflected isolines

- (1) classes of objects under investigation should be refined; geological, petrophysical and geometrical characteristics of typical objects in these classes and corresponding characteristics of host media should be obtained;
- (2) features obtained from the observed field (and from other geophysical fields) and a set of indicators associated with the targets should be substantiated; the methods of their obtaining should be determined, and their anomalous values should be estimated;
- (3) interpretation criteria for singling out the targets according to the given field (and other geophysical fields) and/or to a set of indicators should be generated.

It is generally a good practice to summarize the results of devising a model of medium in a table containing geological, petrophysical, geometrical and geophysical data on the targets and host media, key indicators of these objects and criteria of their singling out. They should be presented as generalized sections with computed field charts placed above them (Fig.4.3).

It is also expedient to present some model elements in the forms of petrophysical maps and schematic geological maps accentuating geological objects which are the probable sources of anomalies and excluding all other objects. Having all data required, these graphic models may acquire the form of block diagram.

Naturally, a model of the medium is authentic only to a certain degree. The more thorough and full is the analysis and the use of prior information, and the more justified are the analogies drawn, the more reliable is a model of a medium. We can assume that a model of a medium is a complex hypothesis of unknown features of the geological structure in the investigation area and its prospects for a certain mineral. The uncertainty is always present (and must be present) in a model. The aim of the subsequent field data interpretation is to reduce the uncertainty and, therefore, to test the hypothesis by the developed criteria [96].

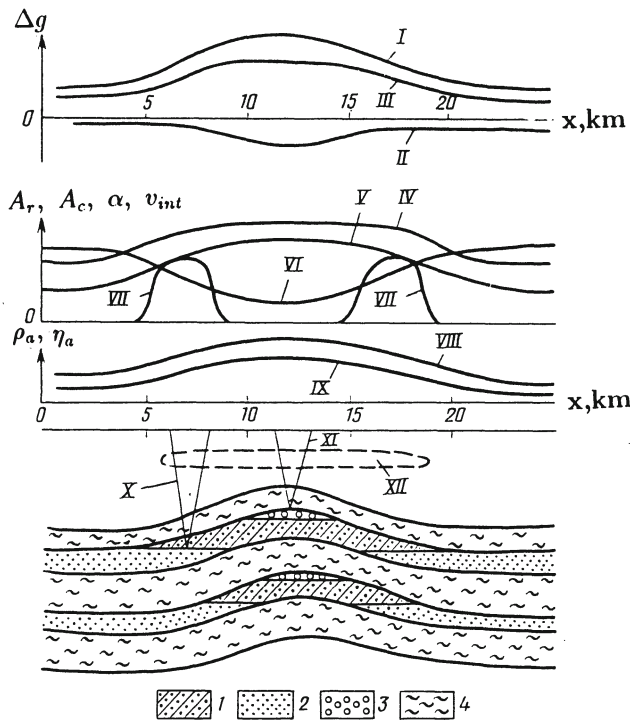


Fig.4.3. A summarized physico-geological model of the oil-and-gas pool of anticlinal type (from [30])

(1) oil-and-gas pool; (2) sandstone; (3) gas; (4) host rocks  
 (I) gravitational anomaly  $\Delta g_s$  from a structure with constant density of layers having no deposit; (II) gravitational anomaly  $\Delta g_d$  from a deposit; (III) total anomaly  $\Delta g_{s+d}$  from the structure and the deposit; (IV) amplitude  $A_r$  of waves reflected from the pool's roof; (V) effective coefficient  $\alpha$  for seismic wave absorption by the oil-and-gas pool; (VI) interval velocity distribution curve  $V_{int}$  within the deposit and outside its contour; (VII) possible amplitudes  $A_c$  of waves reflected from oil-water and gas-water contacts; (VIII) curve  $\rho_a$  for apparent resistivity over the deposit and outside its contours; (IX) polarization curve  $\eta_a$  for rocks in deposit and outside its contours; (X) schematic reflections from contacts; (XI) scheme of reflections from the pool's roof; (XII) rocks of enhanced pyritization due to movable hydrocarbons

## Chapter 5

# INDICATOR SPACE GENERATION

The procedure of indicator space generation covers stages which are usually united under the common name of preliminary processing of observed results. An indicator space is formed in two sequential stages including:

- (1) elimination of the field complication due to known factors, primarily to terrain relief, and
- (2) determination of the secondary derived indicators by the initial field; they are values which have not been and/or can not be measured, i.e. the results of various field transformations.

The indicator space formation is different from the initial processing of measurements results (consideration of gravimeter drift, variations, normal geomagnetic field, etc.). When accomplishing indicator space formation, it is necessary to take into account the data introduced into the model of medium. This is why it forms an integral part of interpretation.

When interpreting, the analysis of variations can also be of interest for the investigator. Geophysical field variations distorting the anomalies due to anomalous objects impede quantitative (and sometimes qualitative) interpretation. Therefore, they deserve a brief discussion in a separate section (see Section 5.1).

Apart from topographic effect, among other known factors that are comparatively easy to consider, are the effects from deep boundaries, regional fault zones and large shallow-seated objects (e.g., intrusions) located on the area under investigation or on adjacent territory. Their geometric and petrophysical parameters can be estimated either by the results of smaller-scale survey, or by other

exploration methods. The fields from these objects are determined in the area under study by solving a direct geophysical problem. Calculated fields are subtracted from the observed field. The fields due to the objects which are not the targets of investigation are excluded. For example, if the desired objects are intrusions, then the effects from the known intrusive bodies are not excluded.

In any case, when eliminating the effects of the known objects, it is necessary to control carefully the correspondence between the objects' parameters assumed in computing and actual parameters. This is necessary to exclude their effect from the observed field and not to complicate the latter with noises of unknown values. If the desired data are not available, then noise effects should be suppressed using transformations based on general ideas on the character of the targets and noise fields. The observed field, being cleared from noise fields and the effects from the known objects, which are of no value for the investigation, are used for obtaining the secondary indicators of the targets.

## 5.1 Elimination of field variations with time

Errors due to variations in the results of observations of some geophysical fields can be represented as a sum of two components. The first (and the main) one is a contribution of the variation of the amplitude (and sometimes of the phase) to the measured field. The second is caused by the secondary variation effects from geological objects which differ from the host medium by contrasting physical properties. As shown above, mountainous regions are characterized by differentiation of physical properties along the vertical and the lateral, which may favor the generation of secondary fields.

Time variations of geophysical signals are observed in all natural geophysical fields under study. The methods for their elimination are the most developed techniques in magnetic and gravity prospecting.

Elimination of geomagnetic variations is vital for conducting high accuracy magnetic surveys. The main principle of their revealing involves continuous or discrete-continuous observations of magnetic field variations at the same point [178]. Continuous inves-

tigations are carried out in observatories with the use of magnetic variation stations (*MVS*), while discrete-continuous measurements are accomplished at control points (*CP*) using *MVS* or magnetometers during field survey. Only short-period and diurnal variations are essential for the field magnetic survey. They are taken into account by introducing corrections: the variations observed on the *CP* are subtracted from the magnetic field values measured on the profile. Secular variations of the magnetic field, changing from one region to another, should be taken into account when linking up the surveys from different years [212]. Observations during magnetic storms are rejected.

The secondary effect of mean diurnal variations over strongly magnetized geological bodies was estimated by Dyadkov [68]. It was found, for example, that if the geological object magnetization is  $5 \text{ A/m}$ , variations cause a secondary effect of 2 to 3 nT. This allows, in most cases to ignore these secondary effects when solving direct and inverse problems in magnetic prospecting.

It is worth noting that magnetic field variations should not be regarded only as a noise. Thus, for example, diurnal geomagnetic variations are used for determining the nature of geomagnetic anomalies [279]. In this way the objects of the desired classes can be singled out by the intensity and shape of variations. Deep structure studies on the basis of electromagnetic field variations are the foundation for corresponding modifications of the electric prospecting.

The methods of eliminating gravitational field variations are adequately described in the literature (for instance, [1,293]). The secondary effects of gravity field variations are negligible.

Self-potential variations depend on hydrogeological conditions, features of soil and vegetation cover and other difficult-to-consider factors [80,240]. As a rule, these factors can not be eliminated.

Time variations bring about considerable errors into the results of observation obtained by *VLF* techniques and near-surface thermal prospecting. In contrast to magnetic prospecting, where variations account for  $10^{-3}$  to  $10^{-4}$  of the constant magnetic field of the Earth, in the *VLF* method electromagnetic field variations are often comparable with an average intensity of the signal. Therefore the

effects caused not only by the initial signal variations, but also by their secondary effects due to the heterogeneity of the section, may arise.

A ground survey method with synchronous variation measurements at the CP, which is similar to magnetic prospecting, was proposed for VLF method. Application of a simple linear filter allows to obtain the VLF field value free from variations for each profile point [77]. This technique makes it possible to eliminate the observation distortions caused by field variations in time and to reduce the observations to a common level. It has been complicated earlier by field variations during a day and intensity changes from day to day (this technique is described in Appendix A).

Among other methods for eliminating seasonal variations in near-surface thermal prospecting [51,154], a more appropriate one has been suggested. It is based on repeated temperature measurements along the observation profile using the data on regional temperature field change obtained from meteorological stations [72,131]. Using the combination of these data as a base, a system of linear algebraic equations can be written, its solution allowing to eliminate the effect of temperature waves coming with retard from the earth's surface (see Appendix A).

## 5.2 Terrain correction and utilization of topography for deriving geological information

### 5.2.1 Problem of terrain correction; two aspects of this problem

#### 5.2.1.1 General information

Elimination of the effect of earth's surface relief is most important for geophysical investigation of mountainous regions. A very rugged relief has an effect not only on the transportation, complicating geophysical prospecting under mountainous conditions (particularly, laid-out routes are not always located across the strike of the target, which limits the interpretation). Relief effect also manifests itself in non-stationary and stationary topographic anomalies.

Consideration of non-stationary anomalies is customarily accomplished visually during the field investigation or by special methods of observation. Filtration anomalies of the self-potential are classified among non-stationary anomalies. Usually their gradient is considerably less than that of "ore" (quick) anomalies, and a mirror reflection of the relief shape by the *SP* anomaly is used for the rejection of barren anomalies. When the *SP* survey profile crosses a mountainous river with a stony bed, a kinetic electric field is observed, which appears as a potential minimum against the background of its total increase due to filtration on the valley slopes. The potential of such a field grows along the stream. Magnetic anomalies on tops of hills, associated with lightning discharges (magnetization of outcropping rocks is severely changed in their vicinity), may also fall into this category, as well as thermal anomalies due to varying meteorological conditions (their effect can be excluded by repeated observations at different time intervals).

The main aspects of terrain correction are connected with stationary noises introduced into geophysical observations. For one thing, the form and physical properties of the topographic masses (i.e. relief-forming morphostructures) are responsible for the effects due to these masses in the anomalous field, which disguise the anomaly effects from the hidden targets. Second, due to uneven observation line, the distance from the field recording point to the source varies, which manifests itself differently in anomalies from various objects.

Note that a fail in eliminating a topographic effect results in the distortion not only of the anomalous field details, but also of the entire idea of geologic structure of the object under study and of its presence. For example, in highlands ore body may be located above the observation point. It is only natural that magnetic, gravitational and electric effects will appear to be opposite to that expected from the body lying below the observation plane.

As an example, consider the *SP* anomaly from a sulfide vein of a thin bed shape (Fig.5.1a). Proceeding from the classical *SP* theory [240], the lower pole line (projected into the point *A*) of the polarized bed has a negative charge, when the groundwater surface is parallel with the slope and intersects the ore deposit. From this theory it follows that a negative *SP* anomaly will be recorded on the earth's

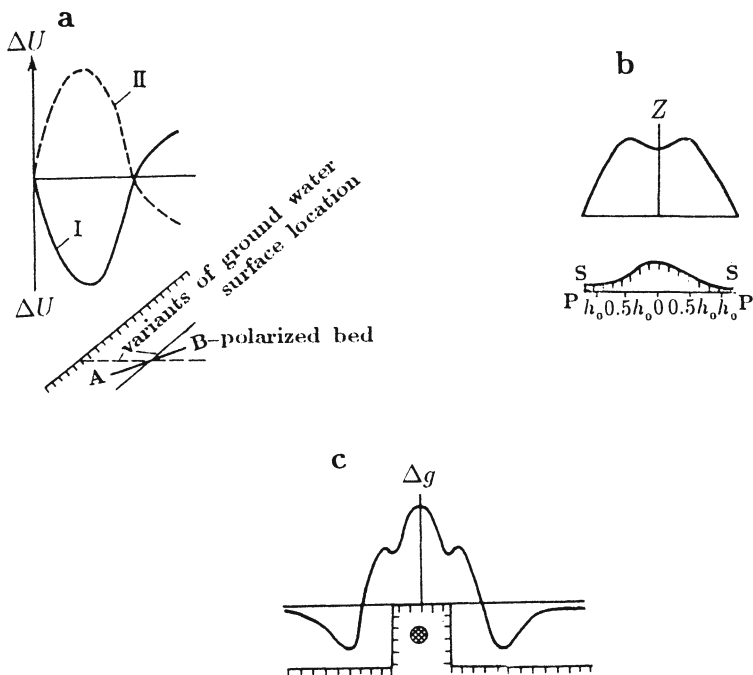


**Fig.5.1. Geophysical anomaly distortions in case of uneven surface of observation for:** (a) self-potential field over the inclined bed; (b) magnetic field over the infinite vertical thin bed; (c) gravitational field over the deposit with a circular section

surface, but it will be considerably displaced from the orebody projection (curve I). By contrast, if the groundwater table follows the horizontal plane and crosses the deposit, then the upper pole line (projected into the point *B*) acquires a negative charge. In this case, the negative anomaly on the earth's surface becomes positive (curve II), and its nature is far from being understood correctly. The negative SP anomaly may completely disappear, if the ore deposit occurs under the low of the relief, which causes a positive anomaly due to filtration. The negative anomaly of filtration potential may appear over the elevation in the absence of orebody.

Similar examples can be cited for other geophysical methods. When the basite dike in the form of a thin vertical bed occurs under the top of a mountain range, the relief of which is approximated

by the Aniezie curl [193], the magnetic anomaly splits into two maximums, which may create an erroneous idea of the presence of two magnetized bodies (Fig.5.1b). A deposit with circular section, resembling some chromite bodies, being arranged inside the elevation with vertical slopes (Fig.5.1c), sets up  $\Delta g$  anomaly of a very complicated form with four additional extreums [182].

Thus, under the conditions of rugged relief, commonly accepted notions of qualitative interpretation, according to which the number and location of geophysical anomalies are correlated with the number and location of geological objects, are open to question.<sup>1</sup>

On the whole, the consideration of the terrain relief effect on gravitational and magnetic fields includes the following two stages: (1) calculation of that part of the field which is due to the known or “missing” topographic masses, and (2) conversion of the observed values to horizontal reference plane (reduction line correction). One should keep in mind that the attraction of morphostructures forming the terrain relief may considerably exceed the anomalies from the target, reaching 1,000 nT and over in magnetic prospecting and 10 mGal and over in gravimetric prospecting. Meanwhile, large objects, which are most clearly detected by gravity survey in mountainous regions, such as acidic intrusions, produce gravitational effect on the same order. Fig.5.2 illustrates the field ratios for some situations involved. Apparently, in one case the Bouguer anomalies and in the other case  $\Delta T$  anomalies caused by geologic boundaries are completely concealed by the relief form attraction.

#### 5.2.1.2 Direct problem solutions

The problem of terrain correction received earlier primary emphasis in gravity prospecting [101] and also in seismic prospecting, where the corresponding procedures introduce so-called statics. The first factor (topographic mass influence), conditioned by the irregularities of physical (density, velocity, etc.) earth-to-air interface, always affects the results of these methods. To correct for the effect of topographic mass attraction, it is necessary to carry out a large amount

---

<sup>1</sup>The cited data and some other evidence from geophysical investigations of mountainous regions were first reported in [131]. They were afterwards reproduced in books on integration of methods [44,275], unfortunately, without corresponding references

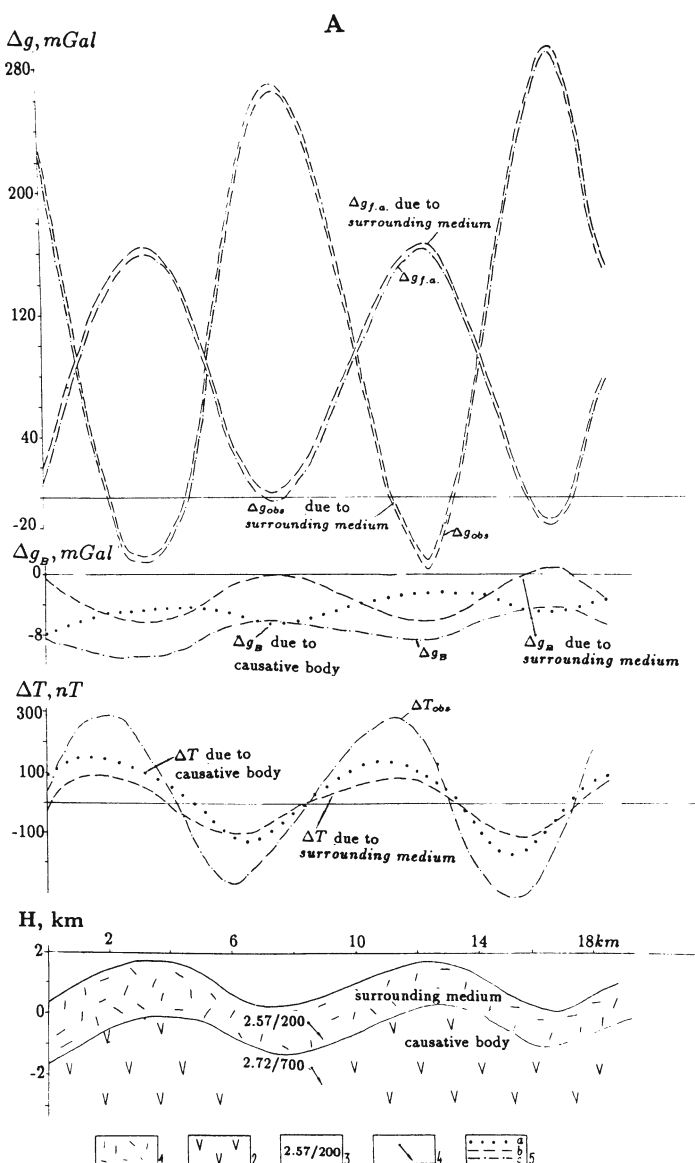
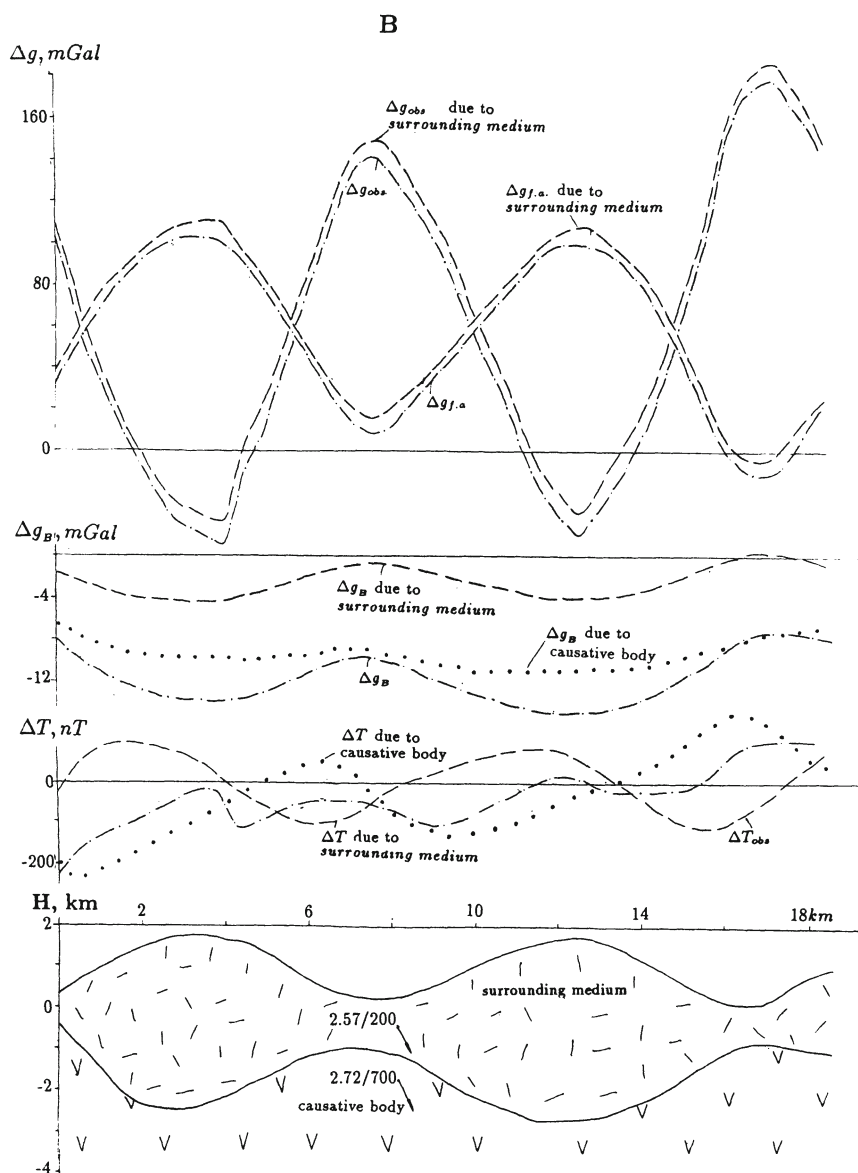


Fig.5.2. Modeling of gravitational and magnetic fields at conformable (A) and discordant (B) depth boundaries with respect to the relief

(1) surrounding medium; (2) causative body; (3) physical properties (numerator=density,  $\text{g}/\text{cm}^3$ ; denominator=magnetization,  $\text{mA}/\text{m}$ ); (4) magnetization vector direction; (5) computed effects using the GSFC program: (a) physical interface, (b) medium, (c) total



of topographic and geodetic works or to employ the available data obtained by ground surveying and aerial survey, as well as the data on the physical properties of the upper portion of the section. The above data are used for computing and eliminating the topographic mass attraction in gravimetric and magnetic prospecting, applying the statics in seismic prospecting, etc. Thus, a direct problem of geophysics is solved. For this purpose, a number of methods is utilized [135]. An effective program for solving a direct 3-D problem of gravimetric and magnetic prospecting under the conditions of complex media and rugged relief, called a Geological Space Field Calculation (*GSFC*) program [143,145], was used in computing the fields by models presented in Fig.5.2. Its characteristics are set forth below in Chapter 10, while the description of the program is given in Appendix B.

The accuracy of various methods is determined on the standard models, their attraction being calculated by analytical formulas.

To determine corrections in the central zone, the following analytical expressions of the simple body attraction can be employed:

(a) for an inclined plane

$$g_r = 2\pi G\sigma_r R(1 - \cos \alpha K_\alpha / K_o); \quad (5.1)$$

(b) for a cone

$$g_r = 2\pi G\sigma_r R \tan \alpha (1 - \sin \alpha); \quad (5.2)$$

(c) for a conical hollow

$$g_r = 2\pi G\sigma_r R \tan \alpha (1 - \cos \alpha). \quad (5.3)$$

Here  $G$  is the gravitational constant,  $\sigma_r$  is the density of rock forming the relief,  $R$  is the central zone radius,  $\alpha$  is the dip angle of the inclined plane as in formula (5.1) and the cone generatrix dip angle as in (5.2) and (5.3),  $K_\alpha$  is the total elliptic integral of the first kind,  $K_o = \pi/2 = 1.5708$  at  $\alpha=0$ .

The gravitational effects of the bodies under discussion were computed by formulas (5.1)–(5.3) for  $\sigma_r=1 \text{ g/cm}^3$  and  $R=0.1 \text{ km}$ , provided  $\alpha$  varied from  $0^\circ$  to  $50^\circ$  with a step of  $5^\circ$  (Fig.5.3).

The plots in Fig.5.3 were used to determine terrain corrections in the central zone with a radius of  $0.1 \text{ km}$  for 8 points located on

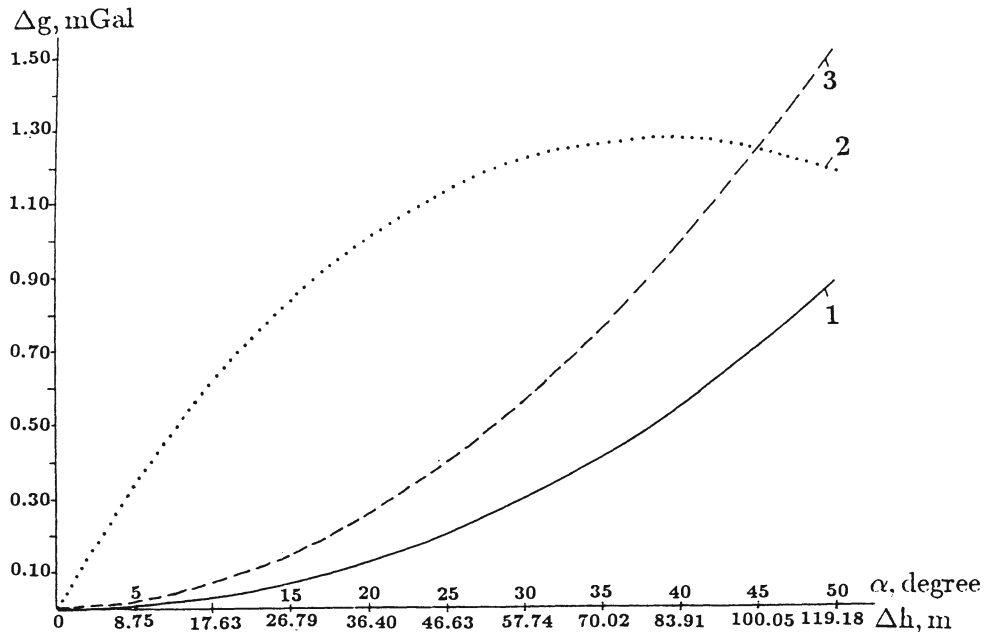


Fig.5.3. Plots of correction for topographic mass attraction within a zone of 0 – 100 m computed from analytical formulas of effective density of  $1 \text{ g/cm}^3$

Terrain relief forms are approximated by inclined plane (1), cone (2) and conical hollow (3)

the slopes and satisfying the model of formula (5.1), and for 2 points on the tops of rounded positive relief forms approximately satisfying the model of (5.2).

The standard deviation ( $SD$ ) of corrections obtained from (5.1) as compared to the corrections determined in the same points by Berezkin's method [28], amounted to  $\pm 0.06 \text{ mGal}$ , while that found from (5.2) ran to  $\pm 0.09 \text{ mGal}$ . However, in the first case a systematic discrepancy of  $0.35 \text{ mGal}$  is observed. It is caused, on the one hand, by the deflection of the real relief from the inclined plane, and, on the other hand, results from the ineffective hyperbolic approximation assumed in Berezkin's method for an even slope. These data point to the necessity of a more careful account for

the terrain relief effect in the central zone during high-accuracy survey. One should distinguish between its internal part admitting approximation by simple bodies, and its outer part. For the latter, terrain corrections can be computed using well-known programs, if respective topographic evidence is available.

#### 5.2.1.3 Statistic analysis of terrain corrections

A direct problem solution is a deterministic process. However, the procedure of terrain correction involves some elements of statistic nature.

For example, the gravitating mass attraction is computed for adjacent zones from topographic maps and leveling data, whereas corrections for remote zones are determined from the plots of their correlation dependence on the heights of the observation point for each survey sheet.

To increase the effectiveness of eliminating topographic effects, the autocorrelation properties of the heights field can be employed. As follows from the data obtained on the Lesser Caucasus [69], there is a close relationship between terrain corrections ( $g_r$ ) and the average slope angle and the index of the relief ruggedness. The latter represents the mean distance along the vertical between adjacent extrema of the relief in the profile interval. Both these characteristics and those of corrections are specific for various types of relief. We may conclude that the values  $g_r$  and their gradients tend to correlate with the relief ruggedness index. Meanwhile, the above mentioned index is a clear analog of the autocorrelation radius described in quite a number of well-known works applying the theory of random functions.

According to [116], it is expedient to treat the terrain correction in all these zones (excluding a central zone) as a sum of two components. The first component is caused by the relief ruggedness, while another – by the point height. The influence of the first component is essential for the adjacent zones, but it decreases with the distance from the point. This allows to apply correlation between corrections and heights, when the topographic effect is accounted for remote zones. This approach improves the process of topographic effect elimination, which can be optimized on the

basis of theoretical analysis of terrain corrections from the statistical standpoint.

Proceeding from the familiar formula for computing terrain corrections by summing-up the effects of unit cells of the “apparent” graticule<sup>2</sup> applied to the topographic map, we also substantiated the subdivision of the correction into two components [7]. In fact,

$$g_r = \frac{1}{2} G\sigma \sum_{i=-n}^n \sum_{j=-n}^n C_{ij} (H_{ij} - H_c)^2, \quad (5.4)$$

where

$$C_{ij} = -\left[ \frac{r_{22}}{x_2 y_2} - \frac{r_{21}}{x_2 y_1} - \frac{r_{12}}{x_1 y_2} + \frac{r_{11}}{x_1 y_1} \right]_{ij}, \quad (5.5)$$

$C_{ij} = 0$  when  $i \wedge j < m$ ,  $x_2 = x_i + a/2$ ,  $x_1 = x_i - a/2$ ,  $y_2 = y_j + a/2$ ,  $y_1 = y_j - a/2$ ,  $a$  is the grid step,  $x_i$  and  $y_j$  are center coordinates of  $(i, j)$ -th cell,  $H_{ij}$  is the height of this unit,  $H_c$  is the height of calculated point,  $n = r_k/a$ ,  $r_k = \max(x_i, y_j)$ ,  $m = r_m/a$ ,  $r_m = \min(x_i, y_j)$ .

The scheme of determining (5.4) is similar to that of the second moment of the random value  $H_{ij}$ . According to Ventsel [292], the second moment is minimal and equal to the random value variance, if it is centered, i.e. if the moment is computed with respect to the average

$$\bar{H} = \sum \sum C_{ij} H_{ij} / \sum \sum C_{ij}. \quad (5.6)$$

Proceeding from (5.6) we can easily show that

$$g_r = \frac{1}{2} G\sigma K D_H + \frac{1}{2} G\sigma K (H - H_c)^2, \quad (5.7)$$

or

$$g_r = g_1 + g_2, \quad (5.8)$$

where

$$D_H = \sum \sum C_{ij} (H_{ij} - \bar{H})^2 / K, \quad (5.9)$$

$$K = \sum \sum C_{ij}. \quad (5.10)$$

---

<sup>2</sup>Graticules (zone charts) have almost not been used for processing geophysical fields for many years. Their principles have been realized in a digital form in various computer programs. However, at the same time, the use of this term is necessary for a more clear explanation of some processing aspects. Therefore, the authors introduced the term “apparent graticule”.

Thus, the correction for terrain relief in the point  $(0, 0, H_c)$  is resolved into a sum of two components, the first ( $g_1$ ) being proportional to the sampling variance <sup>3</sup> of the heights  $D_H$  taken in the nodes of the apparent square graticule with a remote central square. It represents the terrain correction in the point  $(0, 0, \bar{H})$ . The second member ( $g_2$ ) is the constant gravitation of the rock layer with the thickness of  $\bar{H} - H_c$  within the apparent graticule  $(r_m, r_k)$  in the point  $(0, 0, H_c)$  or the point  $(0, 0, H)$  located on the lower or upper surface of this layer.

It is important to emphasize, as suggested also by the authors of [116], that the values  $g_1$  and  $\bar{H}$  do not depend upon the height of selected point  $H_c$ , but are functions of the relief structure in the zone under investigation  $(r_m, r_k)$ . In addition, it is worth mentioning that the term  $g_2 = \frac{1}{2}G\sigma K(\bar{H} - H_c)^2$  depends not only on the heights of the selected (central) point, but also on the relief ruggedness. If the relief is smooth and monotonous, then  $\Delta H = \bar{H} - H_c \rightarrow 0$ . For example, for the inclined plane  $\Delta H = 0$ ; in this case the dip angle is of no importance, whereas  $g_1$ , which is proportional to the sampling variance of heights, depends also on the dip of the relief.

In modern practice isocorrection maps for  $g_r$  values in the square grid nodes are sometimes generated in advance using various computer programs. However, they can hardly be applied to interpolation [16]. If we take  $\bar{H}$  values obtained by formula (5.6) instead of  $H_c$  values, then there is more ground to use the isocorrection maps of  $g_1$  for interpolation, since  $\bar{H}$ , being an averaged relief characteristic, varies more smoothly than  $H_c$ . At the same time, it is necessary to draw isoline maps for weighted average heights of  $\bar{H}$  by their values computed in the nodes. Once the interpolated values of  $g_1$  and  $\bar{H}$  are obtained in the required points, the terrain relief corrections can be easily obtained by formula (5.7), where  $K$  is constant for this size of an apparent graticule.

It is obvious that the more  $H_{ij}$  values we use, i.e. the greater is the apparent graticule's final radius  $r_k$ , the more stable is  $\bar{H}$  and the more close is the sampling variance  $D_H$  to the real variance. The apparent graticule cells are not necessarily equal, since a weighted averaging takes place. On the other hand, the remote cells have small weights  $C_{ij}$ ; their account for any  $H_{ij}$  (in physically accept-

---

<sup>3</sup>For the sampling size of  $4(n^2 - m^2 + n + m)$

able limits) practically does not alter  $\bar{H}$ . This consideration yields a criterion for determining  $r_k$  according to the required accuracy of topographic effect elimination.

Formula (5.7) gives an insight into relief features affecting the correction value. For instance, it is easy to reveal the inadequacy of a frequently used preliminary heights averaging within the limits of elementary squares (rectangles) of the digital terrain model. The point is that the step-wise relief approximation conserves the volume of elementary parallelepipeds (prisms), and not their gravitation. If we make use of formula (5.7) to compute the gravitation of the elementary cell measuring  $0.5 \cdot 0.5$  km and  $x=2$  km,  $y=4$  km distant from the selected point, then we can find that in more detailed relief descriptions and, hence, with more precise stepwise approximation, corrections tend to increase gradually. Thus,  $g_r$ -values are computed with an error in the range of 20 to 30% for 500 m step, and less than 7% for 250 m step. The larger is the inclination of the relief, the more detailed should be the relief description at the corresponding distance from the selected point. This problem has to be solved empirically for each real relief, according to the zones, and selecting a specifying interval for the digital relief model according to the required accuracy of computing corrections.

#### 5.2.1.4 Reduction to line

The account of topographic mass attraction may be of no use, for example, for magnetic investigations directed at singling out a magnetized body among non-magnetic host rocks or for electric exploration for conducting ores in a high-resistance medium. In any case, however, the distorting effect of a non-horizontal observation line takes place, when the object differs from the host medium by contrasting properties and causes the anomalous vertical gradient.

The comparison of anomalies  $\Delta g_B$  and  $\Delta T$  from the local body observed on the inclined and horizontal relief is illustrated in Fig.5.4. Apparently, after applying all corrections (for “free-air”, plane-parallel intermediate layer and terrain relief with correct intermediate layer density  $\sigma_{int}$ ), the singled out Bouguer anomaly corresponding to the local anomaly takes on small negative values (minimum) in the direction of low of the relief, whereas the anomaly

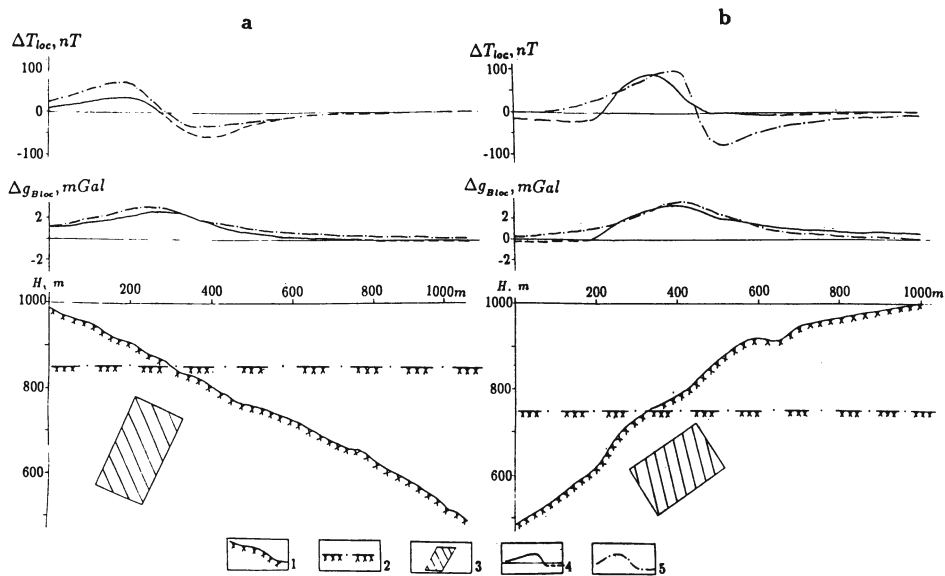


Fig.5.4. Comparison of gravitational and magnetic anomalies from a local anomalous body observed on inclined and horizontal profiles: (a) smooth slope, (b) complicated slope

(1) inclined profile; (2) horizontal profile; (3) anomalous body with excess density  $\sigma_{red} = 1.5 \text{ g/cm}^3$ ,  $I_{red} = 0.5 \text{ A/m}$ , magnetic inclination  $i = 60^\circ$ ; anomalies of  $\Delta T$  and  $\Delta g_B$  from the same body after topographic mass attraction correction: (4) on inclined profile, (5) on horizontal profile

on the horizontal profile has no negative values.  $\Delta T$  anomaly has the form on the inclined profile as if corresponding to a smaller magnetization inclination in contrast to the case of horizontal profile. This shows a good fit to the theoretical results reported in [146]. Thus, applying topographic corrections does not eliminate the effect due to different observation point heights in respect to the anomalous object. The same conclusion has been earlier illustrated by Nemtsov [204].

In a general case, to avoid the analytical continuation through the possible causative masses, it is necessary to reduce these observation results to the common level, usually the highest point level (reduction to line). The above reduction means introducing a correction for anomalous vertical field gradient, i.e. for the gradient

component caused by anomalous bodies and the normal component of the vertical gradient.

Quite a number of methods for reducing to a horizontal level are known [12,27,32,93,146,182,236]. The principle of the majority of them consists in selecting by the successive approximation method of such a field on the intermediate plane that coincides with the measured one when continued to the observation surface. The observed field is assumed to be a zero approximation, i.e. it is thought of as being recorded on the intermediate plane. Then, this field is continued upward to the observation line. The difference between the observed and computed fields is the correction in each point, which is added to the zero approximation (observed field). Thus, the first approximation is computed. Then, the first approximation field is continued again to the measurement line, and the correction is computed. Now it is the difference in the results of the first and the second upward continuations. This correction is added to the first approximation. After this manipulation, we obtain the second approximation, which is subjected to the same procedure until the correction becomes close to the observation error. The final approximation is used for continuing to any horizontal plane. Among these techniques, Aronov's method [16] is the most well-known.

When realizing the above methods, upward continuation is accomplished. As a result, not only the anomalies caused by relief forms collapse or are attenuated, but also those from the objects under investigation (see, for example, Fig.16-5 from [61]). Therefore, the expediency of continuation should be estimated with due account of the type of work, problems and available data.

It is commonly known that for the purpose of estimating the expediency of reduction to the common level, the degree of anomaly distortion can be approximately determined from the formula for any component of the recorded field

$$\Delta U = (\partial U / \partial Z) \Delta H, \quad (5.11)$$

where  $\partial U / \partial Z$  is the vertical derivative of the field; and  $\Delta H$  is the relative elevation of the flight height (observation line), i.e. terrain clearance of aerial survey.

In aerial surveys by sinuous (in the vertical plane) routes and

ground surveys, the sinuosity effect consideration, i.e. reducing observations to horizontal or inclined plans, is, in principle, necessary. It substantiates solution to some problems accompanied by quantitative determination of the anomalous bodies' parameters: neglecting the effect of variation in the observation point heights may bring errors into interpretation. To reduce deterioration of the anomalies under study, the researcher should choose the reduction level as close to the acting masses as possible and, if required, select several levels.

Within the areas with close inclination angles of survey profiles, distortions of the field and its transforms due to the relief are of the same type. Thus, it is not necessary here to carry out reduction to the plane, if the preliminary regioning has been accomplished by the main forms of the relief determining the dominant dips of the routes (Fig.5.5). The subsequent analysis of the field and its transforms should be executed independently within the limits of the singled-out areas. Here one should keep in mind that the results relate to fictitious bodies of identical forms and the sizes similar to those of real anomalous bodies (see Sections 2.2 and 7). According to the available evidence, the positions of fictitious and real bodies in plan do not differ greatly (max. 0.4 of the body depth for the relief dip angle up to  $30^\circ$ ). This is not essential for shallow-seated objects. When the relief is very complicated, in certain plots it may become necessary to reduce the field to the plane which should be inclined and as close as possible to the relief.

#### 5.2.1.5 Non-conventional ways for terrain relief effect reducing

The above approach is the most universal. However in this case the manual calculation is very labor-consuming, as is the setting of models for computer solution of direct problems. The most essential for computing corrections is the detailed investigation of physical properties of the relief-forming rocks. As mentioned above, either involves dramatically increased time and labor input for the terrain correction or results in discarding such considerations in magnetic and electric prospecting, thus restricting the possibilities of geophysical investigations of mountainous regions.

The correlation method of topographic effect elimination is a

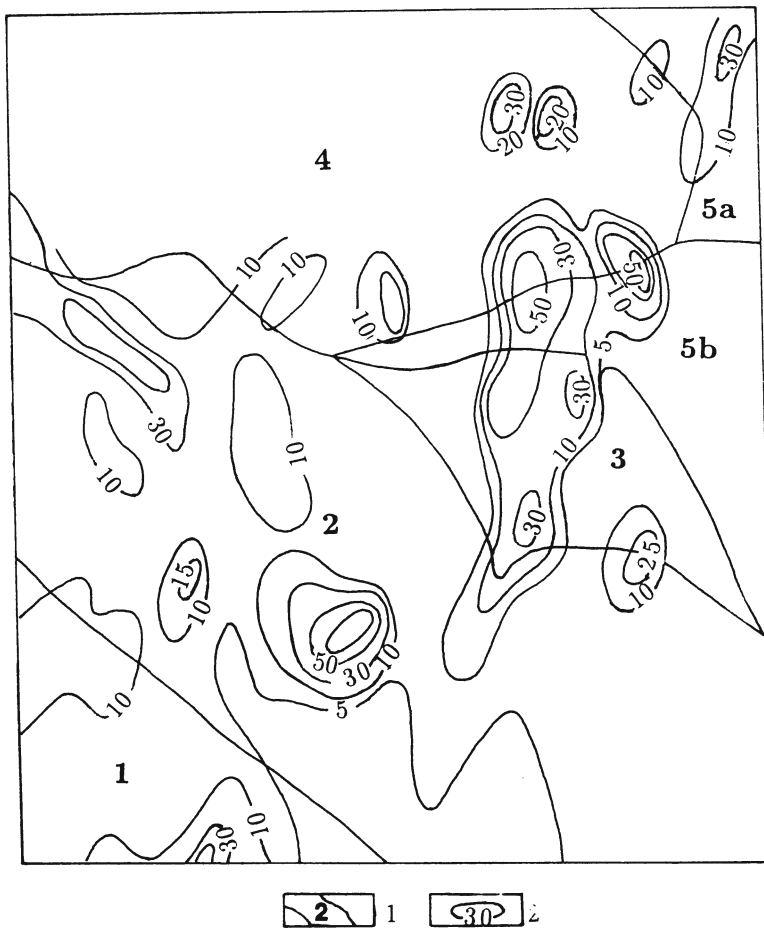


**Fig.5.5. Relief regioning in the Mekhmana ore district (Lesser Caucasus) by the inclination angles as compared to magnetic susceptibility [135])**

(1) area with similar inclination angles; (2) magnetic susceptibility (in  $10^{-3} SI$  unit)

way out of various situations. This technique was known in gravity prospecting as statistic reduction [188]. It was developed in detail in magnetic prospecting [130,136,137] and proved to be effective for other types of geophysical investigation [131,140,142]. For this reason we described it in a separate Section 5.2.2.

There are some other non-conventional ways of eliminating or reducing field distortions caused by terrain relief.

The integration of geophysical methods makes it possible to suppress to some extent the topographic noises. Indeed, making use of the technique for computing the amount of information contained in the results of a separate method application (see Chapter 8) and summing up the amount of information obtained by each method allows to diminish the terrain relief effect by the selection of fields where the terrain relief exerts different influence. For example, valleys are characterized by the decrease in the magnetic field under the conditions of “magnetic” relief, and by growing resistance on profiling arrays.

The possibilities of reducing topographic effects by grouping the points of additional gravimetric observations around the central point located on the survey network were shown in [8]. A group of 4 to 8 additional points is located above and below along the relief approximately symmetrically and equidistant from the central point. The topographic effect is reduced to the obtained difference between the gravity field in the center of the group and its mean value for the whole group. The comparison of local Bouguer anomalies  $(\Delta g_B)_{loc}$  obtained by using a conventional technique for computing corrections at the area of the Kyzylbulakh gold-pyrite deposit in the Lesser Caucasus with the results of grouping the points along 8 rays with the radius of 30 m around the central one showed that the difference field obtained by grouping differs from the  $(\Delta g_B)_{loc}$  value by less than 0.1 mGal both on the slope and on the ridge.

#### 5.2.1.6 Terrain correction as an element of modeling during the interpretation

When solving a number of problems, it seems rather attractive to consider topographic effect elimination as one of the steps in mathematical simulation of the effects due to the entire medium

under investigation, including earth/air interface. Excluding a separate procedure of terrain correction, we reduce the total error of processing and interpretation and save much time. An example of such an approach was obtained at an area of the above mentioned Kyzylbulakh deposit [145].

An isoline chart of  $(\Delta g_B)_{0-50}$ , i.e. Bouguer anomalies including the total correction within the zone of 0 to 50 km (the heights of the surrounding relief elements vary from 0 to 4 km within a radius of 50 km) was compiled using the conventional method of terrain correction (Table 5.1). Variations over the whole area ran from 4.2

**Table 5.1. Terrain correction zones in conventional technique gravity prospecting**

Zone	Radius of zone,km Inner      Outer		Correction method author, SD (mGal)	Scale of topogra- phic materials	Step of digital relief model (km)
Central	0.0	0.1	[28], $\pm 0.06$	1:2,000	–
Near	0.1	2.0	[180], $\pm 0.05$	1:25,000	0.1
Middle	2.0	10.0	[180], $\pm 0.05$	1:50,000	0.3
Distant	10.0	50.0	[181], $\pm 0.05$	1:200,000	–

to 7.4 mGal, with maximums in the brook and crests and minimums on the slopes. The  $\Delta g_B$  chart drawn up with due account of these corrections is characterized by the standard deviation amounting to  $\pm 0.11$  mGal and is not in good agreement with the geological evidence obtained by mining and drilling (Fig.5.6A,B).

Therefore, a special scheme for obtaining the gravitational field of Bouguer anomalies was realized. It is based on determining the difference between free-air anomalies  $\Delta g_{f.a.}$  and gravitational field computed by a 3-D digital model of the homogeneous medium with  $\sigma=2.67$  g/cm<sup>3</sup> and real topography.

According to our method, the terrain relief effect is accounted for simultaneously with the interpretation. The terrain relief is simulated using six selected profiles 2c – 7c in the central portion of the Kyzylbulakh area, crossing the deposit of the same name (their length runs to 800 m). Experimental computations were carried

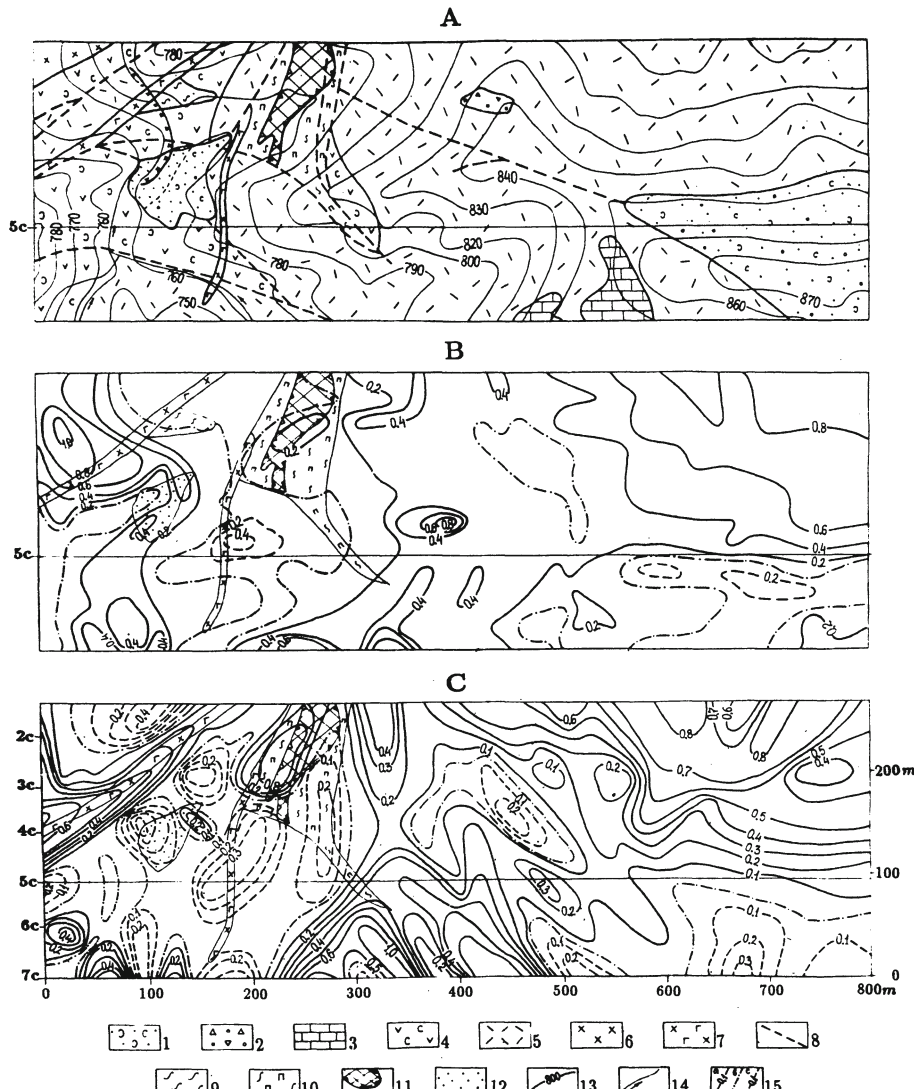


Fig. 5.6. Comparison of corrections in detail gravimetric prospecting: (A) geological map of the central part of the Kyzylbulakh gold-pyrite deposit; (B) and (C) fragments of  $\Delta g$  field charts obtained by conventional and special techniques, respectively

(1) Quaternary deluvial deposits; (2) lens of tuffaceous conglomerate from the Upper Jurassic; (3) lenses of bone chert; (4) tuffs and lavas of andesitic porphyrites; (5) tuffs of liparite-dacitic porphyrites from the Upper Bajocian; (6) subvolcanic body of andesitic porphyrites; (7) dykes of andesite-basalts from the Upper Jurassic; (8) disjunctive dislocations; (9) zones of brecciation and crush with weak pyrite-chalcopyrite mineralization; (10) zones of brecciation lean as to pyrite-chalcopyrite ore content; (11) outcrop of orebody represented by oxidized pyrite-chalcopyrite ore; (12) dead rock and ore component pile; (13) terrain relief isolines; (14) brook bed; (15) isoanomals, mGal: (a) positive, (b) zero, (c) negative

out using the *GSFC* program in order to investigate the relief digital description range. These computations were accomplished along the profile 6c both for 2-D and 3-D models of the medium. For a 2-D model, relief description intervals of 0.8 and 10 km were used, while for a 3-D model – those of 0.8, 10 and 80 km.

For a 3-D model the relief was described for all design profiles and, additionally, for other four profiles, two of them being to the left of the profile 2c and other two – to the right of the profile 7c. The border profiles were selected so that they coincided with those observed in the Kyzylbulakh area. In this case, the  $\Delta g$  values were computed along the profiles 2c – 7c with a unified digital description of the terrain relief. The analysis showed that the difference in the results of 2-D and 3-D modeling was appreciable (up to  $\pm 1.5$  mGal). At the same time, the curves obtained from the 3-D model with a relief description interval of 10 and 80 km are practically identical. This suggests that the description interval of 10 km is sufficient for 3-D model. When the terrain relief recedes from the selected points, it can be described more schematically, singling out solely its major forms.

On executing the above experiment, the further processing of materials from the Kyzylbulakh area involved the following steps. A 3-D terrain relief model with the description interval of 10 km, in the points of profiles 2c – 7c with a step of 8.46 m (95 points per each profile) was employed to compute the gravitational effect of the medium with  $\sigma = 2.67 g/cm^3$  using the *GSFC* program. This effect is equal to incomplete topographic correction ( $(\Delta g)_{ITC}$ ) of opposite sign. These corrections were subtracted from, i.e. added with their own sign to the values of  $\Delta g_{f.a.}$ , and  $(\Delta g_B)_m$  values were thus obtained (subscript “*m*” stands for “model”). The latter were used to construct an isoanomaly map. The accuracy of calculated  $(\Delta g)_{ITC}$  is considerably higher than that of terrain correction by conventional techniques within the zone of 0 to 50 km. The standard deviation of  $(\Delta g_B)_m$  amounted to  $\pm 0.06$  mGal.

The chart of  $(\Delta g_B)_m$  isoanomalies is much more differentiated than the  $\Delta g_B$  chart drawn up by conventional techniques and is in better agreement with the available geological data (Fig.5.6C).

## 5.2.2 Correlation technique for reducing topographic effect

### 5.2.2.1 Terrain correction in magnetic prospecting

There is a distinct correlation between the elevations of the observation point ( $H$ ) and the vertical magnetic field increments ( $\Delta Z$ ) under the condition of relatively homogeneous magnetic medium. In case of direct magnetization, the field maxima correspond to ridges of the “magnetic” relief, while the minima – to its valleys.

An analytical approach was suggested by Khesin [129] to show the possibility of applying the linear relation  $\Delta Z(H)$  to a typical element of mountainous regions – a slope (inclined ledge, or step). All the main relief forms can be approximated with the use of one or another combination of slopes. It appears, then, that rough as it is, a simple and effective method for eliminating the effect of magnetized rock relief is substantiated. It employs only the data on the recorded field and terrain relief. To apply it, a correlation field is drawn up between  $\Delta Z$  and  $H$  values, and then an averaging straight line is plotted. The terrain correction is determined by this line

$$\Delta Z_r = c + bH, \quad (5.12)$$

where  $b$  and  $c$  are factors of a linear equation computed using the least-square method.

The averaging straight line (5.12) is drawn on the basis of many observation points data obtained under the conditions of a medium close to uniform and as distant as possible from sharp bends of the relief. It was shown that

$$b = (8I \cos \alpha)/R, \quad (5.13)$$

where  $I$  is the topographic mass magnetization,  $\alpha$  is an acute angle between the slope face and horizon,  $R$  is the slope length across the strike.

Therefore,  $I$  value can be determined by the angular coefficient of the correction chart.

Elimination of the topographic effect by the correlation technique allows practically complete smoothing out of the anomalies caused by morphostructures (Fig.5.7a). When excluding the topographic effect from the observed field (see Fig.5.7b),  $\Delta Z$  curve is

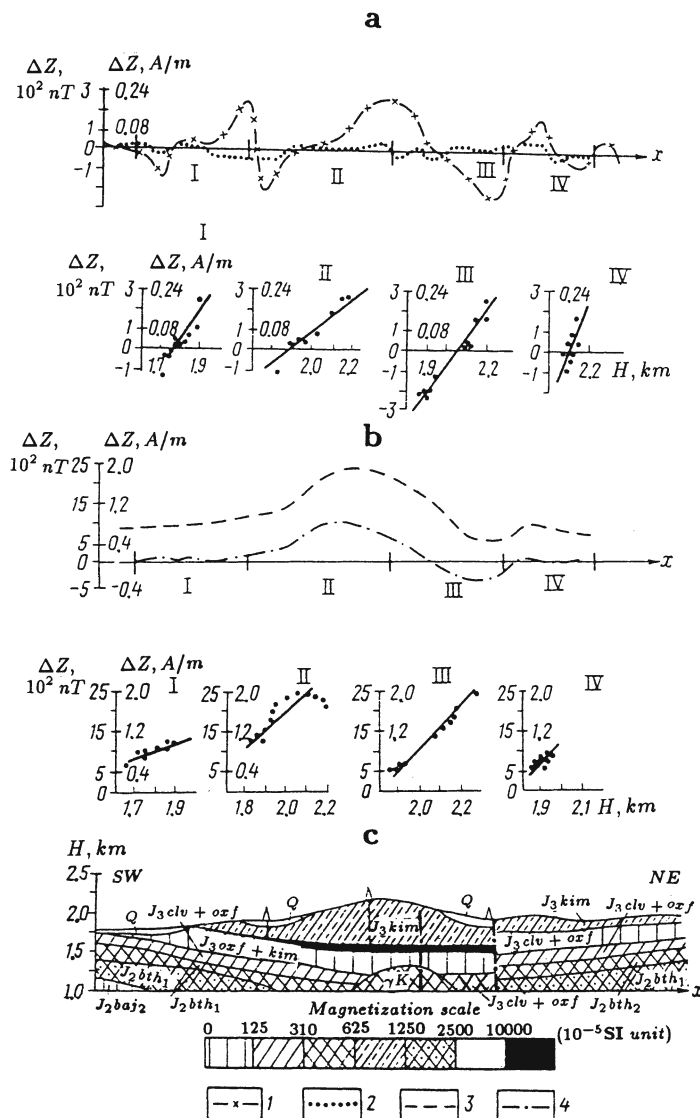


Fig. 5.7. Terrain correction by correlation method basing on ground survey data on a 1:25,000 scale (Dashkesan iron ore district): (a) magnetic field charts and approximating lines for the model c; (b) the same for the observed field; (c) petromagnetic section ( $\gamma K$  = hidden apophysis of the Dashkesan intrusive)

$\Delta Z$  field: (1) computed by the model c, (2) the same, corrected, (3) observed, (4) the same, corrected

in closer agreement with the concept of the field caused by a flat-dipping thin bed (of magnetite deposit) under oblique magnetization.

Along with the linear approximation of the relationship between the field and the height, approximations in the form of the square trinomial (parabolic equation) are appropriate here. Judging by the type of the parabola, one can get useful interpretation evidence. If its vertex is at the top, it means that the vertical gradient decreases with height, which is characteristic of uniform medium. If, however, it is at the bottom, then there are significant inhomogeneities present in the section. The parabolic characteristics carry some other information, too. It makes it possible to judge about the presence of the inhomogeneity and even about its features. However, it has been statistically proved that the parabolic approximation  $U(H)$  can be replaced by the linear approximation, when the correlation between the magnetic field and the relief is known [136].

To reduce correlation distortions, it is recommended, in general, to plot approximation lines for each individual element of the relief.

In the regions with flat-dipping geological boundaries, the features of rocks outcropping onto the earth's surface may markedly differ from those of the investigated section on the whole. In such regions it is expedient to draw unified approximating line by the correlation plotted for the whole surveying sheet. It will be a good idea to determine preliminarily the areas of correlation by visual analysis of geophysical and topographic maps.

The results of eliminating the topographic effect by the correlation technique (Fig.5.8) obtained in the Mekhmana ore district (Lesser Caucasus) can serve as an example. Regioning of the terrain relief was carried out in this district by the dip angles, comparing them with magnetic susceptibility data (see Fig.5.5). No correlation were observed in the zones 1, 4 and 5, which can be explained theoretically by the ratio of inclination angles of the relief and magnetization. For zone 2, the correlation formula is of the following form

$$\Delta Z = 0.765(H - 1150), \quad (5.14)$$

while for zone 3 it takes the form

$$\Delta Z = 1.135(H - 1280), \quad (5.15)$$

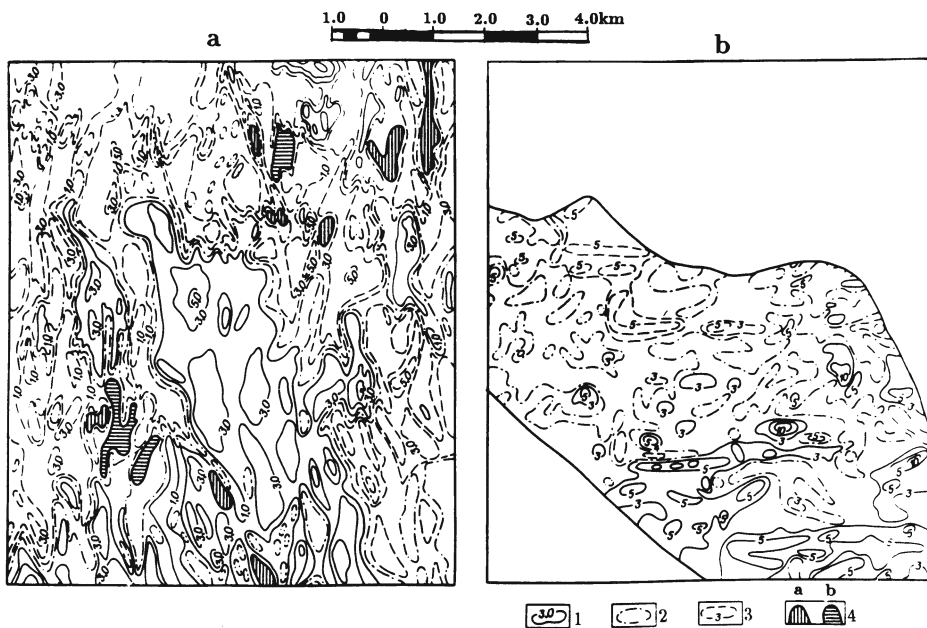


**Fig.5.8. Terrain correction by correlation method:** (a) observed magnetic field  $Z_{an}$ , (b) magnetic field  $Z_c$  corrected for topographic effect (1 – 3) isolines ( $n \cdot 100$  nT): (1) positive, (2) zero, (3) negative field; (4) sites of intense local anomalies: (a) positive, (b) negative

where  $H$  is measured in meters and  $Z$  in nanoTesla.

In Fig.5.8, the isogam map ( $Z_c$ ) drawn up for zones 2 and 3 is compared with the initial field chart. The figure shows that the anomalies and other field features presented in the initial chart have undergone drastic changes. The field pattern became simpler and the strikes of anomalies showed a marked deviation, some of them being smoothed. This allows for considerable reduction in the interpretation errors, and primarily the errors of the first kind (i.e. “false alarm”).

This method can be used to improve the choice of the level for reducing the field to one plane. When plotting a correlation chart, the compared areas of the largest dispersion with respect to

the averaging line correspond to the elevation of the points under which the targets are situated. The presence of dispersion in itself is indicative of the hidden inhomogeneity present in the section.

Examination of the correlation technique potentialities for eliminating the topographic effect shows that the method makes it possible to establish promptly the fact of the terrain relief influence, the presence and some peculiarities of hidden inhomogeneities, and to suppress or reduce the noise caused by the relief. If necessary, it allows to solve additional problems, i.e. to determine the mean magnetization of the medium and the vertical gradients of magnetic field.

Analysis of the spectral composition of geophysical and heights field improves the efficiency of the correlation method [80]. The magnetic field spectrum is much more differentiated and wider as compared to the heights spectrum. Therefore, a more distinct correlation is observed when using averaged values, rather than observed values of  $\Delta Z$  or  $\Delta T$ . If high-frequency magnetic components are involved in the correlation, the relationship is weakened. Such a weakened relationship in correlation at a high frequency testifies to the presence of such geological inhomogeneities as orebodies, dikes, etc.

#### 5.2.2.2 Terrain correction in other geophysical surveys

The correlation between the observed results and the terrain relief heights must be observed in the data obtained by different geophysical methods [216]. Each elevation of the relief with respect to the neighboring one can be considered as an additional pole or a line of poles that change the field intensity in the point of measurement. A sum of fields of such elements filling the relief forms tends to increase with increasing height of the observation point. Mathematical modeling confirms this relationship for an inclined ledge (except portions adjoining its horizontal faces) over which the increments of the total modulus of the magnetic field vector ( $\Delta T$ ), gravimetric and thermal field are computed (Fig.5.9).

According to the theoretical analysis [141], the potentialities of the statistical reduction have broad prospects in gravimetric prospecting at regional [134] and especially detailed investigation

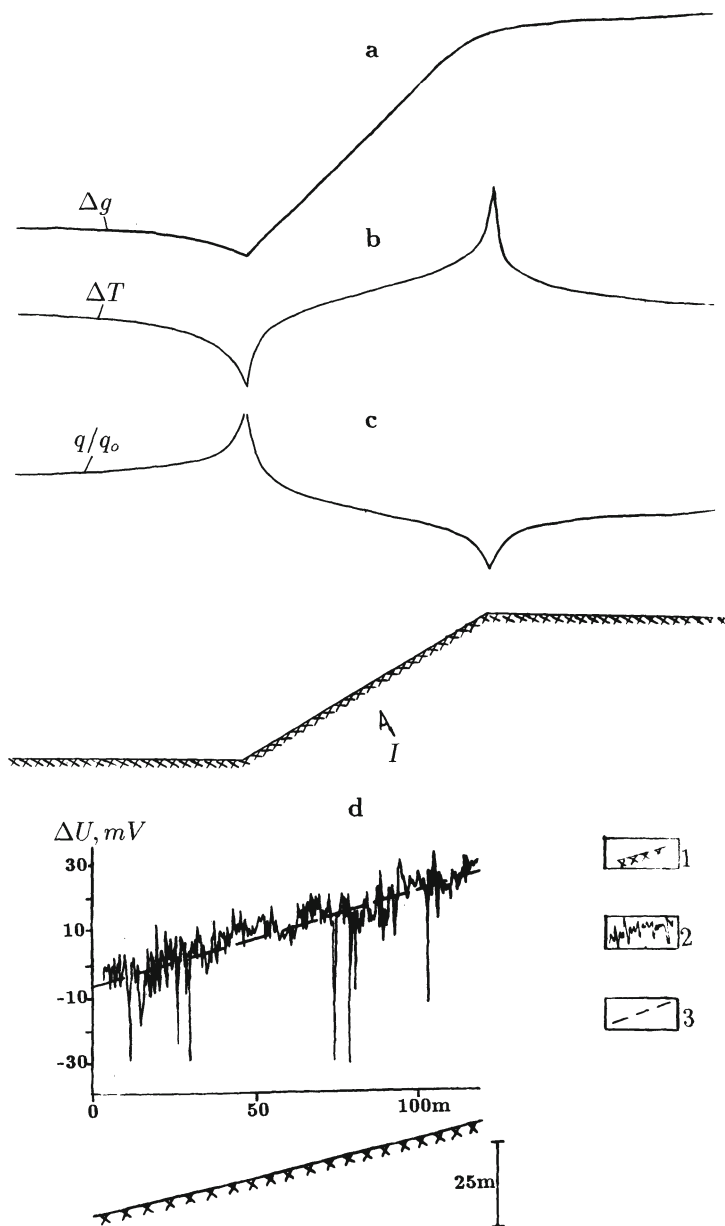


Fig.5.9. Substantiation of the correlation technique for terrain correction in gravimetric (a), magnetic (b) and thermal (c) prospecting, and SP (d) observations  
 (c) and (d) after [170] and [80], respectively  
 (a), (b) and (c) are model results, (d) is real observations on a slope  
 (1) observed SP plot, (2) approximating straight line, (3) relief form

[131,143].

Statistical reduction, which automatically accounts for defects of the Bouguer reduction described in the literature and, particularly, in [135], employs a simple correlation technique, since except the surrounding relief correction, all the corrections exhibit linear dependence on the observation point height. It can be shown that proceeding from the analytical expression of the inclined ledge (slope) gravitation, the attraction of typical relief forms is also linearly dependent on the height on the observation point. According to [141]

$$\Delta g = c + bh, \quad (5.16)$$

where  $c = 2G\sigma\alpha H_o$ ;  $b = 2\pi G\sigma$ ;  $G$  is the gravitational constant;  $\sigma$  is the density of rocks forming the ledge;  $\alpha$  is an acute angle between the inclined face of the ledge and its base;  $H_o$  is the vertical ledge thickness;  $h$  is the difference in levels between the observation point and the ledge base (if the ledge base is at the sea level, then  $h = H$ ).

The relationship between  $\Delta g$  and the difference between heights  $h$  becomes a correlation due to the presence of density inhomogeneities in the volume of the slope and beneath it, and also as a result of the deviation of the earth's surface from the inclined step.

Further inspection of the gravitational anomaly over the slope formed of homogeneous rocks discloses that corrections for relief  $g_r$ , in all points of the slope are equal and proportional to the ledge thickness and to the inclination angle of the relief. Therefore, on a homogeneous slope Bouguer anomalies  $\Delta g_B$  are constant and equal to the attraction of the ledge to the point at its base

$$\Delta g_B = 2G\sigma\alpha H_o. \quad (5.17)$$

Since  $\alpha < 0$ , then  $\Delta g_B < 0$ . When  $\sigma = 2.67 g/cm^3$  and  $\alpha = -30^\circ$ , it is found that  $\Delta g_B = -g_r = -18.6 H_o$  (mGal), where  $H_o$  is expressed in kilometers.

The estimation of  $g_r$  value thus obtained is supported by the results of computing terrain corrections. In practice, these corrections are added to  $\Delta g_B$ , which is usually used as an alternative to the value of the anomaly in topographic reduction ( $\Delta g_T$ ). Therefore, Bouguer anomalies (assumed to be local topographic anomalies) must be equal to zero, provided that the intermediate layer is accounted for correctly and geologic inhomogeneities are absent

Owing to the above defect of the Bouguer reduction, the correlation  $\Delta g = f(H)$  is registered.

The above mentioned paper [141] has shown that the correlation technique is appropriate in considering the terrain relief effect on the free-air anomaly ( $\Delta g_{f.a.}$ ). This is confirmed by a rigorous formula derived by the authors

$$\Delta g_{f.a.} = c_1 + bh, \quad (5.18)$$

where  $c_1 = 2\pi G\sigma H_1 + c$ ;  $H_1$  is the height of the ledge base.

If local geological and topographic inhomogeneities are present, their gravitational effect ( $\Delta g_{an}$  and  $\Delta g_r$ , respectively) may be written as

$$\Delta g_{an} + \Delta g_r = \Delta g_{obs} - g_{corr}, \quad (5.19)$$

where  $g_{corr}$  is the correction determined from the straight line plot of (5.16) type;  $\Delta g_{obs}$  is the relative observed value of the acceleration of free fall ( $\Delta g_{obs} = g_{obs} - \gamma_o$ . Here  $g_{obs}$  stands for the measured acceleration of free fall on the earth's surface, and  $\gamma_o$  stands for the normal acceleration of free fall on the earth's surface).

Obviously, the density of the inclined slope forming rock can be determined using formulas (5.16) – (5.19). The absolute value of  $\Delta g_r$  is slightly varied in detailed investigations. Therefore, the comparison between the statistical anomalies

$$\Delta g_s = \Delta g_{obs} - g_{corr} \quad (5.20)$$

and the local topographic (Bouguer) anomalies shows the possibility of applying the statistical reduction (correlation technique) to singling out quick anomalies in the area of the Katsdag ore deposit (southern slope of the Greater Caucasus). Similar results have been obtained during detailed investigations in Karatau, Kazakhstan.

To support the corresponding postulate theoretically by a direct problem solution is very difficult in electric prospecting. The possibility of the correlation approach, proposed in [131] is corroborated by the results of observations using widely-used modifications and physical modeling. They testify to the applicability of correlation technique for eliminating the terrain relief effect in profiling and in *SP* (see Fig.5.9), *IP* and *VLF* methods [139]. Fig.5.10 illustrates the results of applying the correlation technique to a model of *IP* field.

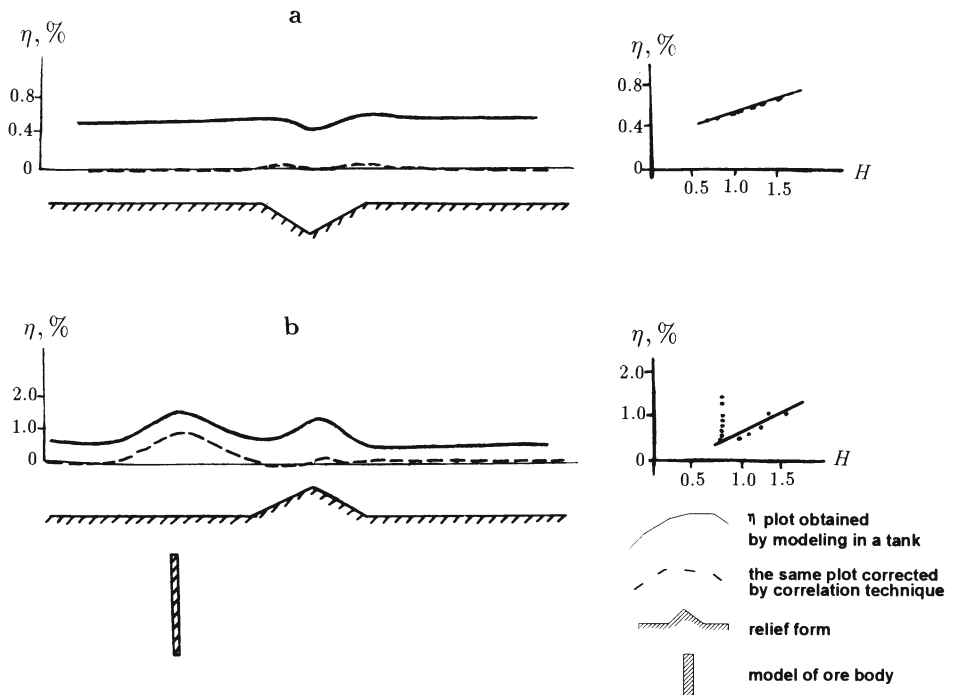


Fig.5.10. Correlation technique testing for terrain correction in the IP method for negative relief form (a), positive relief form with an orebody laying aside (b)

Characteristically, a swarm of points is present in the correlation field caused by the anomalous object.

#### 5.2.2.3 Conducting a correlation procedure

By way of example, consider the procedure of using this technique in investigations by VLF method [76]. The principle of the technique consists in obtaining a linear approximation of the relationship between the recorded field ( $U$ ) and the height of the observation point ( $h$ ), and employing this approximation for computing topographic correction.

The elimination of the terrain relief effect involves three steps:

(1) Plotting of correlation field  $U = f(h)$ . In order to improve the accuracy, correlation fields for individual elements of the relief (for example, for two parts of the slope differing in inclination

angle) are computed separately. The portions of the slope with different geological and, hence, physical characteristics, but equal relief inclination angle should be also considered separately. The number of points used for the computation must be no less than 15–20. The set of points within a narrow range of  $h$  values suggests a hidden inhomogeneity in this range indicated by considerable variations in the amplitude of  $U$ . These portions of the correlation field are ignored when computing approximate straight lines.

(2) Determination of approximate line factors (regression equations)  $b$  and  $c$ .

Terrain corrections are determined from the equation

$$U_{appr} = c + bh. \quad (5.21)$$

(3) Obtaining the corrected values of  $U_{corr}$  in the observation points

$$U_{corr} = U_{obs} - U_{appr}. \quad (5.22)$$

Fig.5.11 shows [73] that the negative topographic anomaly of high intensity impedes interpretation of the plot of the total horizontal component of the VLF electromagnetic field ( $H_{\phi_{obs}}$ )<sup>4</sup>. Three correlation fields were plotted here: one for the southern and two for the northern slope (under the condition of rock variations characterized by different conductivity). All the three regression equations were derived using the least-square method. Table 5.2 sets out the results of computation.

**Table 5.2. Correlation coefficients ( $r$ ) and regression equations for three portions of the profile crossing the Kyzylbulakh deposit**

Profile portion	$r$ value	Regression equation
I	0.96	$H_{\phi_{appr}} = 118 + (3.75 \pm 1.16)h$
II	0.95	$H_{\phi_{appr}} = 103 + (5.60 \pm 1.80)h$
III	0.54	$H_{\phi_{appr}} = 263 + (0.88 \pm 1.37)h$

An anomaly from the anomalous (ore) body is apparent in the northern part of the profile in  $H_{\phi_{corr}}$  plot after the correction for

<sup>4</sup>  $H_{\phi}$  component values (as well as other components of the VLF magnetic field) are given in microVolts due to specific features of the Soviet (Russian) apparatus SDVR-4

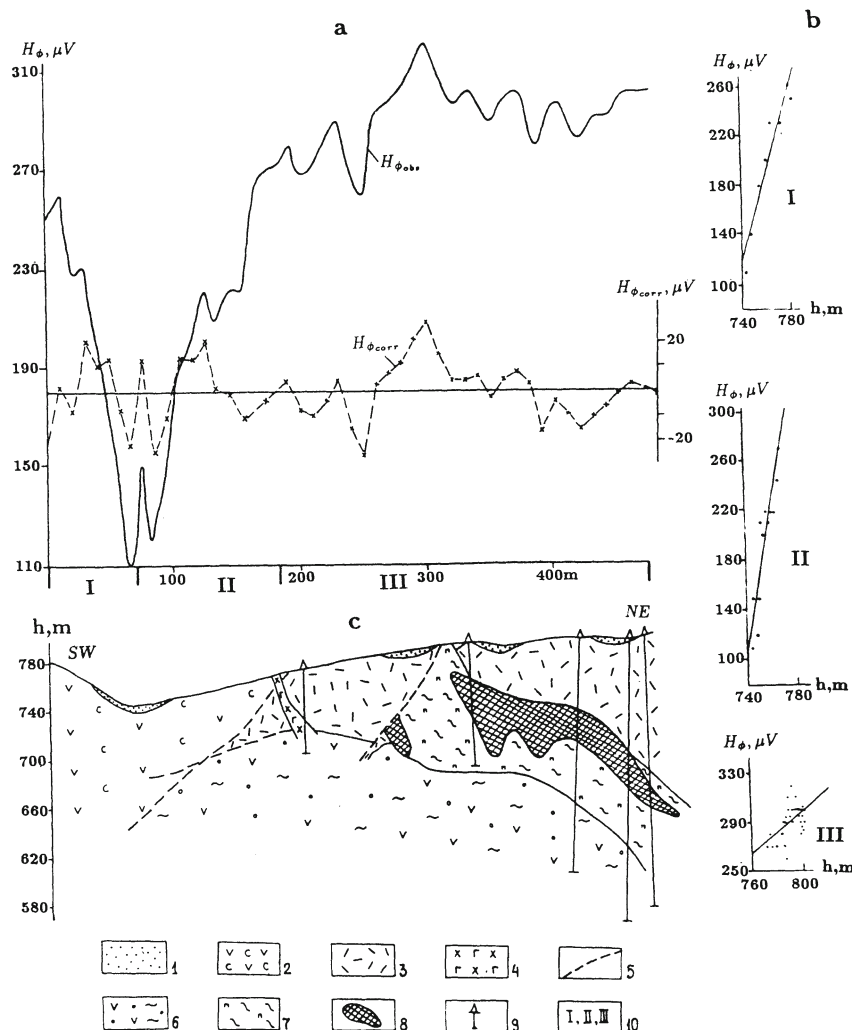


Fig. 5.11. Correlation technique for eliminating terrain relief effect on a portion of the Kyzylbulakh gold-pyrite deposit: (a) plots of observed  $H_\phi_{obs}$  and corrected  $H_\phi_{corr}$  values, (b) correlation, (c) geological section

- (1) deluvial deposits;
- (2) tuffs and lavas of andesitic porphyrites;
- (3) tuffs of liparite-dacitic porphyrites;
- (4) dike of andesite-basalts;
- (5) disjunctive dislocations,
- (6) pyritized and quartzized andesitic porphyrites,
- (7) zone of boudinage and crumpling,
- (8) orebodies,
- (9) prospecting boreholes,
- (10) profile intervals for plotting correlation field  $H_\phi = f(h)$

the relief effect. Its form is similar to the anomalies obtained by physical simulation of flat dipping thin bed [99], which is in good agreement with the available geological data.

Thus, the correlation technique makes it possible not only to eliminate promptly the terrain relief effect, but also to reveal its influence and hidden geological inhomogeneities deriving additional information by the type of correlation. The approximate relationship plot contains information on physical properties of the medium, which enabled us to suggest a special technique described in the next Subection.

### **5.2.3 The use of topographic complexity and height field for deriving additional geological and geophysical data**

#### **5.2.3.1 Estimation of magnetization inclination and information value using $\Delta T$ and $\Delta Z$ observations on the inclined relief**

Two approaches are usually applied for the determination of inclination and value of rock magnetization: (1) Sampling and measurements of oriented samples; (2)  $I_e$  vector selection according to the observed magnetic field (physico-geological modeling). The first way requires considerable additional work. In this case negative effects of near-surface rock alterations and local  $I_e$  variations are not completely excluded. The efficiency of the second approach is conditioned by the reliability of the model of the medium. However, as a rule, reasonable data are absent at the initial stage of a new area study, that is, when the magnetization evaluation is necessary for the design of following survey and interpretation of magnetic anomalies. Hence, the method of  $I_e$  determination according to observed magnetic field using minimum assumptions relevant to geological structure and physical properties of rocks very expedient.

For aeromagnetic survey at a small clearance elevation over the land and for ground magnetic mapping, a linear dependence between the magnetic field and heights of ledge is fixed in the central part of a slope [146]. In case of oblique magnetization, analytical expressions for vertical  $Z_d$  component and  $\Delta T$  field over a slope (inclined at an

angle  $\alpha$ ) are the following:

$$Z_d = -2\pi I_e \sin \alpha \cos(\phi_m - \alpha) + 8I_e \sin(\phi_m - \alpha) h/R, \quad (5.23)$$

$$\Delta T = -2\pi I_e \sin \alpha \cos(\phi_m - \tau_o - \alpha) + 8I_e C_o \sin(\phi_m - \tau_o - \alpha) h/R. \quad (5.24)$$

Here  $I_e$  is the projection of magnetization vector on vertical plane transverse to the strike of the ledge;  $\phi_m$  is the angle of inclination of the magnetization projection  $I_{xz}$  to the horizon;  $h$  is the elevation of the observation point with respect to the middle of the ledge;  $R$  is the length of the ledge;  $C_o$  is  $\sin i_o / \sin \phi_o$ ;  $i_o$  is the geomagnetic inclination;  $\tau_o = 90^\circ - \phi_o$  is the angle completing the geomagnetic inclination to the vertical in the plane of profile;  $\phi_o$  is the angle of inclination of the geomagnetic field vector projection on the plane of profile to the horizon.

We assign:

$$c_d = -2\pi I_e \sin \alpha \cos(\phi_m - \alpha), \quad (5.25)$$

$$b_d = [8I_e \sin(\phi_m - \alpha)]/R, \quad (5.26)$$

$$c = -2\pi I_e \sin \alpha \cos(\phi_m - \tau_o - \alpha), \quad (5.27)$$

$$b = [8I_e C_o \sin(\phi_m - \tau_o - \alpha)]/R. \quad (5.28)$$

As a result we obtain:

$$Z_d = c_d + b_d h, \quad (5.29)$$

$$\Delta T = c + b h, \quad (5.30)$$

i.e. equation of linear relation.

Under real conditions, in consequence of fluctuation of heights and magnetic parameters, the linear relation (5.30) becomes a correlation one. Coefficients in equation (5.30) can be easily determined using the least square method. When  $Z_d$  and  $\Delta T$  observations are available, using these coefficients, it is possible to define not only the value, but also the direction of magnetization vector [142]. Then:

$$\cot(\phi_m - \alpha) = \left( \cos \tau_o - \frac{b}{b_d C_o} \right) / \sin \tau_o. \quad (5.31)$$

This equation is simplified, when the profile is oriented at an acute angle to the magnetic meridian ( $C_o \approx 1$ ).

It follows from the equation (5.31) that the invention [142] does not require the knowledge of normal magnetic field. After  $\phi_m$  value definition, it is possible to determine  $I_e$  value from  $b$  and  $b_d$  coefficients. This technique was successfully applied at the Lesser Caucasus and in other regions of the former USSR.

Fig.5.12 exemplifies such computations based on the results of investigations carried out in the Mekhmana ore district of the Lesser Caucasus.

The investigated rocks (volcanites of the Bajocian of the basic and intermediate composition) were found to be magnetized in parallel with the Earth's field, and the mean  $I_e$  value is in accord with the results of measurements on samples.

In the Belokan-Zakatala ore district (Greater Caucasus) it was also revealed, using the above method, that shales and sandstones of the Aalenian are magnetized in parallel to the Earth's field, and their magnetization (in the range of 30 to 70 mA/m) is closer to the upper limit of the results obtained on samples. The latter results from the fact that when measuring surface rocks, we underestimate the magnetization. It can be determined more accurately with the use of the recommended technique, where a great volume of rock is studied in its natural bedding.

### **5.2.3.2 Estimation of the magnetization inclination and value using the correlation between $\Delta T$ field and the elevations of measurement site**

When only  $\Delta T$  observations are available, using the data on  $c$  and  $b$  factors, it is, generally speaking, possible to calculate the value and inclination of magnetization.  $C_d$  factor depends on local level of the normal geomagnetic field. If the normal field is excluded, expression for  $\phi_m$  determination can be obtained after dividing the equation (5.27) by equation (5.28).  $\phi_m$  value will be substituted in equation (5.28) and subsequently  $I_e$  value will be obtained. If the factor  $b$  is calculated in nanoTesla/meter, then  $I_e$  value (in milliAmper/meter) should be multiplied by the coefficient 0.1.

But if the normal field is not excluded, this solution is unsuitable. What is the way out?

Let us consider two mating slopes with the same magnetization

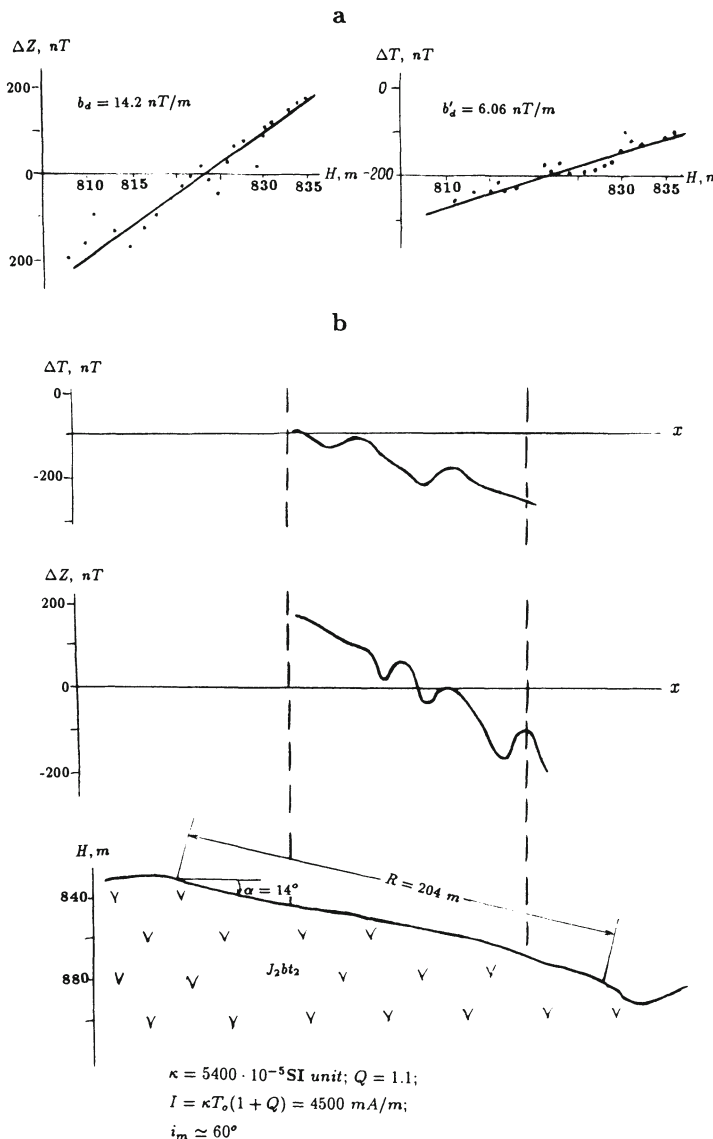


Fig. 5.12. Determining the value and direction of rock magnetization in natural occurrence by the observations of  $\Delta T$  and  $\Delta Z$  on a sloping relief: (a) determination of coefficients  $b_d$  and  $b'_d$ , (b)  $\Delta T$  and  $\Delta Z$  curves, and geological section along the observation profile

and their magnetic fields (Fig. 5.13).

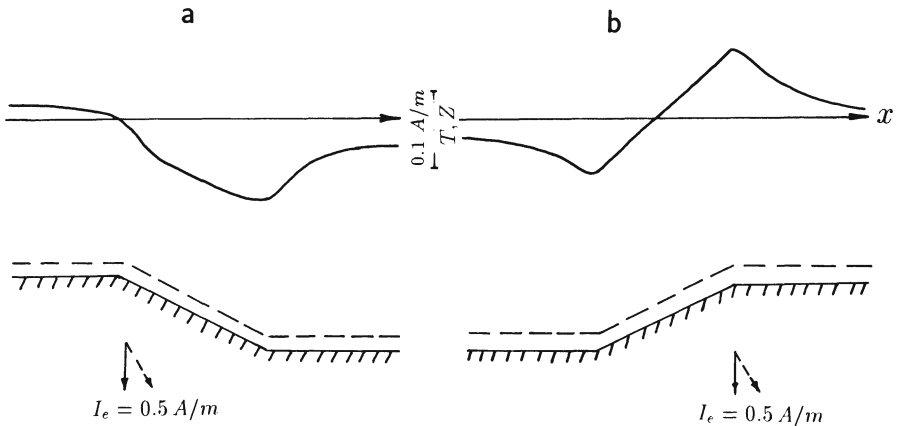


Fig. 5.13.  $\Delta T_a$  model curves for vertical magnetization (or  $Z_a$  for  $60^\circ$  inclination of  $\mathbf{I}_e$  vector) at the level of 100 m over two inclined ledges (a and b)

Let “b” ledge be the first (the slope rises from south to north, i.e. “southern” ledge) and “a” ledge – the second (slope dips from south to north, i.e. “northern” ledge). Then  $b_1$ ,  $R_1$  and  $\alpha_1$  values characterize the southern ledge ( $\alpha_1$  is negative), and  $b_2$ ,  $R_2$  and  $\alpha_2$  values characterize the northern ledge ( $\alpha_2$  is positive). Two pictures taken together make a meridional profile across a valley.

Let us consider a general case when two mating slopes are both composed of the same rock, and  $\phi_m$  is unknown. In this case the magnetization of these ledges is  $\mathbf{I}_e$ . Then:

$$0.1C_o 8I_e = \frac{b_1 R_1}{\sin(\phi_m - \tau_o - \alpha_1)}, \quad (5.32)$$

$$0.1C_o 8I_e = \frac{b_2 R_2}{\sin(\phi_m - \tau_o - \alpha_2)}. \quad (5.33)$$

We equate the two expressions:

$$\frac{b_1 R_1}{\sin(\phi_m - \tau_o - \alpha_1)} = \frac{b_2 R_2}{\sin(\phi_m - \tau_o - \alpha_2)}. \quad (5.34)$$

After several transformations we have:

$$\tan \phi_m = B/A, \quad (5.35)$$

where

$$A = b_2 R_2 \cos(\tau_o + \alpha_1) - b_1 R_1 \cos(\tau_o + \alpha_2),$$

$$B = b_2 R_2 \sin(\tau_o + \alpha_1) - b_1 R_1 \sin(\tau_o + \alpha_2).$$

The inclination angle of magnetization projection  $I_{xz}$  to the horizon  $\phi_m$  is determined by the expression (5.35), which has two possible solutions. It is possible to receive an exact  $\phi_m$  value (Table 5.3) by considering the sign of  $\phi_m$  and kind of correlation  $\Delta T$  vs  $h$ .

**Table 5.3. The determination of magnetization direction**

Sign of $\phi_m$	Kind of correlation $\Delta T$ vs $h$ for a ledge:		Quadrant	$\phi_m, {}^\circ$
	northern	southern		
+	inverse	direct	I	acute angle $\phi_{m,0}$
+	direct	inverse	III	$-180 + \phi_{m,0}$
-	direct	direct	II	$180 + \phi_{m,0}$
-	inverse	inverse	IV	$-\phi_{m,0}$

The quantity  $\phi_m$  is substituted to the equation (5.32) or equation (5.33), and subsequently  $I_e$  is obtained. To exclude mutual disturbances, the distance between ledges "b" and "a" has to be sufficiently long. Northern slope ("a") must be also sufficiently long.

For the verification of this method, checking on a model is most reliable. Magnetic field on the height of 100 m over the model was computed by developed 3-D program (see Appendix B). The model with the extent of 30 km along the strike and thickness of 15 km was investigated (Fig.5.14).

All slopes in Fig.5.14 are numbered from the south to the north. Their length ( $R$ ),  $H$  (height of ledge), dip angle ( $\alpha$ ) and also  $b$  factor and magnetization parameters are shown in Table 5.4. Magnetization in milliAmper/meter (numerator) and slope number (denominator) are presented at the bottom of Fig.5.14. Intervals of  $b$  factor determination (middle part of slope) are hatched by horizontal lines.

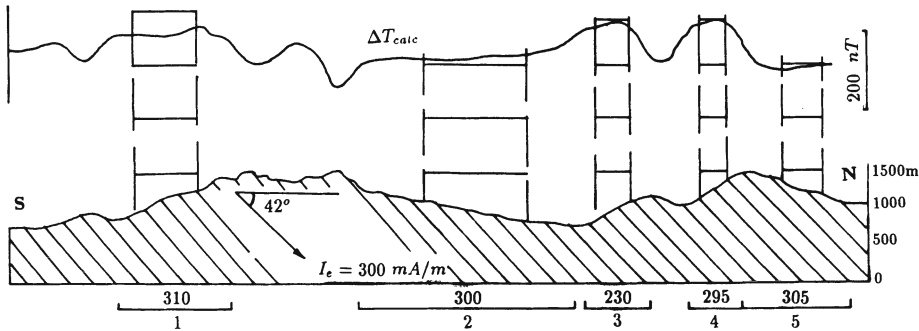


Fig. 5.14. Determination of model magnetization by the new correlation method

In Table 5.4 the average  $I_e$  and  $i_m$  values are  $290 \text{ mA/m}$  and  $39^\circ$ , respectively. The values of  $300 \text{ mA/m}$  and  $42^\circ$ , respectively, were used during the direct problem solution. Thus, the accuracy of average value determination is in the range of 5% for magnetization and 10% for its dip angle. The greatest divergence reaches 25%. In general, the best accuracy of similar investigations is 10% and permissible precision is 30% [212]. Therefore, model examination allows to utilize the above described method.

Precambrian crystalline rocks in Sinai [21] were investigated by this method using aeromagnetic map on a scale of 1:50,000 [156]. Vector  $\mathbf{I}_e$  was also studied using the interpretation of  $\Delta T$  anomalies by rapid methods of inverse problem solution. They were developed for inclined magnetization characterizing the regions of central and low latitudes [146]. These methods allow to estimate the anomalous body magnetization and the generalized angle  $\theta$  which includes the difference between body dip and  $\mathbf{I}_e$  direction. Many kappametrical measurements of sample collections were also performed. Their results basically agree with the results of  $\Delta T$  field analysis obtained by above-mentioned methods. In Table 5.5 are represented the effective magnetization  $I_e$  and inductive magnetization  $I_i$  by the magnetic susceptibility  $\kappa$  and Earth's magnetic field  $T$ .

**Table 5.4. Determination of magnetization for a model (see Fig.5.14)**

Slope	$H, \text{m}$	$R, \text{m}$	$\alpha, {}^\circ$	$b$	$\phi_m, {}^\circ$	$I_e, \text{mA/m}$
1	490	1540	-18.6	0.04	44	310
2	455	2800	9.4	-0.02	40	300
3	350	700	-30.0	0.10		230
4	420	770	-33.0	0.09	33	295
5	420	1340	18.3	-0.10		305
Average values				39		290

It was found that granite-metamorphic basement had, in general, low magnetization. Essential magnetic rocks are distributed in local areas and can not generate considerable magnetic anomalies in the case of deep burial. In southern Israel sources of similar anomalies might be located within the Phanerozoic section. It was hitherto speculated that main sources of these anomalies were associated with Precambrian basement.

Most of obtained magnetization inclinations of Precambrian rocks of Sinai were clustered around modern magnetic field inclination ( $44^\circ$ ). Inverse magnetization was also observed, resulting in a decrease in effective magnetization as a whole. The vertical or sub-vertical  $\mathbf{I}_e$  vectors, most likely, correspond to hidden dike-like bodies including Katharina ring dike.

These data showing a low magnetization of Precambrian rocks in Sinai are significant for a reinterpretation of magnetic field. This suggests the necessity of revaluation of some conceptions regarding different thickness of a sedimentary cover over separate tectonic blocks and their corresponding oil-and-gas potential.

The present correlation method can be further modernized. The integration of the correlation method with kappametrical research opens up new opportunities for the determination of effective angle and the value of natural remanent magnetization ( $\mathbf{I}_n$ ). Combination of this method with paleomagnetic investigation would make it possible to separate  $\mathbf{I}_n$  value into two components: (a) caused by magnetic field that acted during rock formation; (b) caused by other

**Table 5.5.  $I_e$  vector and kappametrical data for exposed rocks of Upper Precambrian in Sinai**

Rock	Correlation method		Median $\kappa$ value, $10^{-5}$ SI unit	$I_t = \kappa T$ , $mA/m$
	$\phi_m, {}^\circ$	$I_e, mA/m$		
Alkaline magmatic series				
Sharm granite	39	135	440	190
- " -	58	1650	1000	430
Calc-alkaline magmatic series				
Umm-Malaq granite	59	500	600	260
Girgar granite	31	850	700	300
Ghashi granite	107	610	800	350
Granitoid	-88	590	350	150
Quartz-diorite and gabbro	43	960	500	220
Diorite and metamorphite	31	320	1000	430
Volcanics of Ferani group	-76	640	1000	430
Metamorphic series				
Granite-gneiss	43	990	600	260

factors.

### 5.2.3.3 Derivation of geological information from the topography complexity

It is expedient to point out the advantages of direct use of topographic maps for geological purposes, which is well-known in geomorphology. Topographic data (digital terrain models) are used to determine topographic corrections in geophysics. However, the data on the terrain relief (height field) in processing and interpreting geophysical observations can be a source of additional geological information.

Geological regularities, which manifest themselves in mountainous relief structure, can be stressed by treating the height field of the area by the techniques employed in geophysical field analysis. For example, application of the predominant strikes of relief isohypsues

for ore prediction was reported by Borovko [38]. Later in [135] it was shown that this transformation allows to single out a very important indicator of endogenic deposits of various compositions and origins (Fig.5.15). Large deposits tend to occur in the corners of blocks having a predominant strike of isohypsces different from the Caucasian on the whole. Therefore, the corresponding areas (with due account of other data) were recommended for drilling deep test wells in the mountainous regions of Azerbaijan.

The relief complexity, which, as described above, governs the spatial distribution of topographic corrections, can be estimated by the map of the specific sinuosity of height isolines. Khesin [6] proposed to apply the specific sinuosity of isolines (*SSI*) for characterizing the complexity of geophysical field.

It is determined as follows: (1) the total length of isolines (*L*) for a given field is computed within a sliding area, (2) area *S* on the sliding cell is determined and (3) the parameter

$$SSI = KL/S \quad (5.36)$$

is computed, where *K* is the scale factor for converting *L* into kilometers, and *S* – into square kilometers.

The *SSI* is, thus, measured in  $km/km^2$ , and the value obtained refers to the center of this cell.

The map not only characterizes the complexity of the terrain relief and determines the requirements for eliminating its effect, but also allows for geological interpretation. For example, when analyzing the large-scale data on the Mekhmana ore district (Nagorny Karabakh), it was established that the oldest associations from the Lower Bathonian are characterized by a reduced specific sinuosity of horizontals, whereas in the areas of younger rocks a corresponding increase is observed. This parameter increases also along disjunctive dislocations, and axes of synclines.

To summarize, the application of height field transformations adds to the informativity of a set of geophysical investigations practically without any expenditures, since the terrain heights data employed are prepared, in any case, for topographic effect consideration. These transformations of digital terrain model can be executed together with the geophysical fields conversion using programs developed for computing field entropy, curvature or standard

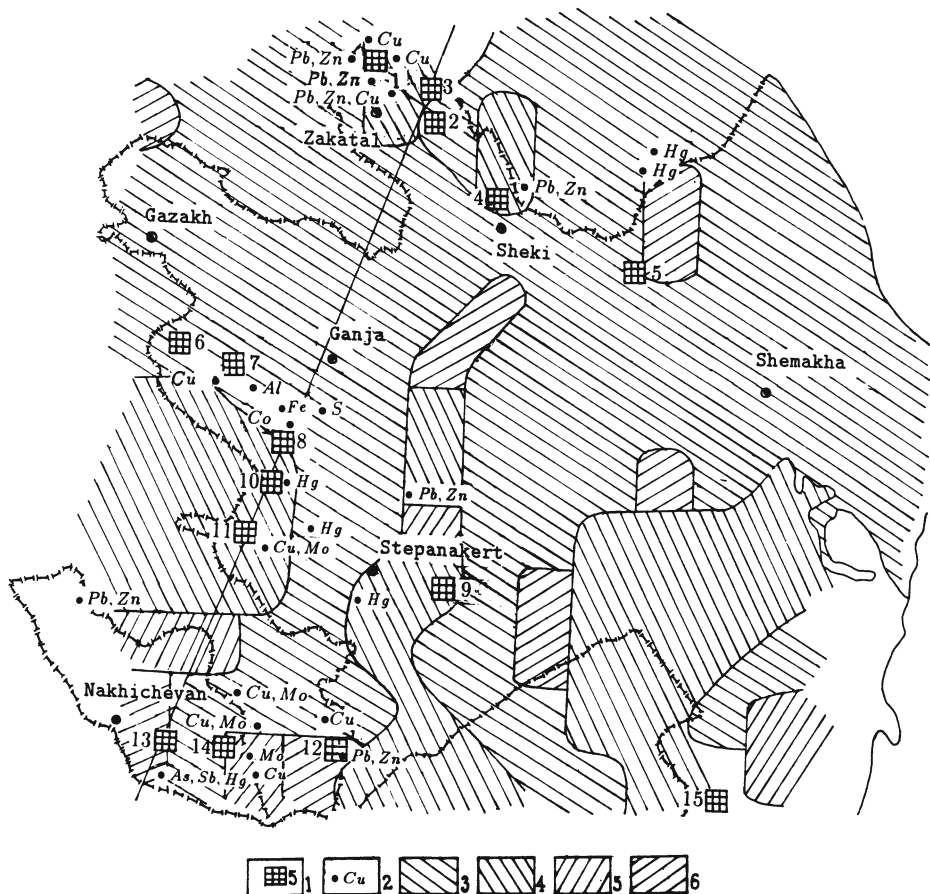


Fig.5.15. Test well drilling site pattern in mountainous regions of Azerbaijan

(1) sites recommended for test well drilling and their numbers; (2) ore deposits; predominant courses of terrain relief isohypsес: (3) W.N.W., (4) N.N.W., (5) N.E., (6) E.N.E.

deviation. Obviously, a spatial distribution of the entropy values will be close to the distribution of the  $SSI$  parameter.

## 5.3 Execution of transformations

### 5.3.1 General characteristic of the problems to be solved and field transformations

To single out certain features of geological structure or objects of the desired class, the researcher has to transform the geophysical field observed for obtaining secondary indicators. The necessity for secondary indicators of the targets required for the interpretation arises at the stage of the initial model formation (see Section 4.2). The methods of deriving them from the initial field, i.e. types and parameters of transformations, are suggested at this stage.

Singling out a hidden body is rather often reduced to revealing a weak anomaly of geophysical field. By this term we mean an anomaly with a mean square close to the mean square (dispersion) of a random normally distributed centered (having a zero mean value) noise. Rather often, an anomaly is thought to be weak if its maximum amplitude is equal to the triple standard deviation. Any components of the investigated field, its characteristics (ruggedness, dispersion), intersection of anomalies with different strikes may be considered as an anomaly. In the latter case, a distribution of two components of the same field is studied, i.e. an anomaly in 2-D space of indicators. Therefore, the computation of the parameter  $I_{cr}$  for localizing structure intersections according to the data of one method (see Subsection 5.3.5) is a particular procedure employed in the integrated interpretation (see Section 8.3.3).

Useful anomalies should be singled out against the background of regular field noise caused by the sources which are of no interest to the researcher and random noise due to instrumental error and fluctuations conditioned by minor inhomogeneities of the medium. This is accomplished by means of smoothing, upward continuation, averaging, computation of local and circular (differential) anomalies, and horizontal and vertical gradients of the geophysical fields [174].

The notions of an anomaly, regional background and random

noise are relative. This relative nature can be reflected in the initial model of the medium. Not only local, but also regional anomalies and even individual components of noise may be of interest (save for noises associated with observation errors containing no geophysical information). In different problems, the same anomalous field components may be considered either as a noise, or as useful local anomalies, or else, as a regional background.

As a result of various transformations and correlation analysis some components of the observed fields are singled out, and others, which are of no value for the given geological problem, are suppressed. These conversions employing various statistical properties of useful signals and noises are directed to the solution of problems of frequency or azimuth filtering [12,90].

The techniques of conversion are based on integrating and calculating the moments of the observed field distribution. For instance, upward continuation is carried out by integrating within certain limits. In this procedure the field values are multiplied by weighting coefficients, which tend to diminish with increasing distance from the point where the transformation (convolution) is accomplished. Computing of correlation functions is of a similar character, when the values of the observed field (autocorrelation) or the field on the neighboring profile (cross-correlation) or ordinates of the given signal (inverse probability method) serve as weighting coefficients.

The effectiveness of the methods of inverse probability [53,207] and cross-correlation [248] is well known. So is the importance of upward continuation and averaging (their results being close), computation of such parameters as predominant strikes, horizontal gradients, residual and differential anomalies. But in each case it is necessary to select the parameter of conversion (averaging radius, height of continuation, dimension of the sliding interval), taking into account geological and geophysical conditions and the aim of the investigation.

When selecting the transformation parameters to fit the character of the revealed (or suppressed) effects, the researcher should also consider that the transforms obtained from different fields have to be in agreement. Anomalies can be separated from the objects of various classes, if there is a difference in their characteristics, which determines the intensity and extension of anomalies, and

in their position. However, in many cases the differences are not large. Rather often a geophysical field is fairly homogeneous in its mean intensity, but heterogeneous in terms of variability in local areas. Under such conditions amplitude filtering is ineffective and, therefore, the methods for deriving information are necessary that exploit the differences in other characteristics of the objects, such as computation of the field ruggedness, predominant strike of isolines, entropy, singling out the nodes of intersecting structures, etc.

The main types of conversion are listed in Table 5.6.

**Table 5.6. The main problems of transformation and methods of treating them**

Problem	Method of solving
Singling out regional isometric anomalies	Averaging [281] Sliding averaging Quantiles (including median [38]) Upward continuation Smoothing with polynomials
Singling out local isometric anomalies	Derivatives of higher order [177] Variations [12,103] Downward continuation [257]
Revealing linear anomalies of non-unidirectional type	Horizontal gradients Anisotropic graticules Self-setting filtering Determination of predominant strikes
Singling out and tracing anomalies of approximately known shape or strike	Inverse probability Cross-correlation [248] Sign correlation [6]
Revealing hidden nodes of anomalies of different strikes	Accentuating of structure intersection areas [131]

A set of results obtained by various transformations makes up the indicator space observed to be used in further analysis.

Oblique magnetization complicates the target indicators. To take this into account when forming the standard indicator space, one has to use the standards appropriate to the conditions of oblique

magnetization at the stage of developing the initial model of the medium.

Oblique magnetization does not impede transformations, which are invariant with respect to it. If field transformations are based on the solution of Dirichlet's problem and those of Neumann for Laplace's equation, it can be shown that corresponding calculation formulas as applied to magnetic field components have been derived without any assumption of vertical magnetization. Thus, the field under oblique magnetization is converted into the field of the same magnetization [90]. This considerably enhances the role of transformations in the interpretation of anomalies under the condition of oblique magnetization and oblique polarization, in general. It should be noted that a well-known technique of the reduction to the pole, eliminating the oblique magnetization effect, is efficient only for some environments (see Subsection 7.2.4). Blakely [33] points out that this technique is not applicable to the magnetic observations in low latitude regions.

Conversions can be executed also for the inclined linear profile of extended type (as compared to the depth of occurrence and the height of continuation), i.e. they are true for inclined semiplane (inclined semispace). In this case, the conversion line must be parallel with the inclined observation profile (see Section 2.2).

The possibility of upward and downward continuations, averaging, computing the horizontal component  $X$  by the field  $Z$  and  $\Delta T$  value by the field values of  $Z$  and  $X$ , vertical and horizontal gradients by anomalies of  $Z$  and  $\Delta T$  in horizontal position is beyond any doubt, as the curves are specified in the horizontal profile points. It is also clear that with a proper accuracy of transformation, the interpretation of transform's curves results in obtaining parameters, in particular, coordinates of a fictitious body (see Section 2.2). Formulas for converting the parameters of the fictitious body to those of the real object for various fields are set forth in Section 2.2 and further in Section 7.2.

For the qualitative interpretation of field isoline charts observed in mountainous regions, continuation of the field should be executed along the vertical without any displacement, since fictitious bodies are considered here, and information on the real anomalous bodies is absent before quantitative interpretation. In contrast, it is more

expedient to perform the analysis of the spatial field structure observed on the inclined profile in inclined coordinates, making field continuation along the normal to the profile. This method provides a correct mutual arrangement of inclined continuation levels, transforms on different levels, which is not the case in the former variant.

It is also advantageous to use the oblique coordinates for reducing the field with complicated observation line to an inclined line. The reduction by the methods based on Poisson's integral is appropriate also in the case of inclined semispace: observation points on the profile of complicated shape are "transferred" along the normal to the inclined reduction line onto this straight line, while the real anomalous bodies remain in their places. The inclined reduction plane can be selected most close to the maximum of the observation profile relief (see Fig.2.2). Here, the origin of coordinates in the inclined system may be chosen arbitrarily.

Both the transformation parameters and their types are determined roughly when devising a model of the medium. Therefore, it is a good practice to compute some other transforms and to employ additional parameters of conversions, because a certain redundancy of the observed indicator space is advisable. Given a proper software and peripherals, deriving additional transforms of different type or parameters presents no problem. It is essential that corresponding requirements were substantiated and qualified during the development of the model of the medium.

When computing indicators (transforms), the researcher should control the accuracy of computation by selecting computer programs. The accuracy can be checked on models by comparing the results of direct transform computation with those obtained by corresponding conversion of the initial field.

To make good the loss on the conversion area edges, it is necessary to transform the field on a surplus area (exceeding the size of the area investigated). This is realized by employing the available geophysical data of the same or smaller scale. Extrapolation beyond the survey area edges is admissible for developing the initial digital model of the field or an isoline chart. The type of extrapolation (linear or more complicated) is determined by the field pattern on the area edges.

### 5.3.2 Field separation into regional and local isotropic components

Various techniques of averaging are used to single out regional isometric anomalies. Among them, the method developed by Tikhonov and Bulanzhe [281] initiated the extensive employment of transformations. Other techniques are analytical upward continuation and smoothing with polynomials. As to the analysis of fields with asymmetric distribution, their averaging using the conventional techniques may result in distorting the regional component by the intensive local anomaly. Therefore, it is recommended to apply here the method of quantiles, in particular, the median method [38]. The 50 percent quantile, a median, corresponds to the middle of the variation series composed of sequentially increasing field values within the transformation cell. For the separation of isometric anomalies by the median method, the radius  $r$  of apparent graticule is chosen according to

$$r = \sqrt{r_1 r_2}, \quad (5.37)$$

where  $r_1$  and  $r_2$  are radii of field features to be separated (regional and local objects, respectively) using half of their amplitude.

Usually the transformation cell (sliding window) size should be bigger than the local noises, less than the background features and close (or slightly higher) to the expected signal. Since there is always a correlation of results when overlapping the neighboring cells in slide processing, it is not recommended to reduce the computation step more than to half a radius of the transformation cell.

The relationship between the averaging area radius  $r$  and the continuation height  $H$  for gravitational field, leading to close results of these transformation is given by Kunin [169]

$$r \approx (2.5 \div 3.5)H. \quad (5.38)$$

The comparison of regional component charts of Azerbaijan obtained by averaging and upward continuation corroborates this conclusion regarding magnetic field, as well (Fig.5.16).

Usually the choice of transformation is of no special importance. A clear physical sense of the transformation by upward continuation suggested by Andreyev [12], and its comparability with aircraft observations testify to the advantages of this method. However, the

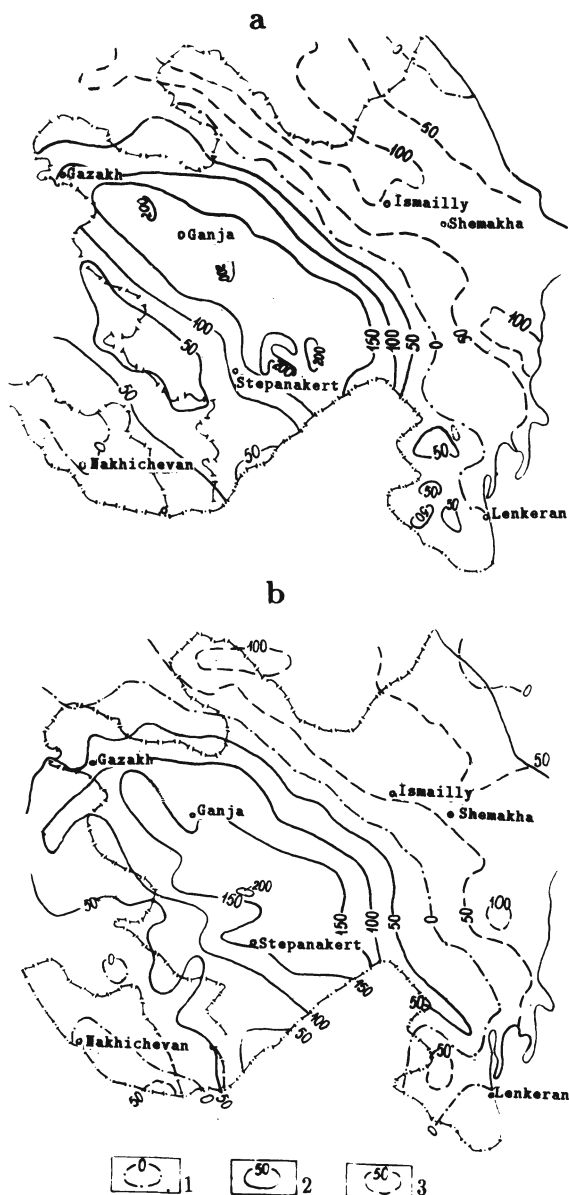


**Fig.5.16. Singling out the regional component of magnetic field in Azerbaijan: (a) averaged within the radius of 60 km; (b) continued upward to the height of 25 km**

Isolines in nanoTesla: (1) zero, (2) positive, (3) negative

uncontrollable influence of the discarded residual term in Poisson's integral often turns out to be very high.

In non-formalized calculations<sup>5</sup>, along with fundamental advantages the productivity plays an important part in the selection of the type of conversion. The above median method is attractive from this standpoint. Actually, the assumption of compensation of random deviations from the average within the limits of the transformation cell (averaging method) may not hold true in smooth fields, while for sharply varying fields the polynomial smoothing is completely inapplicable. The results of application of the sliding average method, as shown in [42], are more dependent on the anomaly amplitude than those of the median method. The latter exhibits a very high productivity, which is confirmed by the experience gained in Azerbaijan.

The polynomial and other types of smoothing allow to localize the targets in plan (for example, to use the isoohm chart for singling out the distribution of water-bearing associations). It should be noted that the same problem can be also solved in vertical plane by the data of vertical electric sounding. It is accomplished by separating the vertical section of the apparent resistivity  $\rho_a$  into the regional and local components.

A high reliability can be basically attained in geophysical field regioning and revealing regional structures, if we use the method of areal autocorrelation analysis. However, the results of this method are highly dependent on the field description interval and on the size of an apparent graticule. Besides, this analysis is accompanied by a big loss of the area on the calculating map edges and makes it possible to derive solely general results, which are rarely of no individual value.

In order to single out general features of geophysical fields (and the height field, as well) it is often advisable to calculate tertiary indicators, i.e.  $SSI$  by formula (5.36), the length of dislocations revealed from the results of interpretation in the slide window [151].

The  $SSI$  distribution (Fig.5.17) reflects certain geological features of the region. Interestingly, this chart correlates rather well with the map of seismic activity [234]. The latter is apt, on the one

---

<sup>5</sup>It is reasonable when the data body is small

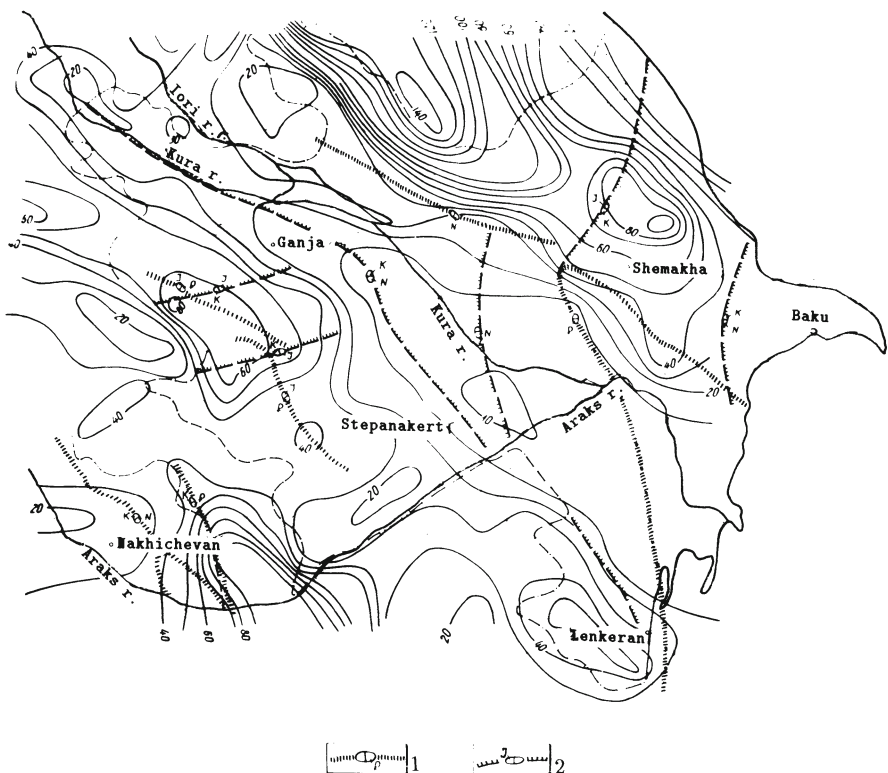


**Fig.5.17. Map of equal lengths of isohyps for the topography of Azerbaijan**

(1) deep fault (dots show buried paths of the fracture); (2) flexures (on the surface as shown by solid lines, and buried, as shown by dashed lines; indices point to the expected section interval dissected by fractures

hand, to contribute into the formation of the terrain relief and, on the other hand, is also caused by some relief-forming factors.

The results of summing up the lengths of disjunctive dislocations revealed from magnetic and gravimetric data on the sites of  $25 \cdot 25 \text{ km}^2$  are presented in Fig.5.18. It is established that relative dislocation density increases in the zones of main disjunctive dislocations. These zones are of prime importance as ore and oil-and-gas controls [135,140], and foci of earthquakes tend to occur there (see Fig.5.18).

To reveal local anomalies, some methods of computing the derivatives of higher order, which correspond to "difference" bodies

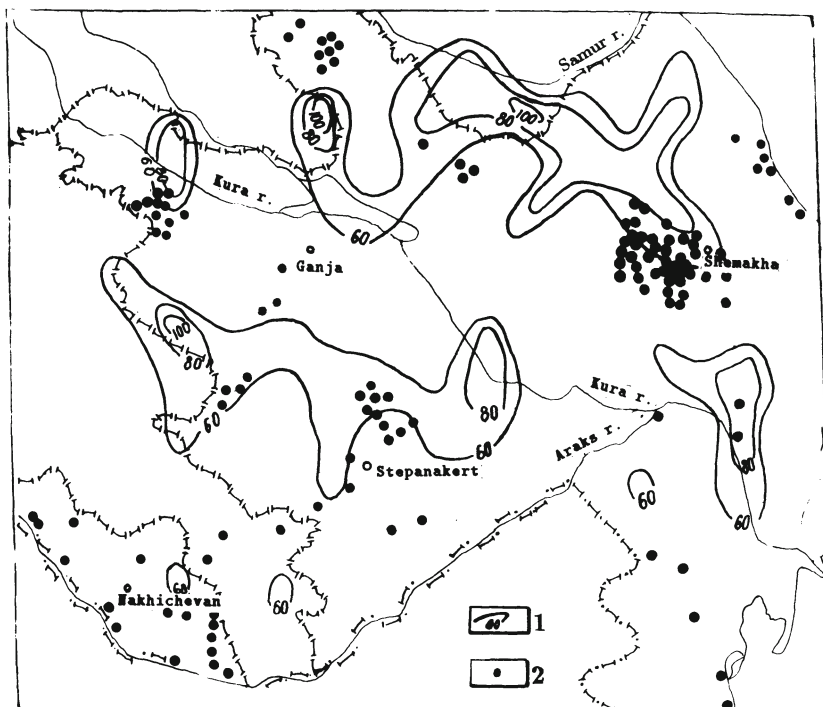


**Fig. 5.18. Summing up the lengths of disjunctive dislocations in sliding cell for the East Caucasus [151]**

(1) density isolines of disjunctive dislocations singling out on the basis of magnetic and gravimetric prospecting data ( $km/1,000 \text{ km}^2$ ); (2) earthquakes of magnitude of 7 and over by macroseismic evidence [250]

developed by Logachev [178], are used, as well as the variation method in 2-D (after Andreyev [12]) and 3-D (after Griffin [103]) variants. Localization of anomalies takes place in the analytical continuation downward using the methods reported by Strakhov (for instance, [262]) and other authors. As the methods of analytical continuation are usually characterized by high sensitivity to surface inhomogeneities, they are more suitable for plane conditions. The influence of oblique polarization is essential for their application.

As is known, the results of analytical downward continuation are applied, along with field continuation upward, for plotting field isoline charts in the vertical plane of the profile. In the case of vertical beds with vertical magnetization or beds magnetized along the dip, isolines, according to [264], have a circular shape and intersect in the angular (singular) points of the bed. In contrast, for oblique magnetization and the inclined dip which does not coincide with the magnetization direction, the isolines have a shape of double logarithmic spirals coiling on the angular bed points. Since the analytical continuation to the level of singular bed points  $H_o$  is impossible due to the field “breaking down effect” [262], the continuation must be stopped somewhat above this level (approximately by  $0.8H_o$ ). The further course of isolines is determined by extrapolation from the vertical isoline chart. It is only natural that in the case of oblique magnetization the above behavior of isolines in proximity to the singular points impedes their extrapolation, and the results of localizing the singular points are less reliable.

Local anomalies are most often computed by the available data on regional anomalies. The most useful in this respect is the method of “ring” involving the difference between the regional anomalies computed with different radii of averaging. In this way, the filtration of high-frequency and low-frequency components is accomplished simultaneously, and the presence of anomalies of the desired classes is emphasized (with the known frequency characteristic). Ring (difference) anomalies allow one to make important interpretation conclusions [86,113,114].

### 5.3.3 Singling out concentric objects

The concentric zonal structures of ring and pipe-like types (such as diatremes, necks, collapse caldera, ring and stock-like intrusive bodies and zones of their contacts) control the deposits of diamonds, rare metals and gold, copper and other metals. The deposits, being of various genesis and type (magmatic and hydrothermal; pyrite, skarnous and carbonatite) frequently have the same morphology. Oil-and-gas deposits are also connected with volcano-tectonic structures and brachy-forms of close to isometric section: brachy-folds, salt domes, diapires. But it is difficult to single out objects of the above form in complex geophysical fields observed in mountainous regions, especially taking into account the commonly employed rectangular network of observation. Besides, one has to discriminate between the anomalies caused by annular structures and the features of the field stemming from its character on the periphery of stock-like bodies (central type volcanos, stock-like intrusives). For this purpose Khesin [146] proposed a special method for distinguishing concentric structures based on summing up horizontal gradients of the field using a circular graticule (zone chart).

Horizontal gradients are determined by the apparent graticule radii drawn with the interval of  $45^\circ$ . When summing up the gradients in various directions, the presence of circular feature should be intensified, whereas other signals are leveled. Here the correlation of the sum of gradients (or the average gradient) for a circle with the radius  $R_n$  and a ring external to this circle limited by  $R_n$  and  $R_{n+1}$  radii makes it possible to determine whether the circular feature revealed reflects the centric or ring structure. The sum of gradients inside a circle tends to zero in the absence of a centric texture.

This method was successfully tested on a model of the inclined circular cylinder magnetized along its dip (Fig.5.19a). The field of the cylinder was complicated by normally distributed random noise comparable with the useful signal. A random value with zero average and a standard deviation equal to 0.3 of the anomaly amplitude over the cylinder, taken from the table of random numbers [168], was added to the model field in all the points of its assignment.

Fig.5.19b presents the total field produced in such a way. A

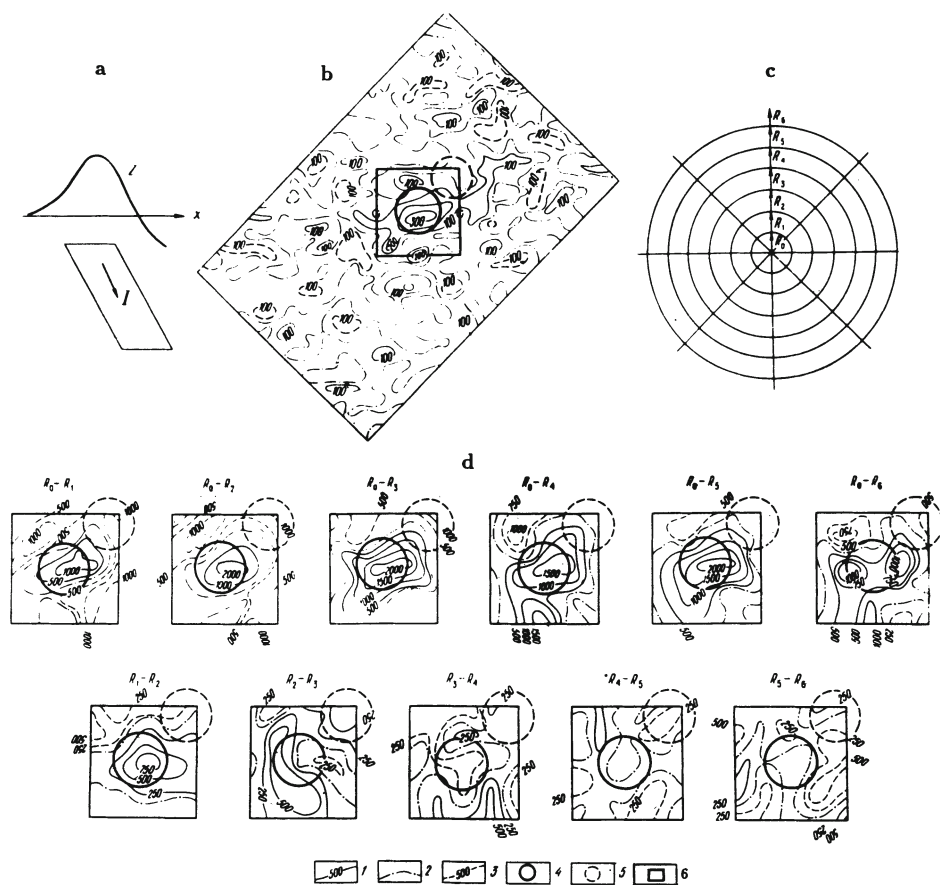


**Fig. 5.19. Singling out a concentric structure:** (a) a model field of inclined circular cylinder calculated along a profile, (b) a model field complicated by random noise (in plane), (c) apparent graticule for concentric structure selecting, (d) singling out a model body by summing up horizontal gradients of field within apparent circular graticule zones

Isogams of a model field (b) and the sum of its gradients (d) in conventional units: (1) positive, (2) zero, (3) negative; cylinder edge projection: (4) upper, (5) lower; (6) contour of the portion treated on the (b)

circular graticule was mounted on it; gradients were determined along the radii and subsequently summed over the circle and the ring zone external with respect to this circle. The object was singled out by maximal horizontal gradient, whereas an irregular field was observed in the remote ring zones.

This example is shown just for illustration. The program realization of this algorithm allows to trace “apparent isolines” in response to the type of the studied geophysical field. Obtained relationships between the field gradients for various directions make it possible to determine the criteria of the presence of concentric structure and also to refer it to a circle or ring type. Program of this kind was briefly exemplified in Subsection 5.3.5.

### 5.3.4 Anisotropic transformations and correlation analysis

Localizing the anomalies caused by extended bodies of various strikes calls for the application of anisotropic conversions. To do this, it is desirable to have information on the variation of autocorrelation radius  $\tau_e$  in different directions. The data on  $\tau_e$  value within localized areas of the stationary field are also employed in regioning. Given a favorable geologic situation, they allow for estimating the mean depth of anomalous bodies (see Section 7.3).

A method for sequential correlation and periodogram analysis of geophysical fields (revealing the latent periodicity) was developed by various authors for a profile. As for an area, the 2-D autocorrelation analysis is employed. There, using the method of self-setting filtering [54], the slide window dimensions are defined from the results of computing the 2-D autocorrelation function. The method consists of turning the window with respect to the direction of profiles and allows to reveal the anomalies of different strikes on the area under survey.

The first methods developed were those of inverse probability and cross-correlation, which formed the base for various commonly used variants of self-setting filtering [208].

The theory of identification, commonly called in radiolocation the theory of optimum reception of the signal extracted from the background of noise, served as the basis for introducing into explo-

ration geophysics an effective method of localizing weak anomalies of a specified form, i.e. the method of inverse probability [53,208]. In order to determine roughly the position of the expected anomaly  $a(x_i)$  by the observed field  $U(x_i)$  corrected for the zero average, it suffices to make a plot for correlation sums of the type

$$S = \sum_{i=1}^n a(x_i)U(x_i). \quad (5.39)$$

The number of points  $n$  in the processing interval is determined by the width of the anomaly  $a(x_i)$  and the step of processing. The computing of correlation sums is analogous to that of the slide average weighted by the expected anomaly ordinates.

The plausibility ratio (likelihood coefficient) is computed by the formula

$$\Lambda_j = \exp\left[-\frac{1}{2\sigma^2} \sum_{i=1}^n a^2(x_i)\right] \exp\frac{S}{\sigma^2}, \quad (5.40)$$

while posteriori probability of localizing the anomaly – by

$$P_j(a > 0 | U_1, U_2, \dots, U_n) = \frac{\Lambda_j}{1 + \Lambda_j}, \quad (5.41)$$

where  $\sigma^2$  is the noise dispersion,  $j$  is the number of a stake (selected point).

It can be easily shown that the first exponent in (5.40) is a constant determined by the square of the target anomaly. If  $\Lambda_j > 1$  (or  $P_j > 0.5$ ), then the anomaly is present here.

The investigations disclosed that the determination of a signal position on the profile after processing is weakly dependent on the anomaly configuration details. Close results can be obtained using a bell-shaped (anomaly from many model bodies) or a rectangular impulse.

The inverse probability method (*IPM*) was used on the Filizchai pyrite-polymetallic deposit which is the largest in the Caucasus. This deposit was revealed by geophysical methods. Application of *IPM* with the purpose of singling out weak magnetic anomalies showed that the ore deposit can be detected using this method (Fig.5.20) even in that part of the area where it is not fixed in the observed field.

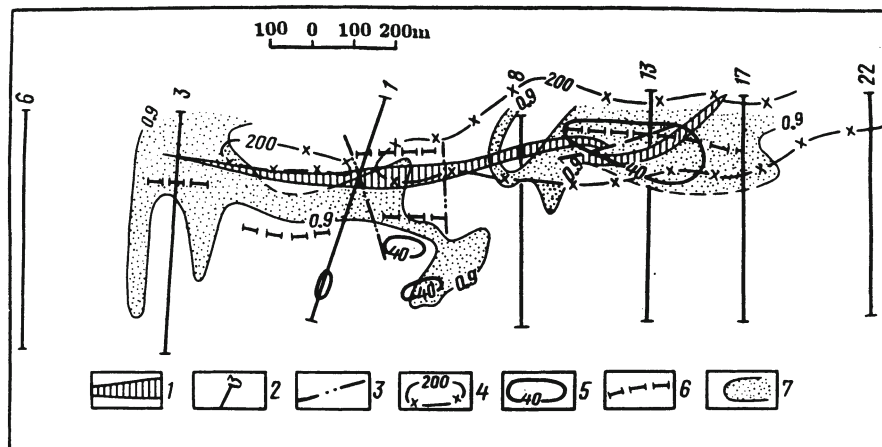


Fig.5.20. Inverse probability and cross-correlation methods testing on the Filizchai polymetallic deposit

(1) upper edge projection of the deposit on the earth's surface by geological data; (2) profiles; (3) disjunctive dislocations; (4) isopotential lines of  $SP$ ,  $mV$ ; (5) isolines  $\Delta Z$ ,  $nT$ ; (6)  $\Delta Z$  anomaly axes obtained with the use of cross-correlation; (7) areas, where after the inverse probability method application the probability of detecting the targets exceeded 0.9.

The effectiveness of *IPM* may be further improved, if we take into account the conditions which partially manifest themselves during the analysis of other methods of this kind.

Identification is not optimum if the width of a noise pulse exceeds that of a signal [19]. Therefore the regional background noise must be preliminarily eliminated. The bodies under study are frequently observed as closely located parallel zones. The nearest anomaly introduces an error into the determination of the target anomaly position, which can apparently be reduced by successive approximations. The assumed condition of equality of prior probabilities is fulfilled solely in the most promising areas and in large-scale investigations for singling out some ore controls. Other situations call for modified variants of the method. To estimate the errors of revealing anomalies and select the threshold of their determination, Kotelnikov's ("ideal observer's") criterion is used which minimizes the average (total) error of identification [211]. Barabash et al.

[19] noted that the criterion can not be applied to the classes of unknown prior probabilities. Moreover, when an average cost of the error is minimum for all the classes, the objects of rare occurrence are misidentified. Economic deposits, in particular, fall into this category. Therefore, it is expedient to employ here the criterion of minimal mean risk considering the error cost as well.

The method of cross-correlation serves to reveal the anomalies of the same direction. A modification of this method makes it possible to single out the systems of magnetic and gravity anomalies of different strikes [160].

The correlation function maximum can not be assigned to a certain point on the profile. Therefore, Shaub [248] suggested a modification with the greatest correlation observed for a certain point in the survey sheet. It is expected that on averaging the product of  $U_1$  and  $U_2$  field values for the neighboring profiles 1 and 2, all random effects tend to 0 on a fairly wide interval, and the useful signal effect is singled out owing to their common source. The type of desired signal is also determined by the character of the cross-correlation extremum  $K(x)$ : the maximum of  $K(x)$  corresponds to an even signal (anomaly from a steeply dipping body, dike), the minimum of  $K(x)$  – to an odd one (ledge anomaly).

The values of  $K(x)$  function referred to the middle of the  $j$ -th interval in the point between two neighboring profiles are computed by the formula

$$K_j(x) = \frac{1}{2n+1} \sum_{\substack{\tau \\ \Delta x}}^n U_1(x_i - \tau) U_2(x_i + \tau), \quad (5.42)$$

where  $\Delta x$  is the step of observation and  $\tau$  is the displacement.

The cross-correlation method is approximate due to the conditional character of some presumptions (primarily, that the cross-correlation function of the anomaly and noise is equal to 0 on the averaging interval) and the possibility of spurious extrema. Therefore, Alexeyev [6] proposed another approximate, but more simple technique of sign correlation, in which instead of the expression (5.42), the sign-correlation function is computed:

$$\omega_j(x) = \frac{1}{2n+1} \sum_{\substack{\tau \\ \Delta x}}^n sgn U_1(x_i - \tau) sgn U_2(x_i + \tau), \quad (5.43)$$

where  $sgn$  is the sign of  $U_1$  and  $U_2$  fields for neighboring profiles reduced to the zero average value. All the rest designations and the method of computation are identical with (5.42).

Computations are highly efficient since they are reduced to multiplication of signs followed by summing up the results.

The methods of cross- and sign-correlation have been tested to advantage on models and in real situations (see Fig.5.20). Thanks to the information measure, the cross-correlation method can be applied not only to the correlation of anomalies of the same type on parallel profiles, but also for revealing signals from a common source on one profile by different fields [131].

Application of various techniques can be successful only when certain geological information on the structure of the area under study is available. Since at the present level of knowledge, geophysical prospecting is based on sufficiently clear geological premises, the above requirement must be fulfilled (see Chapter 4). This approach can be applied to singling out the correlation axes caused by the terrain relief or other surface inhomogeneities. Comparing, for example, the axes of maximums in sign-correlation with the relief shapes, it is easy to exclude the anomalies of non-geological origin (provided, certainly, that the topography does not reflect geologic structures).

With the sign-correlation method, spurious extrema may appear, with axes parallel to the real ones. They do not distort the evidence on the prospects of the area under investigation but, if necessary, they can be rejected on the basis of the results of other geophysical methods or alternative techniques of processing.

Computing the horizontal gradient plays an important role in transformations. This conversion makes it possible to reveal elongated structures against the background of isometric textures. However, even this simple transformation, which is widely used in practice, has its nuances. First, it is necessary to determine the total horizontal gradient by

$$\frac{\Delta U}{\Delta l} = \sqrt{\left(\frac{\Delta U_x}{\Delta x}\right)^2 + \left(\frac{\Delta U_y}{\Delta y}\right)^2}, \quad (5.44)$$

where  $\Delta U_x$  is the mean increment of the  $U$  field along the  $x$ -axis,

computed for the parallel sides of the square transformation cell;  $\Delta U_y$  is the same parameter along the  $y$ -axis;  $\Delta U/\Delta l$  is the average absolute value of gradient in the cell (*grad U*).

Second, the size of the transformation cell (as in other conversions) should be selected basing on the objective sought for. For example, until recently, the results of magnetic survey were believed to be inapplicable to the prediction of long-term seismic activity  $A$ : observed magnetic field and its transforms did not correlate with the distribution of  $A$  values. However, after the magnetic gradient was computed in the same areas where the average activity  $A$  had been determined, the correlation factor between the  $A$  values and *grad U* increased from 0.17 to 0.60 [234]. This allowed for employing the available magnetic data in refining the predicted values of  $A$  in Azerbaijan.

The distinct steps are observed also in regioning of the field using the predominant strike of isolines [304], dispersion [38] “anomalous coefficient” [167], ruggedness of the field and its entropy [42].

The anomalous coefficient, proposed by Kruglyakova [167], is the ratio of field plot length on the sliding interval of the profile to the interval length. The anomalous coefficient is plotted along the profile in accordance with the slide interval. The 2-D variant of this method is analogous to the method for determining the specific sinuosity of isolines described in Section 5.2.3.

To single out the zones of jointing, in particular, those controlling the distribution of underground water, the calculation of the number of geophysical field extrema in the sliding interval can be used. Segments with increased inhomogeneity of geologic structure are more pronounced on the plot of this generalized parameter.

The data on isoline strikes make visual the regioning of the field under study. In most cases, it is sufficient to get the distribution of predominant strikes in octants, as shown in Fig.5.15, which simplifies the processing.

If a distinct unidirectional elongation of the bodies is not observed, then anisotropic elliptical or, more often, rectangular graticules are employed [158]. Gradient and amplitude anomalies are singled out with the use of computer realization of these graticules (Fig.5.21). Graticules divided by transverse lines were also proposed

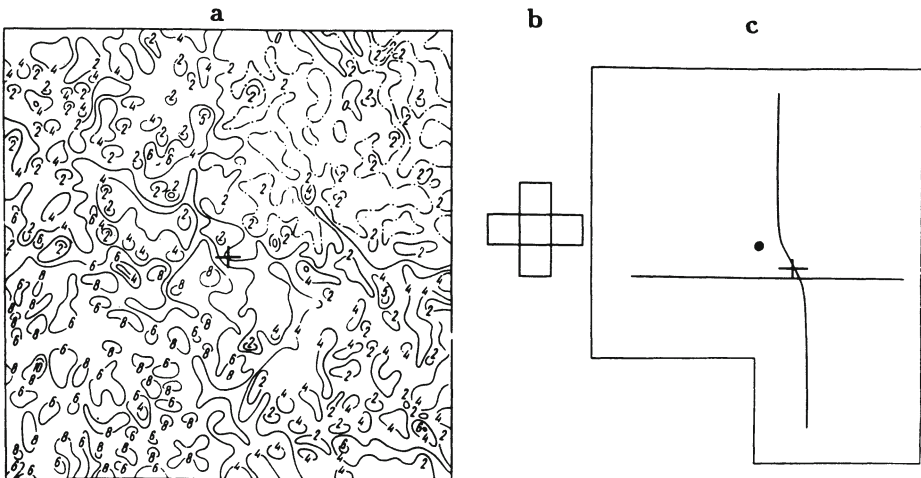


**Fig.5.21. Singling out intersection node:** (a) synthetic magnetic field of mutually perpendicular intersecting linear structures, plus random noise, (b) apparent cruciform graticule, (c) computation results

to suppress anomalies of this type [169]. The apparent graticule dimensions serve as frequency filter, and the azimuth selectivity is determined as the ratio between long and short axes. Additional interval division makes it possible to differentiate over a long or a short axis.

### 5.3.5 Revealing hidden intersections of linear structures

Singling out nodes of linear structures is a crucial problem, since such nodes control the location of economic ore, oil-and-gas and underground water deposits of various types. This problem is also of high priority in earthquake prediction [126]. Therefore, a method was developed for direct localizing structural intersections by digital field models [135].

When structures with different strikes intersect, the field components caused by these structures superimpose. The observed pattern is complicated by random noise. Thus, the problem consists in

suppressing random noise and revealing isoline strikes. The latter, being removed from the intersection area, approximate the strike of anomalous bodies.

In the case of superposition of differently oriented anomalies, false resulting strikes can prevail. The maps of graphs (Fig.5.22a) and isolines (Fig.5.22b) represent a model magnetic field of mutually perpendicular intersecting linear vertical beds. The rose-diagram (Fig.22c) of the isoline strikes shows clearly the false orientation.

The proposed method allows to distinguish the true strikes.

Fig.5.21a shows a synthetic magnetic field (broken lines mark zero contours) of mutually perpendicular, intersecting linear structures, plus random noise. Fig.5.21b shows an apparent cruciform graticule used for computing the number of isolines per area. The result of this analysis is presented in Fig.5.21c. A small cross marks the location of the pre-set structure intersection. The solid lines are anomaly axes determined with an apparent anisotropic graticule using the technique described in [158]. The small disk is the point of ledge intersection defined according to the value of parameter  $I_{cr}$  (at the maximum of information quantity).

Each rectangle of apparent graticules is made up of three elementary squares. The middle square, being common for both rectangles, falls directly within the hypothetical area of intersection and is not involved in computations. For each direction, isolines which cross the external line of outer squares and the internal line parallel to it, are counted ( $\mu$  and  $\nu$ ). According to Brillouin [43], the amount of information obtained as a result of a physical measurement is calculated by

$$I_u = \log\left(\frac{L_u}{\Delta U}\right), \quad (5.45)$$

where  $L_u$  is the span of  $U$  value,  $\Delta U$  is the measurement error.

The isolines are plotted with the intervals close to  $\Delta U$  error. Consequently, if  $\mu$  or  $\nu$  isolines are present on a portion of the map, then their numbers correspond to  $L_u/\Delta U$  values in equation (5.45). Then the amount of information  $I_{cr}$  about the presence of intersection is determined by the ratio of the amounts of information on the presence of anomalies with different strikes  $I_1 = \log_2 \mu$  and  $I_2 = \log_2 \nu$ . In order to reduce the effect of high-gradient zones with

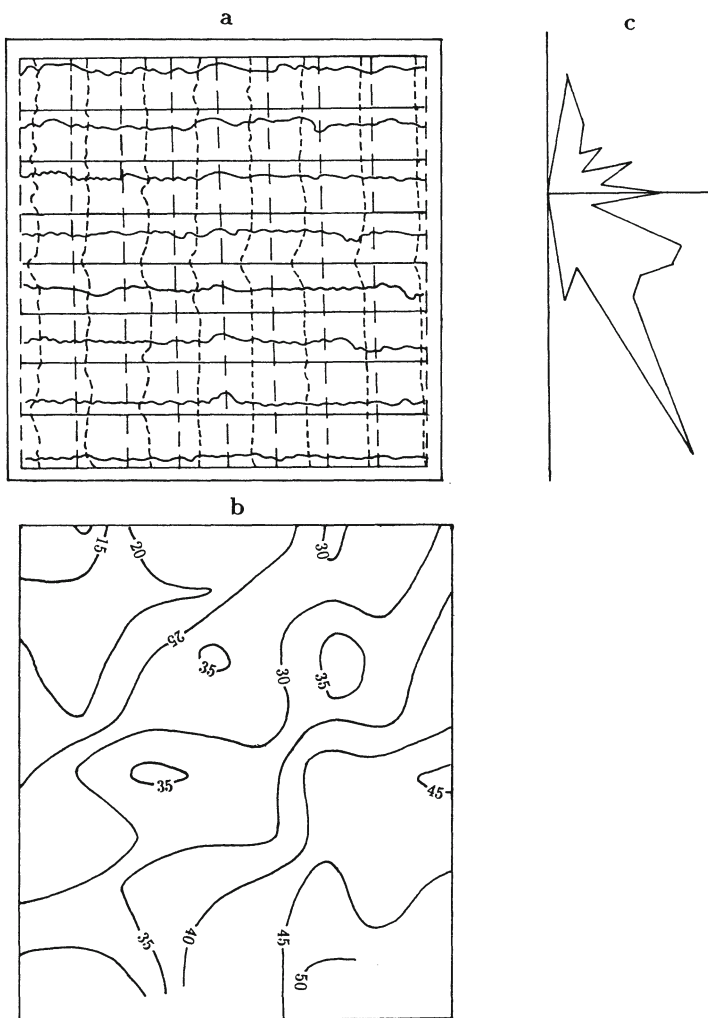


Fig.5.22. Analysis of model magnetic field of mutually perpendicular, intersecting linear structures: (a) map of graphs, (b) map of isogams, (c) rose-diagram of isogam strikes

a common strike,  $I_{cr}$  is calculated by the formula

$$I_{cr} = (I_1 + I_2) \frac{I_1}{I_2}, \quad (5.46)$$

where  $I_1 \leq I_2$ .

As shows Fig.5.21c, the developed method makes it possible to reveal the intersection node to the accuracy of the size of the side of the apparent graticule's elementary square.

For example, the isoanomalies of the gravitational field of the Sinai Peninsula were processed using an apparent graticule (Fig.5.23). Fig.5.24 shows the results of this processing. The gravitational field in incomplete Bouguer reduction (without relief correction) reflects clearly the NW–SE and NE–SW structures. But hidden intersections of regional structures in the N–S and W–E directions were revealed using these calculations.  $I_{cr}$  values are shown in Fig.5.23 and Fig.5.24 by crosses (its dimension is proportional to  $I_{cr}$  value). Ambiguous directions of the crosses are shown by dashed lines. Fractures are shown in accordance with geological data [21].

The lines of nodes are approximately on the northward continuation of Eilat and Suez Gulfs. It is interesting that large nodes in the NE part of Sinai coincide with isometric magnetic anomalies. These anomalies may be caused by intrusive bodies at weakened intersection areas.

The program “Node”, which realizes this algorithm, allows to examine angles between the rectangles of the apparent graticule and rectangle's sizes (22 variants altogether). By applying this program, the apparent graticule is superimposed on a digital model of the investigated field. Field gradients computation plays the role of a graticule. Then a relationship between the gradient zones of various directions and their intensity is computed. On this basis we can draw a conclusion about the presence of a node of intersection of structures according to the developed informational criterion.

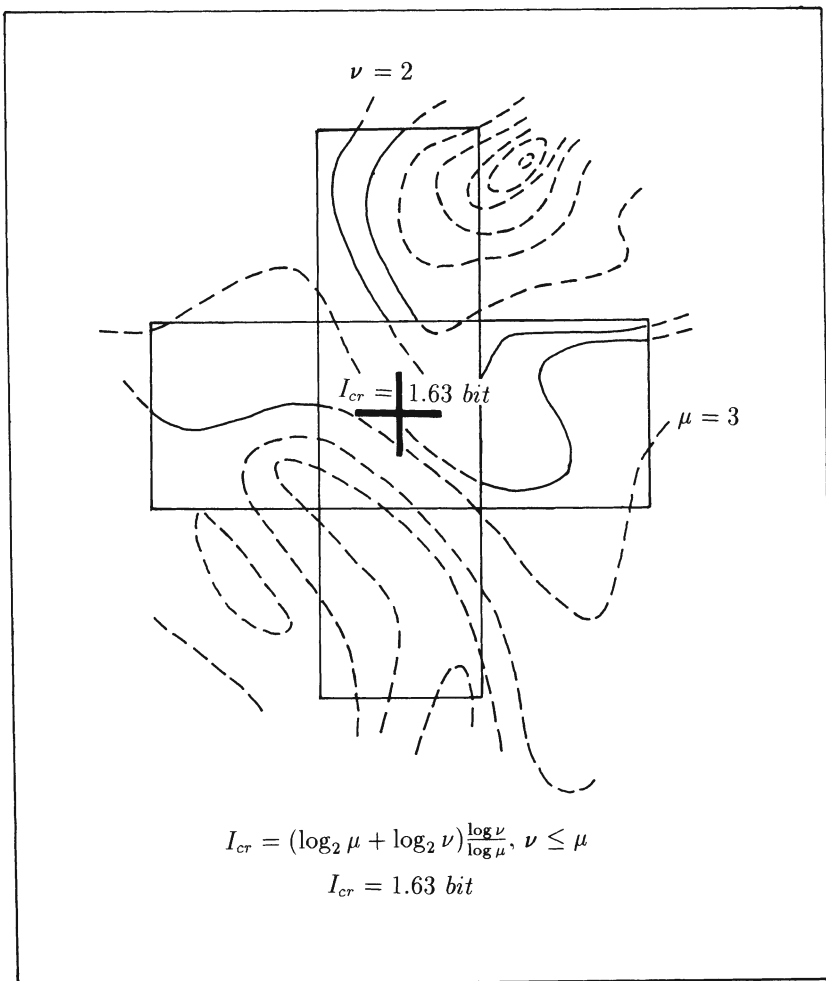


Fig.5.23. Number of  $\Delta g$  isolines obtained using apparent cruciform graticule

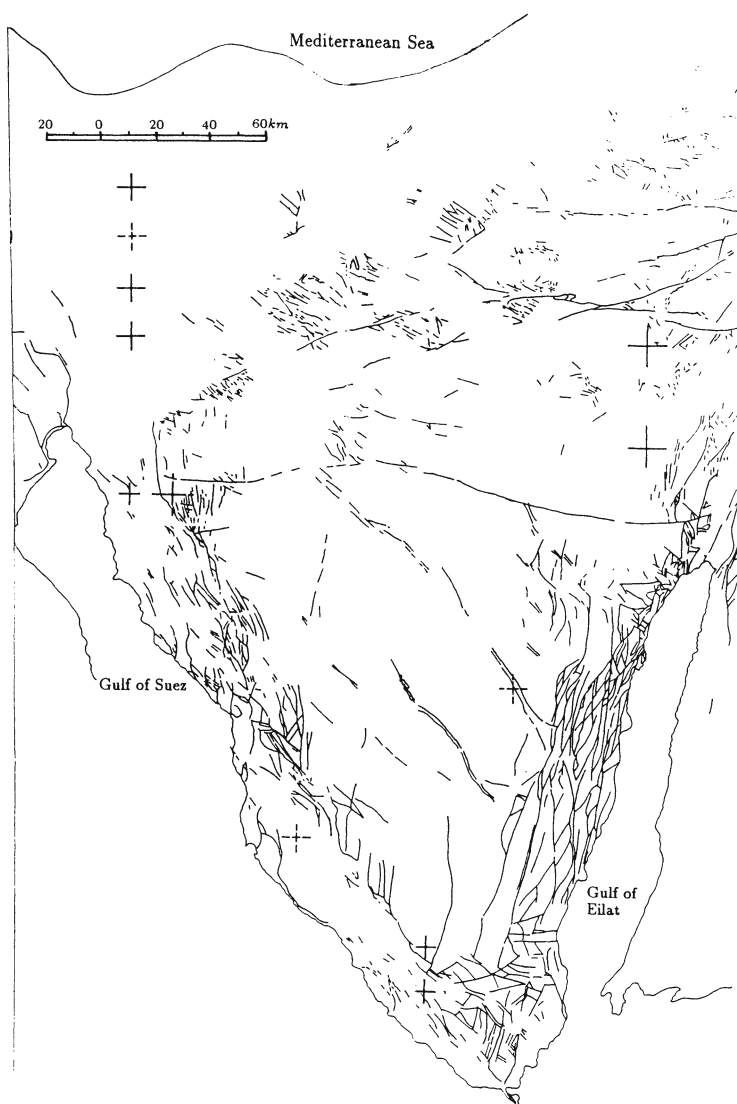


Fig.5.24. Hidden intersections of linear structures (crosses) revealed using apparent cruciform graticule and known fault distribution

# **Chapter 6**

## **REVEALING AND LOCALIZATION OF TARGETS**

Having a common interpretation aim, the methods of revealing and localizing the targets substantially depend upon the types of the areas under study and the types of prospecting. As mentioned above, due to its vector nature, the most essential is the specific character of magnetic field analysis. Therefore, the interpretation procedure will be discussed below for this particular field. For other fields it is similar or even more simple.

### **6.1 Regioning**

If deterministic features are predominant in the observed field (as, for example, during regional aeromagnetic survey when the local changeability of higher orders cannot be fixed), good results can be obtained from visual analysis of the initial field and corresponding transforms (forming the indicator space), their correlation with geological and petrophysical maps of the same scale, i.e. regioning of the field. In the above analysis the region under investigation is divided into districts with different types of fields. A geological sense is attached to these districts and their boundaries. To single out such areas, a set of indicators is employed, which includes the following:

- the sign of the field and its intensity;
- predominant strikes of isolines;
- presence of linear anomalies and gradient zones at the boundaries of the region;

- approximately the same variability within the limits of the region, differing from the variability in neighboring regions;
- sizes, forms and orientation of local anomalies, called sometimes “field pattern”.

Therefore, it is obvious that the regioning process is of classifying or, to be more exact, of taxonomic character, since the number of regions and the particular combination of indicators in each region are unknown prior to geophysical survey and regioning.

In field regioning, the anomalies from many classes of geological objects are discussed. The main objects for open regions include the areas of effusive and pyroclastic (stratified) rock masses, intrusive complexes and isolated bodies and various tectonic dislocations with different directions. These objects are of metallogenetic importance, being ore controls. They are not separated in space, but form complex combinations in plan and in section.

The above geological object manifestations in geophysical fields are well-known [67,135]. They are taken into account when devising an initial model of the medium. Here it is necessary to dwell on the role of model representation involving obliquely magnetized objects which are most commonly encountered.

When interpreting the observed or transformed field, the anomalies of certain morphological features are the first to be singled out and traced. The anomalies thus revealed are correlated (quite often mentally) with theoretical anomalies over simple bodies or with those over known geological objects. In case of their similarity, the anomalous objects are identified, as a first approximation, with these simple bodies or with known geological objects.

In the case of vertical magnetization  $Z$  anomaly shapes from simple symmetric bodies are not intricate and typical. This allows to carry out the analysis of magnetic maps on the basis of several common principles following from the direct problem solution which are formulated in Table 6.1 [5].

The principles set out in Table 6.1 are appropriate in analyzing other types of fields, and primarily gravitational one.

For oblique magnetization (polarization), principles 3 – 7 are not applicable. The shape of anomalies for the vertical component is complicated by the horizontal component effect. This is why in

**Table 6.1. Common principles for analyzing magnetic maps (developed for vertical positive redundant magnetization)**

No	PRINCIPLES	CHARACTERISTIC FEATURES OF ANOMALIES
1	Detection	Positive anomaly testifies to the presence of anomalous object with increased magnetization (in the northern hemisphere)
2	Coulomb	The higher is redundant magnetization of the object, the bigger is its size and the closer is it to the observation line – the higher is anomalous intensity
3	Correspondence	The position in plan and shape (strike) of the anomaly are in correspondence with the position in plan and shape (strike) of the anomalous object
4	Maximum (consequence of the correspondence principle)	Anomaly maximum is observed close to the projection of the body's center (middle of the upper bed edge) on the earth's surface
5	Gradient (consequence of the correspondence principle)	The greatest in magnitude field gradients are observed close to projection of lateral boundaries of the body on the plan
6	Symmetry	Plots of the field along directions across the isoline strike are symmetrical about the vertical straight line which traverses the maximum of the anomaly
7	Limitation	The presence of minimums on both sides of the higher maximum testifies to a dip-limited body

the northern hemisphere anomalies become asymmetric when the body's magnetization is parallel to the Earth's field. Thus, anomaly maximums of sublatitudinal-oriented bodies are shifted southward, while a minimum arises in the northern periphery of the anomaly. If the magnetization inclination with respect to the horizon is not large (in southern latitudes), the maximum is shifted more to the south, and the intensity of the minimum increases. Inflection points (maximum gradients) in the anomaly plots are displaced southward from the projections of lateral sides of the bed on the plan. In case of a depth-limited body, one of the minimums (southern one) may disappear along the maximum periphery. All the distortions described above are typical of  $\Delta T$  anomalies [269].

As to three-dimensional bodies of approximately isometric section,  $Z$  anomaly distortions occur not only due the inclination of the magnetization vector to the horizon plane, but also due to different orientation of the horizontal magnetization projection with respect to the body's axes. For  $\Delta T$  anomalies, the geomagnetic field inclination and orientation of the body's axes relative to horizontal component of the geomagnetic field are also significant. Therefore, the analysis of field graph maps is not sufficient, it is necessary to analyze field isolines maps as well.

$Z$  anomaly distortions similar to those described above are observed for vertical magnetization and inclined dip of bodies toward the side opposite to the magnetization vector inclination. If the inclinations of beds and magnetization are identical, the symmetry of field plots is restored, as well as the possibility to use other principles from Table 6.1.

The general rules of geological object manifestation in the magnetic field, which are systematically used in regioning, are as follows:

- (1) correspondence between the sign and intensity of the magnetic field and the sign and intensity of the object magnetization (other conditions being equal);
- (2) correspondence between the shape and orientation of anomalies (in plan) and object orientation;
- (3) correspondence between the areas with highly rugged field pattern and the areas with increased inhomogeneity of composition and/or magnetization (in magnitude and direction) of the objects.

The division of the survey area into portions with different signs and field intensity is quite a natural operation used for singling out various (in the first approximation) classes of objects. In many cases geological objects of various shapes in plan fall into different classes or relate to different objects within one class (elongated objects, such as disjunctive dislocations, sheet intrusives, dikes, sheet-like ore bodies, veins; isometric objects such as brachyanticlines, granitoid intrusions, volcanos, diatremes, ore stocks). Therefore, when classifying the objects, it is expedient to consider shapes of separate anomalies and single out linear field elements. Differences in orientation and sizes of anomalies (for limited variation of the source depth occurrence) favor the revealing of geological nature of the anomalous bodies on the basis of model concepts.

The first above mentioned relationship is complicated under the conditions of oblique magnetization, since each field maximum (for normal magnetization of the object) is accompanied by a minimum of lower intensity located to the north, north-west or north-east of the maximum. These minimums do not provide information on the presence of objects with insufficient magnetization or on depth limitation of the objects with redundant magnetization. Therefore, an important requirement is to reveal the minimums which accompany the corresponding maximums. Having certain skills, especially in using standard (calculated or observed over similar obliquely magnetized objects) curves, it is not difficult to set up these relations. If one ignores the adjoin minimums when classifying the objects, in other respects the first relation may be used taking into account that the anomalies are shifted to the southern bearings from the anomalous object projections onto the plan. The second and third relations are not violated under the conditions of oblique magnetization, and they can be applied to regioning, provided we take into consideration that the ruggedness of field pattern over the series of obliquely magnetized bodies may be more severe than over similar, but vertically magnetized bodies (with equal heterogeneity of the composition).

The differences in magnetic field ruggedness are useful for dividing into classes (subclasses) with close magnetization vector. They are observed over the rocks of similar composition differing by genetic or age features. The corresponding empirical dependence of field ruggedness on genetic features and age of rocks is as follows

[67]:

- (1) field pattern is more intricate over effusive rocks than over intrusive ones, being more intricate over the latter than over host sedimentary rocks;
- (2) in effusive rocks, the field pattern is more intricate over cenotypal rocks than over paleotypal ones, over lavas than over tuffs;
- (3) in granitoid intrusions field pattern is more intricate over the rocks of the basic phase as compared with artificial phase rocks.

Meanwhile, differences in field ruggedness occur also when the field intensity is varying (in this case they are less important). In contrast to acid rocks, basic effusive ones are characterized by more rugged field. Field ruggedness decreases with increasing depth of object occurrence.

The role and significance of various indicators in the indicator space is different when conducting the regioning. So, the regions with different signs and intensity of the field are mainly singled out by maps of the initial field and the field on a number of levels of the upper semispace with due account of local and difference anomalies. Field region boundaries and other linear elements are traced by horizontal gradients and predominant strike isolines maps using the initial field map and regional anomaly map and employing local elongated anomalies from corresponding charts. The local anomalies are singled out by maps of local and difference anomalies with due account of the horizontal gradient map. All mentioned above gives an idea on the depth extension of the sources.

By way of example, consider the regioning scheme of the gravitational field in Azerbaijan as compared with regional steps of the magnetic field (Fig.6.1). Regional peculiarities of gravitational and magnetic fields determine regional factors of both oil-and-gas and ore control. Shamkhor-Kedabek-Dashkesan ore zone and Mekhmana ore district (Lesser Caucasus), Belokan-Zakatala ore district revealed on the basis of systematic geophysical study, and Kutkashen-Ismailly district, which is promising as to endogenic mineralization according to a number of indicators [135] (Greater Caucasus) are controlled by the positive difference field  $\Delta g_{8-20}$  (zones 8 and 2, respectively, in Fig.6.1). The regional minimums of the same component outline prospective oil-and-gas regions. A

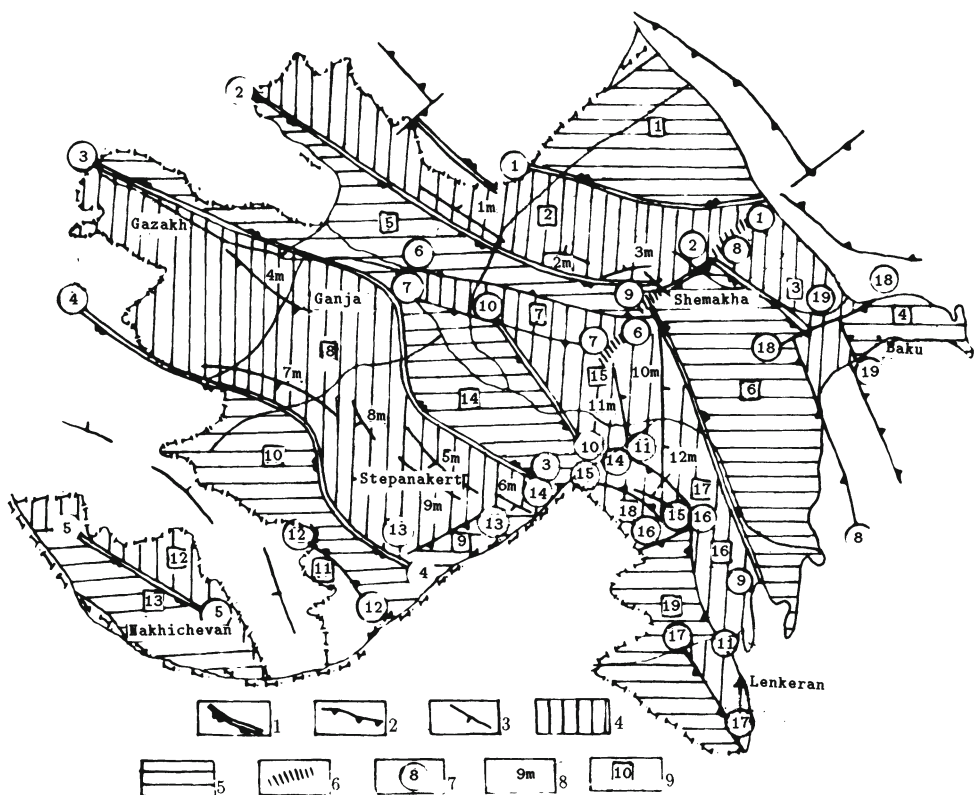


**Fig.6.1. Comparison between the scheme of gravitational field regioning and regional steps of magnetic field**

(1) axes of intense extended gravity steps distinguished in the  $\Delta g_{8-20}$  and  $\Delta g_{4-10}$  difference fields and the field of horizontal gradient obtained from  $\Delta g$  on the level of 2 km; (2) axes of market gravitational steps distinguished in the same fields; (3) axes of regional magnetic steps distinguished in the magnetic field on the level of 10 km and in the field of its horizontal gradient on the level of 2 km; (4)  $\Delta g_{8-20}$  positive gravity field blocks and zones; (5)  $\Delta g_{8-20}$  negative gravity field blocks and zones; (6) weak boundaries of  $g_{8-20}$  positive or negative gravity field areas; (7) gravitational step number (beginning and end of a step are indicated); (8) magnetic step number; (9) number of  $\Delta g_{8-20}$  positive or negative gravity field zones and blocks.

The arrows on the symbols show the direction to the blocks of lower density or magnetization

sharp distinction of terrigenous rock masses of Cenozoic by lower density ( $2.0 \div 2.3 \text{ g/cm}^3$ ) gives all the grounds to define unambiguously the regions of lower density at depth (gravity minimums) as the regions of the largest accumulation of sedimentary rock masses. The latter are promising as to oil and gas resources in the Paleogene-Miocene and Pliocene-Quaternary deposits. Characteristic of these regions are Kuba-Khachmas and Iory-Agrichai zones mating with Kobustan-Lower Kura zone in the east, and Evlakh-Agdjabedy zone (negative field regions 1, 5, 6, and 14, respectively, in Fig.6.1).

The accumulated experience validates the expedience of performing independent regioning using the initial field and regional anomaly maps. Comparison of the results in unified scheme makes it possible to determine common features and differences in deep structure elements and in the upper portion of the section, to reveal the elements (primarily, disjunctive dislocations and blocks) manifesting themselves in various structural stages.

The transforms reflecting the degree of heterogeneity of the field such as anomalous coefficient, dispersion, entropy, etc. are the most useful for singling out field areas in open regions. In different areas, these parameters may acquire different geological sense. They are also appropriate in solving more particular problems, namely, in the regioning of separate portions by the degree of heterogeneity of their lithological complexes. Here, it is convenient to compute the specific sinuosity of isolines (see Sections 5.2.3 and 5.3.4).

Visual analysis of the field character often allows to solve fully enough the geological objective, especially when a set of geophysical methods is employed. The mapping of intrusive rocks by the data obtained by magnetic and emanation surveys at a portion of the Lesser Caucasus enabled us to reveal with sufficient precision an intrusive body which intrudes limestones, and even to classify it by composition (Fig.6.2).

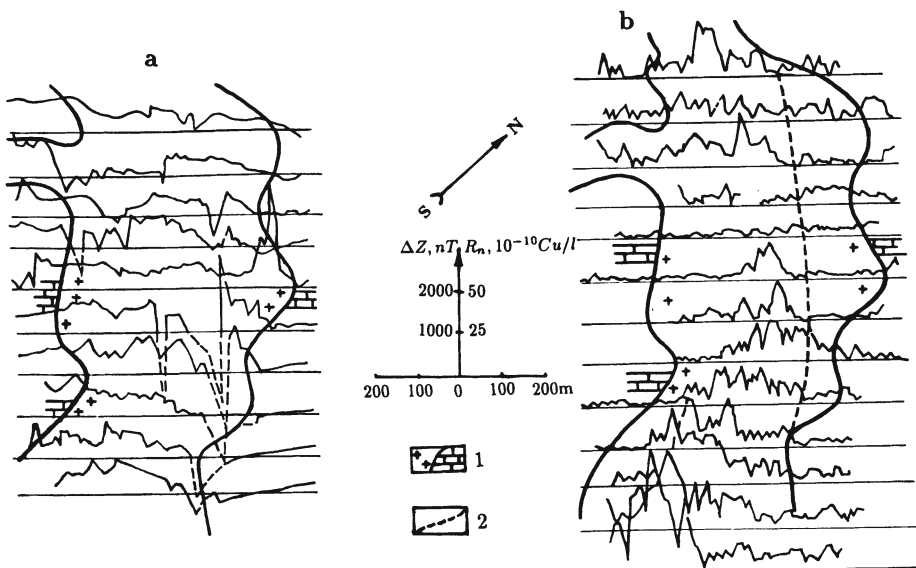


Fig.6.2. Magnetic (a) and emanation (b) survey data employed for intrusive rock mapping (dashed line shows negative values of magnetic field graphs)

(1) intrusion/limestone contact; (2) interface of alkaline rocks and gabbro-diabases by the emanation survey data

## 6.2 Delineation and determination of anomalous body axes; their representation with the results of regioning

During regioning it is necessary to define the contours of anomalous bodies. The normal practice is to delineate the objects, which are approximated by thick (depth-limited or unlimited) beds, by points of inflection in the charts of  $Z$  and  $\Delta T$  anomalies. The latter are plotted by profiles across the strike of the object or by horizontal gradient extrema on a corresponding isoline map, thus realizing the gradient principle (see Table 6.1). The inflection points are shifted from the lateral boundary projection on the plan under the condition of oblique magnetization. The object contour thus obtained in some cases fails to reflect its exact position in plan, since

the displacement depends upon the size of the generalized angle  $\theta$  and the relative semithickness  $\beta = b/h$ , where  $b$  is semithickness and  $h$  is depth of the bed occurrence (depth of its upper edge). The angle  $\theta$  is involved in the general analytical expression of magnetic anomalies ( $Z$  or  $\Delta T$ ) under oblique magnetization for two-dimensional inclined dipping bodies of sheet-like type with bottom edges rather remote into depth [5]:

$$\{Z_{ds}, \Delta T_{ds}\} = \{C_m C_s, C_o C_m C_s\} [Z_{vv} \cos \theta + X_{vv} \sin \theta], \quad (6.1)$$

where for  $Z$  anomalies  $\theta = \gamma_m - \gamma_2$ , for  $\Delta T$  anomalies  $\theta = \gamma_o + \gamma_m - \gamma_2$ ;  $C_m = \sin i_m / \sin \phi_m$ ;  $i_m$  is the inclination of magnetization vector  $\mathbf{I}$  to the horizon;  $\phi_m$  is the inclination angle of the magnetization vector projection on the vertical plane of the profile;  $\cot \phi_m = \cot i_m \cos \delta_m$ ;  $\delta_m$  is the angle between the  $\mathbf{I}$  projection on the horizontal plane and observation profile perpendicular to the body's strike;  $\gamma_m = 90^\circ - \phi_m$ ;  $C_o, i_o, \gamma_o$  and  $\phi_o$  have been determined in Subsection 5.2.3;  $C_s = \sin(\phi_2 - \phi_1) / \cos \phi_1$ ;  $\phi_1$  is the bed's upper edge dip;  $\phi_2$  is the bed dip;  $\gamma_2 = 90^\circ - \phi_2$ ; subscript "d" (dip) refers to magnetic inclination; subscript "s" (slope) refers to inclined dip;  $Z_{vv}$  and  $X_{vv}$  are, respectively, vertical and horizontal components of the magnetic field due to vertically dipping bodies under vertical magnetization with the same singular points.

The common techniques for interpreting magnetic anomalies caused by vertically magnetized bodies of inclined dip type or obliquely magnetized bodies of vertical dip type follow from expression (6.1).

Formula (6.1) is also adequate for analyzing  $Z$  or  $\Delta T$  anomalies of the bodies isometric in vertical section (approximated by horizontal cylinder); in this case  $\phi_1 = 0$ ,  $\phi_2 = 90^\circ$ , then

$$C_s = 1, \theta_z = \gamma_m, \theta_{\Delta T} = \gamma_o + \gamma_m.$$

The generalized angle  $\theta$  reflects the degree of magnetic anomaly asymmetry as a function of magnetization inclination, body dip, magnetization and observation profile azimuths relation. As for  $\Delta T$ , it is also dependent on the geomagnetic field inclination and *geomagnetic declination/profile azimuth ratio*. When the angle  $\theta$  is small (i.e. magnetization is directed almost along the dip), anomaly inflection points define the position of lateral boundaries of a thick bed in plan rather precisely. However, even for greater  $\theta$  values, it

is possible to delineate accurately a sheet-like anomalous body, if one knows in advance the size of the angle  $\theta$  and makes use of other characteristic points in the anomaly plot.

The first step involves the determination of the angle  $\theta$  range by quadrants of a circle. Fig.6.3b shows  $Z_{ds}$  curves over a thick bed with the horizontal upper edge for four  $\theta$  values. Save for  $\gamma_m$  and  $\gamma_2$  angles ratios demonstrated in Fig.6.3.b, case II is possible under conditions of normal magnetization and southern gentle dip of the body, case III takes place when the body has the northward direction of gentle dip, case IV (and also II) – when the remanent inverse magnetization is strong, and the body is of steeply dipping type.

From formulas presented in Fig.6.3b and the behavior of  $Z_{ds}$  curves it is easy to establish that  $Z_{ds}^{IV} = -Z_{ds}^I$ ,  $Z_{ds}^{III} = -Z_{ds}^{II}$ ,  $Z_{ds}^I(+x) = Z_{ds}^I(-x)$ . In other words, curve IV is symmetrical to curve I about the  $Ox$ -axis, and curve III shows the symmetry with curve II; curve III is symmetrical to curve I about the  $Oz$ -axis, and curve II shows symmetry with curve IV. From these relations we inferred the range of angle  $\theta$  change by the anomaly curve shape (Table 6.2).

**Table 6.2. Determining the angle  $\theta$  range by the interrelation of absolute values and relative positions of  $Z_{ds}$  curve extrema**

Extremum absolute value ratio	Position of maximum with respect to minimum	Range of angle $\theta$
$Z_{max} >  Z_{min} $	southward	$0 \div 90^\circ$
$Z_{max} <  Z_{min} $	id.	$90 \div 180^\circ$
$Z_{max} >  Z_{min} $	northward	$-90 \div 0^\circ$
$Z_{max} <  Z_{min} $	id.	$-180 \div -90^\circ$

Table 6.2 can be applied to determining the range of angle  $\theta$  only when the normal background level of the anomaly is determined correctly. Otherwise,  $Z_{max}/|Z_{min}|$  ratio is not true. When the background level is unknown, one should use segments  $d_3$  and  $d_4$  ( $d_3 < d_4$ ). Segment  $d_3$  is obtained as the difference in abscissas of the intersection points of a tangent in the inflection point of  $Z_{ds}$  ( $\Delta T_{ds}$ ) curve with horizontal tangents in extremum points, which determine the greatest amplitude (span) of the anomaly. Segment

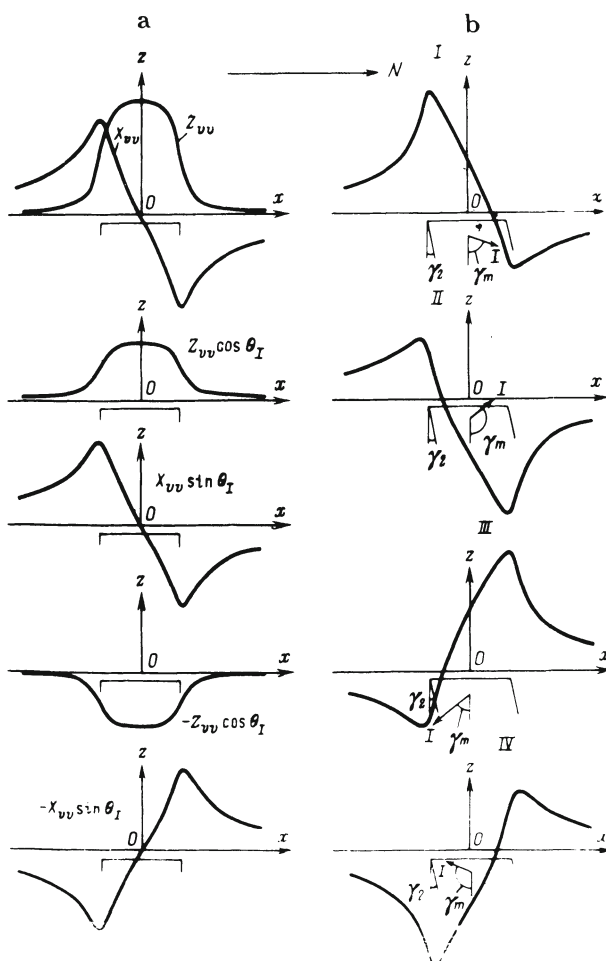


Fig.6.3. Behavior of  $Z_{ds}$  curves over a thick bed for different ranges of  $\theta$  values: (a) graphical expression of formula (6.1) for the  $Z_{ds}$  field, (b)  $Z_{ds}$  curves

(I)  $\theta_I = 0 \div 90^\circ$ , (II)  $\theta_{II} = 90 \div 180^\circ$ , (III)  $\theta_{III} = -90 \div 0^\circ$ ,  
 (IV)  $\theta_{IV} = -180 \div -90^\circ$ ;

when  $\theta_{II} = 180^\circ - \theta_I$ ,  $Z_{ds} = -Z_{vv} \cos \theta_I + X_{vv} \sin \theta_I$ ;

when  $\theta_{III} = -\theta_I$ ,  $Z_{ds} = Z_{vv} \cos \theta_I - X_{vv} \sin \theta_I$ ;

when  $\theta_{IV} = -180^\circ + \theta_I$ ,  $Z_{ds} = -Z_{vv} \cos \theta_I - X_{vv} \sin \theta_I$

$d_4$  is obtained in a similar way on the other branch of the curve. In the inflection points only two tangents are employed which show the greatest (in magnitude) slope toward the  $Ox$ -axis. Segments  $d_3$  and  $d_4$  are taken from the horizontal tangent which intersects sloping tangents at their divergence. The range of angle  $\theta$  is determined from Table 6.3.

**Table 6.3. Determining the angle  $\theta$  range from the positions of segments  $d_3$  and  $d_4$  on the curve  $Z_{ds}$**

Mutual position of segments $d_3$ and $d_4$	Position of segments $d_3$ and $d_4$ relative to inflection points	Range of angle $\theta$
$d_3$ is to the north of $d_4$	below	$0 \div 90^\circ$
$d_3$ is to the south of $d_4$	above	$90 \div 180^\circ$
id.	below	$-90 \div 0^\circ$
$d_3$ is to the north of $d_4$	above	$-180 \div -90^\circ$

Once it is established in which quadrant the angle  $\theta$  is situated, the interpretation of the anomalous curve by corresponding change in the direction of  $Ox$ - and  $Oz$ -axes is reduced to the case of  $0 \leq \theta \leq 90^\circ$  (see Fig.6.3). Thus, when interpreting a curve of type IV, the direction of the  $Oz$ -axis is changed to the opposite, or the curve is mirror reflected about the  $Ox$ -axis, while for interpreting a curve of type III the direction of the  $Ox$ -axis is changed to the opposite or the curve is mirror reflected about the  $Oz$ -axis.

After bringing angle  $\theta$  into the first quadrant, it can be conveniently determined from  $k_\theta = d_3/d_4$  ratio (see Section 7.2). If  $k_\theta = 0.6 \div 0.8$ , then angle  $\theta = 0 \div 30^\circ$ , provided  $k_\theta \geq 0.9$  and  $\theta \geq 60^\circ$ . More accurate estimation of the angle  $\theta$  value can be obtained from the plot  $\theta = f(k_\theta)$ , presented in Fig.7.5.

It is shown in [146] that when  $\theta \geq 30^\circ$  and  $\beta \geq 2$ , the values of intersection point abscissas of the left-hand inclined tangent with the upper horizontal tangent ( $x_{up,l}$ ) and the right-hand inclined tangent with the lower horizontal tangent ( $x_{un,r}$ ) are close, respectively, to the left-hand and right-hand lateral boundary abscissas of a thick bed. Similarly, the left-hand and right-hand inflection point

abscissas ( $x_l$  and  $x_r$ ) are close to the abscissas of the bed angle points, provided  $\theta < 45^\circ$ . Therefore, the lower right-hand and the upper left-hand points of tangent intersection, along with the inflection points in the magnetic anomaly curve, can be employed for contouring anomalous objects in plan, especially taking into consideration the opposite location of the corresponding intersection and inflection points with respect to the bed angle points (see Fig.7.4). Values  $x_{max}$  and  $x_{min}$  are also suitable for the purpose. At  $\theta > 60^\circ$  they are close, respectively, to the abscissas of left-hand and right-hand angle points of a bed, and to the abscissas of points taken between those discussed.

Fig.6.4 shows curves of the abscissas of the points involved (in shares of semithickness of a bed) as a function  $\theta$  for different values of  $\beta$ . The optimal parameter can be selected from Fig.6.4 to contour

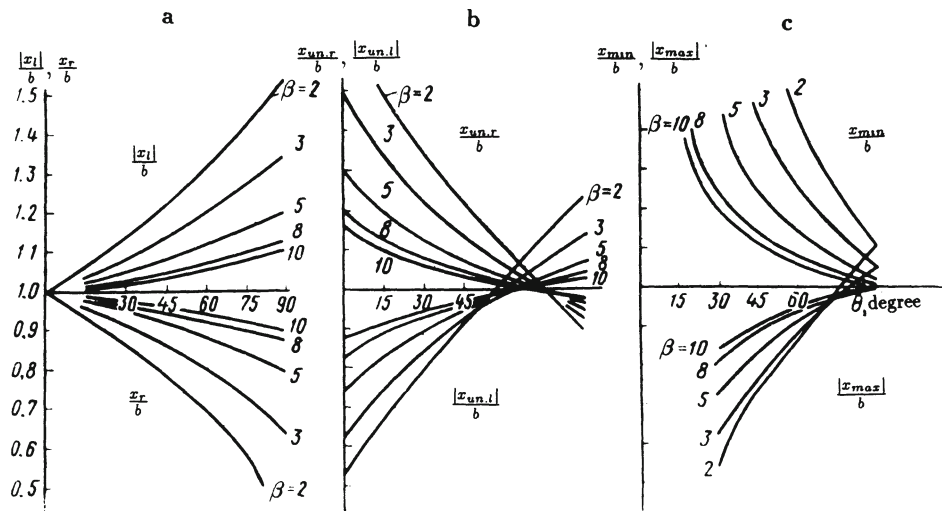


Fig.6.4. Plots of relative abscissas  $|x_l|/b$  and  $x_r/b$  (a),  $x_{un,r}/b$  and  $|x_{un,l}|/b$  (b),  $|x_{max}|/b$  and  $x_{min}/b$  (c) as a function of the angle  $\theta$  for different values of  $\beta$

anomalous bodies in plan for particular values of angle  $\theta$ , even when these values are determined rather roughly. For example, when  $\theta \leq 30^\circ$ , the use of inflection points gives good results, while for the medium values of angle  $\theta = 40 \div 70^\circ$  – that of the selected points of tangent intersection, for  $\theta = 30 \div 60^\circ$  – medium points

between the points of inflection and above mentioned points of tangent intersection, and, finally, for  $\theta = 75 \div 90^\circ$  – medium points between tangents intersection and extremum points. Delineation error does not exceed  $\pm 0.15b$ .

It should be noted that the delineation of bodies can be accomplished by points of inflection with the error not exceeding  $\pm 0.24b$  (or  $\pm 0.15b$ , if  $\beta \geq 3$ ) for  $0 \leq \theta \leq 45^\circ$  angles and by points of tangents intersection for  $45^\circ \leq \theta \leq 90^\circ$ .

The accuracy of delineation considerably increases with growing body thickness (see Fig.6.4). Inflection point position in the plot is not related to the projections of lateral boundaries of thin beds and horizontal cylinders onto the plan, since their horizontal dimensions are indefinable without additional information. It is senseless to delineate these bodies. One should determine the position of the projection of horizontal axis of the body on the plan, which is shifted from maxima's axis. It coincides with the latter for bodies of cylindrical section only under the condition of vertical magnetization, and for sheet-like bodies – when the inclination angle of effective magnetization is equal to the dip angle of the bed ( $\theta = 0$ ). In the case of a thin bed, the horizontal projection of its upper edge axis is easily determined by Reford's points in anomaly plots using a well-known Reford's rule [230] (see Fig.7.1). The upper edge is located under a point in the anomaly plot, in which it is intersected by the straight line joining the maximum and minimum. Theoretical substantiation of this rule is given in [6]. For a cylindrical (isometric in section) body, the position of its axis can be approximately (with an error up to  $\pm 0.24h$ ) determined by the position of its middle point between the points of inflection on the anomaly plot for steep and moderate angles ( $0^\circ \leq \theta \leq 45^\circ$ ) of inclination of the effective magnetization. As to the gentle inclination ( $60^\circ \leq \theta \leq 90^\circ$ ), it is advisable to use (with the same limiting error) the middle point between the maximum and the minimum which is the greatest in magnitude in anomaly plots. A range of the angle  $\theta$  can be easily determined by the ratio of distances between the points of inflection and between the mentioned extremums. If the ratio amounts to  $0.5 \div 0.6$ , the angle  $\theta$  is in the interval of  $0 \div 30^\circ$ . When it exceeds 0.75, then  $\theta > 60^\circ$  (see Section 7.2 and curve  $k'_\theta$  in Fig.7.2).

The above rules for finding the contour or axis of anomalous

bodies hold true for those unlimited along the strike. As to the bodies limited in plan, but having a pronounced strike, the rules remain valid only for the middle portion of the anomaly. In the anomaly edge portions delineation is carried out roughly. It is expedient to use inflection points plotted for a profile along the body strike or the points in which  $Z$  component is half of its value in the anomaly epicenter.

It has been found advantageous to delineate bodies isometric in plan by radial profiles. When a body is magnetized along the Earth's field ( $i_m = 55 \div 65^\circ$ ), the points of inflection in plots are used for the profiles situated in north-eastern and eastern (south-western and western) azimuths. For those situated in north-western and northern (south-eastern and southern) azimuths, the points of tangents intersection are employed.

A map (or scheme) of the results of the anomalous field interpretation includes:

- (1) regional elements, such as singled-out areas with various field pattern, linear field elements, i.e. area boundaries having a sense of boundaries (frequently tectonic) of structural or facial zones;
- (2) local elements such as contours and axes of anomalous objects obtained by delineating local anomalies, linear field elements traced in small areas;
- (3) known elements of geological structure including disjunctive dislocations, intrusives and dikes (possibly, partially exposed) with indicated basicity, effusive-pyroclastic rock fields, as well as deposits, ore shows, etc.;
- (4) results of previous geophysical observations;
- (5) results of interpretation of other geophysical field data, geochemical anomalies.

Joint analysis of all elements, comparison of the elements revealed in the given geophysical field with the geological materials presented in the scheme and with the results of other geophysical methods application, taking into account the information introduced into the initial model of the medium allow to define the geological nature of most of them. This done, the singled out field elements are represented in the scheme using symbols of geological content.

Special marks are used to indicate the elements of geological structure, which are established reliably (supplementing and refining known geological objects), and those which are established hypothetically (hidden objects that were assumed in the initial model of the medium), and the elements (objects) which are especially tentative (a lack of information in the initial model does not allow to reveal their nature). The nature of the latter should be refined during subsequent geophysical investigations, in some cases using quantitative interpretation (after determining such parameters as magnetization, density, polarizability, etc.) and interpretation of different geophysical fields observed in integrated investigations.

Often the evidence accumulated at this stage of interpretation is sufficient for solving the given problem and determining the directions of further geological-geophysical investigations.

# **Chapter 7**

## **DETERMINATION OF THE ANOMALOUS BODY PARAMETERS**

### **7.1 General issues of quantitative interpretation**

#### **7.1.1 Basic ideas and methods of the inverse problem solution**

The inverse problem solution is often called “inversion procedure” or simply “inversion”. The interpretation problem at the stage of determining the anomalous bodies parameters consists in a detailed description of the sources of anomalies by the measured field taken into account with prior geological and geophysical information [258].

As mentioned above, determination of the anomalous bodies quantitative characteristics is also often called quantitative interpretation. Yet some features quantitatively characterizing an object (such as the body position in plan, the strike direction and, in some cases, the approximate plan dimensions of the anomaly sources), can be obtained by qualitative interpretation as well. However, the qualitative interpretation does not provide such parameters as the occurrence depth of the upper edge or center of the body, its dip angle or magnetization. These parameters are only roughly estimated in comparison with neighboring anomalies with known source parameters.

The above parameters can be determined more exactly provided there exist:

- (1) a fairly clear model notion of the sources resulting from the

qualitative interpretation, taken into account prior geological and geophysical information;

(2) available methods to determine the desired parameters with due regard to the existing model notions.

These are the most significant requirements.

A great number of methods employed in practice to determine quantitative characteristics of the anomaly sources are based on the inverse problem solution with the deterministic notions of the sources and the fields they induce. Though the deterministic approach is limited under the conditions of open regions, comparatively simple situations where this approach can be efficiently used are numerous enough.

The deterministic approach is realized in the form of a variety of analytical approximations. The real source distribution is approximated by a certain model distribution. The field, generated by the real source distribution, which occurs only in discrete points or along discrete lines, is approximated by a model field, i.e. the field of the model source distribution. It is essential that, like most real sources, the above model ones are stationary and generate potential fields, and an experimental field can be approximated by the potential fields of the sources. In this case the interpretation can be based on the potential theory, which enables one to solve the direct and inverse problems of geophysics for model sources and a model field, respectively.

However, an experimental field to be approximated, along with the model part proper, involves fields of noise sources (both systematic and random), which are not the target of investigation and interpretation. It also involves observation errors, which can be formally assumed to be caused by some geological sources. An experimental field thus complicated makes the quantitative interpretation approximate, irrespective of the source and field approximation quality.

In the framework of the fundamental idea of analytical approximation, the inverse problem can be solved in two ways [259].

(1) The first way involves variation of the model source distributions. If for each individual model situation we compute the field using the known formulas and compare it to the observed one, then

the discrepancy between the fields can be reduced to minimum (or be less than a certain given value). The model distribution thus obtained is assumed to be the distribution of real sources. In such a way the selection idea is realized – the inverse problem is solved by successive solving a series of direct problems.

(2) The second way employs certain principles of the potential theory. They postulate that the harmonic functions approximating an experimental field cease to be continuous, harmonic and satisfying Laplace's equation in some points of the area occupied by anomalous masses, i.e. in singular points associated with the field sources. The observed field can be transformed so that the obtained distribution of the field or some values determined by the field will fairly exhaustively characterize the sources. Thus, the information transformation idea (in terms of Strakhov [259]) is realized – that of an immediate solution of the inverse problem.

The idea of the approximate optimization based selection is most commonly used in the framework of the selection conception. This conception incorporates also the idea of the characteristic points method, or an interpolation selection. Here the approximating model parameters are determined from the system of equations resulting from equating the values of the model field in some points with the corresponding experimental values (or quantities obtained from the experimental data). The tangent (inflection-tangent-intersection) method is a version of the characteristic point method. Yet it differs from the latter drastically, since along with the field as such, the values of horizontal gradients of the field are also used in some individual points. The potentialities of the interpolation selection are limited by the fact that there are no criteria to bring the selected model field in conformity with the real one (hence, the model as such with the real source). Another factor is the instability with respect to the noises in the observation data. Moreover, the information taken from the observed field is far from being complete, though the portions (points) of the anomaly plot with the greatest informativity are undoubtedly used. Still the interpolation selection is rather straightforward and fairly acceptable in simple situations with a low level of noises. Being fast enough, it ensures rapid interpretation. The best results can be obtained with the characteristic points applied to get an interval estimation of the parameters (not a point-wise one, in the form

of particular numbers) in the framework of a mixed deterministic-statistical model of the experimental material [98].

According to [259], the integral method can be also classified as an interpolation selection – the selection is accomplished by certain values representing the functions of the experimental data. However, the integral method can be interpreted within the framework of the information transformation conception as well. The classical technique of determining the sources integral characteristics by computing certain integrals of a field with weights as functions of coordinates is the method of transforming the information into interpolation functionals [259]. An interpretation functional enables the field sources to be located, i.e. a multitude of points, its certain submultitude (including a one-point submultitude) belonging to the field sources. Similar functions are the coordinates of the field singular points [104,295].

In the framework of the concept of information conversion, the idea of the field's spatial distribution determination has been developed [259]. The concept of information conversion differs from the selection concept in that it employs basically analytical field models (the field complicated by random noises), while the sources models are used only in an indirect way. As a result, instead of anomalous bodies parameters, the field's singular points are obtained, associated with the anomalous bodies in a certain way. They occur either on their boundary (on the breaks in the body contour) or inside the bodies. In case of a smooth contact surface, the distance between the latter and the singular points may be arbitrarily large. The method of a complete normalized gradient [29] can also be considered a realization of the above concept.

The ideas just discussed give rise to a number of techniques (varieties of methods) of the quantitative interpretation with different requirements to prior model information, conditions of applicability, degree of accuracy and labor-consumption. Table 7.1 gives a list of the main groups of methods with the mentioned peculiarities in common (on the example of magnetic prospecting where the procedures are most developed).

**Table 7.1. Characteristics of major methods for the inverse problem solution in the framework of the fundamental idea of analytical approximation**

Ideas forming the basis of the methods (in terms of [259])		Groups of methods	Applicability conditions								Prevailing sensitivity to errors	Labour intensiveness Needed		Average relative error, %	
			Direction of the body magnetization		Observation line		Body shape					Systematic	Random	Preliminary transformations	
Conceptual	Functional	Arbitrary	Given-inclined	Vertical	Arbitrary	Inclined	Horizontal	Complex	Simple	Systematic	Random	Preliminary transformations	Computers		Average relative error, %
Selection	Selection based on linear programming methods	-	+	+	+	+	+	+	+	+	-	-	+	5 - 20	
		-	+	+	+	+	+	+	+	+	-	-	+		
	Interpolation selection	Characteristic points	+	+	+	-	+	+	-	+	-	+	+	-	10 - 30
		Tangents	+	+	+	-	+	+	-	+	-	+	-	-	
	Field transformation	Spatial graticules	-	+	+	+	+	+	-	+	+	-	-	-	5 - 25
		Integral	+	+	+	-	+	+	+	+	+	-	+	-	
Transformation	Transformation into a set of interpretation functionals values	Singular points localization	+	+	+	-	+	+	+	+	-	+	-	+	5 - 25
	Determination of a spatial distribution of a field	Analytical (approximation) continuation	+	+	+	-	+	+	+	+	-	+	-	+	5 - 25

(1) If the selection methods based on approximation optimization admit the selection of a background component of the field, then the methods are not sensitive to systematic errors.

(2) The interpolation selection methods have been developed primarily for vertical magnetization. Modifications for arbitrary magnetization are available.

(3) The interpolation selection methods and methods of the field transformation have been developed for a horizontal profile and modified by the authors for an inclined plane. In the case of preliminary field reduction to the inclined plane, the methods are acceptable for a complex profile as well.

(4) With an arbitrary direction of magnetization the integral methods have been developed for bodies of a simple shape.

(5) Preliminary transformations are required in the method of the latter when characteristic points are employed at different levels.

It follows from Table 7.1. that the groups of methods have diverse and generally controversial conditions of applicability. This should be taken into account when selecting a way of interpretation (see Subsection 7.4.1).

The data on the degree of accuracy of the interpretation methods (see Table 7.1.) are valid only when applied correctly. Otherwise the errors in the interpretation results can amount to hundreds per cent.

Table 7.1. gives an idea of potentialities, advantages and disadvantages of different groups of methods under oblique magnetization and rugged terrain relief. The table does not include the methods which cannot be applied in the mentioned conditions.

### **7.1.2 Possibilities of interpretation of the field observed on an inclined terrain relief**

It is essential that the selection methods based on approximate optimization can be applied to under conditions of a complex terrain relief. In this case the tentative parameters of the bodies, including the direction of magnetization (or the range of probable changes in the parameters), should be specified. However, oblique magnetization and rugged terrain relief make it difficult to develop model notions, as compared with the vertical magnetization and smooth relief.

The interpolation selection methods have been developed earlier for bodies of a simple shape, basically under vertical magnetization and horizontal observation line. For these shapes certain modifications have been developed [5], which are applicable under arbitrary direction of the bodies magnetization and conditions of inclined profiles.

According to the data reported in [146], if a magnetic field is observed on an inclined profile, but described on horizontal projections of the observation points onto the plan, then the field thus given can be interpreted by all the techniques developed for the horizontal relief. In accordance with Section 2.2, the same is valid for other geophysical methods discussed. In this case the parameters obtained by interpretation refer to some fictitious bodies related in

a certain way to the real sources. The relations of the parameters are established and given in general terms in Section 2.2.

Table 7.2 presents the formulas to compute the real body's parameters by those of a fictitious one for different components of the magnetic field. The fictitious body's parameters are denoted by a tilde.

**Table 7.2. Conversion formulas for the parameters of a 2-D body of an arbitrary shape proceeding from the parameters of a fictitious body**

Parameters to be determined	Conversion formulas	Applicable to anomalies
$z_s$	$(\tilde{z}_s + \tilde{x}_s \tan \omega_o) \cos \psi$	$Z, \Delta T, X$
$x_s$	$(-\tilde{z}_s \tan \omega_o + \tilde{x}_s) \cos \psi$	$Z, \Delta T, X$
$S$	$\tilde{S} \sec^2 \omega_o \cos \psi$	$Z, \Delta T, X$
$I$	$\tilde{I}$	$Z, \Delta T$
$I$	$\tilde{I}_c \sec \psi$	$X$
$C_m$	$\tilde{C}_m$	$Z, \Delta T, X$
$\gamma_m$	$\tilde{\gamma}_m - 2\omega_o$	$Z, \Delta T, X$

As mentioned above, if the inclined observation profile with the inclination angle  $\omega$  does not cross the strike of the anomalous body, then the observations are first reduced to the inclined profile across the body strike. The angle of inclination  $\omega_o$  for this profile is calculated by the formula

$$\tan \omega_o = \tan \omega \sec \psi, \quad (7.1)$$

where  $\psi$  is the difference in azimuths of the profiles under study.

It should be noted that when a field observed on the inclined profiles not across the body strike is represented as a plan of plots or a plan of isolines (i.e. in horizontal projections), all the real anomalous bodies are replaced by fictitious ones. So, the qualitative interpretation will yield information about the fictitious bodies only. Their cross-section in the vertical plane of the profile is similar to that of real bodies and turned counter-clockwise by the angle  $\omega_o$  (see Fig.2.1). Each fictitious body is magnetized by a fictitious vector of the same value as that of the corresponding real body. Yet the projection of the fictitious vector onto the plane of the profile

is deviated from the vertical by an angle which is  $2\omega_0$  larger than the angle of deviation of the real vector projection onto the vertical plane, normal to the real body strike [146]. It is possible to pass from fictitious bodies to the real ones only with the help of quantitative interpretation.

In case the observation profiles have a complex configuration admitting no approximation by inclined straight lines, the field should be previously reduced onto the inclined plane parallel to the mean inclination of the relief. This possibility has been discussed in Section 2.2. These results greatly extend the applicability range of methods based on the information transformation concept.

### 7.1.3 Choice of parameters to be determined

An important stage of the interpretation is establishing a list of parameters which are open to inspection. It is well known that geological objects approximated by simple bodies have a number of parameters that cannot be determined, unless there are some additional data, since they are not included into the approximating analytical expressions irrespective of other parameters. If there are no independent data, then a separate determination of interrelated parameters is practically impossible, even with the help of selection methods, since the range of their admissible values cannot be reduced to the desired extent.

In some cases (with high accuracy of observations, low level of noises, considerable intensity of the anomaly) the ratio of the parameters characterizing the body cross-section to the depth of its occurrence can be changed by upward or downward continuation, making use of appropriate schemes securing the desired accuracy of the continuation. For example, an anomaly caused by a depth-limited thin bed, after the downward continuation to a due level, can be treated as an anomaly caused by a thick bed extending to a large depth. The anomaly thus modified permits the horizontal thickness of the bed and the effective magnetization to be determined separately. The upward continuation makes it possible to view above mentioned anomaly as an anomaly due to a circular cylinder, thus enabling to determine the inclination of the effective magnetization, and then the bed's dip angle. Examples of such

approach are described in [146] and presented in Section 7.2. (see Fig. 7.9).

For bed-like bodies of great thickness, the latter is determined accurately enough by the inflection points of the anomaly plot irrespective of the value of the generalized angle  $\theta$ . Therefore, the interpretation problem for such bodies should consist in obtaining the depth of the upper edge occurrence, inclination and value of the magnetization. The latter parameter is essential for specifying the nature of anomalous bodies. If the structure of the field (i.e. the presence of lateral minimums) indicates to a depth-limited character of the body, then the depth of the lower edge should also be classified as a parameter to be determined. It generally requires some additional, independent data about the bed thickness and its upper edge depth. It is also essential that there were no distortions in the area of the anomaly minimums. In this case a downward continuation may be of use (with corresponding smoothing). This will permit us to somewhat increase the accuracy of determination of the upper edge depth, employing the techniques designed for beds unlimited along the dip.

#### 7.1.4 Preparing the anomaly plot for inversion

The basic operation necessary to prepare the anomaly plot for inversions is a choice of an interpretation profile with consideration of 3-D peculiarities of real medium. In some cases it is required that the angle  $\theta$  was reduced to the first quadrant.

The available interpretation techniques have been primarily developed for anomalies due to the bodies unlimited along the strike. This can be accounted for by the fact that the interpretation profile is assumed to be horizontal and pass across the strike of the anomaly (the body). The strike of body is usually determined by the direction of the anomaly axis. Quantitative calculations by the interpolation selection technique require plots which are not complicated by any side effects, have a pronounced minimum to the right or left of the maximum and straight-line portions without distortions (in the proximity of the inflection points).

Rather often the interpretation profile cannot be drawn across the strike of the anomaly axis because of distortions in the anomaly's

boundary portions due to the proximity of other anomalous bodies. In case a direction is chosen not across the strike, so that any distorting effect of the neighboring objects is excluded, then the parameters resulting from the quantitative determinations refer to a fictitious body. The formulas for calculating real bodies' parameters by those of fictitious ones, are presented in Table 7.2 and those for other fields follow (see Section 7.3).

The condition of the body's ideal two-dimensionality is never met in practice, since real bodies are finite along the strike. Therefore, there arises a question as to the expediency of applying the procedure for interpretation of anomalies from 2-D bodies to interpretation of anomalies from 3-D bodies.

A thin vertical bed with vertical magnetization and limited strike can be replaced by a bed infinitely extended in plan, provided the value of  $q$  (i.e. the ratio of the bed extension along the strike  $2l$  to the depth of its upper edge occurrence  $h$ ) is greater or equal to four [178]. The same is valid for a horizontal circular cylinder (here  $q$  is the *cylinder length/center depth ratio*). To replace a thick strike-limited bed by a strike-unlimited one, the following relation is of importance:

$$q_1 = l/\sqrt{b^2 + h^2}, \quad (7.2)$$

where  $b$  is half-thickness of the bed.

If the bed thickness in several times as great as the depth of its occurrence, the replacement is possible at  $q_1 = 2.5 - 3$ .

The authors of the present book have examined the conditions for a strike-limited body to be approximately replaced by an infinite one under oblique magnetization. The results indicate that this conditions generally hold for the interpretation of  $Z_d$  anomalies, excluding the case of a thin bed, which requires  $q \geq 6$  at  $\theta \geq 30^\circ$ . The  $\Delta T_d$  anomalies make the conditions imposed on  $q_1$  more strict. In the case of the same  $q_1$  values, the divergences of amplitude-normalized fields due to 3-D and 2-D bodies are greater for the  $\Delta T$  anomalies than for the  $Z$  anomalies.

A relationship of the long and short axes of some isolines of an anomaly indicates to the value of  $q$  or  $q_1$ . Yanovsky [299] reported that for a thin bed this relationship is about 0.5  $q$  for the isoline  $Z = 0.5 Z_{max}$ . It is easy to show that for a horizontal limited

cylinder the relationship of the axes of the isoline  $Z=0.5Z_{max}$  is approximately equal to  $q$ . For a thick bed it equals  $q_1$  with higher accuracy.

Fig.1.2 of Section 1.1 shows the distribution of geological bodies dimensions both along and across the strike. For open areas, on the average,  $2l=5$  km,  $2b=0.8$  km, so that  $q_1=6$  (for semiclosed areas  $2l=5.5$  km,  $2b=1.3$  km and  $q_1=4$ ). Therefore, the condition of approximate replacement of strike-limited bodies by infinite ones is satisfied on the average. In this case the interpretation should be carried out by the profiles normal to the long axis of the anomaly and passing across its central portion.

If the above conditions are not satisfied, it is necessary to reduce a 3-D field to a 2-D one. For this purpose, a special technique has been worked out. It consists of averaging an anomalous field along the lines, which are parallel to the strike [12,244,287]. However, this transformation has not been widely used, since on the periphery of the anomaly under examination other anomalies are generally observed, which distorts the field averaging process.

According to Tyapkin [287], the initial values of  $Z$  anomaly, summed up over the intervals corresponding to a 3-fold extension of the body, yield a  $Z$  curve which is very close to the curve for a 2-D body. However, fairly good results can be derived if the averaging is performed only within the bounds of the anomaly (the last closed isoline) by the following formula

$$Z(x) = \frac{1}{n} \sum_{i=1}^n Z(x_i, y_i), \quad (7.3)$$

where  $n$  is the number of profiles in the summation interval.

In some cases the computations should be preceded by the reduction of  $\theta$  to the first quadrant. For details see Section 6.2.

## 7.2 Techniques of magnetic anomaly interpretation under oblique magnetization

Let us dwell on the techniques developed or improved by the authors for the conditions of oblique magnetization. We described them in

the order recommended for their application, outlined in Section 7.1.

### 7.2.1 Interpolation selection of parameters

#### 7.2.1.1 General information

The techniques of anomaly interpretation under oblique magnetization and unknown background level, which are most thoroughly studied, are considered here for such simple 2-D bodies as an inclined depth-unlimited thick bed, inclined unlimited thin bed and horizontal circular cylinder (see Table 1.1). The calculation formulas are given for the observations performed in horizontal profiles across the strike. The interpretation results for inclined profiles, given in a horizontal projection, refer to fictitious bodies. They should be converted to the real sources parameters by the formulas of Table 7.2. For more complicated profiles, the magnetic field ( $Z$  or  $\Delta T$ ) should be first converted to the inclined straight line, which is the nearest to the observation profile.

The techniques are described with  $Z$  component taken as an example. However, the same methods can be applied to the interpretation of  $\Delta T$  anomaly.

The following values should be determined in the course of interpretation.

(1) Effective magnetic moment  $M_e$ . Properly speaking, it is, respectively, for an inclined unlimited thick bed – an effective magnetic moment of its volume unit, i.e. effective magnetization ( $M_e^v$ ), for an inclined unlimited thin bed – a magnetic moment of its cross-section unit, i.e. linear effective magnetization ( $M_e^l$ ), and for a horizontal circular cylinder – a magnetic moment of the length (along the strike) unit, i.e. effective magnetization of its cross-section area ( $M_e^a$ ). Their respective expressions are:

$$M_e^v = I_e \sin(\phi_2 - \phi_1); \quad M_e^l = I_e 2b_o; \quad M_e^a = I_e S, \quad (7.4)$$

where  $I_e = IC_m$  is the effective body magnetization (for anomalies of  $\Delta T$  the value  $C_m$  is replaced by  $C_m C_o$ );  $\phi_1$  is the angle of inclination for the upper edge of a thin bed;  $\phi_2$  is the same for lateral faces of thin and thick beds;  $2b_o$  is the normal thickness of a

thin bed;  $S$  is the cross-section area of the cylinder;  $C_m$  has been determined in the notations to the formula (6.1),  $C_o$  – in Subsection 5.2.3.

(2) Generalized angle  $\theta$ , equal correspondingly to

$$\theta = \gamma_m - \gamma_2 + \phi_1, \quad \theta = \gamma_m - \gamma_2, \quad \theta = \gamma_m, \quad (7.5)$$

where  $\gamma_2 = 90^\circ - \phi_2$  (for  $\Delta T$  anomaly  $\gamma_m$  should be replaced by  $\gamma_o + \gamma_m$ ).

(3) Coordinates of angular points  $(x_1, h_1)$  and  $(x_2, h_2)$  for the upper edge of a thick bed (here  $x_2 - x_1 = 2b$  is the horizontal thickness of the bed), coordinates of the upper edge mid-point  $(x_o, h)$  of a thin bed, coordinates of the center of the cylinder  $(x_c, h_c)$ .

(4) Abscissa of the epicenter (projection onto the plan of the mid-point of the upper edges of thick and thin beds, or of the center of the cylinder), with respect to an arbitrary origin, since under the oblique magnetization the epicenter does not coincide with the abscissa of the anomaly maximum.

The need to localize the epicenter and to determine the generalized angle  $\theta$  is a specific feature of the anomaly interpretation under oblique magnetization. Another task of the interpretation in this case is the determination of the normal background level ( $\Delta Z_{backgr}$ ) for the anomalies.

In the techniques described below the angle  $\theta$  is taken to be in the range of  $0 \div 90^\circ$ ,  $Ox$ -axis is assumed to have an approximate north-wise direction to the right (in figures),  $Oz$ -axis – downward, the field  $Oz$ -axis – upward. With other values of  $\theta$ , the angle  $\theta$  is reduced to the first quadrant, employing the corresponding reflections of the anomalous curve with respect to  $Ox$ – or  $Oz$ -axes, according to the rules reported in Section 6.2. When the value of the reduced angle  $\theta$  is obtained from the interpretation results, it is necessary to restore its true value; for  $\Delta T$  the value of  $\gamma_o$  should be subtracted.

#### 7.2.1.2 Method of characteristic points

The following characteristic points are used in the interpretation: abscissas and ordinates ( $x$  and  $y$  coordinates) of the anomaly

maximum ( $x_{max}, z_{max}$ ) and minimum ( $x_{min}, z_{min}$ )<sup>1</sup>,  $x$ -coordinates of the right and left points of the anomaly semi-amplitude ( $x_{0.5z_A}$ )<sub>r</sub> and ( $x_{0.5z_A}$ )<sub>l</sub>, respectively;  $x$ -coordinates of the right and left inflection points of the anomaly plot  $x_r$  and  $x_l$ , respectively (Fig. 7.1), and  $x$ -coordinate of the maximum  $x_{max}$  ( $\Delta h$ ) of the curve, obtained from the initial one by converting to a higher level  $\Delta h$ . The origin of

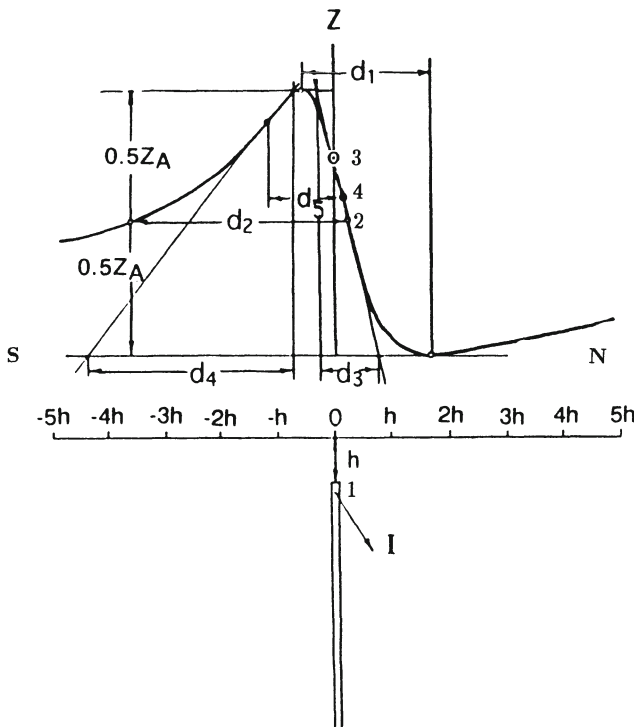


**Fig. 7.1. Position of characteristic points and tangents on  $Z$  anomaly due to an obliquely magnetized thin bed**

(1) a model of thin bed situated in non-magnetized medium; (2) points of extrema and half-width; (3) Reford's point; (4) inflection points of the anomaly plot

the practical curve is chosen arbitrarily and not at the epicenter, as its position is unknown. The normal background level is not known either. Bearing this in mind, we use the differences in  $x$  and  $y$  coordinates for the corresponding characteristic points (these differences being independent of the mentioned unknown values, see

<sup>1</sup> For an anomaly due to a cylinder, one distinguishes between the right minimum with coordinates  $(x_{min,r}, z_{min,r})$  and the left minimum with coordinates  $(x_{min,l}, z_{min,l})$ .

Fig.7.1):

$$d = x_{max} - x_{min} (\Delta h); \quad (7.6)$$

$$d_1 = x_{min} - x_{max}; \quad (7.7)$$

$$d_2 = (x_{0.5Z_A})_r - (x_{0.5Z_A})_l; \quad (7.7)$$

$$d_5 = x_r - x_l; \quad (7.9)$$

$$Z_A = Z_{max} - Z_{min}. \quad (7.10)$$

For a cylinder equation (7.7) is substituted by

$$d_{1r} = x_{min,r} - x_{max}; \quad d_{1l} = x_{max} - x_{min,l}. \quad (7.11)$$

The obtained relations describing the links of the characteristic points coordinates and the corresponding characteristic differences with the model parameters, are used to derive the calculation formulas for these parameters (Table 7.3).

The interpretation is performed as follows. The desired characteristic points are found on the anomaly curve. The corresponding characteristic segments are measured and substituted into formulas in Table 7.3 following the order they are listed in this table. Fig.7.2 facilitates the determination of some coefficients in the function of angle  $\theta$  for the case of a horizontal cylinder. Fig.7.2 shows that for rapid estimation of the depth  $h$  with any  $\theta$  in the range of 0 to  $90^\circ$  for the case of a horizontal cylinder with  $k_5 \approx 0.9$  the formula can be used:

$$h_c = 1.1d_5. \quad (7.12)$$

If there are more than one formula in Table 7.3 to determine a parameter, all its values thus obtained should be averaged.

The case of a thick bed fails to yield simple analytical expressions of the relations between the parameters and characteristic points. The bed epicenter can be defined by the curve of the horizontal gradient  $Z_x$ . If  $2b \gg h$ , then there will be two weakly-interrelated pulses registered on the curve  $Z_x$ , each of them proportional to the  $Z$  anomaly of a thin bed. The upper edges of the "beds" corresponding to these pulses, fall on the angular points of a thick bed. The magnetization of the R.H. (right hand) bed is negative.

It is possible to obtain the exact position in plan of the thick-bed lateral faces by Reford's point determined on each pulse of

**Table 7.3. Formulas for interpreting anomalies over a thin bed and a horizontal circular cylinder by the method of characteristic points**

Parameters to be determined	Parameters employed for anomalies due to models		Formulas to calculate parameters by the anomaly due to models	
	bed	cylinder	bed	cylinder
$\theta$	$d, \Delta h$		$\tan(\theta/2) = d/\Delta h$	$\tan(\theta/3) = d/\Delta h$
	$d_1, d_2$	$d_{1r}, d_{1l}$	$\tan \theta = d_2/d_1$	$\cot(\theta/3) = \sqrt{3} \frac{(d_{1l}+d_{1r})}{(d_{1l}-d_{1r})}$
$h, h_c$	$d_1, d_2, \theta$	$d_{1r}, \theta$	$h = \sqrt{d_1 d_2}/k_{1,2}$ , where $k_{1,2} = 2/\sqrt{\sin \theta \cos \theta}$	$h_c = d_{1r}/k_{1r}$ , where $k_{1r} = 2\sqrt{3} \frac{\cos(60^\circ+\theta/3)}{\cos \theta}$
	-	$d_{1r}, (\Delta h)$	$h = d_5/k_5$ , where $k_5 = 2\sqrt{3} \frac{\sin(\theta/3)}{\sin \theta}$	$h_c = \frac{d_{1r} \Delta h}{d_{1r} - d_{1r}(\Delta h)}$ $k_5 = 2\sqrt{2} \frac{\cos(\theta/2)-1}{\cos \theta}$
$M_e$	$Z_A, h, h_c$		$M_e = 0.5 Z_A h$	$M_e = Z_A h_c/k_m$ , where $k_m = (3\sqrt{3}/2) \cos(30^\circ - \theta/3)$
$x_o, x_c$	$h, \theta, x_{max}, x_{min,r}$		$x_o = 0.5(x_{max} + x_{min,r}) - h \cot \theta$	$x_c = 0.5(x_{max} + x_{min,r}) - h_c \frac{\sin(60^\circ + \theta/3)}{\cos \theta + h_c \tan \theta}$
	$(x_{0.5Z_A})_r, (x_{0.5Z_A})_l$	-	$x_o = 0.5[(x_{0.5Z_A})_r - (x_{0.5Z_A})_l] + h \tan \theta$	
	$h, \theta, x_r, x_l$		$x_o = 0.5(x_r - x_l) - h \cot \theta + h \frac{\cos(\theta/3)}{\sin \theta}$	$x_c = 0.5(x_r + x_l) + h_c \tan \theta - \sqrt{2} h_c \frac{\sin(\theta/2)}{\cos \theta}$
$\Delta Z_{backgr}$	$Z_{min}, Z_A, \theta$		$\Delta Z_{backgr} = Z_{min} + Z_A \frac{k_o}{1+k_o}$ , where $k_o = \frac{1-\cos \theta}{1+\cos \theta}$	$k_o = \frac{\cos^3(60^\circ + \theta/3)}{\cos^3(\theta/3)}$

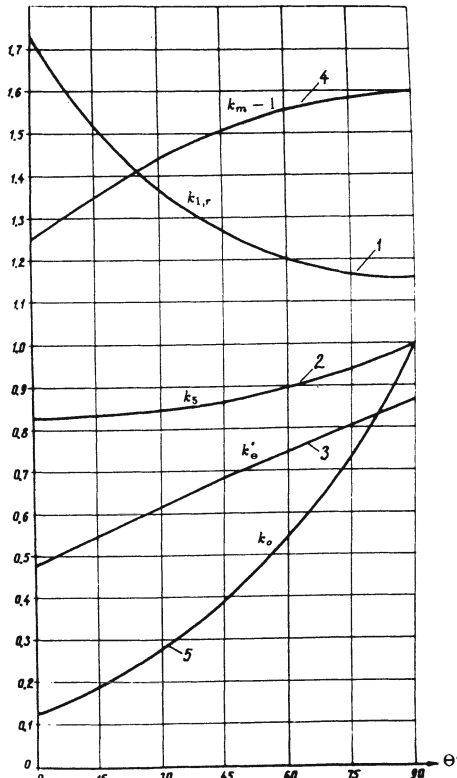


Fig. 7.2. Plots of variable coefficients  $k_{1,r}$  (1),  $k_5$  (2),  $k'_\theta$  (3),  $k_m - 1$  (4) and  $k_o$  (5) as functions of  $\theta$  for interpreting the anomalies of  $Z$  over a horizontal circular cylinder by the method of characteristic points

the obtained curve  $Z_x$ . The distance between these points equals the bed thickness (within the bounds of the gradient determination accuracy). The origin occurs at the mid point. We may go on interpreting the above mentioned pulses of the curve  $Z_x$  by the formulas for a thin bed.

When  $h_1 = h_2$  (the upper edge of the bed is horizontal), the bed parameters can be determined as follows. If we make use of the origin of the coordinates, obtained either by the above technique or by the tangent method (see below), then it is not difficult to single out the symmetrical and antisymmetrical portions on the curve  $Z_{ds}$  which has been determined in the denotations to the expression (6.1):

$$Z_{vv}(x) \cos \theta = 0.5[Z_{ds}(x) + Z_{ds}(-x)];$$

$$X_{vv}(x) \sin \theta = 0.5[Z_{ds}(x) - Z_{ds}(-x)].$$

The values of  $h$  and  $b$  are calculated by the curve  $Z_{vv} \cos \theta$  using the known technique of the characteristic points  $(x_{0.5}, x_{0.25})$ . To determine  $M_e$  and  $\theta$  it is necessary to employ the amplitudes of both curves. Proceeding from the analytical expressions for  $Z_{vv}$  and  $X_{vv}$ , one can readily make sure that the amplitude of the symmetrical curve equals  $(Z_{vv})_A \cos \theta$ , while that of the antisymmetrical one makes up  $(X_{vv})_A \sin \theta$ . The two values of the coefficient  $k_m$  ( $k_m$  is the amplitude of the anomaly at  $h = 1$ ,  $2M_e = 1$  and given  $\theta$  and  $\beta$  values), i.e.  $k_{m_0}$  and  $k_{m_{90}}$  are found. They are obtained in terms of  $\beta = b/h$  with  $\theta = 0$  and  $\theta = 90^\circ$ , using the nomograph given in Fig. 7.7b (see below). The formula  $M_e = Z_A/2k_m$  is applied to obtain  $M_e \cos \theta$  by the first amplitude and  $M_e \sin \theta$  by the second. These two values serve to determine the magnetic moment  $M_e$  and the angle  $\theta$ . A similar procedure can also be used for other models of anomalous bodies.

#### 7.2.1.3 Tangent method

Unlike the method of the characteristic points, the tangent method employs not only  $x$  and  $y$  coordinates of maximum and minimum points, inflection points and their differences, but also the first horizontal derivative in inflection points (where the first derivative has its extrema). These values can be readily obtained from the anomaly plot as tangents of the inclination angles of the tangents to the curves at the inflection points. This fact, along with the acceptable accuracy of the method, favors a wide application of the method.

Semenov proposed in 1948 the simplest version of the tangent method to interpret self-potential anomalies [240]. Gratchev [177] developed a similar method to estimate the occurrence depth of the magnetic anomalous bodies. A somewhat different variant of the tangent method, was suggested by Peters [223]. Quite a number of modifications of the tangent method are available today ([67, 194, 229, 230], etc.). Yet, practically no variant, intended for reducing the inclined magnetization effect, determines  $\theta$ , which is an important parameter of the obliquely magnetized anomalous bodies.

The modification discussed below does not suffer from such a

limitation. It is designed specially for the conditions of oblique magnetization and inclined relief. This technique permits us to determine  $\theta$  and to locate the origin (i.e. position of the body's epicenter) not beforehand, but in the course of the interpretation. Four tangents are used: two inclined ones, passing through the inflection points with the largest in absolute value horizontal gradients of the field, and two horizontal ones, passing through the maximum and the largest in absolute value minimum of the anomaly. The inflection points at the inclined tangents are the nearest to the largest in absolute values extrema of the anomaly and are found to their left for  $\theta = 0 \div 90^\circ$  and the axis  $Ox$  running approximately to the north bearings (to the right in figures).

When interpreting the anomaly  $Z$  due to a thin bed or a circular cylinder, the segments  $d_3$  and  $d_4$  are used, taken from the anomaly plot (see Fig.7.1). Their analytical expressions

$$\left. \begin{aligned} d_3 &= Z_A / |Z_{xr}| \\ d_4 &= Z_A / Z_{xl} \end{aligned} \right\} \quad (7.13)$$

have the following form:

for an anomaly due to a thin bed:

$$\left. \begin{aligned} d_3 &= h / \sin^3(60^\circ + \theta/3) \\ d_4 &= h / \sin^3(60^\circ - \theta/3) \end{aligned} \right\}, \quad (7.14)$$

for an anomaly due to a horizontal circular cylinder:

$$\left. \begin{aligned} d_3 &= \frac{3\sqrt{3}}{8} h \frac{\cos[(90^\circ - \theta)/3]}{\cos^4[(90^\circ - \theta)/4]} \\ d_4 &= \frac{3\sqrt{3}}{8} h \frac{\cos[(90^\circ - \theta)/3]}{\cos^4[(90^\circ + \theta)/4]} \end{aligned} \right\}. \quad (7.15)$$

In both cases the ratio  $k_\theta = d_3/d_4$  is a function of the angle  $\theta$  only and is used to determine this angle either by the formulas

$$\left. \begin{aligned} \tan(\theta/3) &= \sqrt{3} \frac{(1 - \sqrt[3]{k_\theta})}{1 + \sqrt[3]{k_\theta}} \\ \cot(\theta/2) &= 1 + 2 \frac{\sqrt[4]{4k_\theta}}{1 - \sqrt{k_\theta}} \end{aligned} \right\} \quad (7.16)$$

or by the curves  $k_\theta = f(\theta)$  in Fig.7.3.

The depth  $h$  is obtained by the formula

$$h = d_i/k_i, \quad (7.17)$$

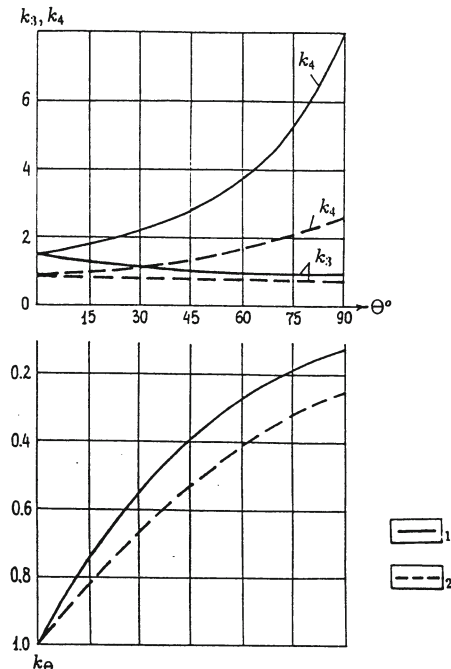


Fig.7.3. Nomograph allowing to determine the angle  $\theta$  and the coefficients  $k_3$  and  $k_4$  by the tangent method from the anomaly over a thin bed (1) and a circular cylinder (2)

where  $i$  is equal to three or four.

The coefficients  $k_3$  and  $k_4$  stand for the values of  $d_3$  and  $d_4$  when  $h = 1$ . They are functions of  $\theta$ . Fig.7.3 shows the plots for  $k_3$  and  $k_4$ . This figure can be used to determine  $k_3$  and  $k_4$  after  $\theta$  has been obtained from  $k_\theta$ .

Other parameters of a thin bed and a cylinder (magnetic moment  $M_e$ , the epicenter location), as well as the normal background level  $\Delta Z_{backgr}$  correction are determined from the obtained values of  $\theta$  and  $h$  as in the method of characteristic points by the formulas of Table 7.3. A change in  $\theta$  in the range of  $0 \div 90^\circ$  causes only a slight change in  $k_3$  for an obliquely magnetized cylinder, i.e. within the range of 0.77 to 0.65 (see Fig.7.3). Therefore, in a simplified way, the occurrence depth can be obtained using only the R.H. branch of the anomaly curve, if the average coefficient is taken to be  $k_3 = 0.7$  and the following formula is used:

$$h = 1.4d_3. \quad (7.18)$$

For a thick bed with a horizontal upper edge, besides the segments  $d_3$  and  $d_4$  expressed by (7.13) or by the relations

$$\left. \begin{aligned} d_3 &= x_{un.r} - x_{up.r} \\ d_4 &= x_{up.l} - x_{un.l} \end{aligned} \right\}, \quad (7.19)$$

the following segments are also used (Fig. 7.4):

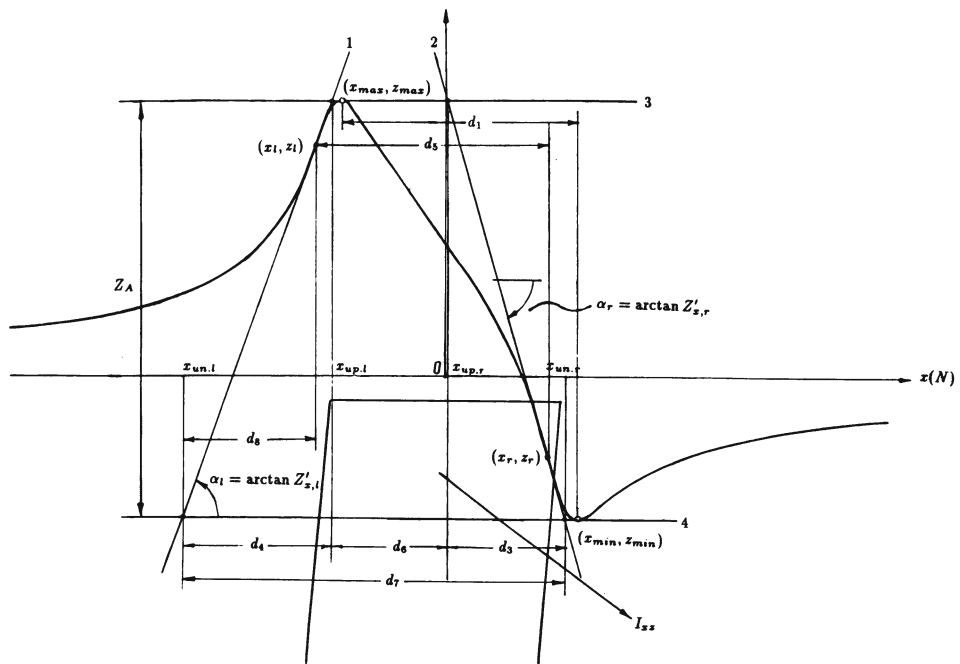


Fig. 7.4. Tangents and characteristic segments employed for the interpretation of  $Z$  anomaly caused by obliquely magnetized thick bed

Tangents: 1,2 – left-hand and right-hand inclined ones, respectively;  
3,4 – upper and lower horizontal ones, respectively

$$\left. \begin{aligned} d_6 &= x_{up.r} - x_{up.l} \\ d_8 &= x_l - x_{un.l} \end{aligned} \right\}. \quad (7.20)$$

Here  $x_{up.r}, x_{un.r}, x_{up.l}, x_{un.l}$  are, respectively,  $x$  coordinates of the upper right, lower right, upper left and lower left points of intersection of the inclined tangents with the horizontal ones:

$$\left. \begin{aligned} x_{up.r} &= x_r - \frac{Z_{max} - Z_l}{|Z_{xr}|} \\ x_{un.r} &= x_r + \frac{Z_r - Z_{min}}{|Z_{xr}|} \end{aligned} \right\}, \quad (7.21)$$

$$\left. \begin{aligned} x_{up.l} &= x_l + \frac{Z_{max} - Z_l}{|Z_{xl}|} \\ x_{un.l} &= x_l - \frac{Z_l - Z_{min}}{|Z_{xl}|} \end{aligned} \right\}, \quad (7.22)$$

$x_r$  and  $x_l$  values are determined from equation  $\partial^2 Z / \partial x^2 = 0$ ,  $Z_{max}$  and  $Z_{min}$  values are obtained from equation  $\partial Z / \partial x = 0$ .

The desired values in the R.H. sides of (7.21), (7.22) and (7.19), (7.20) are calculated for  $\theta$  equal to 15, 30, 45, 60, 75° and  $\beta$  equal to 0.1, 0.5, 1, 1.5, 2, 3, 5, 8, 10. These values indicate to a variety of cases ranging from a thin bed to a very thick one. It is assumed that  $h = 1$ ,  $2M_e = 1$ ,  $b = \beta$ . The values obtained are denoted by a tilde. The values of  $d_3, d_4, d_6$  and  $d_8$  for  $h = 1$  are denoted by  $k_3, k_4, k_6$  and  $k_8$ , respectively.

Fig.7.5 presents the relationships  $k_\theta = f(\theta)$ ,  $k_{\beta\theta} = f_1(\theta, \beta)$  and  $k'_{\beta\theta} = f_2(\theta, \beta)$ , where

$$k_\theta = k_8/k_4 = d_8/d_4, \quad (7.23)$$

$$k_{\beta\theta} = k_3/k_4 = d_3/d_4, \quad (7.24)$$

$$k'_{\beta\theta} = k_4/(k_6 + k_3) = d_4(d_6 + d_3). \quad (7.25)$$

Fig.7.5 is a nomograph for calculating  $\theta$  from  $k_\theta$  and the half-thickness  $\beta$  by the obtained  $\theta$  using  $k_{\beta\theta}$  and  $k'_{\beta\theta}$ , determined experimentally. The need to employ  $k'_{\beta\theta}$  along with  $k_{\beta\theta}$  can be accounted by the fact that  $\beta$  value obtained by  $k_{\beta\theta}$  for small  $\theta$  is not reliable.

Fig.7.6 shows nomographs used to determine  $k_3, k_4$  and  $K_6$  by  $\theta$  and  $\beta$ . Fig.7.7 gives nomographs serving to obtain  $\tilde{x}_{un.r}$  and  $\tilde{x}_{un.l}$ ,  $k_m (k_m = Z_A$  when  $h = 1$ ,  $2M_e = 1$ ) and  $k_o = |\tilde{Z}_{min}| / |\tilde{Z}_{max}|$ .

The nomographs in figures 7.5 – 7.7 are employed to interpret the anomalies due to a thick bed. The interpretation is performed as follows.

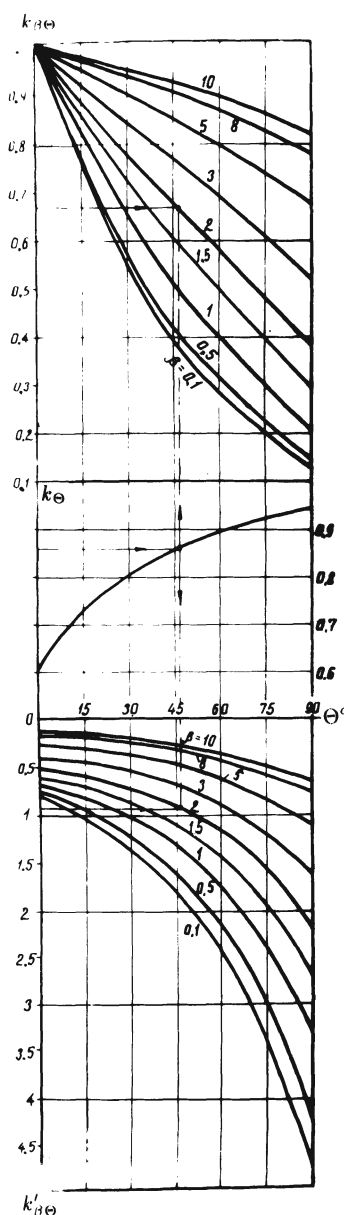


Fig. 7.5. The tangent method: key nomograph for the determination of the angle  $\theta$  and the relative half-thickness  $\beta$  in the case of an anomaly over a thick bed

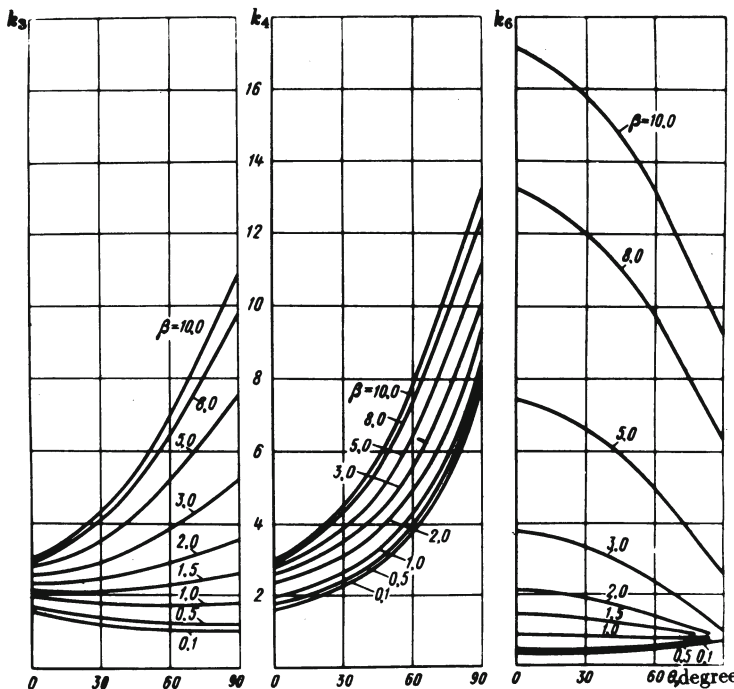


Fig. 7.6. The tangent method: nomographs for the determination of  $k_3$ ,  $k_4$  and  $k_6$  coefficients using  $\theta$  and  $\beta$  values for a thick bed

(1) Determination of  $\theta$  and the relative half-thickness  $\beta$ . The necessary tangents to the anomaly curve are plotted (see Fig. 7.4) and the segments  $d_3$ ,  $d_4$ ,  $d_6$ ,  $d_8$ ,  $Z_A$  are determined from the drawing. The coefficients  $k_\theta$ ,  $k_{\beta\theta}$  and  $k'_{\beta\theta}$  are calculated by formulas (7.23) – (7.25). Then, with  $\theta$  obtained from  $k_\theta$  in Fig. 7.5, two values of  $\beta$  are obtained from  $k_{\beta\theta}$  and  $k'_{\beta\theta}$  and averaged, if they are close.

(2) Determination of the depth  $h$  of the bed upper edge. The coefficients  $k_3$ ,  $k_4$  and  $k_6$  are obtained from  $\theta$  and  $\beta$  by the nomographs in Fig. 7.6. The depth  $h$  is calculated using equation (7.17), where  $d_i$  is some characteristic segment,  $k_i$  is a coefficient corresponding to this segment. Then an average value of  $h$  is derived.

(3) Determination of the half-thickness  $b$  by the following formula

$$b = \beta h. \quad (7.26)$$

(4) Determination of the effective magnetic moment by the

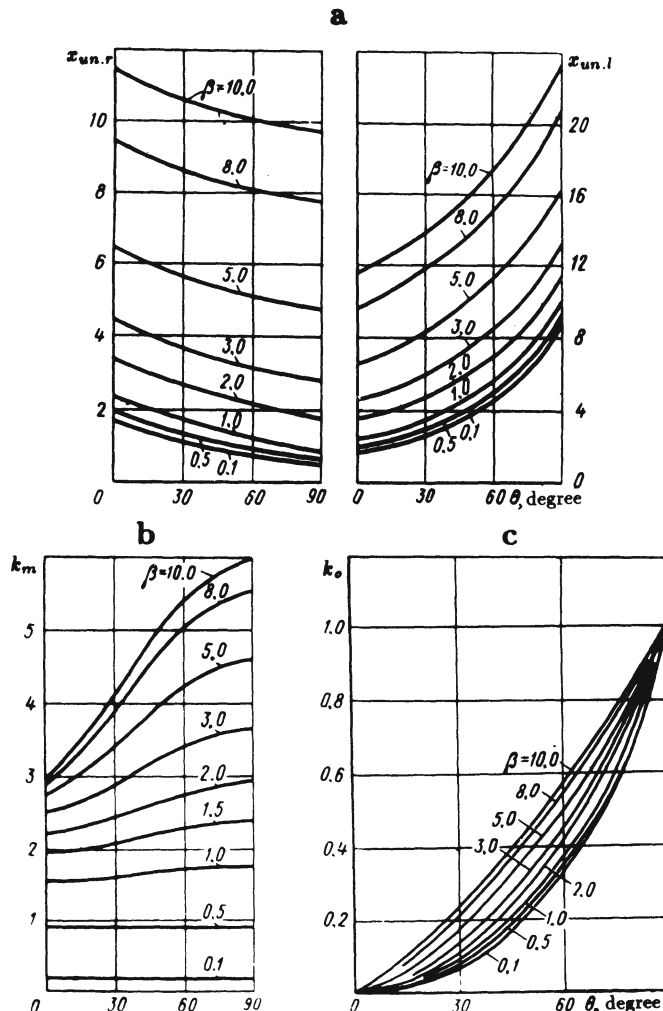


Fig. 7.7. The tangent method: nomographs for the determination of (a)  $\tilde{x}_{un,r}$ ,  $\tilde{x}_{un,l}$ ; (b)  $k_m$  and (c)  $k_o$  coefficients using  $\theta$  and  $\beta$  values for a thick bed

formula

$$M_e = Z_A / 2k_m. \quad (7.27)$$

The coefficient  $k_m$  is obtained from the known values of  $\theta$  and  $\beta$  by the nomograph in Fig. 7.7b.

(5) Localization of the epicenter (the origin of coordinates). This operation is performed with the use of  $x_{un.r}$  and  $x_{un.l}$ , which are calculated by the formulas:

$$\begin{aligned} x_{un.r} &= h\tilde{x}_{un.r} \\ x_{un.l} &= h\tilde{x}_{un.l} \end{aligned} \Bigg\}, \quad (7.28)$$

where  $\tilde{x}_{un.r}$  and  $\tilde{x}_{un.l}$  are obtained from the known values of  $\theta$  and  $\beta$  in Fig. 7.7a.

The segments  $x_{un.r}$  and  $x_{un.l}$  are plotted from the corresponding points of intersection of the inclined tangents and the lower horizontal one. The mid-point between the ends of these segments defines the epicenter location.

(6) Determination of the correction  $\Delta Z_{backgr}$  in the normal background level. It is calculated by an appropriate formula from Table 7.3. The value of  $k_o = |Z_{min}| / |Z_{max}|$  is obtained from Fig. 7.7b.

This modification has been tested on typical (theoretical) curves of  $Z(\Delta T)$  anomalies due to a depth-limited thick bed with  $\theta$  equal to 0, 30, 60 and 90°,  $\beta = 1 \div 10$ . The results indicate to the following average errors in the parameter determination: 1  $\div$  2° for  $\theta$ , 2  $\div$  3% for  $h$  and  $b$ , 1.5% for  $M_e$  (Table 7.4). This fact suggests that the version just discussed has a high theoretical accuracy.

**Table 7.4. Results of the tangent method modification test on the model of  $Z(\Delta T)$  anomalies due to obliquely magnetized beds**

Anomalous bodies (beds)	Determination error			
	$\theta$ , degree	$h$ , %	$b$ , %	$M_e$ , %
depth-unlimited	1 $\div$ 2	2 $\div$ 3	2 $\div$ 3	1.5
depth-limited with $H/h = 8$	11	10	12	15
depth-limited with $H/h = 4$	19	15	13	25

This modification has been also tested on typical curves of the  $Z$  component due to the oblique ( $\varphi_2 = 45, 60, 90, 120^\circ$ ) inductively

magnetized ( $i_m = 60^\circ$ ) beds of a variable thickness ( $\beta = 1 \div 4$ ) with the lower edge at the depth of  $H$  ( $H/h = 8$  or  $4$ ). The results testify to the fact that the modification can be applied to interpret anomalies due to depth-limited beds. Naturally, the errors in the parameter determination for depth-limited beds tend to increase in comparison with the case of depth-unlimited beds. Still, they are practically acceptable (max  $15 \div 20\%$ ).

The above method has been widely tested on  $\Delta T$  and  $Z$  anomalies observed in the areas of the Greater and Lesser Caucasus and Middle Kura depression, either in open areas investigated geologically, or in closed areas investigated by drilling. Over fifty anomalies have been subjected to interpretation. The average error in the determination of the upper edge depth has been estimated as  $11 - 12\%$ , which is in good agreement with the results of model investigation.

#### 7.2.1.4 Other techniques and examples of their combination

As to other methods of the interpolation selection, the integral method (method of characteristic areas) and the method of apparent spatial graticules can be applied in the conditions under review. These methods have been modified in [146] for the case of oblique magnetization.

Fig.7.8a exemplifies the use of the tangent method and that of characteristic points, while Fig.7.8b gives a clear example of the method of characteristic areas (for inclined thin bed model). The model of a thick bed along the profile in the mid-portion of the Guton anomaly (Fig.7.9) has been interpreted by different techniques. The resulting average values are the following:  $61^\circ$  for  $\theta$ ,  $4 \text{ km}$  for the upper edge depth ( $4.2 \text{ km}$  by the tangent method,  $4.0 \text{ km}$  by the integral method,  $4.3 \text{ km}$  by the method of characteristic points,  $3.3 \text{ km}$  by the method of singular points);  $10.6 \text{ km}$  for the half-thickness,  $274 \text{ mA/m}$  for  $M_e$  ( $297$ ,  $291$  and  $265 \text{ mA/m}$  for the tangent method, integral method and method of characteristic points, respectively);  $4^\circ$  for the inclination angle of the upper edge. The determination of the latter parameter was based on the depth of the bed's angular points.

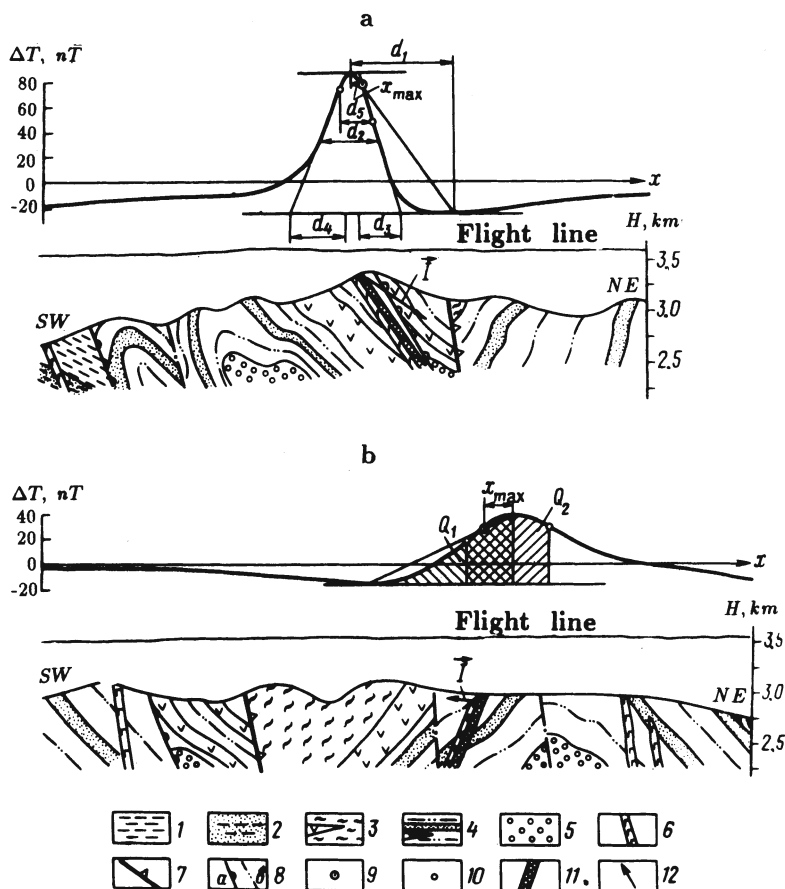


Fig. 7.8. Examples of the quantitative interpretation of  $\Delta T$  plots along the profiles 171 (a) and 181 (b) in the area of the Big Somalit

- (1) Yalakhkam suite  $J_2aal_2$ ; (2) Zainkam suite  $J_2aal_1$ ; (3) Nagab suite  $J_1toa_3$ ; (4) Tseilakhan suite  $J_1toa_1$ ; (5) the Lower and Middle Toarcian suite  $J_1toa_{1-2}$ ; (6) dikes of the gabbro-diabasic association; (7) the Major Caucasian upthrust-overthrust; (8) ore controlling (a) and ore distributing (b) upthrust-overthrusts; (9) Reford's point; (10) inflection points; (11) anomalous body according to the interpretation results; (12) obtained direction of the magnetization vector projection

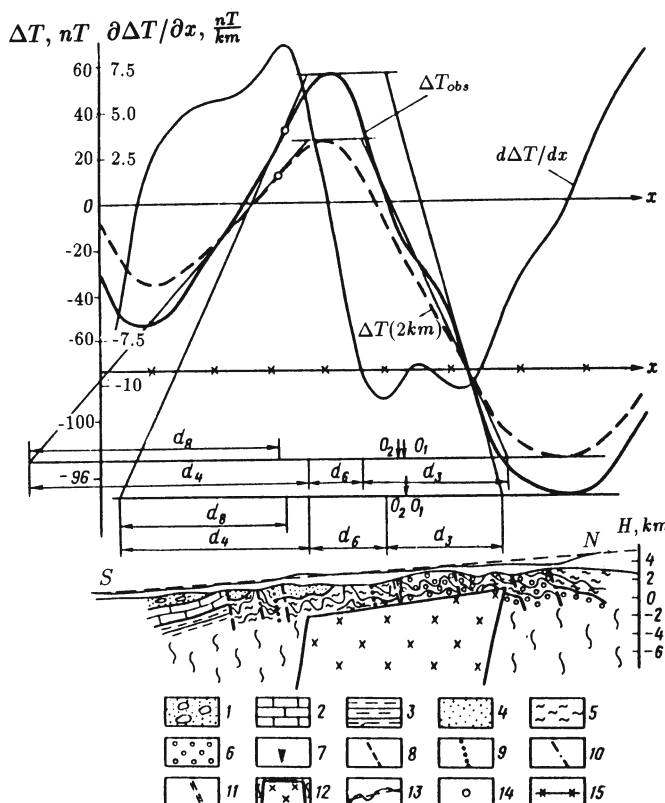


Fig. 7.9. Example of plotting tangents and results of interpretation of  $\Delta T$  graphs on two levels along the profile 28 through Guton anomaly (southern slope of the Greater Caucasus)

(1) recent alluvial deposits; (2) limestones, tuff sandstones, clay shales ( $K$ ); (3) mudstones, tuff sandstones ( $J_3$ ); (4) monolith clay shales and coarse-grained tuff sandstones ( $J_2$ ); (5) sandy-clay shales with horizons of sand flysch, metamorphosed clay shales and sandstones ( $J_2$ ); (6) phyllitized clay shales, sandstones, spilites ( $J_1$ ); (7) dikes and sheet bodies of the gabbro-diabasic association ( $J_2$ ); (8) regional upthrust-overthrusts; (9) upthrust-overthrusts separating the longitudinal tectonic steps of the second order; (10) upthrust-overthrusts complicating the longitudinal tectonic steps; (11) transverse fractures; (12) magmatic intrusion of intermediate-acid composition according to the interpretation data (in non-segmented  $J_{1-2}$  complex); (13) the lines of flight and averaging inclined straight line; (14) inflection point of the plot  $\Delta T$  nearest to the maximum on the left; (15) corrected zero line of the plots  $\Delta T; O_1, O_2$  are locations of the origin (middle of the anomalous body's upper edge) obtained from  $x_{un.r}$  and  $x_{un.l}$ , respectively

### 7.2.2 Revealing singular points of the field

The method of the potential field singular points modified by Troshkov [284] is applicable to anomalies due to 2-D obliquely magnetized bodies of a complex shape. This technique is rather sensitive to local noises, yet it can't be disregarded, since it yields highly informative and visual results. Until recently the method has been employed to interpret observations made on horizontal rectilinear profiles across the strike of anomalous bodies.

The major limitation of the method consists in the requirement that the singular points were sufficiently widely distributed along the profile in comparison to their occurrence depth. This difficulty is removed by a modification which estimates the probability of attributing a dense group of points to a single object [295]. The latest versions of the method make it possible to determine the type of a singular point, thus forming an idea of the anomalous bodies configuration.

Some of the versions are designed for interpreting a complex field due to 3-D objects [104]. The respective algorithm is relatively universal and requires minimal prior information. It generalizes the formulas of the planar inverse problem and can be readily included into a computerized system of processing and interpretation.

One of the most valuable features of the method consists in that the shape of the body under examination is not specified *a priori*. Another advantage is its noise tolerance to the regional fields. Any potential field imposed on the anomaly under survey has no bearing on the computation results, if the singular points (sources) of this field are much further from a certain fixed point chosen within the anomaly than those investigated. That is why the choice of the correct level of the normal field presents no problem in this case. Yet the method has a drawback which restricts its application in the areas with highly heterogeneous upper portion of the geological section. This limitation lies in a strong dependence of the results on the noise fields whose sources are located above the object under examination.

It is possible to improve the method realizing the following idea [135]: the influence of singular points nearest to observation surface is excluded from observed field, then singular points situated at a

larger depth are successfully singled out. This operation is repeated sequentially up to obtaining the deepest singular points.

The version of singular point method developed by Troshkov [104,284] has been modified by the authors of this book for observations on an inclined profile. The basic computations, i.e. determination of the derivatives of various orders at the height  $\Delta h$ , remains unchanged. The distinctions are the following: (a) the magnetic field observed on an inclined profile is given in a horizontal projection; (b) the coordinates of singular points, resulting from the processing, refer to fictitious bodies and should be converted to the real bodies' singular points coordinates using the formulas from Table 7.2 (Fig.7.10).

### 7.2.3 Analytical (approximation) continuation of the field

The magnetic anomalies interpretation based on the downward analytical continuation was first proposed by Strakhov [257]. The improved version of the method applied to a complex field was described in [264].

The technique is used under the assumption that the occurrence depth  $H_o$  of the upper edges of all bed-like anomalous bodies is approximately the same. That is why this parameter is the first to be determined. It can be obtained by a downward continuation of the autocorrelation function calculated by the field  $Z$ . The latter has a strong singular point with the coordinates  $(0; 2H_o)$ .

If the beds have a steep dip and dipping magnetization (the asymmetry of  $Z$  plots over individual beds can be ignored), then the inverse problem can be solved by the analytical continuation of  $Z$  field only. If the magnetization is inclined or the bed dip is far from being vertical, a spatial distribution should be obtained for the components of  $Z$  field and  $X$  ( $X$  is calculated by the field  $Z$ ). A spatial distribution of the field  $T = \sqrt{Z^2 + X^2}$  may also be of use, if the regional component of the observed field is not large.

The determination ranges for the above elements are:  $0 \leq Z < (0.75 \div 0.8)H_o$  for the lower half-plane and  $0 > |Z| > (1.0 \div 1.5)H_o$  for the upper half-plane. The following levels (upward) are employed:  $0.8H_o, 0.6H_o, 0.4H_o, 0.2H_o, -(0.3 \div 0.4)H_o, -(0.6 \div$

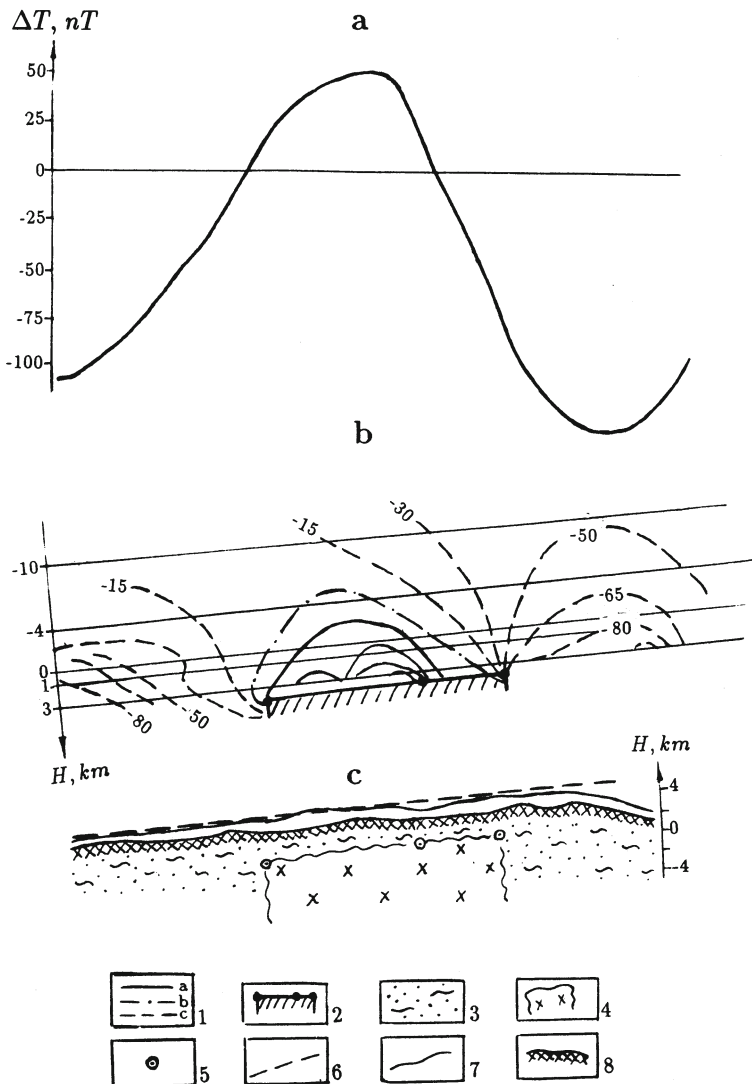


Fig. 7.10. An interpretation example for Guton anomaly by the methods of analytical continuation and singular points: (a) the plot of  $\Delta T$ ; (b) an isoline chart based on the results of analytical continuation in an inclined half-space; (c) a schematic section of the anomalous object

(1) isolines,  $nT$ : a – positive, b – zero, c – negative; (2) magmatic intrusion of an intermediate-acid composition (according to the interpretation results); (3) the upper edge of the anomalous object, obtained by the method of analytical continuation (black points show logarithmic peculiarities of the field); (4) singular point; (5) inclined straight line approximating the observation profile

$0.8)H_o$ ,  $-(0.9 \div 1.2)H_o$ ,  $-(1.2 \div 1.6)H_o$ . Smoothing employed in this case, ensures stable results in presence of random noises in the observed data. In this way the continuation problem is regularized.

The spatial distribution computation results for anomalous field elements can be given either in the form of plot charts for the levels  $Z = \text{const}$  or in the form of isoline charts for these elements in the vertical plane.

The inverse problem (i.e. determination of the upper edges for bed-like anomalous bodies) is solved by isoline charts. The isolines of the field elements are extrapolated into the lower half-plane area, adjacent to the latter calculation level. Extrapolation allows for the regularities in the behavior of the isolines of the given field element for an individual bed on the basis of the localization principle, since in the area close enough to the upper edge of the bed at issue, the field isolines behave as if the field were due to this bed only.

The isolines of  $Z$  and  $X$  components are mutually orthogonal. That is why a simultaneous determination of the spatial distribution for both elements adds to the interpretation accuracy. If the initial data is not exact enough, orthogonality fails to hold, especially in the proximity of the upper edges of the anomalous bodies.

The key advantage of the interpretation method just described is that it employs practically all observed values, and the interpretation accuracy depends on the observation network density and the field measurements accuracy rather than on the field complexity.

We conclude from the foregoing that the analytical continuation method has a limited application in open areas with a complex geological structure and higher level of various noises. Yet some of these areas, in particular those with weakly magnetic rock masses, favor the method application (see Fig.7.10). Fig.7.10 illustrates the field continuation in an inclined semispace. Here computation levels are parallel to the inclined straight line averaging the line of flight.

#### 7.2.4 Reduction to the pole. Anomaly division into symmetrical and antisymmetrical components

The procedure of “reduction to the pole” developed by Baranov [20] is often used in conditions of oblique magnetization for the

conversion of magnetic anomalies into vertical magnetization. The procedure was called as computing of pseudogravimetric anomalies and this name are used in geophysics many years. Nevertheless, as was noted in [33], the transformation really is a conversion from magnetic field to magnetic potential.

Clarity of the approach is rather attractive, and this procedure was elaborated by many authors. Among them we should note a modification of the method of Nabighian [201], which is more convenient than the basic Baranov's method. However, the procedure of reduction to the pole is limited by situations when all anomalous bodies in the studied area are magnetized in parallel to the geomagnetic field and have a subvertical dipping. Only in this case the magnetic fields conversion will be completely correct, and the obtained graphs will be symmetrical and may be undoubtedly used for further interpretation by conventional methods.

The possibilities of anomaly division into two components were mentioned in the Paragraph 7.2.1.2. Naudy's [203] method includes both the division of registered field into odd and even functions and application of the procedure of reduction to the pole. The observed curve is divided into a symmetrical  $\Upsilon_1(x)$  and antisymmetrical  $\Upsilon_2(x)$  components with respect to an arbitrarily chosen center in such a way that  $\Upsilon_1(x)$  does not change its value when  $x$  is replaced by  $-x$  and  $\Upsilon_2(x)$  does not change its sign if the sign of  $x$  is changed. Then the curve  $\Upsilon_2(x)$  is converted into the curve  $\Upsilon'_1(x)$  using the reduction to the pole. After this both curves  $\Upsilon_1(x)$  and  $\Upsilon'_1(x)$  are correlated with a set of theoretically computed master curves of symmetrical model dikes. The model dikes give a large range of depths and widths, and the model with the greatest correlation coefficient is selected from model set. The selected model is used for estimating the source depth of each anomaly on the investigated profile. Using the series of models covering the possible range of depths, quantitative parameters of many dikes can be estimated at different depths. Application of this procedure is effective at the preliminary stage of aeromagnetic survey interpretation.

### 7.2.5 Computation of analytic signal

A method developed by Nabighian [201] is based on the computation of analytic signal  $A(x)$  defined by

$$A(x) = \frac{\partial T}{\partial z(x)} + i \frac{\partial T}{\partial z(x)}, \quad (7.29)$$

where  $T(x)$  is the magnetic field along a profile in the  $x$ -direction at  $z=0$  ( $z$  is in the positive downward direction).

Any 2-D geological body may be approximated as a polygon drawn through the characteristic points of the body. The analytic signal is computed for all vertices of the polygon, and the obtained set of curves is used for interpretation. As a result, quantitative parameters including magnetic susceptibility of the anomalous body may be estimated. However, application of this method under complex geological conditions (rugged relief and oblique magnetization of bodies), taking into account sensitivity of this method to the topographic unevenness and to inhomogeneities of the medium, is complicated.

### 7.2.6 Parameter selection based on the approximation optimization

The techniques that fall under the mentioned category implement the simulation method most adequately. In case of a graphic selection we deal with a visual correlation of the fields. Formalization of the interpreter's actions gives rise to the approximation problem formulation.

The use of computers makes it necessary to set some strict criteria for the choice of a theoretical (model) curve that would be the least deviating from the measured one. In other words, it is essential to define an approximation measure. For this purpose, one group of methods employs the decision-making theory, the other one uses methods of linear programming.

The decision-making theory treats the divergence between an experimental and a theoretical field as a set of a number of components, at least one of them being random, with partially or

fully known statistical properties. That accounts for the randomness of the divergence in general, and the randomness of the measurement field, in particular [96,97]. Such an approach to geophysical problems was first substantiated by Khalfin [128]. The maximum likelihood criterion (which coincides with the minimum-square one in a normal distribution), the Bayes' criterion, criterion of a minimum average risk and others can be used as decision-making criteria. At each step of the interpretation the model parameters are subjected to certain changes or alterations so as to maximize (minimize) the response function. Thus the optimization idea is realized. Interpretation is completed either after the response function reaches some prescribed threshold (limit) or the given number of iterations have been performed. Kalinina [117] was among the first to apply such an approach in magnetic prospecting.

Shalayev [244] points out that simulation errors due to the substitution of real geological structures by simplified models are not always representable in the form of a component, which changes randomly from point to point along the profile. Any error  $n(x, y, z)$  involves as a whole the errors of observation field and modeling. In magnetic prospecting (as well as in other geophysical methods) we may deal with the worst possible case when practically nothing is known about the errors except for that their absolute values do not exceed some small positive number. In other words, we may expect a random variation of the whole level of anomalies, along with some changes in adjacent points. Under such an assumption methods of linear programming can be applied to the approximation of measured curves by the corresponding analytical expressions [48,49,165,244,254].

Linear programming deals with problems of maximum or minimum of a linear form called a target function, provided there are some constraints in the form of a system of linear equations or inequalities. These problems are often solved by a simplex method (with various modifications). It provides a means for obtaining the solution in a finite (not necessarily small) number of steps. A variant which satisfies the constraints is taken as an initial solution. Each subsequent iteration is also performed with the constraints taken into account. However, the transition is not arbitrary; it is accomplished so as to decrease the linear form to be minimized. Additional geological and geophysical information

about the object's parameters in the form of inequalities is naturally included into the constraint system to search for the target function minimum.

## 7.3 Quantitative interpretation of gravitational, electric, electromagnetic and thermal anomalies under inclined terrain relief and oblique polarization of objects

Section 2.1 dealt with investigations relevant to developing a general interpretation scheme for some geophysical fields. Avdevich and Fokin [18] studied analytical expressions for gravitational, magnetic, electric (*SP*) anomalies to obtain a unified system of their electrosimulation. Nepomnyashchikh [205] worked out graticules to interpret these fields. However, these graticules were not widely used, because the account of the boundary conditions presented considerable difficulties.

We may conclude from Chapter 2 that the rapid interpretation methods (those of characteristic points and tangents reported by Alexeyev [5]), designed for complex physical and geological conditions, can be applied (with some modifications) to other geophysical fields. In this case the objects of geophysical investigation can be approximated by bodies with shapes allowed for by the above techniques (see Table 1.1). For each particular geophysical method listed below only the interpretation peculiarities are described. As for the major aspects of the interpretation, they are fully described on the example of magnetic prospecting in Section 7.2.

### 7.3.1 Gravimetric prospecting

It follows from a general survey of the literature [61,184,195,etc.] that there is yet no technique of solving the inverse problem by gravity anomalies observed under above-mentioned complicated conditions. For example, the method of tangents described in [198] and the method of characteristic points given in [184] call for a normal field level, which is often unknown in the investigations carried

out under mountainous conditions. Interesting results, reflecting a separate direction in the potential field theory, were obtained in the work [45]. Applicability of this and similar procedures to complex geological conditions should be examined in concrete geological situations. However, possibilities of application these and some similar procedures in the complicated geological conditions are not clear. It is also noteworthy that despite the lack of polarization effect as such in gravimetric prospecting, the dip of observation lines is equivalent to the manifestation of vector properties of the density (see Section 2.2). This being ignored can cause fictitious sources of anomalies, somewhat shifted from real sources both on the plan and in depth.

Therefore, rapid interpretation of gravity anomaly has been practically rejected, which, in turn, has brought about an urgent need in selection methods used from the very beginning of the interpretation process. However, the lack of the first approximation model obtained by rapid interpretation results in a dramatic increase of computer time consumption and is fraught with gross errors. It is highly important, therefore, that acceptable techniques of rapid interpretation [143] were developed.

The model examples below illustrate the rapid interpretation of gravity anomalies registered on the rugged terrain relief by the mentioned improved methods. The plots of  $\Delta g$  have been computed by the GSFC program under conditions of a homogeneous (a) and heterogeneous (b) media (Fig.7.11). A horizontal circular cylinder (HCC) stands for the approximation model of orebody. The interpretation accuracy diminishes when passing from the homogeneous host medium to the heterogeneous one. Yet, even in the latter case it is still about 15%. For mountainous conditions such an accuracy of the rapid quantitative interpretation proves to be quite adequate.

The interpretation of gravity anomalies is marked by the following special characteristics:

- (1) The angle  $\theta$  determined from the nomograph (see Fig.7.3) must be approximately equal to the angle  $\omega_o$  ( $\omega_o$  is the dip angle of the terrain relief;  $\omega_o > 0$ , if the relief is inclined towards the positive direction of the axis  $x$ ). This equality can be used to estimate the exactness of the interpretation, since  $\omega_o$  is known.

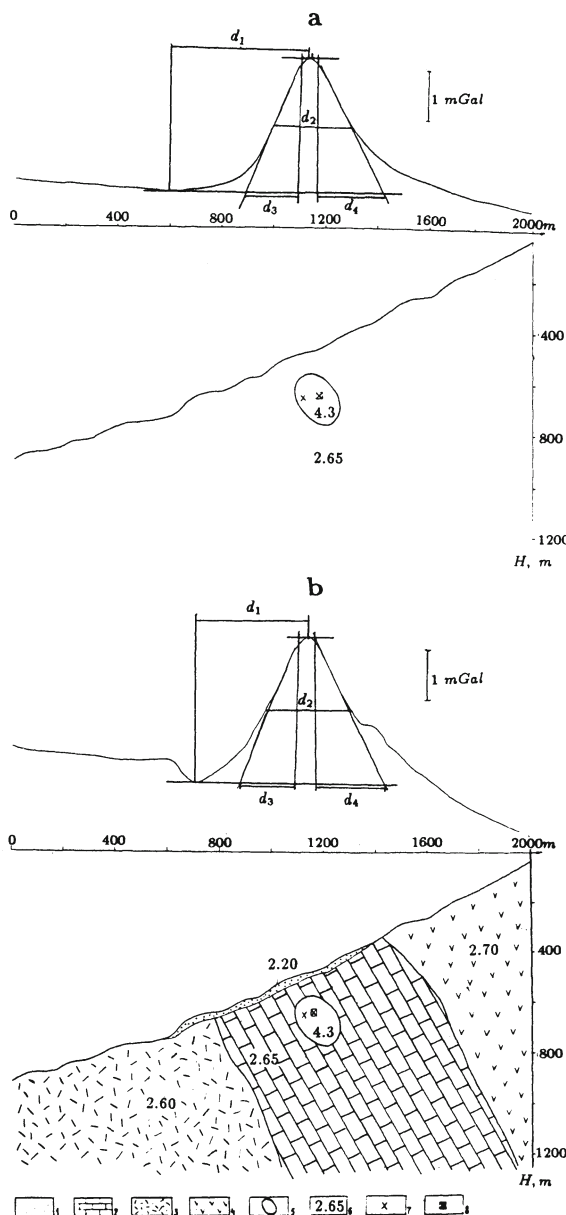


Fig. 7.11. Rapid interpretation of  $\Delta g$  anomaly over the model of a skarn deposit occurring in a homogeneous (a) and heterogeneous (b) medium  
 (1) loose deposits; (2) limestones; (3) acid volcanites; (4) andesites; (5) contour of the skarn deposit; (6) density,  $g/cm^3$ ; location of the HCC center according to the results of  $\Delta g$  interpretation: (7) fictitious, (8) real

(2) Besides the geometrical parameters of an object, the gravity moment can be also determined [7]:

$$M_{\Delta g} = \frac{1}{2} \Delta g_a h, \quad (7.30)$$

where  $\Delta g_a$  is the amplitude of the gravity anomaly (in  $mGal$ );  $h$  is the occurrence depth of HCC center (in meters).

It is possible to pass over to the real source parameters as follows:

$$M_{\Delta g,s} = M_{\Delta g} \cos \omega_o. \quad (7.31)$$

### 7.3.2 The self-potential method

The calculation of theoretical anomalies due to *SP* has long been based primarily on the well-known Petrovsky's solution derived for a vertically polarized sphere [300]. Later on, solutions for sheet-like bodies and inclined plates were obtained [240,274]. The polarization vector was generally considered to be directed along the ore objects dip (along the longer axis of the conductive body).

To perform quantitative interpretation of anomalies due to *SP*, the anomalous body is approximated by a body of a simple geometrical shape. Its parameters (i.e. the occurrence depth, the angle between the horizon and the direction of the polarization vector) are usually determined either graphically, using characteristic points of the anomaly plot [240], or by the trial-and-error method, visually comparing the anomaly with the set of master curves (graticules) [274].

In works [200,240,300] the *SP* anomaly generated by a plate and registered along the profile across its strike, is calculated by the following formula:

$$U(x) = \frac{J\rho}{2\pi} \ln \frac{r_1^2}{r_2^2}, \quad (7.32)$$

where  $J$  is the current per unit length,  $\rho$  is the host medium resistivity,  $r_1$  and  $r_2$  are the distances from the plate ends to the observation points.

However, the techniques suggested in the above works require the normal field level to be known. They are also unacceptable for rugged terrain relief.

The work [83] presents a method of *SP* anomalies computation for field sources of an arbitrary shape. The method is based on numerical integration using Green's function. This approach calls for a considerable computer time consumption.

It follows from the survey of researches by west scholars that there is a number of interpretation techniques recently developed, which are based on minimizing the difference between an observed anomaly and a theoretical one. The minimization is performed by sequential optimization of the interpretation parameters in the course of the computer-aided iterations. These techniques are also complicated and inapplicable for prompt interpretation under field conditions.

In 1984 a paper was published [155] which acknowledged the existing analogy between the current density of *SP* and the magnetic induction. It suggested to interpret *SP* anomalies on the basis of methods developed for magnetic prospecting. A similar approach was proposed by Alexeyev as far back as in 1971 [4] and elaborated later in his subsequent investigations.

Fig.7.12 presents the results of *SP* anomaly interpretation by the developed techniques.

The inclination angle of the natural polarization vector  $\varphi_p$  is calculated from the expression

$$\varphi_p = 90 - \theta; \quad (7.33)$$

on an inclined relief

$$\varphi_{p,s} = 90^\circ - \theta + \omega_o. \quad (7.34)$$

It should be noted that the investigation of this area under fields conditions in order to get information about an ore object called for measuring the *SP* in the wells [247], while the technique substantiated in Section 2.2 and described in Section 7.2 permits to determine the orebody's parameters by the *SP* measurements on the earth's surface.

Fig.7.13 depicts the position of the *HCC* center, which evidently fixes the undrilled edge of a flat-lying orebody.

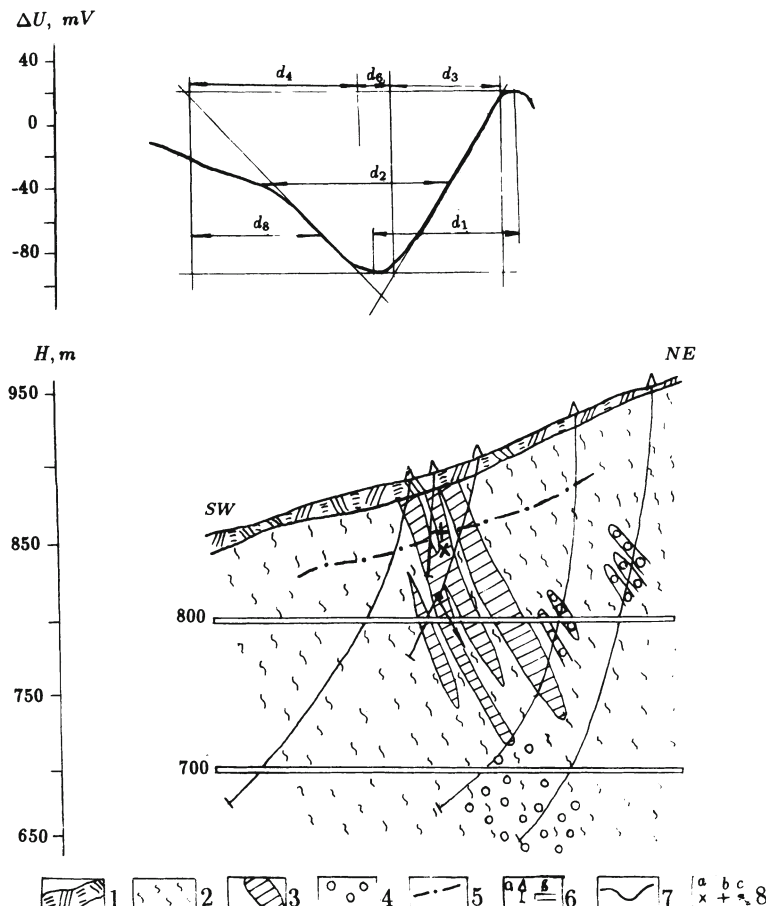


**Fig. 7.12. Interpretation by the developed techniques of SP anomaly in the area of deposit Potentsialnoe in Rudny Altai (initial data from [241])**

(1) soil-vegetative layer; (2) alternation of lavas and tuffs of acid composition and chlorite-sericitic schists; (3) sulfide ores; (4) sulfide impregnation, pyritization; (5) level of ground waters; (6) drilling wells (a) and adits (b); (7) plot of SP potential; (8) interpretation results: (a) mid-point of the dipping thick bed's upper edge, (b) upper edge of the dipping thin bed, (c) center of a horizontal circular cylinder (arrow indicates the direction of the polarization vector obtained by the interpretation)

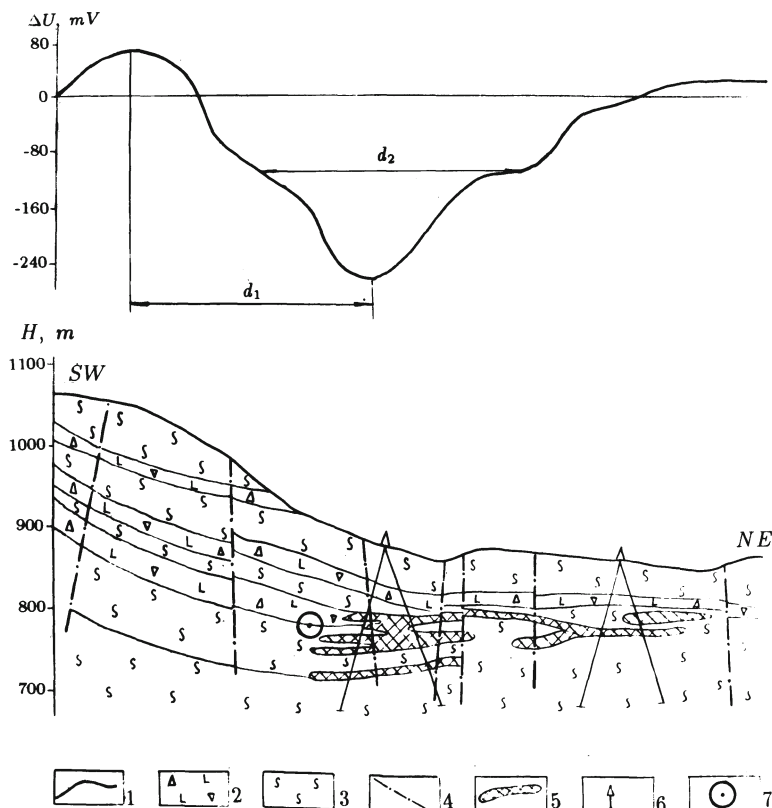


Fig. 7.13. Interpretation of SP anomaly by the method of characteristic points in the area of the Uchambo ore field of the Adjara group of copper-polymetallic deposits (Georgia)  
 (1) observed values of SP; (2) heteroclastic tuff breccia and their tuffs; (3) cover trachyandesite-basalts with pyroclastic interbeds; (4) disjunctive dislocations; (5) zones of increased mineralization; (6) drilled wells; (7) location of HCC center according to the interpretation results ((1-6) from [47])

### 7.3.3 The induced polarization method

The induced polarization method is one of effective techniques applied for prospecting ores and other economic minerals, solution of problems of hydrogeology and engineering geology. This method is most widely used for ore deposits [162,219,277]. Such an extensive application can be accounted for by its sensitivity to the presence of conductive minerals. Still, the techniques of the *IP* anomalies quantitative interpretation are characterized by significant limitations. Among the works dealing with *IP* method, we can single out [237] and [161], relevant to the analytical revealing isometric anomalies and the tangent method, respectively. Of special interest is paper [227], which suggests to interpret *IP* anomalies, obtained with the help of a gradient array, by the potential field theory. To this end the author recommends the technique of characteristic points, well-known in magnetic prospecting. All the mentioned techniques suffer from the same faults which have been examined in detail when analyzing the interpretation of other fields.

Certain conclusions about the parameters of the ore object's geological section can be made with the help of three-layer curves of the *IP* vertical sounding or by computer modeling [162,274]. However, the above mentioned specialized techniques (see Subsection 2.1.2 and Section 7.2) are much more acceptable for rapid interpretation.

Fig.7.14 shows the results of the model curves  $\eta_a$  interpretation for a gradient and potential array on an inclined relief. The figure indicates that boreholes above the obtained fictitious center of *HCC* will not encounter the anomalous object. As to the obtained real sources, they reflect the anomalous object's position with a sufficient accuracy.

Fig.7.15 presents interpretation results for the observed anomaly  $\eta_a$  obtained with the use of a gradient array. The orebody of a complex composition occurs in a sand-shale strata of the Upper Aalenian. The values of its upper edge depth obtained by the methods of characteristic points and tangents for a thin bed model practically coincide. The *HCC* centers, determined by the same techniques, are shifted with respect to each other. This fact testifies to a higher reliability of the bed model. The inclination angle of the

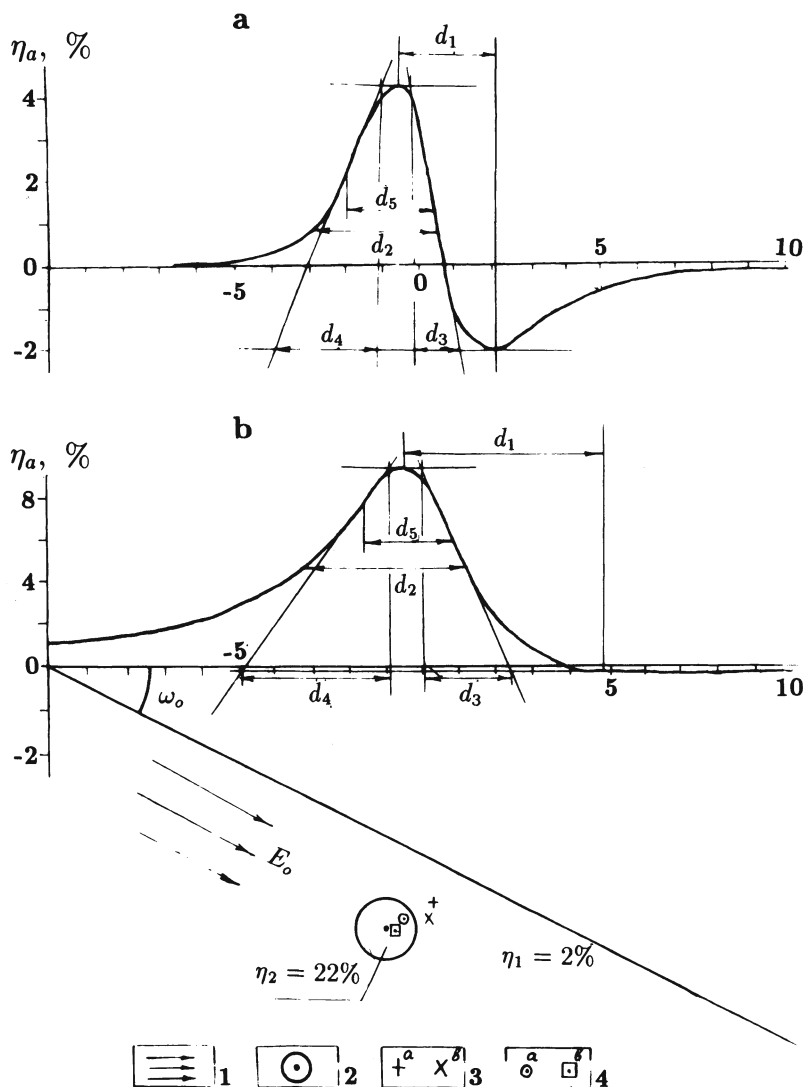


Fig. 7.14. Interpretation of model curves  $\eta_a$  on an inclined relief from a polarized cylindrical body: (a) for a gradient array, (b) for a potential array

(1) uniform polarizing field; (2) model polarized body; (3) center of the fictitious body: (a) by the curve (a), (b) by the curve (b); (4) center of the real body: (a) by the curve (a), (b) by the curve (b)

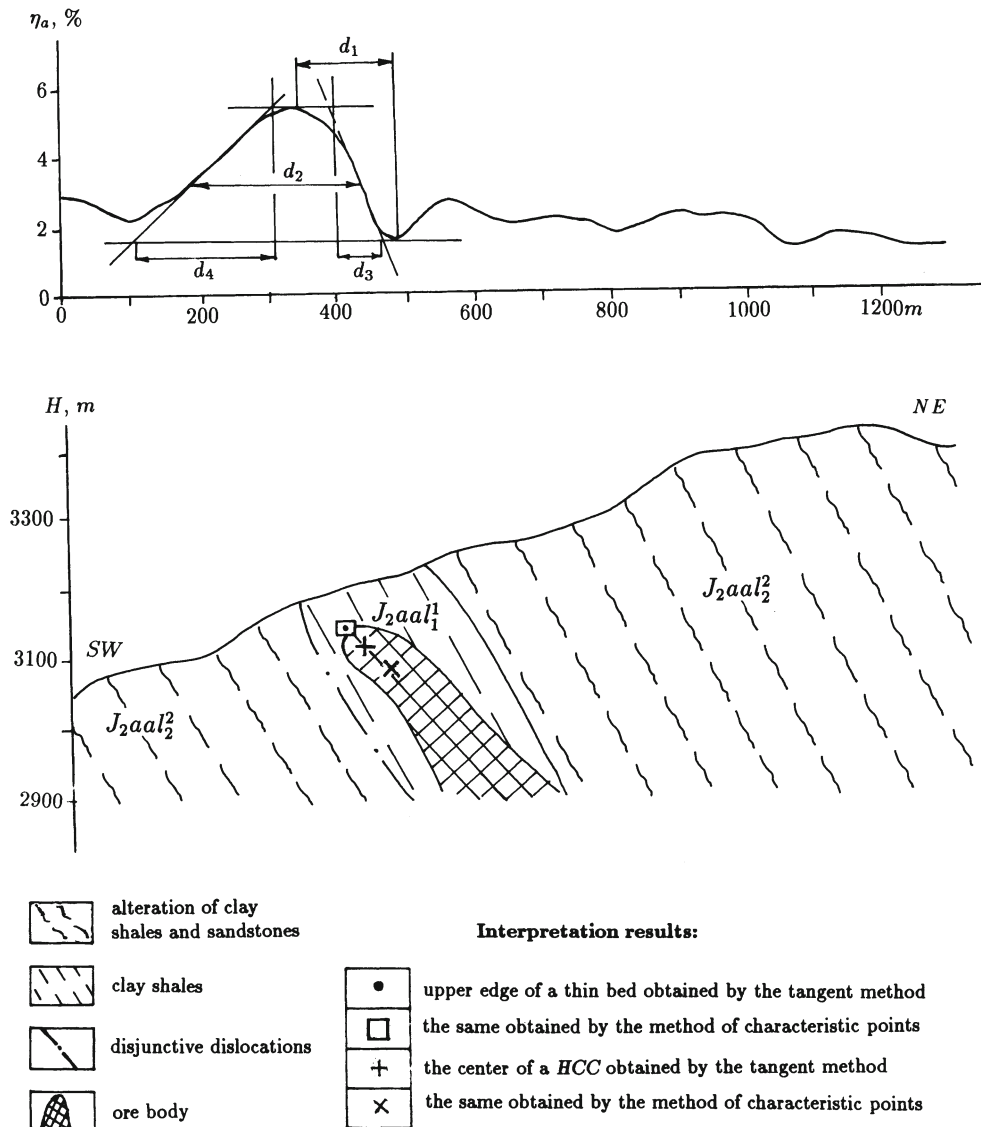


Fig.7.15. Interpretation of the  $\eta_a$  anomaly (gradient array) in the area of Bazaryuzyu (southern slope of the Greater Caucasus) by the developed techniques

*IP* vector  $\varphi_{IP}$  may be calculated by the following expression:

$$\varphi_{IP} = \varphi_2 - \theta + 90^\circ, \quad (7.35)$$

where  $\varphi_2$  is the dip angle of the bed (counted from the vertical).

For the case of a sloped relief we have, respectively,

$$\varphi_{IP,s} = \varphi_2 - \theta + 90^\circ + \omega_o, \quad (7.36)$$

( $\omega_o$  has been determined in Subsection 7.3.1).

Fig.7.15 shows that the inclination of relief and vector of polarization are caused by a displacement of anomaly maximum relatively to the projection of the body's upper edge onto the earth's surface. As a result, a prospecting hole located without the quantitative interpretation and drilled on the  $\eta_a$  maximum can go past of the desired object.

#### 7.3.4 VLF method

It seems from a general survey of the literature that there are practically no reliable and prompt techniques of quantitative interpretation in *VLF* method. The methods suggested by Tarkhov [273] are half-quantitative. The procedure developed by Fraser [85] is useful, mainly, on the stage of revealing anomalous objects. The techniques presented in [99,100], based on calculating the anomaly extreums ratio, require that the zero line (or a normal field) were known. The wrong choice of the zero line entails large errors in determination of the anomalous object's quantitative parameters. Moreover, these techniques are not intended for rugged terrain relief.

Dmitriyev [58,59] solved the direct problem by a number of electromagnetic methods (including the *VLF* method). In his works Dmitriyev gave a numerical analysis of the anomalies due to bed-like bodies depending upon their electric properties, dimensions, position with respect to the earth's surface area and the observation profile. However, mathematical computation difficulties restricted the range of models to be calculated by only simple ones.

According to [303], the finite differences method is the most effective method of electromagnetic field mathematical simulation available at the present moment. But the expediency of its application depends on the size of the design area and the desired

accuracy of computations. For a large area of calculations or for setting the simulation problem with a higher accuracy, the amount of computations performed by the above method goes beyond all possible limits even if large modern computers are used. The programs developed by Druskin et al. [63] for solving the direct 3-D electric prospecting problem in time and frequency domains, call for high-capacity computers. The possibilities of employing these programs in mountainous conditions and the potentialities of such application are not clear so far.

It is necessary to note that some approaches developed for magnetotelluric sounding [123,303] may be used in *VLF* method. However, the application of these procedures is limited by the strong changeability of electric properties in the studied (upper) part of geological section.

Gordyev and Sedelnikov's works [99,100] cover the physical (analog) simulation of *VLF* curves by the models of a vertical and inclined thin bed. The accuracy of the physical simulation and that of numerical computations (for simple models) is at present approximately the same and amounts to about 8 – 10%.

Numerous other works, in many respects close to those mentioned above, deal with the anomaly interpretation in *VLF* method. Thus, for instance, the works [121,214] give the calculation of plots for vertical and horizontal components of the magnetic field of *VLF* due to the model of an inclined thin bed with different dip angles. The depth of occurrence for the upper edge of the bed varies as well. In the works [214,224,280] were computed components of *VLF* fields for different types of geoelectric section. The work [192] gives the calculation of the magnetic components of *VLF* field due to another model of an anomalous object – that of a conductive cylinder placed into a homogeneous medium (the cases of both **E**-polarization and **H**-polarization are discussed).

Olsson [215] solves the direct problem for an ideal conductive half-plane with different dip angles, the half-plane being covered by variable-depth loose deposits. Besides, he proposes techniques for a simplified interpretation of *VLF* data, which are based on the utilization of the extremum points in the anomaly plot.

These techniques suffer from the same limitations as those ex-

amined above.

In this context, the special techniques presented in [9,72] are of practical interest.

As shown in Chapter 2, in *VLF* method it is expedient to apply the interpretation techniques developed in magnetic prospecting for the models of inclined thin bed and horizontal circular cylinder. It should be noted here that the total horizontal component of the *VLF* magnetic field  $H_\phi = \sqrt{H_x^2 + H_y^2}$  most frequently measured in practice, can be interpreted as  $H_x$  component, since the contribution of  $H_y$  component is usually relatively small.

The essential distinctions reflecting quasi-potential nature of the *VLF* electromagnetic field are as follows. In magnetic prospecting the inductive magnetization vector of an inclined bed is approximately parallel to the geomagnetic field vector, irrespective of the bed dip direction, with the magnetic susceptibility not exceeding 0.1 SI unit. In electric prospecting by the *VLF* method under **E**-polarization for highly conductive objects, the equivalent vector of polarization, causing the anomalies of  $H_x$  and  $H_z$ , approaches the body axis, with a slight deviation toward the vertical for gently sloping bodies. That is why the generalized angle  $\theta$ , resulting from the interpretation by the proposed methods and representing the difference of the inclination angles for the bed and the polarization vector, can be used to estimate the bed dip angle by the following empirical formulas [76]:

(a) for  $H_x$  anomaly

$$\alpha = 3\theta + 90^\circ; \quad (7.37)$$

(b) for  $H_z$  anomaly

$$\alpha = 3\theta - 180^\circ, \quad (7.38)$$

where  $\alpha$  is the dip angle of the bed.

For the case of observations on a sloping relief, the angle  $\alpha$  is calculated as follows:

(a) for  $H_x$  anomaly

$$\alpha_s = 3(\theta - \omega_o) + 90^\circ, \quad (7.39)$$

(b) for  $H_z$  anomaly

$$\alpha_s = 3(\theta - \omega_o) - 180^\circ, \quad (7.40)$$

( $\omega_o$  has been determined in Subsection 7.3.1).

The above rapid techniques require a detailed representation of the curves under interpretation. This, in turn, calls for more closely spaced observation steps in anomalous areas (the number of the observation steps should be increased by a factor of 2 or 3).

It should be noted that the obtained position of the upper edge can be slightly shifted from real upper edge downward along the bed dip. This is accounted for by the fact that linear currents are focused in the upper portion of the conductive object. This portion may be situated below its upper edge.

Fig.7.16 gives an example of interpretation. The distortion in the  $H_x$  plot along the profile through a copper-pyrite deposit is due to the terrain relief effect and inclined polarization of the anomalous object. A borehole drilled on the anomaly maximum projection onto the earth's surface area will not expose the ore object. The position of the orebody's upper edge and the direction of its dip are determined by the interpretation results. A slight error in the upper edge determination is due to the fact that the anomalous object, according to its parameters ( $h \simeq b$ ), is intermediate between a thick and a thin bed. However, as to the anomaly shape, the anomalous object falls into the category of thin bed models. The direction of the object is determined more reliably.

Fig.7.17 illustrates the interpretation results for the curve  $H_\phi$  along the profile across the Kyzylbulakh gold-pyrite deposit, the Mekhmana ore district (the Lesser Caucasus). The anomaly over the ore object exposed by prospecting boreholes is interpreted in the central portion of the profile. In the south-western portion the anomaly over an anticipated object is interpreted. In both cases the approximation model is represented by an inclined thin bed.

As shown in Subsection 2.1.2, the magnetic field  $\Delta Z$  is an analogue of  $H_x$  and  $H_\phi$  components in the VLF method for the case of an inclined thin bed. A model magnetic field  $\Delta Z_m$  due to the host medium and near-surface ore body was computed for the central part of the profile. For model computation the following parameters were introduced: magnetization value – 300 mA/m for

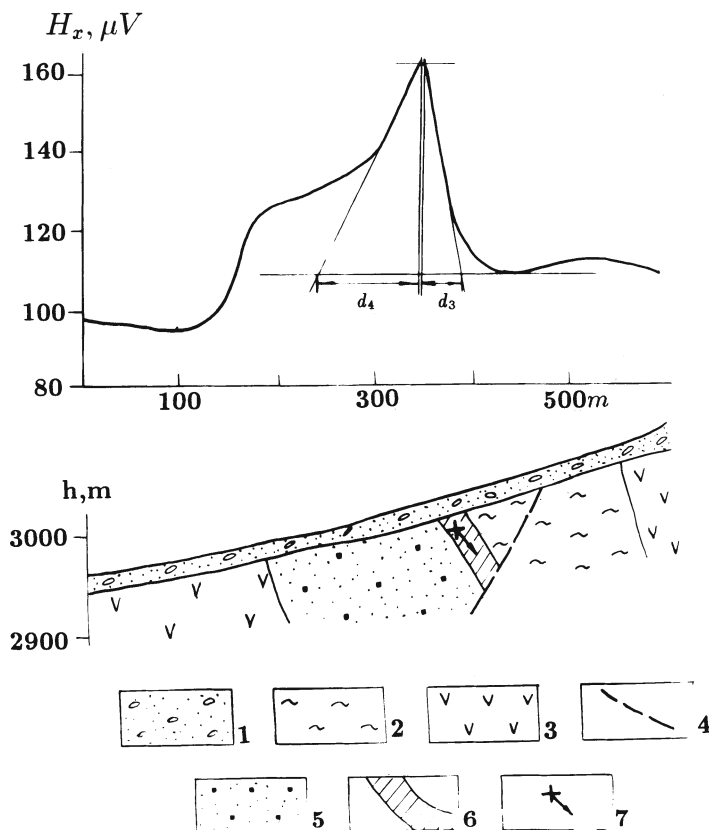


**Fig. 7.16. Quantitative interpretation of  $H_x$  anomaly in the area of a copper-pyrite deposit (initial data from [100])**

(1) loose deposits; (2) spilites; (3) andesitic porphyrites; (4) disjunctive dislocation; (5) mineralized zone; (6) massive ore; (7) location of the upper edge of the conductive object and direction of its dip according to quantitative interpretation results

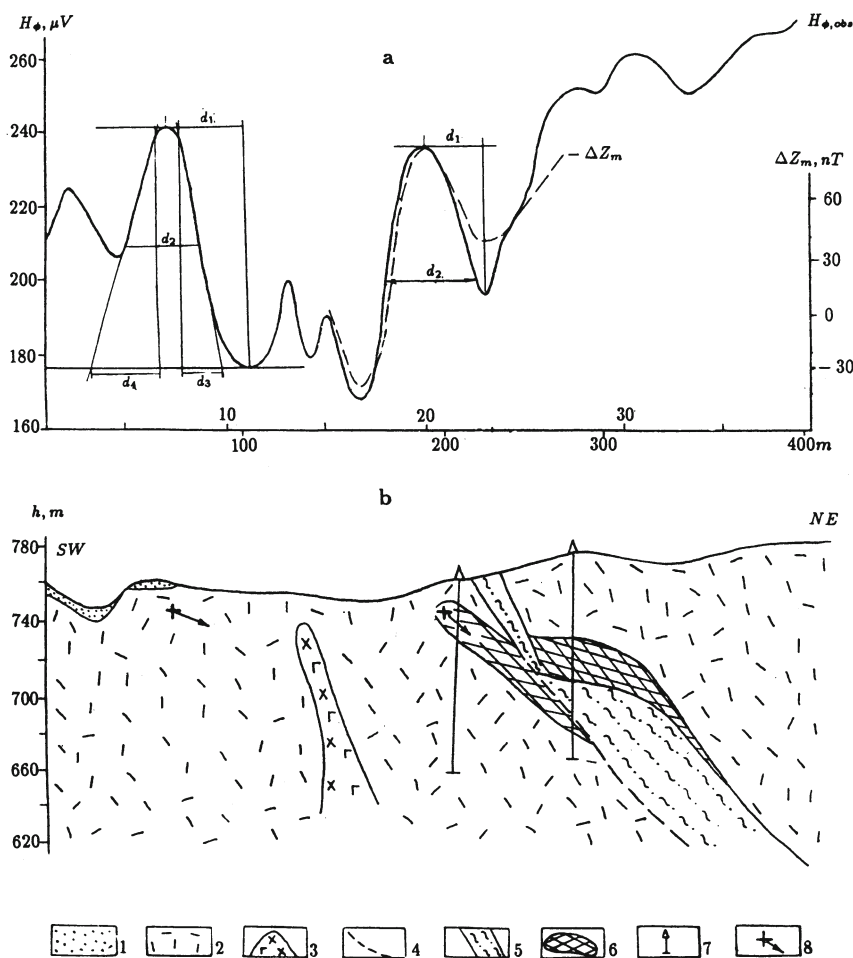


Fig. 7.17. Quantitative interpretation of  $H_\phi$  field in the area of the Kyzylbulakh gold-pyrite deposit: (a) the plots of  $H_\phi$  and model magnetic field  $\Delta Z_m$ , (b) geological section

(1) loose deposits; (2) tuffs of liparite-dacitic porphyrites; (3) dike of andesite-basalts; (4) disjunctive dislocation; (5) ore body; (6) zone of boudinage; (7) prospecting wells; (8) location of the conductive bodies' upper edge and direction of their dip by quantitative interpretation results

the host medium and 1000 mA/m for the anomalous (ore) body; vector of magnetization – vertical for the host medium and along the dipping for the orebody. The azimuth of the selected profile was assumed to be 70°, which corresponds to the angle between the incoming VLF field and the real azimuth of the profile. It is apparent from the figure that  $H_\phi$  and  $\Delta Z_m$  curves are in good agreement. So, we obtained an additional proof of a common nature of these fields.

### 7.3.5 Near-surface thermal prospecting

The first mentions of thermometry as applied to prospecting of sulfide deposits dates back to the mid-thirties, when Sofronov and Rodionov accomplished geothermal investigations in shallow (2–5 m) wells in the Degtyarsk copper-pyrite deposit, Middle Urals [235]. The temperature increase by 1.5°C was observed over the orebody in the profile across the strike. For the first time the thermal balance of the oxidation reaction for pyrite-zinc ore was calculated. At the same time, the method was used by van Bouwhuysen [289] to study a faulted structure near Vintersweek (The Netherlands) and by Paul [221] to study a salt stock near Hannover (Germany).

The near-surface thermal prospecting of ore deposits was further developed by Lakhtionov and Tarkhov [171,172], Khutorsky [153], Dmitriyeva, Skornyakov and others [60,62]. The observations were primarily subjected to a qualitative analysis. Basic geothermal observations were carried out in horizontal underground mines (adits) to lower the level of noises. Of certain interest is the near-surface thermal survey based on the Shallow-Temp technique described in [175]. Many stages of this technique, including reduction of noises of any kind, are automated. However, no details are given in respect to the specific way of noise reduction.

Analysis of thermal fields, based on approximate solutions to direct problems of the heterogeneous media thermal conductivity by the finite-difference grid technique, is covered in [186,187]. However, solving these problems, even with modern computers, takes a lot of time and efforts. A similar approach involves computer-aided selection of temperature fields by successively solving direct problems [187], as in other geophysical methods.

The authors of [266] derived certain functional dependencies between the physico-geothermal parameters of a geological body and the pattern of geothermal anomalies due to this body, occurring in uniform strata of the host rocks. The anomalous object is approximated by a horizontal circular cylinder, which has the radius  $R$  and the center located at the depth  $H$  from the earth's surface. It is shown [266] that prospecting proves to be most effective for the anomalous bodies with parameters satisfying the following conditions:

$$0.1 \leq \lambda_2/\lambda_1 \leq 10; \quad H/R < 5, \quad (7.41)$$

where  $\lambda_2$  and  $\lambda_1$  are the thermal conductivity values for the host medium and the anomalous object, respectively.

Simmons [251] suggested a method for interpreting heat flow anomalies analogous to those used in gravimetric prospecting. The similarity between gravity and temperature anomalies has been also noted by Poley and Steveninck [225] and Kappelmayer and Hänel [118]. However, in these studies examples of quantitative interpretation application are not given. Zorin and Lysak [307] made an attempt to use the proportionality of analytical expressions for gravimetric and temperature fields of a point source. They applied the techniques developed in gravitational prospecting for the interpretation of anomalies in thermal prospecting. The regional anomaly caused by a deep-seated source in a rift zone of Lake Baikal (Russia) was interpreted as an example. The quantitative interpretation was carried out, employing Smith's inequalities developed in gravimetric prospecting [218]. However, the use of these inequalities under complicated conditions (e.g., rugged topography, moderate inhomogeneities, inclined polarization, and unknown level of the normal field) is ineffective.

It follows from the foregoing that the modification of rapid methods for the inverse problem solution worked out by the authors of this book, are very important for thermal prospecting from the practical point of view [148].

Fig. 7.18 presents the results of the interpretation of a temperature anomaly performed by the developed techniques. In the figure, temperature anomaly interpretation results are given for a district with severely inclined relief of the Katekh deposit (the Greater Caucasus). The temperature was measured in 1.0 m deep

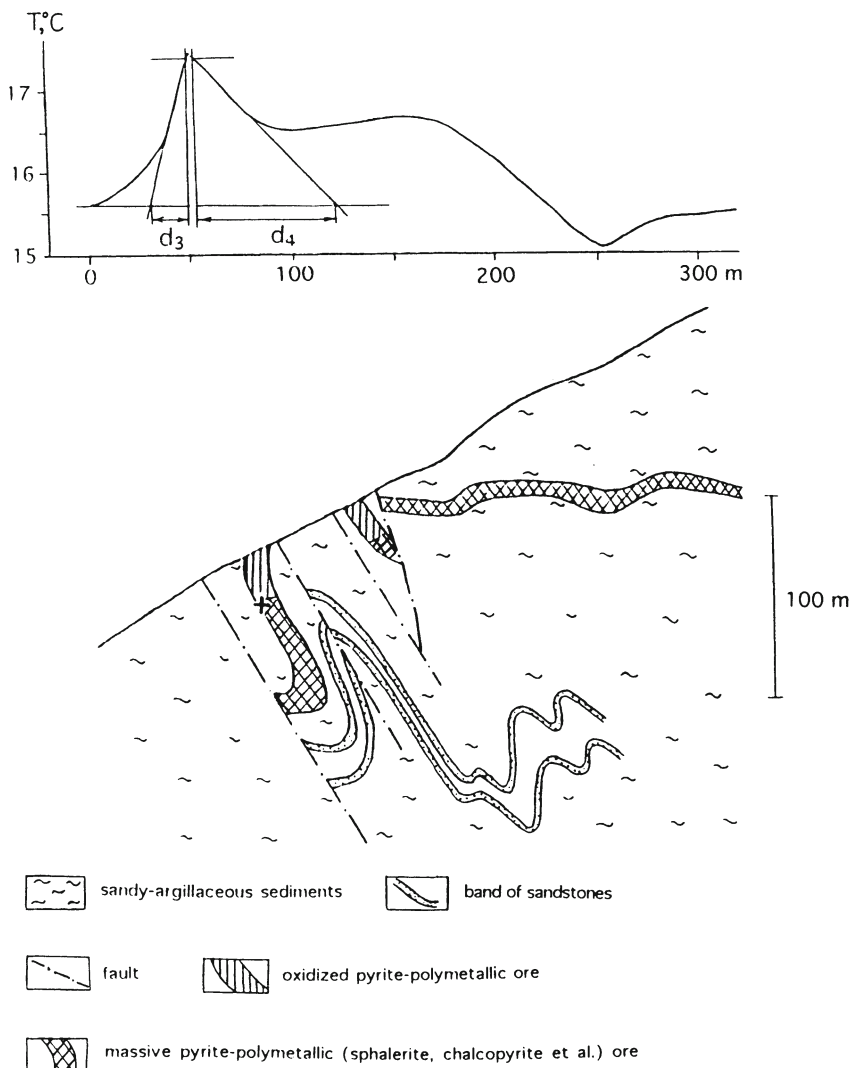


**Fig. 7.18. Quantitative interpretation of the temperature anomaly at the Katekh pyrite-polymetallic deposit (Belokan-Zakatala area)**

The observed temperature and geological sections are taken from [308] and an unpublished report of "Azerbaijangeologiya" Association. The "+" symbol marks the position of the upper edge of the interpreted thin body obtained from the analysis of the anomaly profile

blastholes.  $T^\circ$  plot shows two anomalies, one of which is due to the subhorizontal ore deposit and is less pronounced. The thermal conductivities for the host rock and thick pyrite-polymetallic ore were  $1.45 \pm 0.35$  and  $3.87 \pm 0.57 \text{ W/m} \cdot ^\circ\text{C}$ , respectively [308], i.e. their ratio exceeded 2.5. The upper part of orebody was completely oxidized and did not differ in thermal conductivity from the host medium. The interpreted results permitted to localize the upper edge of the subvertical orebody within allowable error.

Fig.7.19 illustrates the temperature anomaly observed by the geophysical team (Central Research Institute of Non-Ferrous and Precious Metals, Moscow) along the profile across the Kvaisa pyrite-polymetallic deposit (the Greater Caucasus). The anomaly ampli-

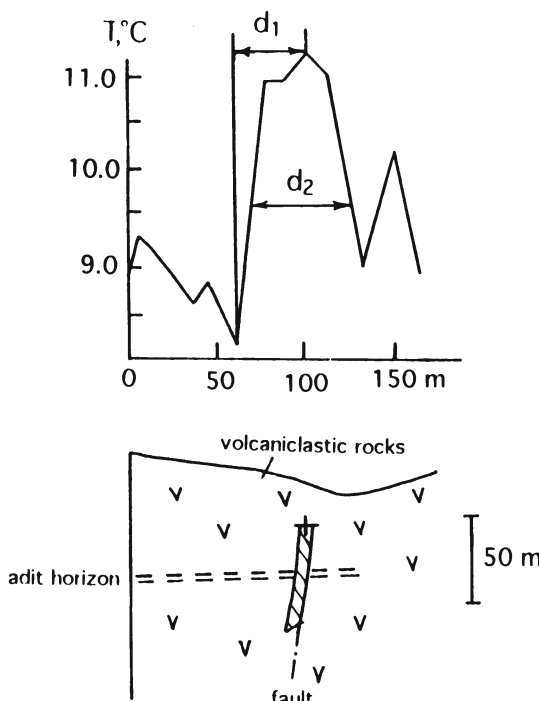


**Fig.7.19. Quantitative interpretation of temperature anomalies in the area of the Kvaisa pyrite-polymetallic deposit (Southern Osetia)**

The massive sulfide orebody is shaded. The “+” symbol marks the position of the upper edge of the interpreted thin body, as obtained from the analysis of the anomaly profile

tude exceeds  $2^\circ\text{C}$ , which is traceable to the additional effect of the

fracture located at the edge of the orebody. The temperature was measured in 1.0 m deep blastholes. The ore was of pyrite-sphalerite composition and a subvertical occurrence in volcaniclastic host rocks. Thermal conductivities for sandy-argillaceous host rocks and thick pyrite-polymetallic ore were  $2.0 \pm 0.5$  and  $5.0 \pm 1.0 \text{ W/m} \cdot ^\circ\text{C}$ , respectively, differing by a factor of 2.5.

Quantitative interpretation was carried out using the characteristic point method. This enabled us to locate the upper edge of the ore deposit occurring within unconsolidated volcaniclastic deposits from the Middle Jurassic. The results were confirmed by mining.

When interpreting plots of a temperature field under an inclined relief, one should bear in mind that the thermal field and the heights of the observation points are inversely correlated (see Fig.5.9). Under equal conditions, this fact accounts for the temperature anomaly plot rotation by  $180^\circ$  about the vertical axis in comparison with the magnetic  $Z$  anomaly, depicted in Fig.7.1 (the relief slope is equivalent to the polarization vector inclination). In this case the segments  $d_3$  and  $d_4$  exchange places, while  $d_1$  is measured from the opposite side (see Fig.7.18 and 7.19).

Developed methods may be successfully applied to the solving problems of oil-and-gas and engineering geology [149], search of underground waters and to other fields.

## 7.4 Combinations of quantitative interpretation techniques

### 7.4.1 Choice and order of the inverse problem solution technique application

The calculation techniques should be chosen at the stage of the development of the initial model of medium (see Chapter 4). After the field work is completed, the set of quantitative interpretation techniques may be corrected, proceeding from a particular type of the anomalies registered. Included into the set are techniques intended for obtaining the parameters of a certain class of model bodies, typical of the area under survey. The major requirements for the techniques to be chosen are as follows: applicability in the specified conditions of geophysical investigations, particularly, under oblique polarization and rugged terrain relief characteristic of the open areas in central and low latitudes; independence of the normal background level and of the choice of the origin of coordinates. The optimal techniques are those which permit to obtain the above mentioned parameters. Of special interest are the selection<sup>2</sup> techniques and some other methods applicable under rugged terrain relief.

It is necessary to consider the results of the research and development presented in Chapters 5, 6 and, especially, 7. They are summarized in Table 7.5.

The parameters should be determined using a combination of the available techniques, so that independent data on the parameters values could be obtained. With the 2-D condition satisfied, it is expedient to perform the calculations along a series of profiles in the mid-portion of the anomaly, where the field isolines are nearly parallel. The calculation results should then be averaged. This will ensure a higher validity of the parameter determination.

To obtain the anomalous bodies parameters, the first stage should involve interpolation selection methods (the method of characteristic points, the tangent method, the areas method, etc.). They

---

<sup>2</sup>The well-known term “selection” implies an approximation selection, if not stated otherwise

**Table 7.5. General scheme of author's modification for geophysical fields processing and interpretation under complicated environments**

FIELD	Time variation correction	Terrain correction using correlation method	Inverse problem solution in conditions of:				Integrated 3-D interactive modeling of complicated geological media
			rugged relief	arbitrary polarization	approximation of anomalous object by	1 or 2 models	4 or 5 models
MAGNETIC	+	⊕	⊕	⊕	⊕	⊕	⊕
GRAVITY	+	⊕	⊕	*	⊕	+	⊕
THERMAL	⊕	⊕	⊕	⊕	⊕	—	—
SP	+	+	⊕	⊕	⊕	—	—
VLF	⊕	⊕	⊕	⊕	⊕	—	—
IP	*	⊕	⊕	⊕	⊕	—	—

*Note. Symbols “+” and “—” designate availability and unavailability of procedures, respectively. Symbol “⊕” designates the authors' modification. Symbol “\*” designates the absence of necessity for calculation*

make it possible to obtain a large number of parameters in a fairly simple way. As to the next stage, it seems reasonable to employ the methods of singular points and analytical continuation, because by this moment one has already gained the necessary information about the object's quantitative characteristics. Comparing the computation results obtained by the methods of interpolation selection to those achieved by the method of singular points, one will get a more reliable and valid classification of singular points. The same refers to the method of analytical continuation. In this case, the range of the upper edge occurrence depth being known, one can avoid the risk of the field continuation into the neighborhood of the sources.

To check the calculations by the values of  $Z$  and  $X$  under oblique magnetization, it is advisable to calculate these components under vertical magnetization [6] with the following interpretation of the obtained curves using the known simple techniques [178].

Having made necessary corrections in the calculation results (due to the profile being non-horizontal and non-perpendicular to the body strike, etc.), we get a set of values for each parameter to be determined. Since the results of the numerical computations have

a probabilistic sense, it is useful to describe them not only by an average value of the parameter under determination, but using a standard deviation, as well. Therefore, for each of the anomalies the average value of parameters and standard deviation should be calculated, the latter being an estimate for the inner convergence of the calculation results obtained by different techniques.

The selection methods are used at the final stage of [145], when a sufficient amount of data on the object's parameters has been gained. These data permit to make important corrections and modifications in the initial medium model, thus forming an initial approximation to realize the selection. The better the initial approximation, the faster is the selection.

The initial approximation involves tracing the average parameters, obtained by the above techniques, onto the section (scheme) plotted previously when developing the initial model of the medium by prior data. The information on the sources' shapes and dimensions gives necessary grounds for selecting the type of the approximating expression. The mean-square divergence in the parameters, with prior information and field work experience taken into account, are used to impose constraints on the range of possible values of the parameters. With sufficient prior geological and geophysical data, ensuring a valid initial approximation, there is no need in other ways of interpretation. On the contrary, prior information being inadequate, physical simulation [18] proves to be useful for efficient preliminary rough estimates of the object's parameters. This is followed by an interactive selection. So, we may speak about a successive application of relatively simple techniques (the methods of tangents, singular points, etc.), admitting the determination of individual features of an object, followed by a more complicated selection, which permits to obtain an overall characteristics of the causative masses.

Under field conditions and at the very beginning of the interpretation with a large amount of computations, it is rather expedient to estimate the change ranges for a number of values by some very simple calculations of the limiting parameters [90,131].

To enhance the reliability of the anomalous object parameters determination, it is necessary to apply jointly the techniques which employ different individual elements of the anomaly or the curve

as a whole. These may be the methods of interpolation selection, singular points, analytical continuation and selection based on approximation optimization. The optimum combination of the mentioned techniques is determined by the specific nature of the region under survey and by the character of the material. For the example, density of the observation network and the accuracy of the field measurements impose certain restrictions on the method of singular points. The results of this method also depend on the noise fields of the sources occurring above the singular points of the objects being localized.

The requirement of the method applicability under rugged terrain relief is not, in most cases, a decisive one if the observed anomaly is initially converted to a horizontal or inclined plane. The necessity of the studied anomaly reduction is determined by the chose of set techniques.

When performing the quantitative interpretation of anomalies, it is essential to combine techniques that differ in the imposed constraints. For instance, while the limiting inequalities determine the largest possible depth, the method of singular points gives an underestimated depth of the upper edge of the object under survey. The latter method is characterized by a higher susceptibility to random errors and a lower sensitivity to the background effects, and the opposite is valid for the method of areas. The parameters determined by techniques with diverse constraints (and close by their informativity) make it possible to obtain the mean-square error in the determination of a parameter. In this case the obtained results will be represented in the form of a confidence area rather than in the form of a point in the section. Note that the intersection of confidence areas for the results obtained by different geophysical methods will permit us to choose the most reliable interpretation variant with the account of geological data.

It is interesting to compare the average parameters obtained by the statistical approach with the results of the deterministic interpretation. The technique worked out by Klushin and Tolstikhin [159] allows to estimate the average occurrence depth of magnetized masses by computing the normalized autocorrelation function  $R_n(\tau)$  of a field with sources represented by a set of thin vertical beds. This technique applied to the meridional profile through western

Azerbaijan confirmed the available Paffenholz's geological concepts [217] relevant to the section (Fig. 7.20). The average depth of the upper edge of magnetized masses is calculated by the formula

$$\bar{h} = \frac{1}{\pi} \int_0^\infty R_n(\tau) d\tau = \frac{\tau_e}{\pi}, \quad (7.42)$$

where  $\tau_e$  is the autocorrelation radius.

We obtain  $\bar{h}$  value of 4.3 km, which is close to the average depth of the field's singular points.

Thus, with the consideration of the data of Section 7.1, the major criteria for the choice of the techniques for inverse problem solution are the following:

- (1) feasibility of this or that version of the deterministic approach;
- (2) applicability under specific conditions;
- (3) low sensitivity to errors (high accuracy);
- (4) small labor-intensiveness and high rapidity;
- (5) combination of techniques subject to diverse (opposite) constraints.

#### **7.4.2 Refining the inverse problem solutions through iterative solutions of the direct problem**

The interpretation results obtained by rapid methods permit us to make necessary amendments into the model of medium available before the interpretation starts, and to form the initial approximation for selection-based interpretation. The following stage, though the most complicated one, plays the key role in analyzing the data of gravimetric and magnetic prospecting [45, 185, 263]. The electric anomaly sources represent rather sparse and isolated objects, while the gravity and magnetic sources with variable properties fill in the geological medium under survey, occupying the greater part of it, if not the entire medium.

Complicated media with a large number of anomalous bodies and parameters to be determined hinder the implementation of automated schemes of selection. In these conditions it would be more effective to use interactive computer selection system, where the direct problems of magnetic and gravimetric prospecting are solved by a computer, while the comparison of calculated and observed

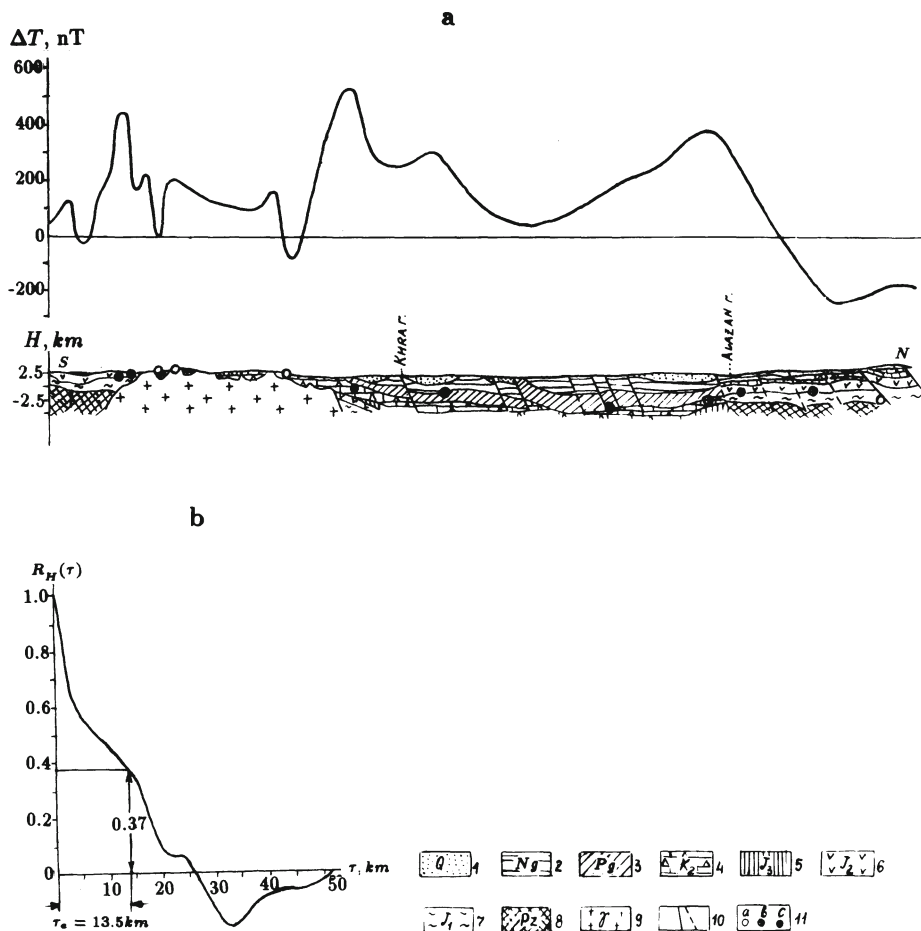


Fig. 7.20. Determination of the average occurrence depth of magnetized masses by the autocorrelation function of the magnetic field along the profile Kedabek-Belokany: (a) the plot of  $\Delta T$ , (b) the plot of the autocorrelation function

Deposits: (1) Quaternary, (2) Neogene, (3) Paleogene, (4) Upper Cretaceous, (5) Upper Jurassic, (6) Middle Jurassic, (7) Lower Jurassic, (8) Paleozoic, (9) intrusive rocks of the granodiorite series; (10) disjunctive dislocations; (11) singular points of the magnetic field with the following magnetization values: (a) up to  $0.5 \cdot 10^{-3}$ , (b) from  $0.5$  to  $1 \cdot 10^{-3}$  cgs, (c) larger than  $1 \cdot 10^{-3}$  cgs

curves, as well as registration of divergences and modification of the petrophysical model is carried out by an experienced interpreter. Thus, the interpreter uses an interactive system. For this purpose an effective *GSFC* program [144,145] with graphical subroutines has been developed (see Appendix B).

The advantage of the interactive computer selection system is that it reduces a great number of iterations, which are inevitable in automated selection by a given algorithm of a successive parameter variation search within the specified range.

A system of automated selection of geophysical fields (for gravitational field, for instance, the basis of this approach was developed by Bulakh et al. [48] and Goldshmidt et al. [92]) has certain limitations. It should be noted, first of all, that the selection should be meaningful, e.g. changing of physical properties and 3-D geometrical parameters should be carried out in definite numerical and space intervals. Principally, these limitations may be provided in the automated program. However, we have more important circumstance, sufficiently limiting the selection. Suppose, we conduct a 3-D integrated gravity and magnetic selection over a non-complicated section consisting of ten geological bodies. Each geological body has 3 petrophysical variables (density, value and inclination of magnetization vector), geometric variables: left-hand ( $y_1$ ) and right-hand ( $y_2$ ) end faces of the body and, finally, its geometric parameters in the plane of geological section. Number of points (variables) necessary for describing bodies in the plane of section *a priori* is unknown. For simplicity and taking into account that many of these points are calculated two times by contouring objects, we can assume that the number of these points is ten. To calculate the possible number of combinations of all variables by the combined 3-D modeling, we should carry out approximated ranging of variables (Table 7.6). Undoubtedly, this ranging is relative and is executed only for an estimation of necessary order number of combinations.

So, for one body we have the number of combinations  $C_{30}^1 \cdot C_{60}^1 \cdot C_{24}^1 \cdot C_{30}^1 \cdot C_{30}^1 \cdot C_{100}^1 \approx 4 \cdot 10^9$ . Correspondingly, for ten bodies we have  $\approx 4 \cdot 10^{90}$  combinations (for non-complicated section). Such a number of combinations considerably complicates an automatic 3-D integrated selection even using large modern computers.

**Table 7.6. Calculation of the number of possible combinations of variables**

Variable	Interval of changing	Ranging	Number of variants
Density, $g/cm^3$	2.3 – 2.6	0.01	30
Magnetization, $mA/m$	0 – 3000	50	60
Inclination of magnetization, degree	0 – 360	15	24
Left-hand end face, $y_1/x^*$	0 – 20	non-linear	30
Right-hand end face, $y_2/x$	0 – 20	non-linear	30
Coordinates of body in the plane of geological section	min 10 points	–	min $10 \cdot 10$

\* $x$  is the maximum length of a selected profile.

Moreover, it rules out the burden of attaching a geological sense to the obtained distribution of physical sources resulting from automated selection. An interactive computer system permits an interpreter to modify a model with the use of geological categories expressed in the form of petrophysical sources.

A method of geological space approximation is mostly important for the selection of a concrete algorithm. Often algorithms based on the approximation of the studied body cross-section by geometric forms of a circular cross-section are used for this purpose due to their simplicity. However, such approximation involves essential errors which can introduce dramatic mistakes into a model of geophysical fields. It is essential that these errors can not be reduced by decreasing the radii of approximating cross-sections. Let us consider a simple example: let a circle with a radius  $R$  be inscribed into body's cross-section which is approximated by a square with a side  $2R$ . Clearly, the difference between the areas of the square and the circle is  $4R^2 - \pi R^2$ , and the error value is above 20%. Now let us fill the area of the square with circular cross-sections with radii  $R/n$ . Their total number is  $n^2$ . Then their total area will also amount to  $\pi R^2$ . So, the error value will be the same for an arbitrary number of approximating circles.

GSFC program allows to compute simultaneously the gravity and magnetic effects due to the model of a medium with an arbitrary number of boundaries (up to 1,000). The influence of the boundary

“earth-air” can be also computed using this program. This allows to conduct interpretation using the selection method without a separate procedure for terrain relief influence (see Subsection 5.2.1).

It is noteworthy that the development of quantitative models without taking into account the 3-D nature of the medium can involve essential mistakes. Fig.7.21 shows that the selection of the profile to be interpreted near the anomalous body can distort the amplitude of gravitational field and dramatically change the form of magnetic field. Therefore it was necessary to develop an integrated software for computing 3-D fields under the conditions of complex geological media and rugged relief. This software is described in Appendix B.

The combination of rapid methods of potential and quasi-potential field interpretation with the selection based on GSFC program may be treated as a system of quantitative interpretation under rugged terrain relief and oblique polarization of objects. Its last stage is reduced to a geological interpretation of the geological space model selected (Fig.7.22). Such a system can assist in optimizing the selection of test wells and mines, thus ensuring a considerable economy.

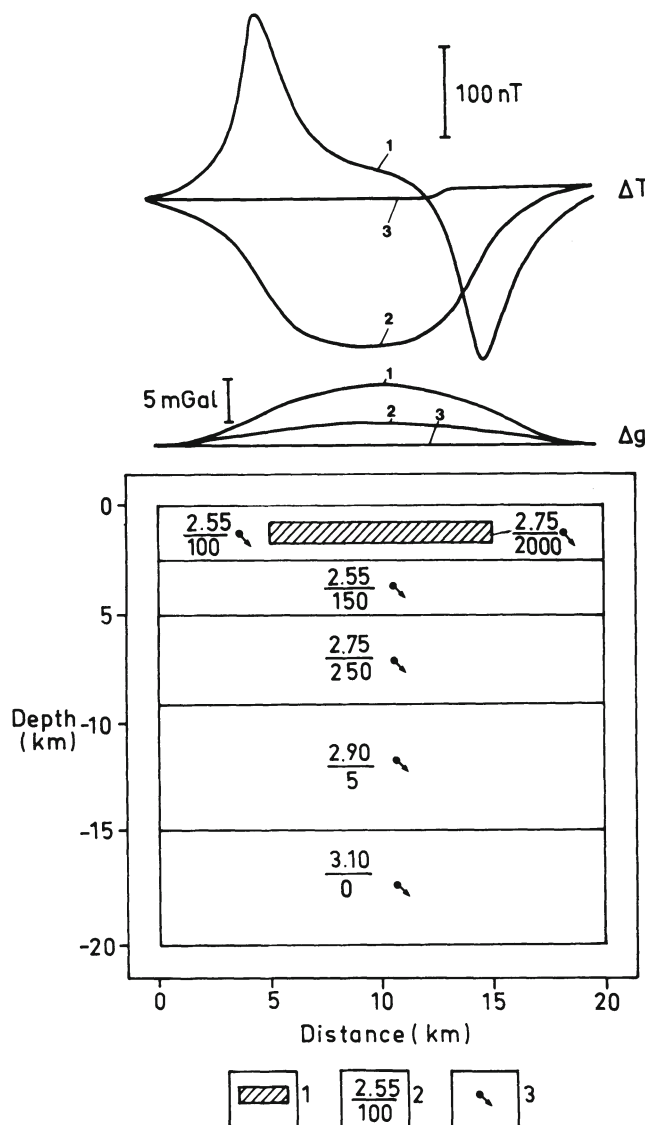
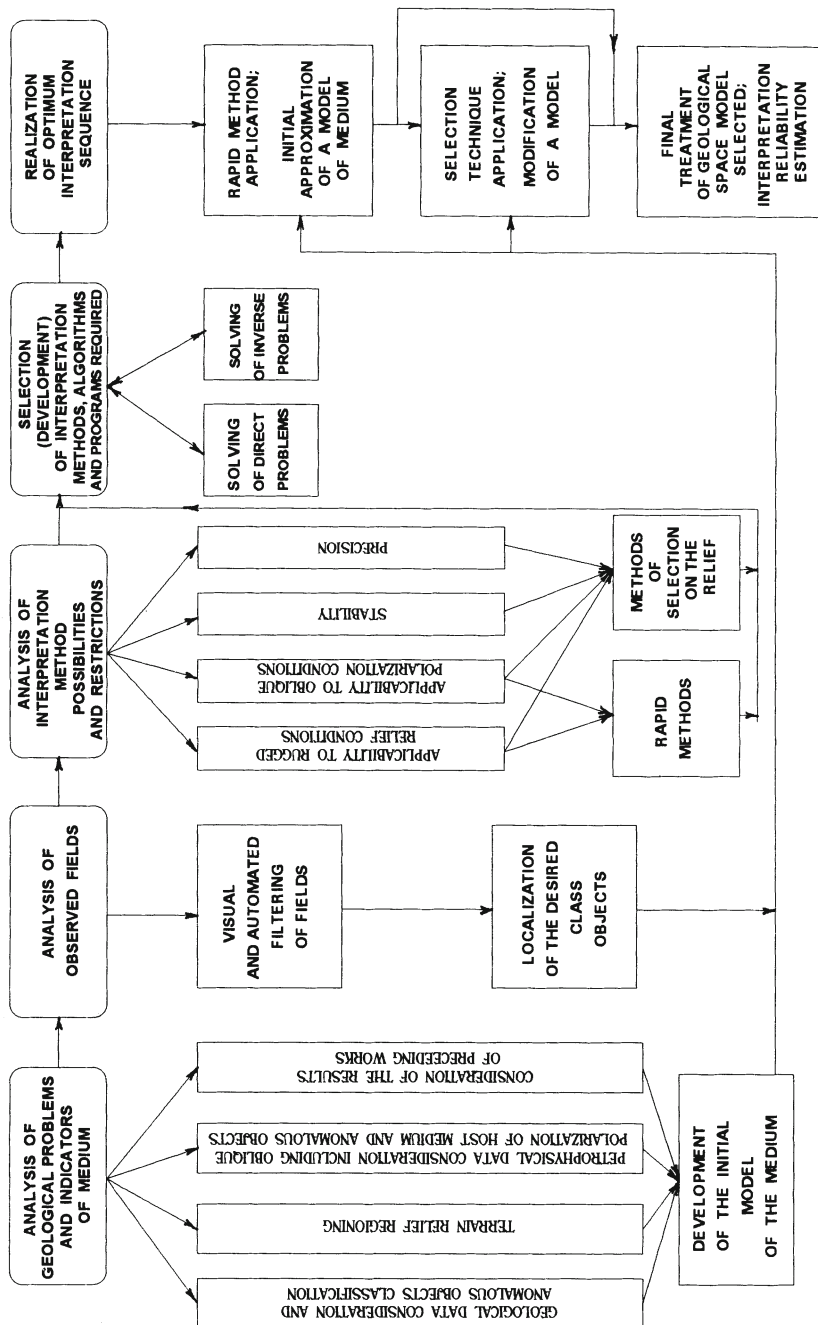


Fig. 7.21. Comparison of  $\Delta g$  and  $\Delta T$  fields computed with various location of end faces of the bed

Disposition of end faces, km: (a)  $(-\infty, +\infty)$ ; (b)  $(-0.5, 10)$ ; (c)  $(5, 10)$   
 (1) anomalous body; (2) physical properties: numerator=density,  $g/cm^3$ , denominator=magnetization,  $mA/m$ ; (3) direction of magnetization vector

(Additional data used in computing: azimuth of the selected profile is  $50^\circ$  and magnetic declination is  $5^\circ$ )



**Fig. 7.22. Flow-chart of a system of geophysical fields quantitative interpretation for complicated terrain and geological conditions**

# **Chapter 8**

## **INTEGRATED INTERPRETATION**

### **8.1 Fundamental advantages of integration**

The intricacy of geological problems, incorrect nature of some techniques and ambiguity of the interpretation results call for integration of geophysical methods [44,79,135,219,246,297,etc.]. Integration is one of the most important principles of geophysical exploration. Telford et al. [277,p.820] note: “The fact that this type of operation is so common space is because the exploration geophysicist, by a suitable selection of, say, four methods, may obtain much more than four times the information he would get from any one of them alone”.

By an integration (set) of geophysical methods we mean their combination based on the employment of different physical properties (magnetization, density, specific resistivity, polarizability, elastic, thermal and radioactive properties). This combination is necessary and sufficient to solve a particular problem under certain geological conditions.

Along with this, an intra-method integration involves different modifications of a single geophysical method [131], used to investigate various indicators of the geological structure. Integration is applied to airborne and ground magnetic surveys, thus making it possible to estimate the depth of anomaly sources. Different components are measured to obtain some additional information about the anomalous masses.

The advantages of integration can be well demonstrated using the information theory. While two independent experiments fail to furnish necessary information about the object of experiment, it

is possible to obtain exhaustive information, if they are performed jointly [298]. At increasing accuracy of measurement the amount of the information  $J_u$  obtained by a single geophysical method is growing far slower than the accuracy  $\Delta U$  due to a logarithmic nature of their interdependence (see equation (5.45)). Therefore, we are bound to come to the conclusion that an integrated approach is preferable as compared to infinite perfection of some individual method taken separately.

The efficiency of integration can be quantitatively estimated. If a set of methods is focused on investigating some independent indicators of equal value, then the anomaly detection reliability  $\gamma$  can be described by an error function (probability integral) expressed [211] as:

$$\gamma = \operatorname{erf}\left(\sqrt{\sum_i \rho_i}/2\right), \quad (8.1)$$

where  $\rho_i$  is the ratio of the anomaly square to the noise dispersion for each  $i$ -th geophysical field.

Bearing in mind that for a single method the anomaly detection reliability of a known form and intensity by Kotelnikov's criterion [292] is expressed by  $\operatorname{erf}(\sqrt{\rho_i}/2)$ , let us show how the integration of methods increases the reliability of a weak anomaly detection. If a mean square of anomaly for each method is equal to the noise dispersion, then the value of reliability  $\gamma$  for individual methods is 0.61, and that of a set of two and three methods is 0.77 and 0.87, respectively, according to equation (8.1). This means that the risk of an erroneous solution at the integration of two or three methods is decreased by a factor of 1.7 and 3, respectively. A comparison of the risk with the expenditures enables one to find an optimum set of methods.

When choosing a set of methods at each stage of investigation, a number of factors should be taken into consideration, namely, the resolution of geophysical methods (i.e. their ability to detect an anomaly due to the desired object at the minimal depth), their economical efficiency and portability. To evaluate the competitiveness of the methods, it is essential to determine their informativity or factor loads by the method of major components [46,288].

## 8.2 Variants of integrated interpretation

There exist different approaches to integrated interpretation, including those using traditional visual comparison of fields, and quantitative expression of the investigated peculiarities of fields and media. The benefits of integrated interpretation become more evident when passing from qualitative integrated interpretation to quantitative one.

Quantitative integrated interpretation usually involves quantitative estimation of parameters by a set of data. This concept seems to be wider; it comprises primarily the determination of the object's nature (quality) by a set of data employing quantitative criteria. Quantitative criteria which make it possible to judge about the nature of the objects under examination may be of different types [41,135].

Integrated interpretation can be deterministic, probabilistic and mixed (probabilistic-deterministic). The latter actually includes elements of both types, as in case of the single-method interpretation. An interesting sophisticated description of the probabilistic-deterministic approach for a common case was presented in [189].

Integrated interpretation based on the deterministic approach can be successfully accomplished provided one is certain that the anomalies of different methods are due to the same sources. In this case one applies the known Poisson's ratio between the magnetic and gravitational fields [202] and the linear programming technique applied to interpretation problems in [49,244].

The most universal means of deterministic interpretation is the selection of geophysical field for the model of the medium obtained from data of another geophysical method, and the comparison of the selected field with the observed one. Such a consecutive integrated interpretation can yield results which cannot follow from separate study of data obtained by different methods. For example, comparing the data obtained by vertical electric sounding (VES) and gravimetric prospecting, one can detect geoelectric horizons which do not manifest themselves in VES curve [231].

If we draw a rough analogy with electric engineering, it can also be series or parallel [139]. However, series interpretation with

each of the stages employing the results of the preceding one, actually performs ordinary interpretation of individual fields. So, we will basically confine ourselves to the parallel interpretation, which involves simultaneous utilization of data obtained by different geophysical methods. Geophysical investigations of oil-and-gas potential in Appalachians is an example of such integration [238]. Characteristics of such cooperative inversion of geophysical data has been given in [176]. These ideas seem most perspective, as confirmed by investigation both in the West and in the former Soviet Union [94,255].

Some additional information can be derived from parallel integrated interpretation (these may be tentative values of vertical and horizontal thickness and the dip angle), if different approximations of an anomalous object are admissible when interpreting anomalies caused by diverse fields<sup>1</sup>. This can be exemplified on the model of a pyrite-polymetallic deposit in the Middle Jurassic shale strata of the Greater Caucasus (Fig.8.1). Rapid methods of quantitative interpretation make it possible to determine the following parameters: position of the mass center of the anomaly-forming body by the plot of  $\Delta g$  (model a); position of the upper edge by the plot of  $\Delta Z$  (model b); position of the horizontal circular cylinder's center in the upper portion of the orebody at the ground water level by the plot of self-potential (model c). The specific models thus obtained reflect the contrasting character of the physical properties of the object and the host medium. They allow a fairly exhaustive description of the geometric parameters of the objects [71]. The model obtained with the help of mentioned data is in good agreement with the initial (prescribed) one (Fig.8.1d). A similar example can be made for a pyrite deposit occurring in a volcanogenic rock mass (Fig.8.2).

The mountainous conditions are usually unfavorable for deterministic integrated interpretation. That is why in this case the deterministic techniques are basically used to quantitatively interpret the results of some individual methods.

Regression-correlation integrated interpretation (e.g., drawing up structural maps by the gravimetric data on the basis of the correlation between these data and the position of seismic bound-

<sup>1</sup>Potentialities of various models of an object and ways of their application in the interpretation of a single field have been studied in Subsection 7.4.1.

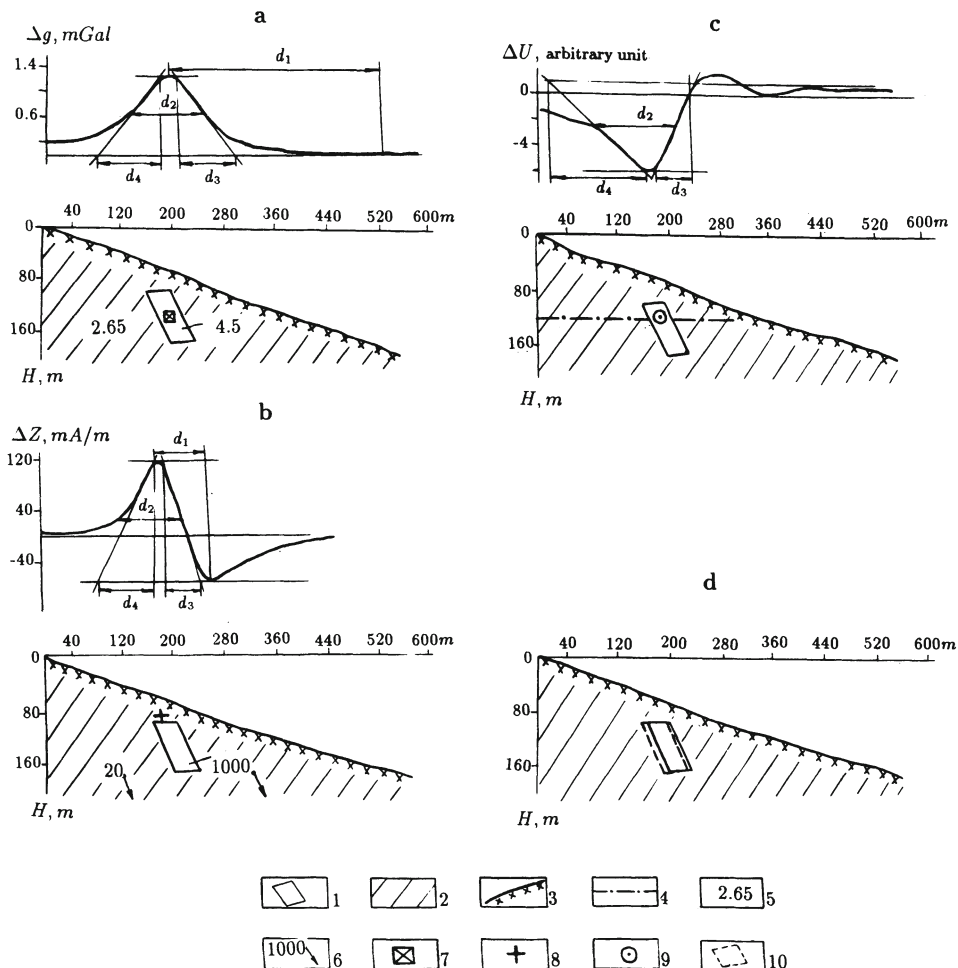
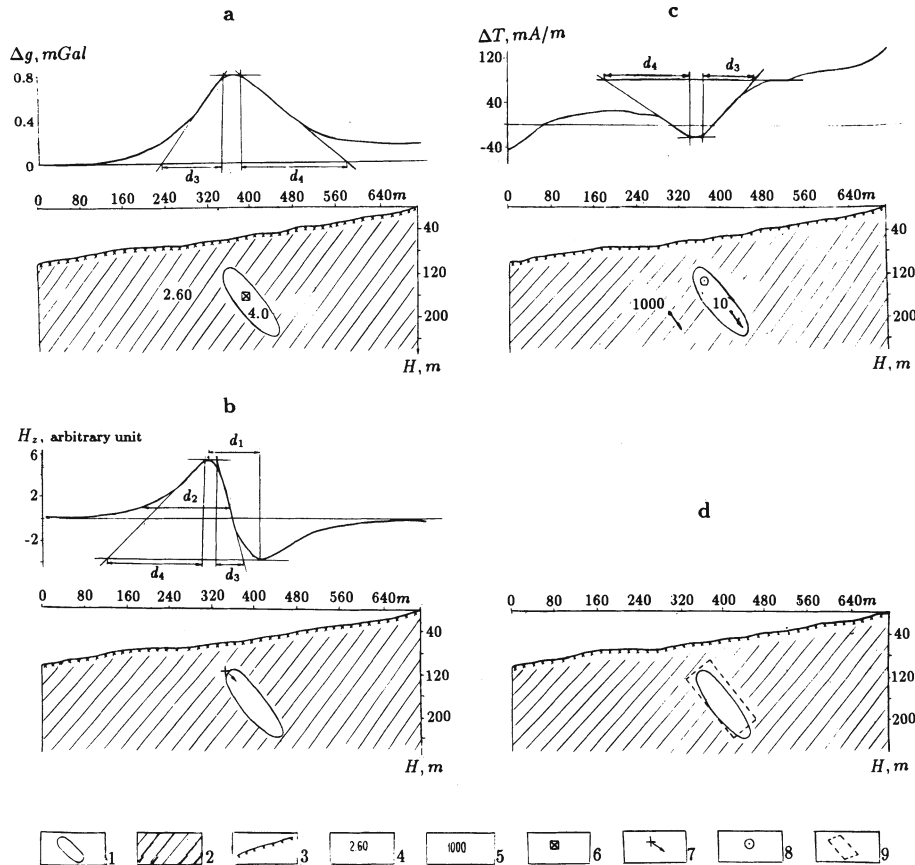


Fig. 8.1. Interpretation of the model fields  $\Delta g$ ,  $\Delta Z$ ,  $\Delta U_{SP}$  due to deposits of the Filizchai type under different approximation of the anomalous body: (a,b,c) results of the model fields rapid interpretation, (d) anomalous object according to the integrated interpretation results

(1) anomalous body; (2) host medium; (3) topography; (4) position of the ground water level; physical properties: (5) density ( $g/cm^3$ ), (6) magnetization ( $mA/m$ ); (7) mass center (of a circular horizontal cylinder) by  $\Delta g$  plot; (8) mid-point of the upper edge of an inclined thin bed by  $\Delta Z$  plot; (9) position of the center of HCC inscribed into the upper portion of the anomalous body at the ground water level by  $\Delta U_{SP}$  plot; (10) contour of the anomalous body obtained from the results of integrated quantitative interpretation



**Fig.8.2.** Interpretation of the model fields  $\Delta g$ ,  $H_z$ ,  $\Delta T$  due to deposit of the Lesser-Caucasian type under different approximations of the anomalous object: (a,b,c) results of the model fields rapid interpretation; (d) the anomalous object by the results of integrated interpretation

(1) anomalous body; (2) host medium; (3) topography; physical properties: (4) density ( $\text{g}/\text{cm}^3$ ), (5) magnetization ( $\text{mA}/\text{m}$ ); (6) mass center (of a circular horizontal cylinder) by  $\Delta g$  plot; (7) mid-point of the upper edge and direction of an inclined thin bed by  $H_z$  plot; (8) position of the HCC center in the upper portion of the anomalous object by  $\Delta T$  plot; (9) the anomalous object contour obtained by the results of integrated quantitative interpretation

aries) is most often used to solve the problems of oil geology. Such an approach to interpretation has become widely known due to the works by Karatayev, Shraibman and others [119,249]. This kind of interpretation has features characteristic of probabilistic-deterministic interpretation. That is why the techniques based on computation of the correlation coefficient between the results obtained by different methods, do not fall under this category, if they have no data on the seismic boundaries location and other information obtained by deterministic method. The above mentioned techniques should be rather classified as information-statistical ones. Thus, Lyubavin and Shaub [183] made use of the direct results of measurements to obtain the function of cross-correlation of the electric field with the magnetic one and its derivative during the flight period.

The most important problem of information-statistical (logico-statistical) integrated interpretation is the determination of an object's class on the basis of probabilistic or informational criteria. The evaluation of the probable presence of desired geological bodies by formalized features facilitates decision making according to the results of geophysical explorations. Under certain conditions it admits strict analysis of possible errors in the solution [46,84].

The major variants of quantitative interpretation are listed in Table 8.1.<sup>2</sup>

### 8.3 Revealing of the desired objects by a set of indicators

The above arguments testify to the importance of elaborating investigating problems of information-statistical integrated interpretation (including methods based on mathematical logic), which is gaining wide-spread application in predicting commercial minerals, revealing seismically active zones and solving other important geological problems. A great number of appropriate methods, algorithms and computer programs have been recently proposed.

---

<sup>2</sup>The classification of integrated interpretation methods was first given in [137,139]. This classification was repeated in the book [44], unfortunately without a respective reference.

**Table 8.1. Main types of quantitative integrated interpretation**

Approach	Interpretation principle
Deterministic	Application of Poisson's ratios between magnetic and gravitational fields at their joint analysis and other deterministic relations
Regression-correlation	Application of regression equations linking the results of geophysical investigation with the known characteristics of objects
Information-statistical	Application of informational and statistical criteria to refer the objects under study to a certain class of objects according to a set of results obtained by different methods

Therefore, it turns out essential to classify the suggested techniques and estimate their applicability for the solution of some particular problems. This challenge has been viewed in works by a number of leading authors [39,46,84,259,etc.].

### **8.3.1 Pattern recognition by standard and control sets of objects**

The best known techniques of integrated interpretation are those based on utilization of standard objects for teaching purposes. This, in fact, is the main limitation of the techniques of this group (group I), since the number of standard objects of large deposit type is extremely small, and moreover, it may happen that a given area of investigations completely lacks such standards.

The techniques of group I include statistical, empirical and informational methods.

The statistical techniques (it is preferable to view them from a somewhat broader standpoint of statistical game approach [46]), are

based on the statistical theory of decision making, which provides for optimal solutions under uncertainty conditions. The statistical techniques comprise the techniques of discriminant functions with linear and non-linear solving rules, Shaw's algorithms and others [66]. The most well known are linear discriminant functions [84].

The principal advantage of the statistic game techniques lies in the possibility to estimate theoretically the recognition reliability. However, their application is restricted by a number of factors. In particular, application of the discriminant functions calls for the following essential condition: the indicator distribution should not contradict the normal law. This condition does not always hold in practice. Next, Shaw's algorithms can only be used when all the descriptions of standard samples have a non-zero probability of occurrence. The statistical techniques are highly efficient if independent indicators are employed. These techniques are totally useless, when the material for teaching is represented solely by objects of a single class (e.g. deposits).

The empirical techniques make use of the decisive rule (an integrated criterion), whose reliability is estimated by the number of empirical errors only. Such are the computer programs realizing the algorithms "Crust-3", "Image-3", "Voting by deadlock testers" and others. They differ in the way computations, indicator selection and encoding are performed, in the number of different classes and other peculiarities [39,105].

The "Crust-3" program realizing the well-known Bongard's algorithm [35], sorts out 3 indicators combinations, that vote for attributing an object to a certain class after teaching. Program "Crust-3" initiated the development of a number of programs of a similar type. The advantage of this and similar programs is that they allow for the links between indicators. However, these programs can hardly be applied in practice, as there remain unsolvable theoretical problems, such as the choice of code and others. The "Crust-3" program, for example, is organized in such a way that the results obtained depend on the order in which the features are listed.

The approach based on pattern recognition of distributed regional seismicity was developed by Keilis-Borok [125]. This approach, particularly, includes clustering of events and changes in

aftershock statistics [196]. The developed algorithms were realized prior to the destructive Armenian (1988) and some other earthquakes [285].

If the indicators are supposed to be independent, one can apply some simple procedures to solve the recognition problem, which includes selecting of information-carrying indicators and generating an integrated criterion. It is the decisive rule providing an integrated estimation of prospects in the form of a function of the selected indicators. For example, the weights of different geophysical indicators of copper-nickel mineralization in the Karelian-Kola region (Russia) are defined by the authors of [95] as the ratio of the indicator distribution area to the total area of investigation. Borovko and others [42] suggest more accurate definitions for indicator informativity in predicting stanniferous mineralization. The integrated criterion of prospects is determined as a sum of informational weights in each information cell.

As to the informational techniques, one of the first was the algorithm by Vysokoostrovskaya and Zelenetsky [296], which employs only deposits (one pattern) as a standard. This technique has been successfully applied in Azerbaijan [132]. The presence of deposits in new areas is estimated by a data set in the following way. It is well known [292,298] that the amount of information contained in the test  $\alpha$  (in our case – geophysical observation) with respect to the test  $\beta$  (estimation of the deposit's presence under the observation point) is determined by the difference between the uncertainty (entropy) in the results of the test  $\beta$  before and after the test  $\alpha$ . Entropy, as well as the amount of particular information, is determined by the value of logarithm of the test's outcome probability taken with the negative sign.

Let  $P(A_i|B)$  denote posteriori probability of finding the  $i$ -th gradation of the indicator  $A$  (e.g., intensity of the field  $\Delta T$ ) over the desired objects  $B$ ;  $P(A_i)$  is prior probability of finding the same gradation on a survey sheet. Then the particular information contained in the registered  $A_i$  gradation with respect to the presence of the object takes the form

$$J_{A_i \rightarrow B} = \log[P(A_i|B)/P(A_i)], \quad (8.2)$$

as the uncertainty in  $A_i$  registration before the survey was  $\log P(A_i)$ , and after the survey  $\log P(A_i|B)$ . Statistically, the probabilities (or,

to be more precise, relative frequencies) are expressed by the ratios of areas:  $S$  is the sheet area,  $S_i$  is the area occupied by the interval of isolines  $A_i$ ,  $S_p$  is the total area of ore objects (or other prospecting objects) projections,  $S_{pi}$  is the area, common for the interval  $A_i$  and the objects projections. Then

$$P(A_i) = S_i/S;$$

$$P(A_i|B) = S_{pi}/S_p.$$

In absence of the object (case  $\bar{B}$ ) we make appropriate substitutions in designations

$$J_{A_i \rightarrow \bar{B}} = \log[P(A_i|\bar{B})/P(A_i)]. \quad (8.3)$$

The increments of information about the presence of the object

$$\Delta J_i = J_{A_i \rightarrow B} - J_{A_i \rightarrow \bar{B}} = \log[P(A_i|B)/P(A_i|\bar{B})] \quad (8.4)$$

are summed up in each elementary cell of the area under investigation. On the plotted map of isolines of information increments, the objects of the desired class (in our case these are ore deposits) stand out more clearly. This has been confirmed by the experience in the techniques application in the Greater Caucasus [132].

Beyond any doubt, geophysical work employing the techniques of group I is of great practical benefit. However, application of these techniques involves some difficulties. The number of indicators and standards being used sometimes amounts to a hundred and even more. As pointed out by Duda and Hart [66], the increasing number of indicators makes the requirement for the amount of standard information more strict. A great number of standards of the same type is available only in well studied regions. However, in such regions quantitative prognosis seems less important in contrast to regions that have not been investigated properly. Small and non-commercial objects can prevail among the standards ones, so similar deposits will be revealed as a result of prognosis [41]. As to the large and unique deposits, which should be the main aim of searching, their indicators can differ from those of standard deposits.

### 8.3.2 Classification of objects into compact groups in an indicator space

Difficulties in the choice of reference objects led to the development of techniques of group II based on the analysis of observed fields, anomalies correlation and differentiation between the obtained groups of similar combination.

To single out anomalies, the filtration-correlation techniques employ correlation analysis and different kinds of filters. In self-setting filtering [54] the anomalies parameters are not specified beforehand, but determined during the processing. The areas, where anomalies obtained by different methods form identical combinations, are joined by a common contour. After that a certain geological content is assigned to each contour. This method provides a vast amount of unbiased information. Nevertheless, being based on sorting, it has certain limitations. Some anomalies singled out by this technique can be of no interest as far as predicting and prospecting problems are concerned.

Among the methods of automatic classification two large groups are distinguished by Bugaets and Dudenko [46]. These are hierarchical and cluster techniques. They serve to determine inter-group and intra-group characteristics of similarity, respectively. As a similarity measure, one can take a distance in a multi-dimensional space, a cosine of the angle between the vectors of indicators or a potential, as in the method of potential functions. This method is known as a general method of constructing a differentiating surface by the data on standard images (learning “with a teacher”). However, it can be equally applied to dividing sets of objects into classes “without a teacher”. Automatic differentiation of objects according to their typical indicators or, vice versa, unique characteristics, aids to form an opinion as to their value. The algorithm “Association” developed by Dorofeyuk can be considered as an example of automatic classification [46].

The results of application of the automatic classification techniques depend, to a great extent, on the changes in the set of indicators, especially if their number is large. Moreover, the analysis of the content of selected groups is impeded, as in case of filtration-correlation techniques.

### 8.3.3 Revealing of objects (classes of objects) with expected properties

Before we pass to the techniques of group III, it is necessary to make an essential proviso. Let us imagine such a situation (which is practically unfeasible), where all the properties inherent in the objects under classification are known exactly, observations and analysis of the observation results have been accomplished without a single error. In this case it is possible to perform an unambiguous partitioning into classes. Therefore, a deterministic solution of the recognition problem is a special case of the probabilistic one. Applying the above considered techniques, except the statistical ones, we can form an unambiguous opinion about the assignment of the object to one or another class. Theoretical error probability in determining the objects nature is taken to be zero. In this connection, some authors call such techniques logical (deterministic). A logical character of interpretation manifests itself when the techniques of group III are employed. However, under certain assumptions as to anomalies and noises, one can give a solving rule with an estimate of the integrated interpretation reliability [210].

The techniques of group III are simpler than the greater part of the methods listed above, but the estimates they yield are more rough. Yet, when it is necessary to single out, for example, the largest and richest orebodies against the background of noises, or sufficiently typical ore controls, such as deep faults, acid or basic intrusions, these techniques of geophysical data interpretation prove to be highly promising, since they use most common “through” indicators for different kinds of the desired objects.

One of the first techniques of integrated interpretation of group III was suggested in oil geophysics for direct prospecting for oil and gas by Medovsky [30]. The technique (graphical integrated interpretation) and its digital modification were further developed by Berezkin. He proposed a method of summation of complete normalized gradients [29].

In ore geophysics, following the developments in integrated interpretation of geochemical data [157], it was suggested to employ the “reduction” of petrophysical or geophysical [288] exploration results, alongside with the computation of a complex index (“index

of contrast”, “generalized function”). The latter is obtained as a sum or a product of centered and normalized anomalies of each indicator under examination. Good results have been obtained using this logical approach. The most precise quantitative content of this approach is due to Khesin’s method of summation or cross-correlation of information obtained by different methods [131,133,146].

At each piquet the amount of information  $J_i$  due to the application of the  $i$ -th method is

$$J_i = -\log P_j \quad (8.5)$$

or

$$J_i \approx \log \left| \frac{U_i}{\Delta U_i} \right|, \quad (8.6)$$

where  $P_j$  is the relative frequency of the  $j$ -th interval of the  $i$ -th indicator on the histogram of its distribution,  $U_i$  and  $\Delta U_i$  are the amplitude and the error of this indicator’s determination, respectively.

After summing up the information elements which enable one to conclude *a priori* that the object of the desired class is present, random noises and components caused by different geological features, are suppressed. To avoid singling out fictitious objects by the plot of  $\frac{1}{n} \sum_{i=1}^n J_i$ , which is possible with a great amount of information contained in the data of only one or two methods, an additional integrated criterion should be computed. It depends on the number of significant indicators, if their relative influence is leveled:

$$J_{compl} = \sum_{k=1}^{\frac{n(n-1)}{2}} \frac{(J_p)_k}{(J_p)_{max}}, \quad (8.7)$$

where  $J_p$  is determined similarly to  $J_{cr}$  in equation (5.46) using pairwise combinations of the results of  $n$  methods used.

To avoid missing deep-seated objects, it is expedient in some cases to use relative frequencies of average values or average field estimates on a sliding averaging interval instead of  $P_j$  and  $U_i$  values, respectively.

Along with a simplified version based on summing up informants obtained from (8.6), the method has been realized as an

“Integration” program. The latter allows to compute and plot the sums of informants by equation (8.5) and the corresponding  $J_{compl}$  index. Unlike other methods, this index is capable of revealing the objects characterized by the maximum number of indicators of different intensities and, at the same, to avoid missing an object which for some reason did not manifest itself by any indicator. The combination of indices permits to make certain interpretative conclusions (Fig.8.3).

In practice  $J_i$  is usually replaced by the relative amount of information, called also a coefficient of informativity [41,133]:

$$K_i = J_i / \bar{J}_i. \quad (8.8)$$

The value of  $\bar{J}_i$  determines the information obtained when the result of  $U_j$  falls into the  $x_j$  interval of histogram at an equal probability of falling into any of  $R$  intervals. According to [292], it is equal to average (complete) information, contained in the results of measuring by a single method,

$$\bar{J}_i = \log R. \quad (8.9)$$

Application of  $K_i$  enables one to take into account differences in the ranges of different fields. However, the application of expressions (8.5) and (8.7) – (8.9) may be not effective for scant sampling.

### 8.3.4 Classification of logico-statistical (information-statistical) techniques

From the foregoing it follows that the most promising approaches under the given conditions are the following: classification of objects by association of indicators forming compact groups in the space of indicators, and revealing of objects (classes of objects) with expected properties. The first approach implies subsequent interpretation of the nature of each class obtained. It is, therefore, applicable at the last stage of thorough examination of all the peculiarities of the singled out area. The second approach, in accordance with the task set, permits us to estimate promptly the presence of desired bodies on the reference profile or in the area of integrated geophysical exploration. These approaches are realized in the techniques of groups II and III listed in Table 8.2.

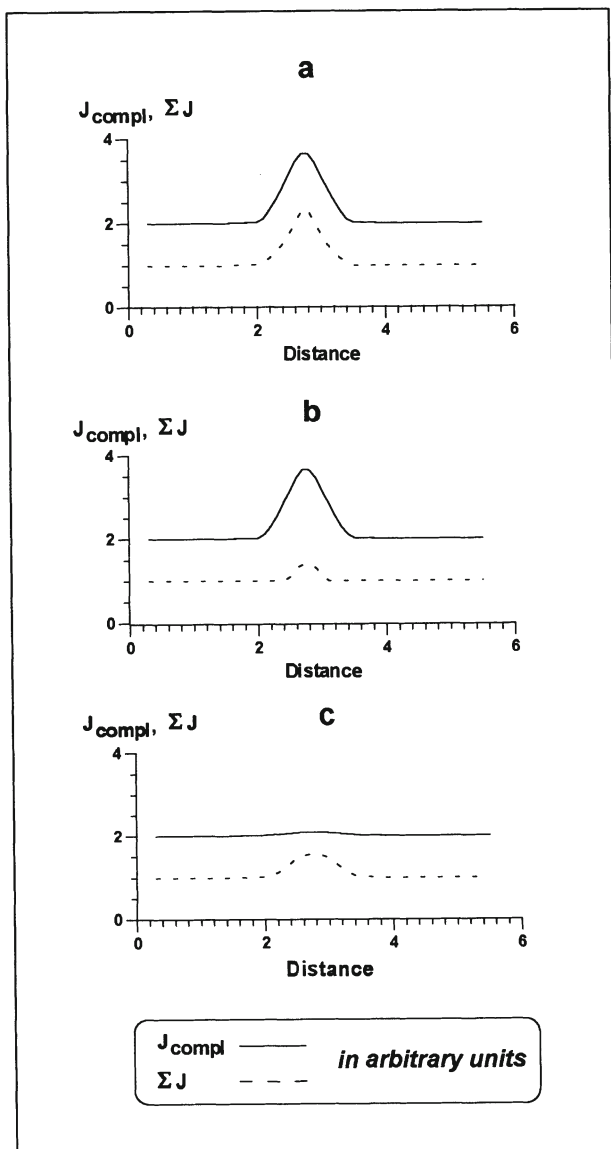


Fig.8.3. Variants of integrated interpretation results by two information indices: (a) the object is singled out reliably by all the features and occurs at a relatively small depth, (b) the object is singled out reliably by all the features and occurs at a large depth, (c) the object is singled out unreliably (not by all the features)

**Table 8.2. Varieties (groups of techniques) of information-statistical integrated interpretation**

Group of techniques	Basic peculiarities	Techniques	Characteristic modifications (programs)
I	Learning on standard objects	Statistical	Discriminant functions [84]
		Empirical	“Crust-3” [105]
		Informational	Developed by Vysokoostrovskaya and Zelenetsky [296]
II	Revealing of anomalies and their groups	Filtration-correlational	Self-setting filtering [55]
		Automatic classification	“Association” [46]
III	Revealing of objects with given properties	Heuristic	Summation of complete gradients [29]
		Logico-informational	Developed by Khesin [131]

The techniques of group I listed in Table 8.2 and called empirical are usually known as heuristic, in terms of Fotiadi [84]. However, a more general notion – heuristic – is more suitable for the techniques of group III. Empirical dependencies manifest themselves in statistical processing. As to heuristic techniques, they use empirical dependencies along with theoretical abstractions [228].

Evidently, all variants of integrated interpretation employ certain model representation. This is well illustrated by the techniques of group I, where learning is accomplished with the aid of natural standards. In the techniques of group II field realizations of one or another standard are used. The techniques of group III are actually based on the utilization of some imaginary (model, ideal) standards.

## 8.4 Stages of physico-geological modeling

The above techniques of processing and interpretation form a continuous sequence of procedures aimed at a final geological product – a resultative map, a section, etc., i.e. a plot representing a final

physico-geological model (*PGM*) of the investigated medium.

For example, summing up the amounts of information contained in  $\Delta g$ ,  $\Delta T$  fields and in the vertical component of *VLF* magnetic field  $H_z$ , we get the anomaly of the parameter

$$\frac{1}{3} \sum_{i=1}^3 J_i,$$

which is more marked and reveals a gently sloping ore object on the profile 5c through the Kyzylbulakh gold-pyrite deposit in the Lesser Caucasus (Fig.8.4A). <sup>3</sup>

The rapid interpretation of  $\Delta g$ ,  $\Delta T$ ,  $H_z$  and  $H_\phi$  plots (see Fig.8.4B) confirmed the available geological ideas and permitted to form an initial approximation of the model of the medium for its further refinement in interactive physico-geological simulation of  $\Delta g$  and  $\Delta T$  fields (see Fig.8.4C).

The bases of such modeling are set forth in Section 7.4. Here we give a detailed description of the order of execution for this process. It enables one to form a 3-D *PGM* of the area under investigation by the results of observation of the gravitational and magnetic ( $\Delta Z$  or  $\Delta T$ ) fields under rugged terrain relief conditions and arbitrary magnetization of objects and the host medium.

There are 3 major stages:

(1) preparation of the initial model of the medium using methods of rapid interpretation for magnetic and gravity anomalies developed for the conditions of rugged terrain relief and oblique magnetization of objects;

(2) interactive selection of geological space models using the 3-D *GSFC* program;

(3) construction of 3-D *PGM* of the area under investigation.

All the stages are typical for any type of prospecting, ranging from regional to detailed ones. They differ basically in the quantity

---

<sup>3</sup>Taking into account a limited sampling, equation (8.6) was used. During this computation  $\Delta U_i$  was taken as a doubled standard deviation of  $U_i$ . The zero line of  $\Delta T$  field is represented by the level of anomaly maximum. The values of  $U_i$  were counted proceeding from this level in the direction of the field decrease (since pyrite deposits are marked by lower magnetization with respect to volcanogenic host rocks).

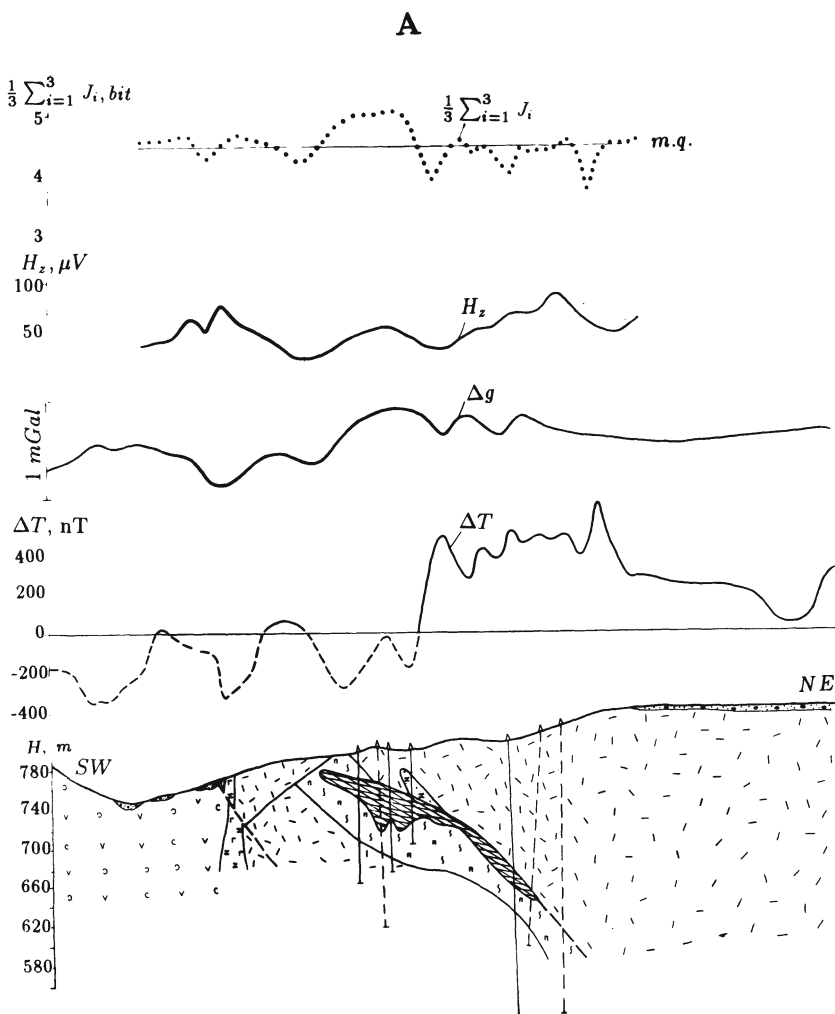


Fig.8.4. Stages in geophysical data interpretation at the Kyzylbulakh gold-pyrite deposit

Fig.8.4A. Singling out of the desired object (ore deposit) by summing up the amounts of information obtained by different geophysical methods

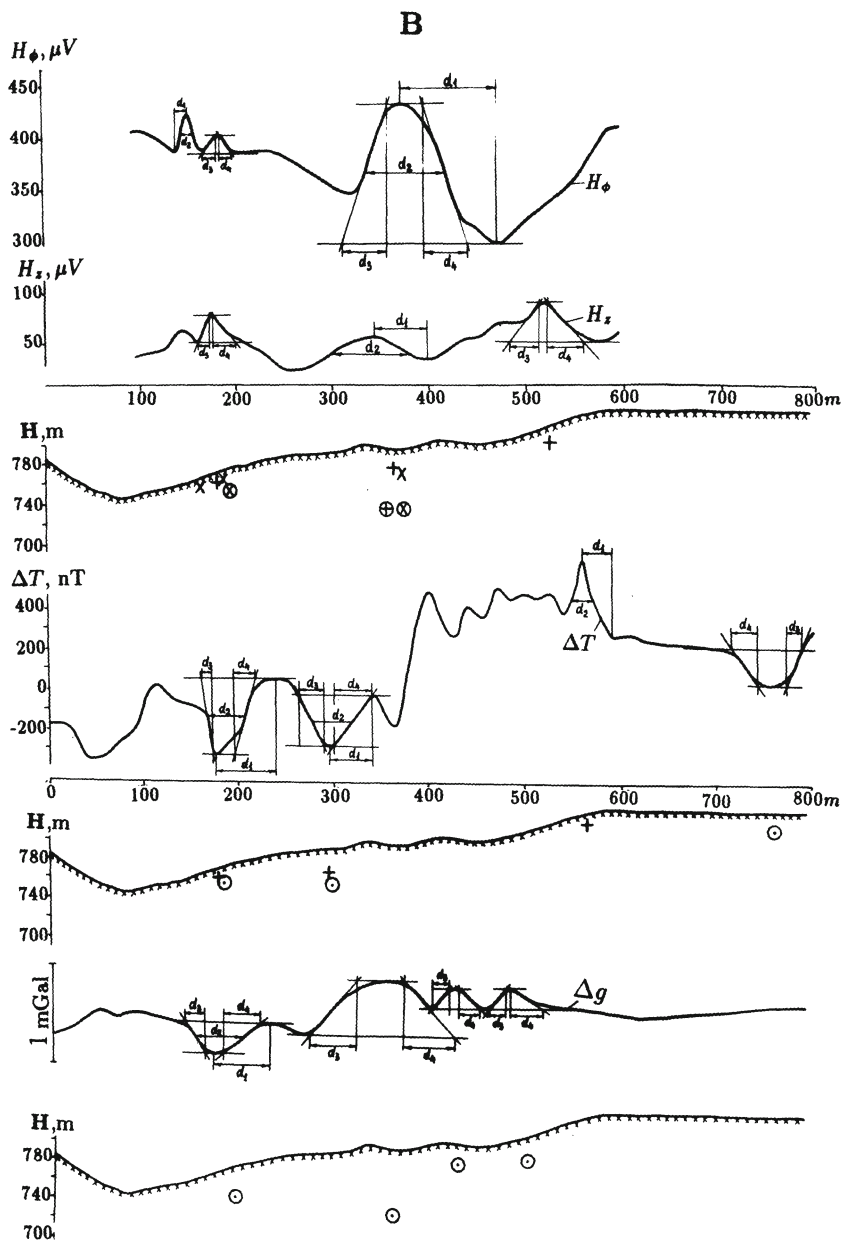
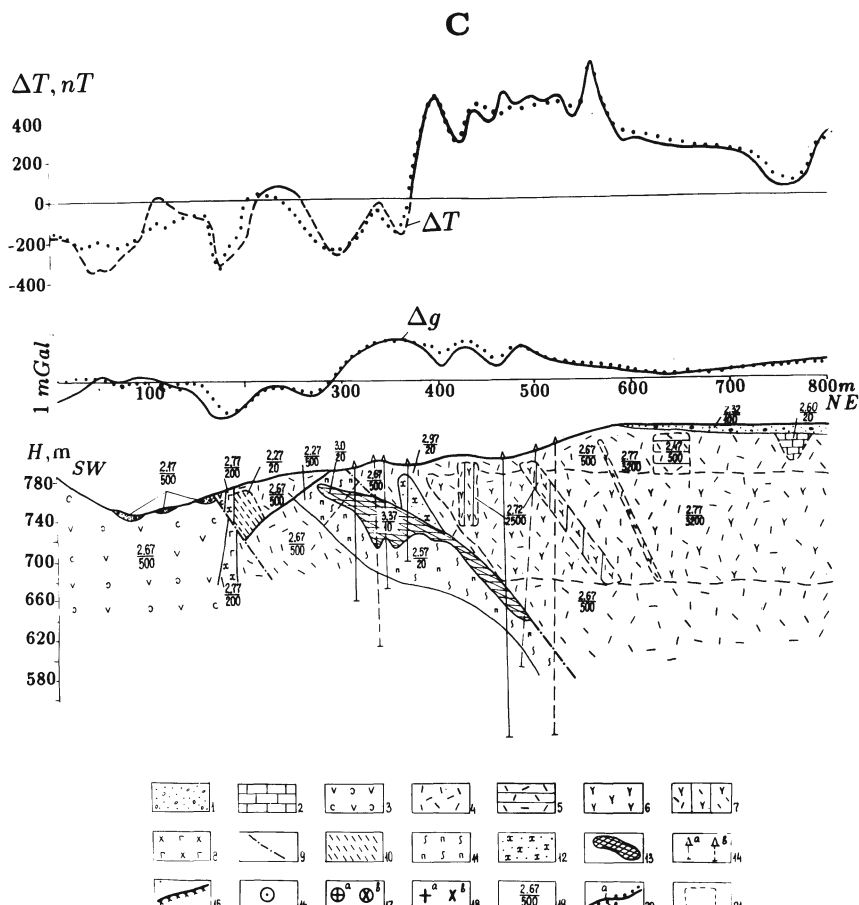


Fig.8.4B. Quantitative rapid interpretation of  $\Delta T$ ,  $\Delta g$ ,  $H_z$  and  $H_\phi$  fields



**Fig.8.4C. Selection of a geological section on the basis of gravimetric and magnetic data**

(1) Quaternary deluvial deposits; (2-8) Middle and Upper Jurassic rocks: (2) silicified limestone lens, (3) tuffs and lavas of andesitic porphyrites, (4) tuffs of liparite-dacitic porphyrites, (5) deconsolidated tuffs of liparite-dacitic porphyrites\*, (6) lavas of dacitic porphyrites\*, (7) consolidated lavas of dacite-porphyrites\*, (8) dikes of andesite-basalts; (9) disjunctive dislocations; (10) zone of brecciation and crush\*; (11) zones of brecciation, crush and boudinage with lean pyrite-chalcocite ore; (12) zone of brecciation, crush and boudinage with rich impregnating mineralization; (13) massive pyrite-chalcocite ore; (14) drilled wells: (a) on the profile, (b) projected on the profile; (15) terrain relief in the profile (in Fig. 8.4B only); results of rapid interpretation; (16) location of the center of horizontal circular cylinder ( $HCC$ ) from the interpretation of  $\Delta g$  and  $\Delta T$  plots, (17) location of the  $HCC$  center from the interpretation of the  $H_z$  (a) and  $H_\phi$  (b) plots, (18) location of the upper edge of thin bed from the interpretation of  $H_z$  and  $\Delta T$  (a) and  $H_\phi$  (b) plots; (19) physical properties (numerator=density,  $g/cm^3$ ; denominator=magnetization,  $mA/m$ ); (20) gravitational and magnetic fields: (a) observed, (b) selected; (21) body contours introduced during the selection using GSFC program

Note. \*Results of selection

and quality of the available initial data and sizes of the objects under study. Therefore, they are described on the example of the 1:200,000 scale explorations along the Lesser-Caucasian segment of one of the profiles crossing the Caucasus in the north-north-east direction (Fig.8.5).

**The first stage** involves the following:

(A) A special geological section is formed, where all the representatives of intrusive, effusive and other associations, as well as disjunctive dislocations and the surface of folded foundation are selected on the basis of geological data within a strip 15-20 km wide. The section is located in the middle of this strip. It characterizes the upper portion of the Earth's crust with 2-3 to 5-8 km thick from the earth's surface to the Baikalian basement. Deeper parts of intrusion bodies and of certain disjunctive dislocations are constructed by extrapolation with the account of occurrence mode, geological considerations of general character and results of preceding geophysical explorations. They are characterized by higher uncertainty.

(B) A preliminary petrophysical model of the section is developed. Here all the representatives of geological associations acquire density and magnetization values according to the data of the preceding petrophysical and geophysical investigations. In absence of any data relevant to magnetization direction, it is assumed parallel to geomagnetic field. Further, the magnetization direction is refined in the course of mathematical modeling. Petrophysical model includes deep-seated layers of the Earth's crust: (1) "basaltic", (2) intermediate between the crust and the upper mantle and (3) the upper mantle. Their surfaces are plotted and physical properties are accepted according to the data of earlier seismic and other deep investigations.

(C) The initial (preliminary) petrophysical model includes, as well, hidden bodies. Their location, thickness, depth and magnetization are obtained by the results of the quantitative interpretation of magnetic and gravitational anomalies by rapid methods. The latter have been developed for the conditions of non-horizontal observation lines, arbitrary polarization of object and unknown level of the normal field.

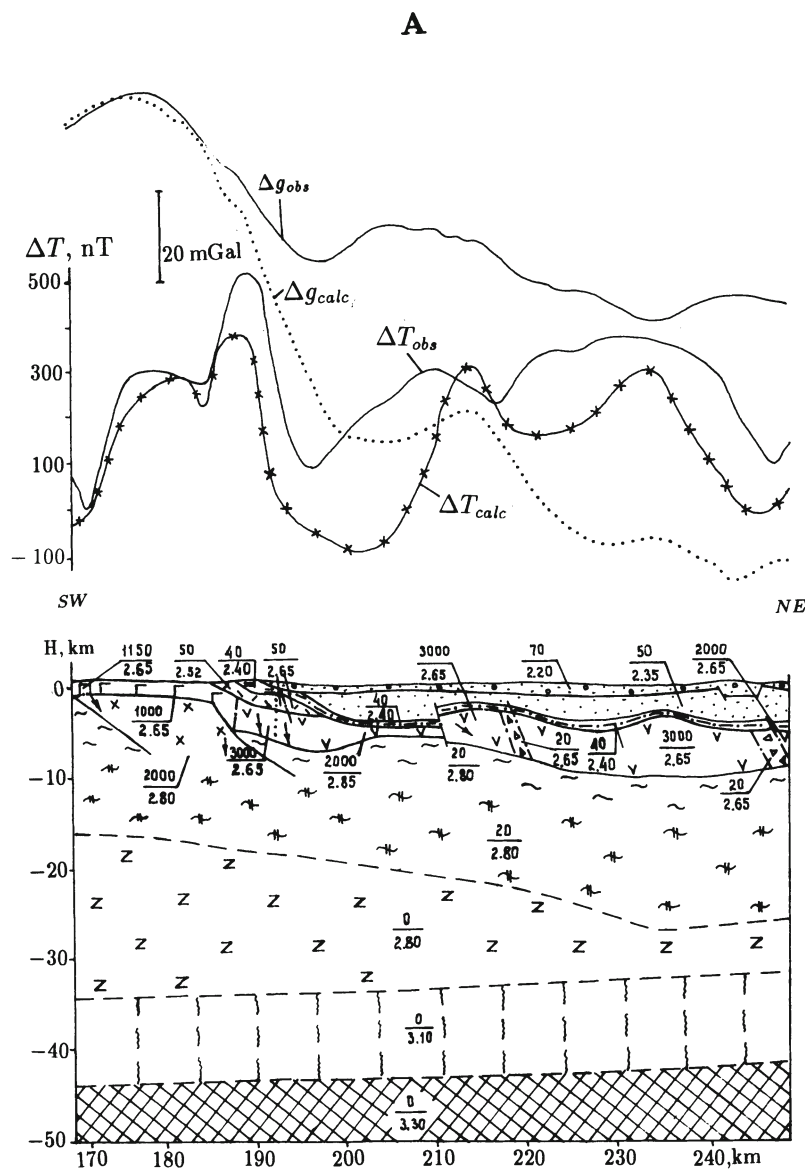
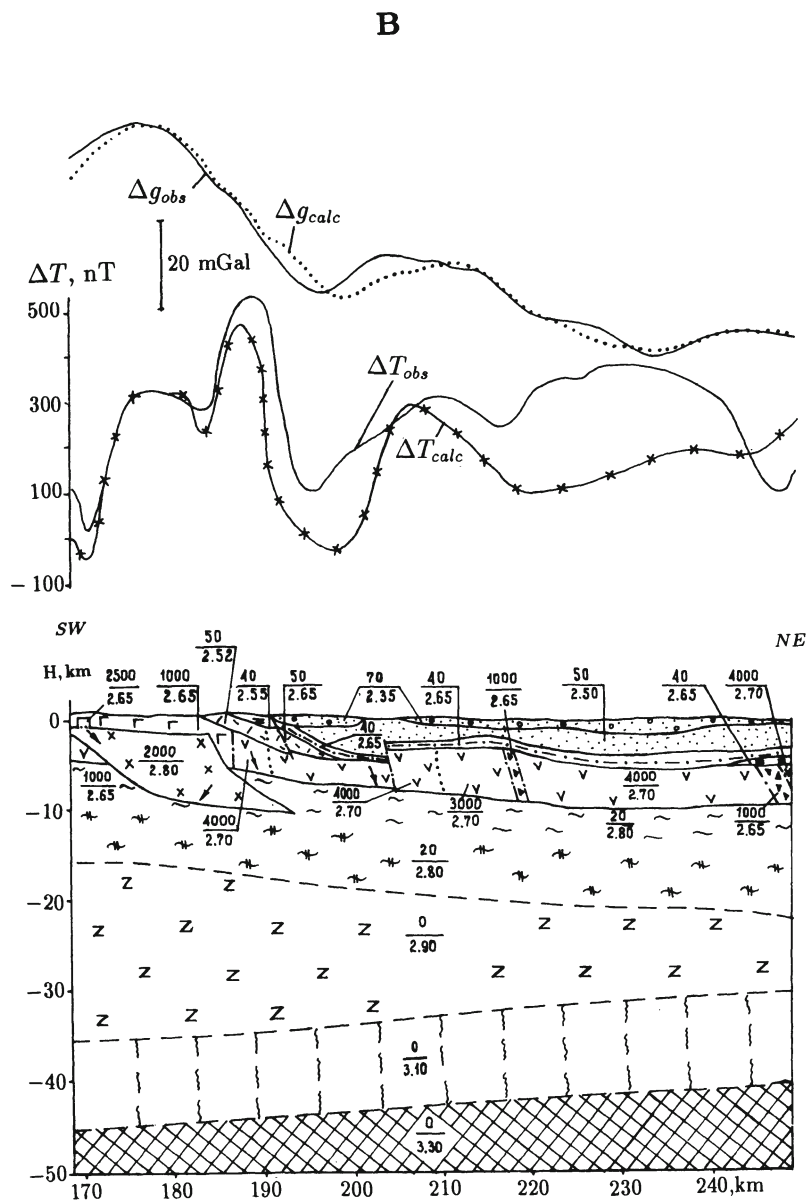
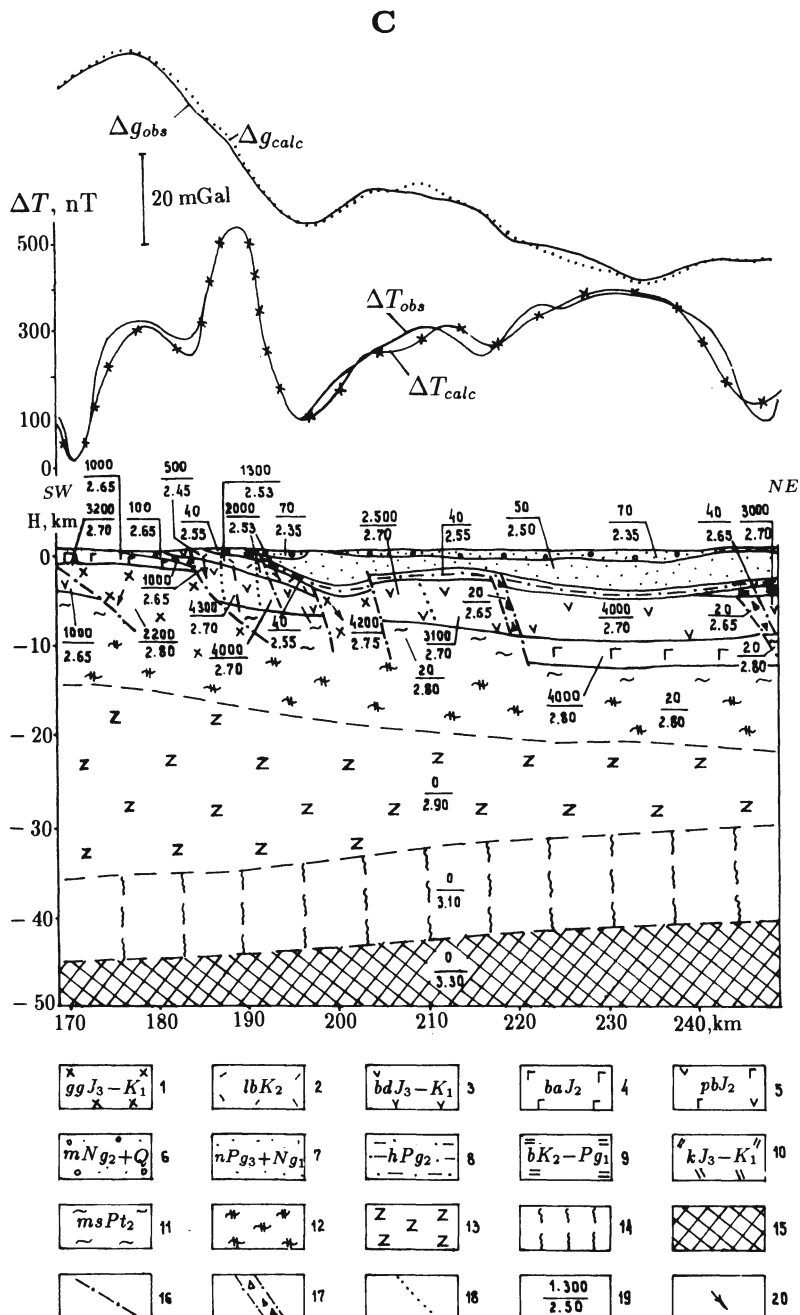


Fig. 8.5. Construction of a physico-geological model (for stakes 700 – 1350 of profiles 3 – 4)  
(A) A zero approximation model (initial)



#### (B) The third approximation model



### (C) The eleventh approximation model (final)

*Caption to Fig.8.5.*

(1) intrusive gabbro-diorite-granodioritic association; (2-5) effusive associations: (2) liparite-basaltic, (3) basalt-andesite-dacitic, (4) basalt-andesitic, (5) basalt-andesite-plagioparitic; (6-11) background sedimentary deposits: (6) upper molassic, (7) lower molassic, (8) terrigenous, (9) terrigenous-carbonaceous, in some places flyschoid, (10) carbonaceous-sandy, reef rocks; (11) metamorphic schists and other metamorphites; (12-15) deep-seated complexes: (12) granites and gneisses, in some places amphibolites, (13) basic rocks, (14) basic rocks – eclogites, (15) uppermantle peridotites; (16) faults, upthrusts; (17) crush zones; (18) boundaries of physical properties changing within the same association; (19) physical properties (numerator=magnetization,  $mA/m$ , denominator=density,  $g/cm^3$ ); (20) direction of the magnetization vector differing from the geomagnetic field inclination

On the basis of the developed initial model of the medium for the area under study and processing from the classification of the desired objects, typical simple models are determined, which approximate the anomaly sources (see Table 1.1 in Section 1.2). The anomalies of the above methods, observed along the profiles in a rugged terrain relief approximated by an inclined plane are interpreted by rapid methods of characteristic points and tangents. When it is impossible to perform such approximation, the anomalies are reduced in the inclined half-space onto an inclined plane which is the nearest to the relief surface. The plots of anomalies for the examined fields are constructed in the horizontal projection. The interpretation of such plots results in quantitative parameters of some fictitious bodies. Then, applying the formulas of Chapter 7, one can pass to the parameters of real anomaly sources. Rapid interpretation methods for anomalies due to different fields are also presented in detail in Chapter 7.

On the basis of the interpretation results some necessary changes are introduced into the initial model of the medium, and conditions are formed to make initial approximations, necessary for the interpretation along the profiles using the selection method.

**The second stage** employs the method of selection of gravitational and magnetic fields along the profiles using *GSFC* program.

Each time the fields due to different bodies, groups of bodies and the model as a whole are computed and displayed or printed in the form of plots, the latter are compared to the observed

fields. Using the results of comparison, some changes matched with the gravity and magnetic effects are introduced into the model of the medium. Computations, comparison of fields and model modification are repeatedly executed until the desired conformity between the computed and observed fields is attained.

In a particular case illustrated in Fig.8.5, the selection was accomplished in the following order. Each printed plot of computed gravitational and magnetic fields was compared to a corresponding plot of observed fields. The comparison started with the total effect of the bodies that formed regional fields, and continued with gradual introduction of effects due to local bodies. On the basis of the comparison, a decision was made as to the necessity of introducing modifications into the configuration or physical properties of the bodies determining regional fields, local anomalies, introduction of new local bodies or exclusion of some of the available ones. These modifications were included into the model. Then the computation was resumed (see Fig.8.5A,B).

First, a regional gravitational field was roughly selected. As a rule, the densities of deep-seated complexes were not changed, the modifications concerned only the shape of their roof. Then, fields of local bodies were selected. If necessary, this was followed by the verification of the regional field and the field of local bodies, as well.

At each step of computer counting, a separate analysis of gravitational and magnetic fields was performed. Coordinated variations verified at the subsequent steps, were then introduced into the model. Thus, integrated quantitative interpretation was actually accomplished for anomalous gravitational and magnetic fields. The selection was stopped (see Fig.8.5C), when the computed gravitational and magnetic fields coincided, on the average, with the observed ones within the accuracy of measuring the latter.

**The third stage** involves geological interpretation of geological space models selected by the profiles, and tie-in of these models. Taking into account the data of rapid interpretation, as well as qualitative interpretation, a 3-D physico-geological model of the area under investigation is developed. This results in final geological documents characterized by a greater completeness of mapping geological objects, mineral controls and mineral deposits, including deep-seated ones.

The geological interpretation of the complexes and local bodies of the selected (final) petrophysical model does not usually present any difficulties, since in the implementation of interactive selection system nearly all the bodies of the model acquire some specific geological content. The geological nature of new sources, introduced into the model during the selection and reflected neither in the initial geological section, nor in the initial physico-geological model, is determined according to the similarity of their physical properties, dimensions, mode of occurrence with respect to the known objects. The age of the introduced bodies is determined according to their interrelation with host rocks.

Such a method of an integrated interactive simulation of fields observed under rugged terrain relief, where geological objects can have an arbitrary direction of polarization (magnetization) vector has not yet been developed in the geophysical practice. The advantages of this technique as compared to the level achieved by the present time, are as follows: (a) more complete consideration of real topographic and geological conditions of the region under investigation; (b) determination of up to six quantitative parameters of anomalous bodies with the admissible error of 10-20% for each field; (c) development of integrated 3-D physico-geological model of the region under investigation; (d) drawing up final geological documents marked by a greater completeness, profoundness and reliability of the geological structure mapping.

## 8.5 Examples of modeling

The developed system allows to solve a wide spectrum of geological problems in mountainous, submountainous and plain regions: prospecting of mineral deposits, prediction of seismic hazards and other geological phenomena [114]. An essential similarity of ore and oil geophysics was shown in [140]. Methods that were primarily developed for ore geophysics, are successfully applicable to the search for oil and gas deposits of new types in Azerbaijan. These deposits are associated with buried highs of magmatic rocks, overthrusts and underthrusts.

For a long time, a dominating point of view in Azerbaijan

consisted in that in Kura depression separating meganticlinoriums of the Greater and the Lesser Caucasus, thick sedimentary deposits occurred on the crystalline Pre-Alpine basement, and these structures were divided by subvertical deep faults. On the buried uplift of the basement, presumed earlier on the basis of high densities and velocities of elastic waves, Saatly super-deep borehole SD-1 has been designed in 1965. The area for drilling was selected using the analysis of seismic profiles 9, 16 and 18 (Fig.8.6). However, the analysis of magnetic properties of rocks and magnetic survey results allowed to conclude that the basement was not magnetized, and a large part of the geological section for Middle Kura depression was occupied by the Mesozoic magmatic associations of basic and intermediate composition with high magnetization [135]. The above mentioned (chiefly, Jurassic) associations are widely distributed in north-eastern part of the Lesser Caucasus. The associations have a deep-seated gently sloping underthrust under sand-shale thick series of the Greater Caucasus Jurassic.

The validity of the interpretation was fully confirmed by the results of the SD-1 drilling (Fig.8.7).

The borehole exposed the Mesozoic volcanogenic rocks at the depth of 3.6 km and did not come from there to its bottom at 8.2 km [113].

The map of deep structure of Azerbaijan with its adjacent regions [114] is an example of the final document mentioned in the end of Section 8.4 (Fig.8.8).

This map has been plotted on the basis of the results of physico-geological modeling along several profiles (see Fig.8.6). The conducted investigation allowed to obtain new data about geotectonic blocks, fractures, folded structures and geological associations in the investigated region. Depth and composition of the intrusive and effusive associations, as well as the depth of Moho and basement discontinuities are presented (see Fig.8.8).

3-D geological model developed for this complicated region allows to solve various geological problems including those of searching for economic minerals. Comparing Fig.8.8 with Fig.1.7 (a map where the distribution of principal deposits of various types is shown), we can indicate the relationship of their localization and

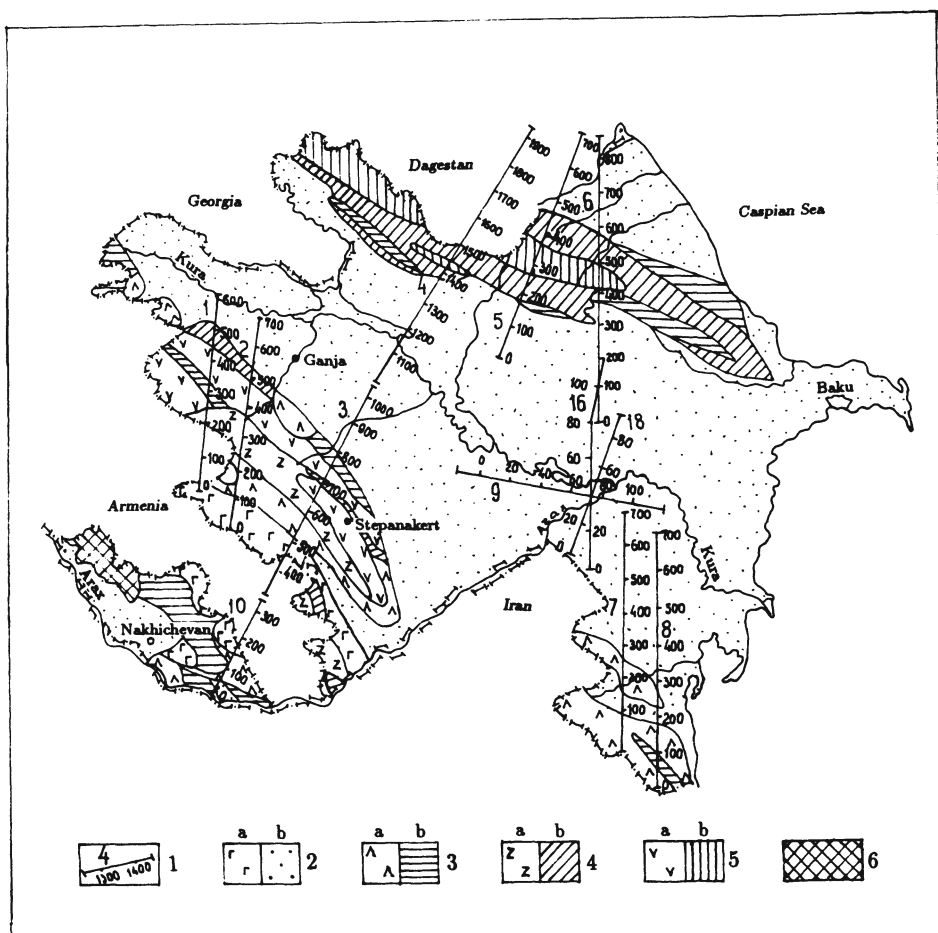


Fig.8.6. Scheme of disposition of major profiles used for physico-geological modeling

(1) profiles and piquets; (2)  $Pg_3-Q$ : (a) orogenic magmatic associations and (b) background sedimentary deposits; (3)  $K_2-Pg_2$ : (a) Pre-orogenic magmatic associations and (b) background sedimentary deposits; (4)  $J_3-K_1$ : (a) Late-geosynclinal magmatic associations and (b) background sedimentary deposits; (5)  $J_1-J_2$ : (a) Early-geosynclinal magmatic associations and (b) background sedimentary deposits; (6)  $Pz$ : Sub-platform deposits

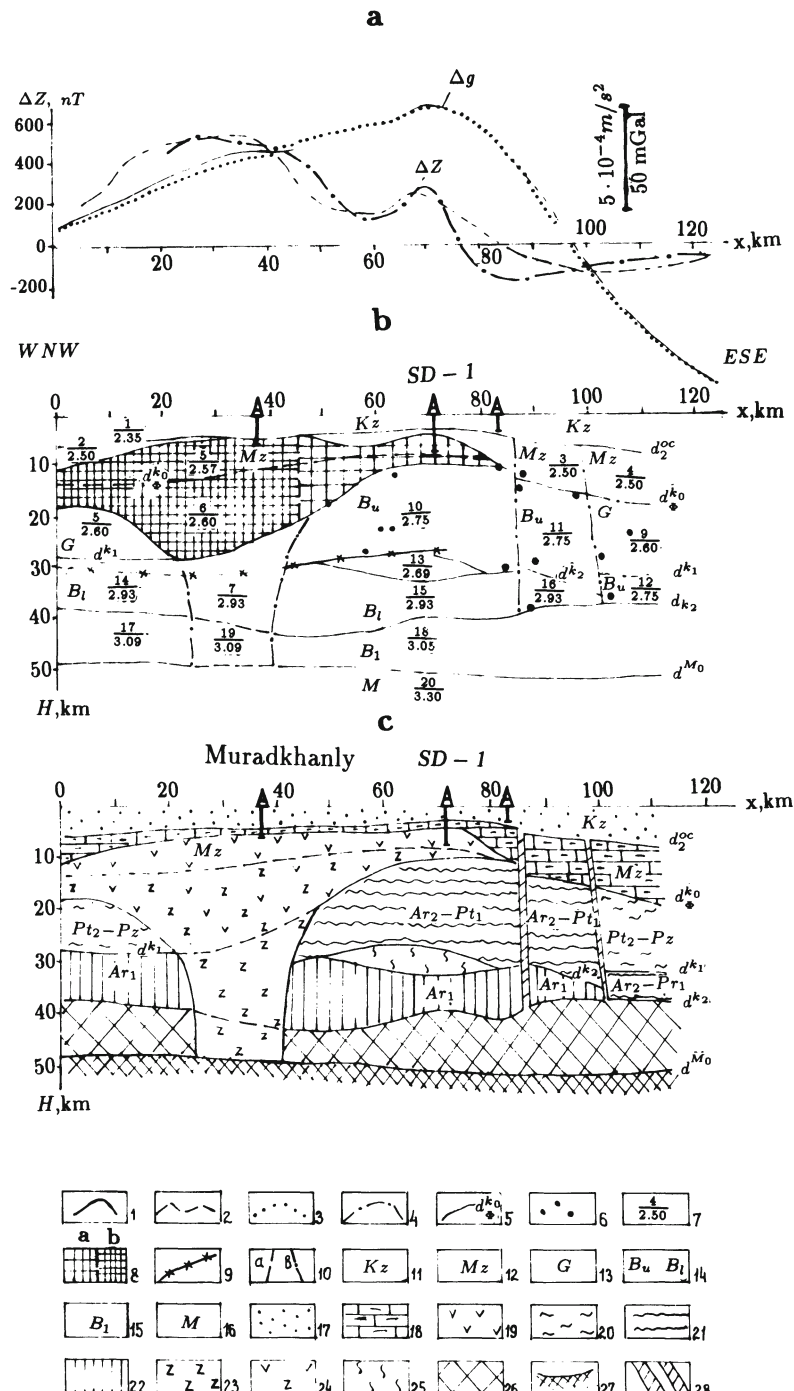


Fig.8.7. Deep geological section of the Earth's crust in SD-1 area (for 9 profile in Fig.8.6)

*Caption to Fig.8.7*

a – gravitational and magnetic fields, observed and computed by the model  
 b; b – petrophysical model; c – geological model

Observed curves: (1)  $\Delta g$ , (2)  $\Delta Z$ ; curves computed by the model b: (3)  $\Delta g$ , (4)  $\Delta Z$ ; (5) boundaries of the velocity and the density inhomogeneities and their indices; (6) diffraction points; (7) body's number (numerator) and density value,  $g/cm^3$  (denominator); (8) geological bodies with the magnetization of 2,500  $mA/m$  (a) and 2,800  $mA/m$  (b); (9) projection of Curie surface on the basis of geothermal data; (10) subvertical boundaries of bodies on the basis of the selection of magnetic (a) and gravitational (b) fields; (11) Cenozoic; (12) Mesozoic; (13) G complex (velocity analogue of the "granitic" layer); (14)  $B_u$  and  $B_l$  subcomplexes of B complex (complex B is the "basaltic" layer velocity analogue); (15)  $B_1$  complex (supposed basite and eclogite composition); (16) M complex (supposed peridotite composition); (17) Cenozoic complex: mainly, terrigenous deposits; Mesozoic complex: (18) terrigenous-carbonaceous formations, (19) mainly effusive associations of basic and intermediate composition; (20) mainly Baikalian complex ( $Pt_2-Pz$ ): metamorphic (primarily terrigenous) associations (the presence of younger deposits is possible in the upper part); (21) Pre-Baikalian complex ( $Ar_2-Ar_1$ ): mainly gneisses and marbles; (22) ancient complex ( $Ar_1$ ): gneisses and amphibolites; (23) root of the basic magmatism; (24) undivided effusive-intrusive complex; (25) rock complex of a low density (serpentization zone ?); (26) complex of associations corresponding to crust-to-mantle transition; (27) upper mantle roof position; (28) large fault zones

determine a prognosis strategy. It would be sufficient to note that the use of the above approach promoted the discovery of a new polymetallic province at the Greater Caucasus (and first of all, of a group of deposits in the Guton magnetic anomaly area [114,135]).

Investigations of similar kind were conducted with our participation on profiles across Caspian sea from Azerbaijan to Turkmenistan. These investigations were directed to the estimation of oil-and-gas potential of South Caspian depression at large depths. The main peculiarity of this work was the use of large amount of seismic information including data of seismostratigraphy. This allowed to develop informative integrated models of media on the base of cooperative interpretation of seismic, gravimetric and magnetic prospecting, as well as magnetotelluric sounding (unpublished report of Southern Branch of VNIIGeofizika, Baku, 1990).

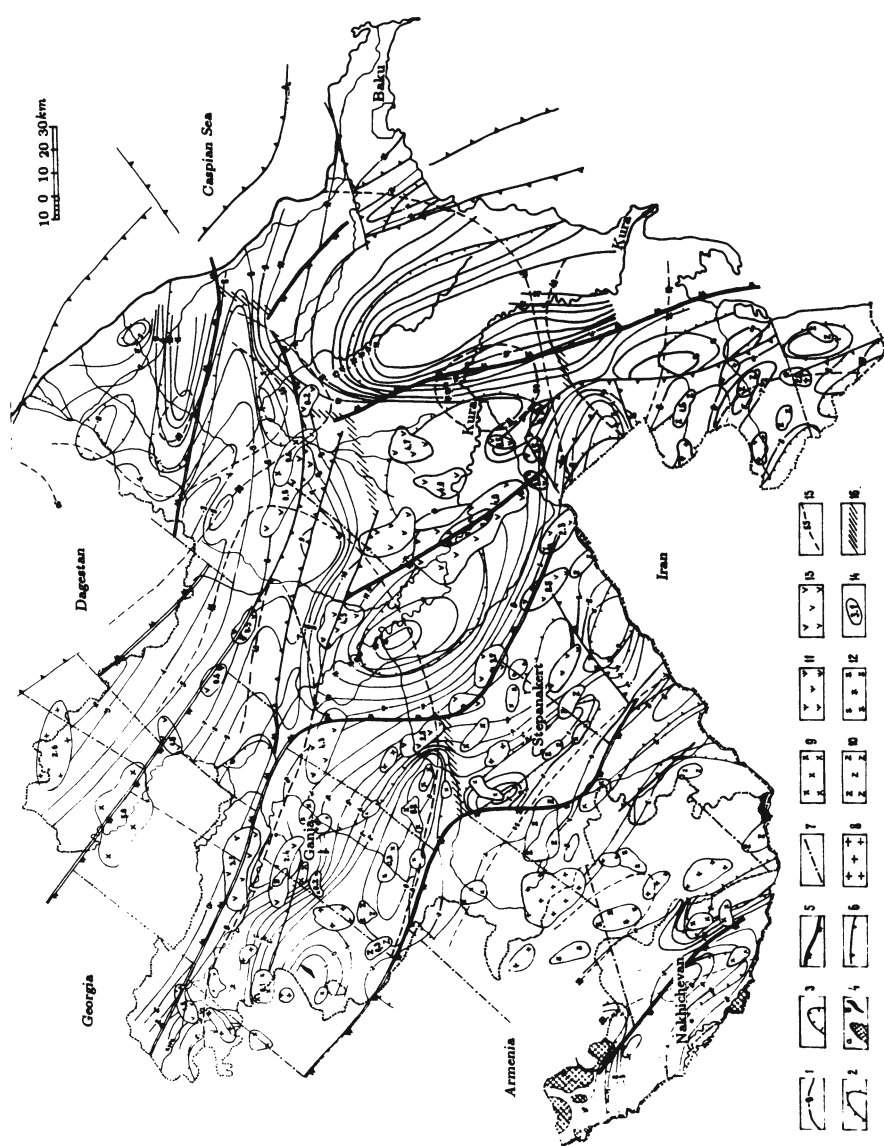


Fig. 8.8. Map of deep structure of Azerbaijan with its adjacent regions according to gravity and magnetic data

*Caption to Fig.8.8.*

Characteristic of the Pre-Alpine basement: (1) isodepths of roof from sea level, km, (2) uplifts, (3) depressions, (4) exposures of Hercynian (a) and Baikalian (b) complexes; disjunctives: (5) deep faults (boundaries of geostructure zones), (6) less deep faults (boundaries of tectonic blocks), (7) fragments of through transverse dislocations; magmatic objects: (8) acidic, (9) intermediate, (10) basic, (11) ultrabasic, (12) alkaline; (13) intermediate-basic effusives; (14) contour and average depth of upper edge occurrence of a magnetized body (km); (15) earth crust isopachs (km); (16) junction districts of geostructures and blocks, having no direct reflection in the gravitational and magnetic fields

# **Chapter 9**

## **REVISION OF A MODEL OF A MEDIUM; REPRESENTATION AND EVALUATION OF INTERPRETATION RESULTS**

### **9.1 Developing a final model**

In Sections 8.4 and 8.5 it was shown how to revise geological notions about the structure of the investigated media with the use of physico-geological modeling. The corresponding integrated interpretation allows to derive substantially new geological information. As an example, consider the detailed prospecting in the Katekh pyrite-polymetallic deposit (southern slope of the Greater Caucasus) and regional investigation in the same region.

The deposit is represented by two subparallel stratified deposits of sheet-like type. It was investigated by mining and drilling up to depth of 500 m. However, the geologists note that due to extremely complicated tectonics those operations failed to delineate completely ore deposits.

To reflect essential features of the deposit a profile was selected which passed through its central portion (Fig.9.1A). As follows from the figure, the plots of  $\Delta Z$  and  $\Delta U_{SP}$  bear scarce information. It can be attributed to the peculiarities of mineralogical composition of ores in the Katekh deposit. Absence of magnetic pyrrhotite causes their almost non-magnetic nature, while a fairly large lead content impedes the normal course of oxidation-reduction reactions and the formation of the intense *SP* anomalies. From this it follows

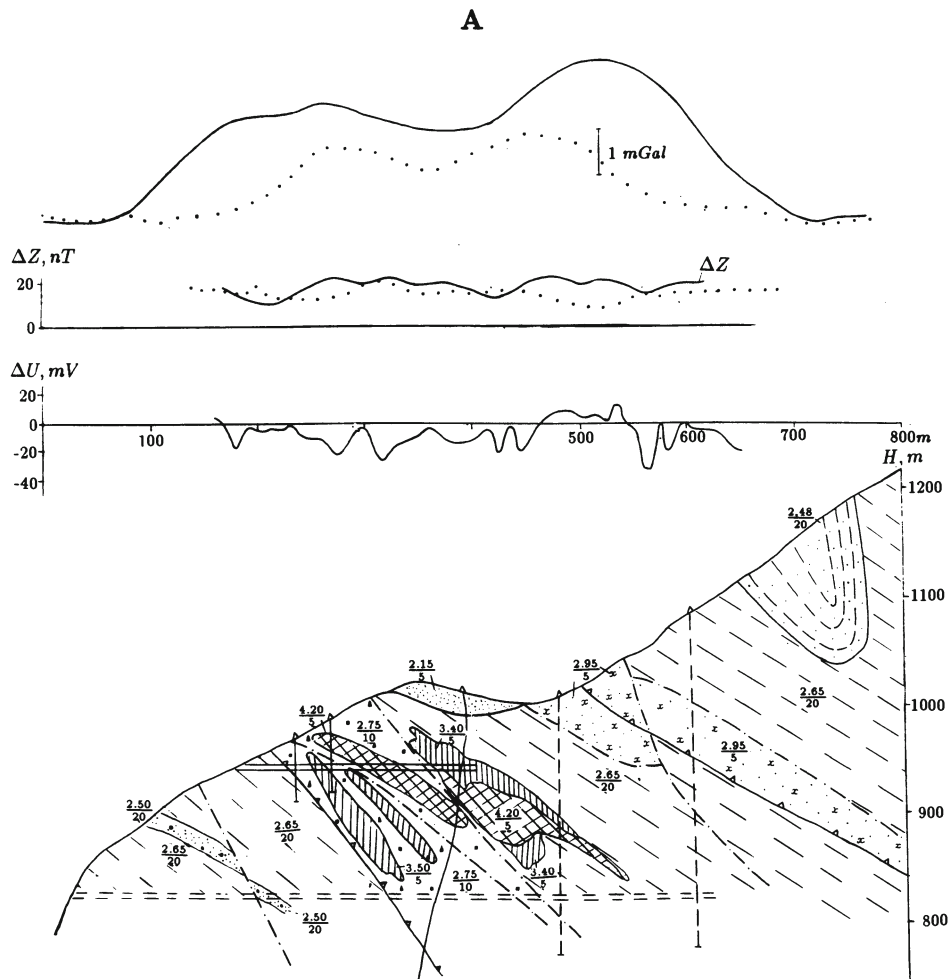


Fig. 9.1A. Computation of a geophysical effect due to a known geological section in the Katekh pyrite-polymetallic deposit

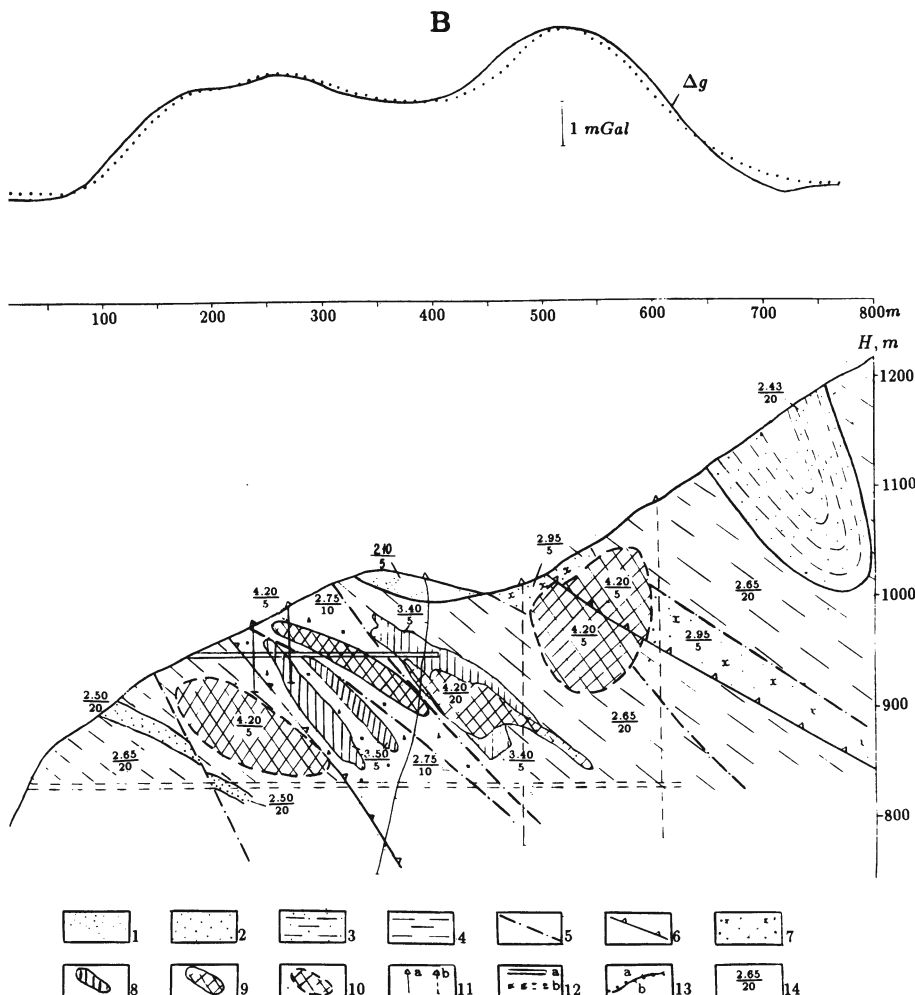


Fig.9.1B. Selection of the section model by geophysical data

(1) loose Quaternary deposits; (2-4) Middle Jurassic deposits: (2) massive fine- and meso-grained sandstones, (3) interstratification of clay shales and sandstones, (4) rhythmical alternation of aleurolites and clay shales; (5) disjunctive dislocations; (6) upthrust-overthrusts; (7-9) pyrite-polymetallic ores: (7) spotty, (8) stockwork-veiny, (9) massive; (10) contour of orebodies introduced during selection; (11) prospecting boreholes: (a) on the profile, (b) projected on the profile; (12) adits: (a) in the plane of the geological section, (b) projected onto the plane of the geological section; (13) curves of gravitational and magnetic fields: (a) observed, (b) selected; (14) physical properties: numerator=density,  $g/cm^3$ , denominator=magnetization,  $mA/m$  (1-9 and 11-12 according to mining and drilling data)

that a basic geophysical information should be derived from the curve  $\Delta g$ . Gravitational field simulation was accomplished using several sequential iterations. It allowed to obtain the following results (Fig.9.1B). An orebody of massive composition was singled out in the south-western portion of the section, which had not been reflected in the geological observations. It also enabled us to define more precisely the location of a massive ore object in the central zone anticipated from previous geophysical observations [7]. The conclusions concerning the presence of a hidden ore object in the south-western portion of the profile are consistent with the results of independent observations obtained by underground geothermal investigations and ground geochemical survey. A temperature anomaly of 0.5 to  $0.8^{\circ}\text{C}$  was recorded in adit 8 during geothermal investigations in the piquets 250–300; the earth's surface zone containing a great amount of lead and zinc was revealed in the area of stakes 150–200.

When simulating gravitational and magnetic fields along the traverse across the strike of the Eastern Caucasus (Fig.9.2), we managed to refine considerably deep geological structure of the region. It is most essential that we had to introduce deep gently sloping magnetized bodies of sheet-like type. This corroborated earlier considerations about the extension of the Mesozoic magmatic associations of the Lesser Caucasus far to the north under the thick Cenozoic sedimentary cover of the Middle Kura depression, about the Greater Caucasian underthrust of the Lesser Caucasian structures [130,135]. These underthrusts are not only of theoretical interest in the deep structure of the Caucasus, which is a standard region when evaluating various tectonic conceptions. They are also of practical interest for oil-and-gas deposits prospecting in overlap-overthrusting associations [253].

## **9.2 Graphic representation of the interpretation results and forming geological conclusions; Physical-geological models**

Once the quantitative parameters of anomalous objects have been determined, the obtained data are plotted on a chart of the inter-

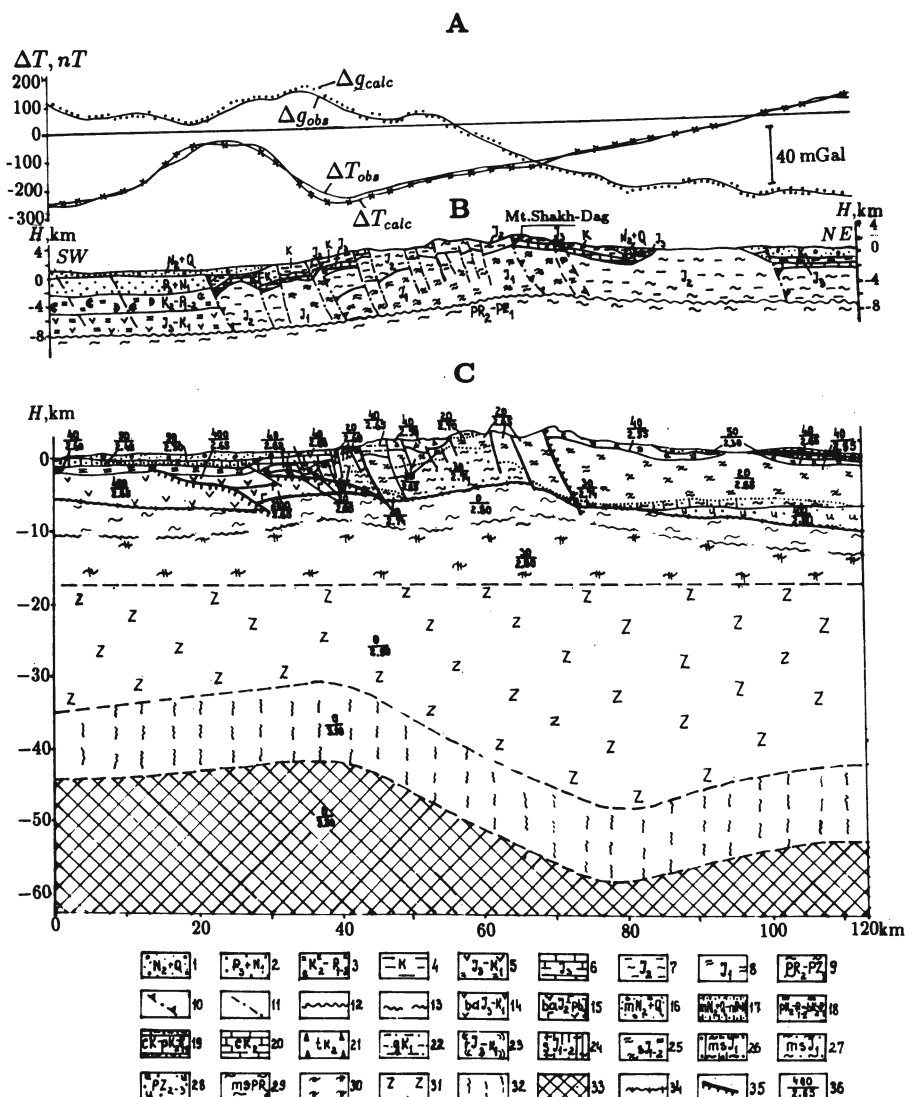


Fig. 9.2. Three-dimensional modeling results obtained using GSFC program along the profile 5 (location of the profile is shown in Fig. 8.6; captions according to [114])

### Caption to Fig.9.2

(A) Gravimetric and magnetic observation results and fields selection on the basis of the model C

(B) Initial geological section

(C) Final physico-geological model

(1) upper molasse; (2) lower molasse; (3) terrigenous and carbonaceous flysch, reef limestones; (4) aleurolites, clay-calcareous shales, marls and sandstones with tuffaceous admixture; (5) volcaniclastic deposits with limestone interlayers; (6) pelitomorphic limestones, clay shales and sandstones; (7) interstratification of the clay shale and sandstones; (8) micaceous coarse-grained sandstones and clay shales; (9) metamorphic schists; (10) deep faults; (11) faults, upthrusts, overlaps; (12) upper boundary of the Pre-Alpine basement; (13) upper boundary of the Pre-Baikalian basement; magmatic associations: (14) basalt-andesite-dacitic, (15) non-segmented basalt-andesite and basalt-andesite-plagioplaritic; (16–23) sedimentary deposits: (16) upper molassic, (17) non-segmented upper-lower-molassic, (18) non-segmented terrigenous-carbonaceous, in some places flyschoid and aleurite-clayey, (19) non-segmented carbonaceous flysch and aleurite-clayey, (20) carbonaceous flysch, (21) carbonaceous-terrigenous flysch, (22) sandy-clayey, flyschoid, (23) terrigenous-carbonaceous flysch, reef limestones; sandy-shale deposits: (24)  $\sigma = 2.69 \div 2.70 \text{ g/cm}^3$ , (25)  $\sigma = 2.65 \text{ g/cm}^3$ ; metamorphic clay shales and micaceous sandstones: (26)  $\sigma = 2.80 \text{ g/cm}^3$ , (27)  $\sigma = 2.74 \text{ g/cm}^3$ ; (28)–(31) Pre-Mesozoic complexes: (28) Upper Paleozoic volcanogeno-sedimentary, (29) mainly alkal-an: metamorphic schists, (30) Pre-Baikalian: gneisses, marbles, amphibolites, (31) basites; (32) associations of a crust-to-mantle transient, presumably with a basite-eclogitic composition; (33) upper mantle's peridotites; (34) roof of the Baikalian complex, (35) overthrusts and underthrusts; (36) physical properties: numerator=magnetization, mA/m, denominator=density,  $\text{g/cm}^3$

pretation results composed after regioning and delineation. The object's contours and axes obtained on delineation, are substituted by more accurate calculated ones. Information on the magnetization value and direction, as well as other physical parameters of hidden objects, allows to refine substantially their geological nature. It is reflected in the interpretation chart as a corresponding change in the legend.

The results of quantitative interpretation are also displayed in the form of sections (3-D models) reflecting a set of available geological and geophysical evidences on the medium. It is expedient to correlate the series of sections into extended geological-geophysical profiles, which makes it possible to study the lateral change in the

section structure and the mode of conjugation of heterogeneous blocks.

The section is often to be drawn in the plane of the profile, non-perpendicular to the anomalous body strike. It is primarily the case when the profile intersects several anomalies due to bodies of different strikes. In this case the parameters of the body intersected by the profile plane are calculated. Horizontal coordinates are multiplied by  $\sec \psi_j$ , where  $\psi_j$  is the angle between the profile planes and the normal sections of the  $j$ -th body, and vertical coordinates remain unchanged. The validity of composite sections has to be verified by the direct problem solution.

The geophysical interpretation map, where the singled out field regions are substituted by geological (tectonic) blocks and the linear field elements by geological ones (most often by faults) is displayed in the form of tectono-magmatic chart. The contours and axes of geological bodies (including hidden ones) revised on the basis of quantitative calculation results are plotted in this chart along with such parameters as depth (mode of occurrence), physical properties, and composition.

The tectono-magmatic chart of the area under study, composed using the integrated interpretation materials, presents the revised model of the medium and is the main document illustrating the results of the interpretation (see Fig.8.8).

Using near-surface geophysical investigations [297], one may study not only geological, but also artificial (anthropological) objects: piping, various communications and other hidden artificial targets. Detailed near-surface investigations are also used for prospecting archaeological objects (see section 9.4). Nevertheless, the procedure of developing and presenting a model remains the same.

The geological conclusion drawn on the basis of the interpretation results, crowns the interpretation process and comes, in general, in a wordy description of the revised model of the medium illustrating separate issues by corresponding graphical materials of previous stages.

When preparing the conclusions, the major focus should be on comparing the revised model of the medium with the initial one. The contribution of the investigation in question into the study

of geological structure of the region should be also evaluated, as well as its prospects as to economic minerals and other peculiarities essential for the solution of actual problems.

As a rule, a revised model of the medium is developed on the basis of a set of data. Not always there is a possibility (and necessity) to evaluate the specific contribution of each method of this set. In contrast to the design stage, where the informativity of geophysical methods included into the prospecting set was calculated [41], at the stage of preparing the conclusions, the investigator should evaluate their real informativity and compare it with the accepted one. This makes it possible to come to the conclusions about the efficiency of the set employed and to elaborate recommendations as to the methods of geophysical investigation of this or more detailed scale under similar conditions.

When compiling geological conclusions, it is necessary to do once again the following:

- to determine the completeness of the application of prior geological-geophysical information;
- to evaluate the quality of the initial model of the medium and the correctness the indicator space selected;
- to estimate the correctness and completeness of applying the object's indicators and the rules of regioning and delineation;
- to verify the validity of the methods of quantitative interpretation and accuracy of calculated parameters of anomalous objects;
- to control the quality of graphic documents, primarily those having geological content.

If any operations have some drawbacks, they should be repeated. It may call for a complete (over the whole area of work) or partial repetition of the subsequent steps. Interpretation is considered completed, if it is impossible to derive any more information necessary for solving the target problem. A geological conclusion should contain information on the completeness of the solution of the problem stated, and recommendations as to the direction and the areas for detailed geological-geophysical investigations, drilling and mining.

The most easy-to-grasp results of the interpretation are physico-geological models (*PGM*), which are displayed both in graphical and tabulated form. Graphical *PGM* of a concrete section is shown in

Fig. 9.2C. It is *PGM* that enables one to solve the double problem of interpretation in the most reliable way:

- (1) to enhance the informativity and reliability of geophysical data interpretation;
- (2) to substantiate the selection of a set for further geophysical investigations and their strategy.

Two types of pyrite deposits, namely Filizchai and Lesser-Caucasian, may serve as an example of the *PGM* development under mountainous conditions. They are typical representatives of two large groups of deposits:

- (1) pyrite-polymetallic deposits concentrated in pyrite-bearing provinces with the predominance of carbonaceous-terrigenous sediments;
- (2) copper-pyrite deposits occurring in pyrite-bearing provinces with the predominance of volcanogenic rocks [37].

Characteristic pyrite-polymetallic deposits of the Filizchai type are [102,286] Sullivan (British Columbia, Canada), Coeur d'Alène (Idaho, USA), Mount-Isa (Australia), Rammelsberg (Germany), Ozernoye and Kholodninskoye (Baikal region, Russia), Filizchai and other deposits (Katsdag, Katekh) on the southern slope of the Greater Caucasus. The latter are situated in a severely rugged relief and occur in sandy-shale rock masses of the Jurassic. The *PGM* for this type of deposits can be represented in the form of steeply dipping massive sulfide deposits of sheet-like type, which differ from the host medium by a number of contrasting properties such as excess density ( $1.3 \div 1.8 \text{ g/cm}^3$ ), higher (by a factor of  $10^2$  to  $10^3$ ) conductivity, thermal conductivity (2 to 3-fold) and polarization (up to 10-fold) and in some cases magnetization (10 to 50-fold) [199].

The development of numerous disjunctive dislocations impeding geophysical data interpretation is typical of the deposits under discussion.

As reported in [286], the following provinces are classified as the Phanerozoic pyrite provinces of the Lesser-Caucasian type: the Caledonian (Tuva, Salair, Western Sayan), the Hercynian (Central Kazakhstan, Mountainous Altai), the Cimmerian (Canadian Cordillera, Sierra-Nevada, Lesser Caucasus) and the Alpine (East-

**Table 9.1. Geophysical effects for different types of PGM**

Type	<i>h</i> value, <i>m</i>	Anomaly				
		gravity, <i>mGal</i>	magnetic, <i>nT</i>	<i>SP</i> , <i>mV</i>	VLF, %	temperature, <i>°C</i>
Filizchai	20	1.0 ÷ 2.2	150 ÷ 200	-(120 ÷ 300)	25 ÷ 50	0.7 ÷ 2.0
	60	0.6 ÷ 1.2	50 ÷ 70	-(60 ÷ 100)	10 ÷ 15	0.2 ÷ 0.7
	100	0.4 ÷ 0.6	25 ÷ 30	-(20 ÷ 40)	2 ÷ 5	0.05 ÷ 0.10
Lesser-Caucasian	20	0.3 ÷ 0.5	-(70 ÷ 100)	-(20 ÷ 50)	15 ÷ 30	0.5 ÷ 1.2
	60	0.08 ÷ 0.15	-(20 ÷ 30)	-(15 ÷ 30)	5 ÷ 10	0.1 ÷ 0.3
	100	0.05 ÷ 0.08	-(5 ÷ 10)	-(5 ÷ 10)	1 ÷ 3	0.03 ÷ 0.05

ern Serbia, Bulgarian Middle Upland, Anatolian Pont, Lesser Caucasus, Northern Iran, Japan, Taiwan, Philippines) geological structures. The pyrite deposits of this type, which are also termed South-Uralian or Kuroko, are investigated in detail in the Lesser Caucasus.

Copper-pyrite deposits of the Lesser-Caucasian type in the Somkhit-Karabakh zone (Alaverdy, Kedabek, Kyzylbulakh) are located in middle-height relief and localized in volcanogenic and volcanogeno-sedimentary associations of the Jurassian and Cretaceous. Physical-geological model of the Lesser-Caucasian type deposits is complicated by the fast variability of rocks and ores and distinct tectonics. A PGM can be schematically presented as a set of small flat-dipping bodies of lens-like form, which differ from the host medium by certain contrasting properties. They are excess density (from 0.4 to  $0.9 \text{ g/cm}^3$ ), higher conductivity (by a factor of  $5 \cdot 10$  to  $5 \cdot 10^2$ ), polarizability (several-fold) and thermal conductivity (1.5 to 2.5-fold) and lower magnetization (by a factor of  $5 \cdot 10$  to  $2 \cdot 10^2$ ).

The fields expected by the typical PGM of the Filizchai (Fig.9.3) and Lesser-Caucasian (Fig.9.4) types deposits were computed using GSFC program for different depths of occurrence of the upper orebody edge *h* (Table 9.1).

For *SP*, VLF and thermal prospecting methods, the determinations of expected effects are accomplished with due account of the results of physical and mathematical modeling, and also of the results of field investigations. IP anomalies at the depth of 20 m amount to 7 ÷ 15% for the Filizchai type and 4 ÷ 12% for PGM of the Lesser-Caucasian type.

The developed physico-geological models substantiate the inter-

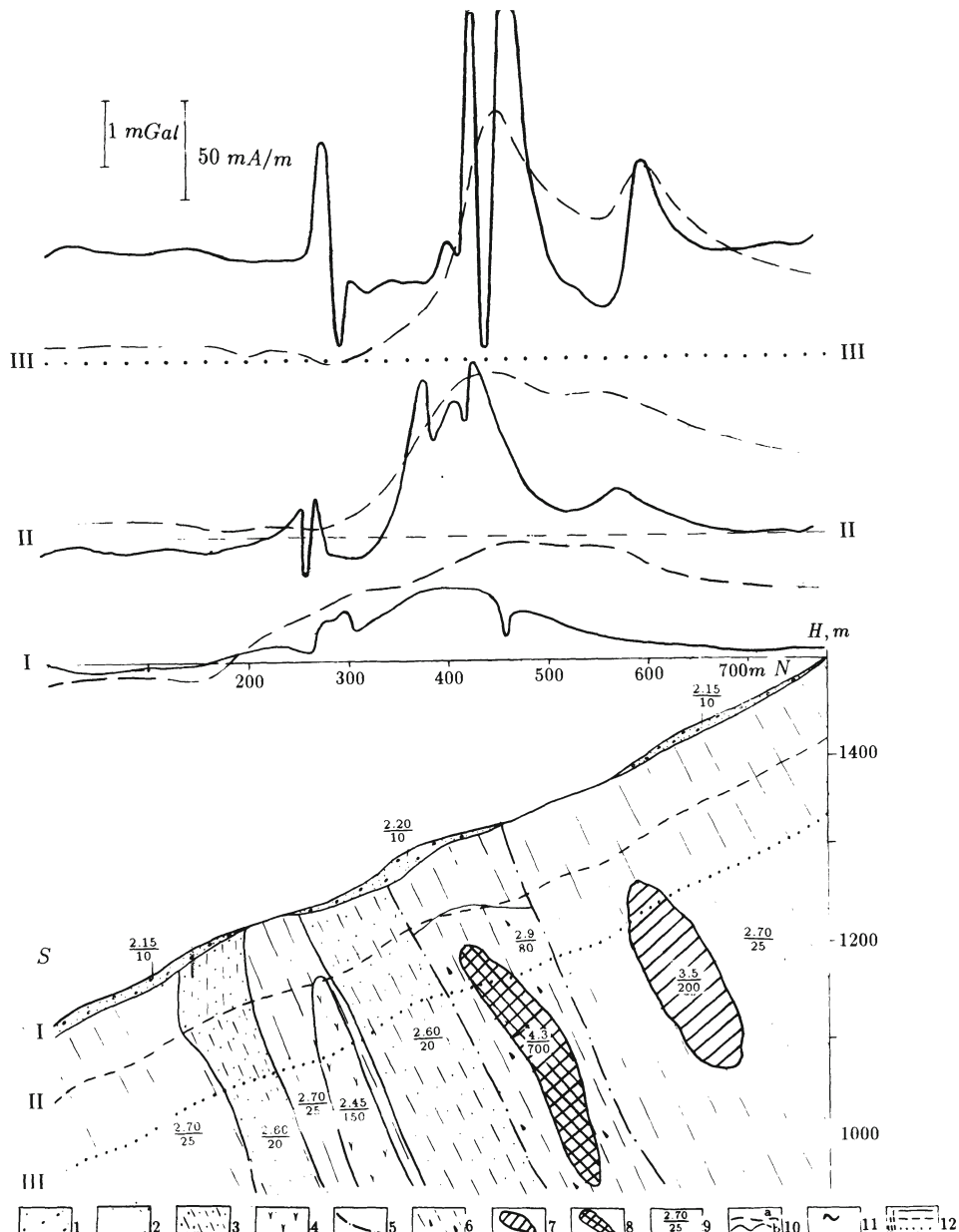


**Fig.9.3. Physical-geological model of the pyrite-polymetallic deposit of Filizchai type**

(1) loose deposits; (2) clay shales; (3) clay shales with sandstone bands; (4) liparite-dacites; (5) disjunctive dislocations; (6) ore zone; pyrite-polymetallic ores: (7) impregnated-veined, (8) massive; (9) physical properties: numerator=density,  $g/cm^3$ , denominator= magnetization,  $mA/m$ ; (10) computed values: (a)  $\Delta g$ , (b)  $\Delta T$ ; (11) boundary line for the anomaly plot overstepping the limits of the drawing; (12) levels of the erosional truncation: (I) – earth's surface, (II) and (III) depths of 80 m and 160 m from the earth's surface, respectively

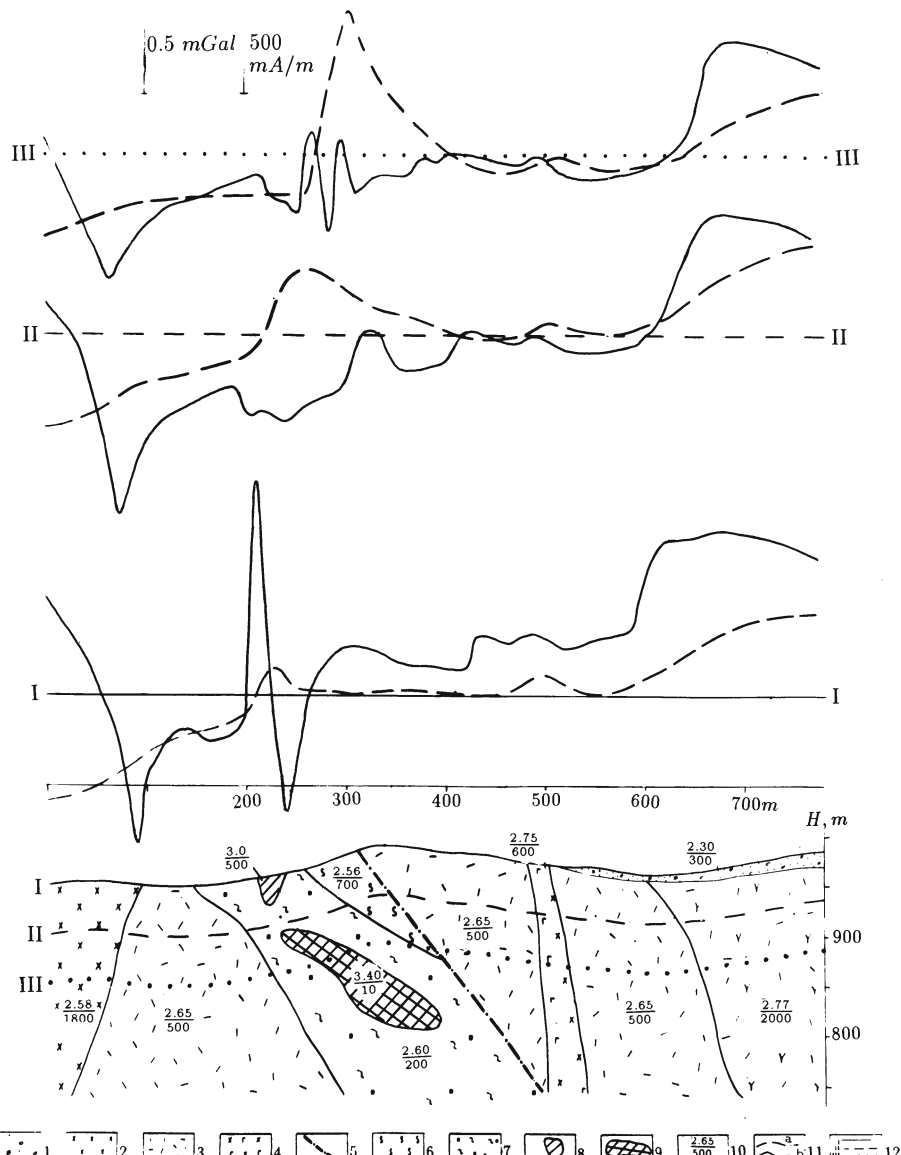


**Fig. 9.4. Physical-geological model of the copper-pyrite deposit of Lesser-Caucasian type**

(1) deluvial deposits; (2) andesitic porphyrites; (3) tuffs of liparite-dacites; (4) lavas of dacitic porphyrites; (5) dike of andesite-basalts; (6) disjunctive dislocations; (7) zone of brecciation and crush with weak traces of pyritization; (8) zone of brecciation, crush and boudinage, with lean ore; (9) oxidized orebody; (10) massive pyrite-chalcopyrite ore; (11) physical properties (numerator=density,  $g/cm^3$ , denominator=magnetization,  $mA/m$ ); (12) computed geophysical fields: (a)  $\Delta g$ , (b)  $\Delta T$ ; (13) levels of the erosional truncation: (I) earth's surface; (II) and (III) depths of 50 and 100 meters from the earth's surface, respectively

pretation criteria and optimal geophysical sets of prospecting and estimation work. For deposits of Filizchai type this set comprises gravimetric and magnetic prospecting and *SP* method. If ore objects differ only slightly by their magnetic properties from host sandy-shale deposits, it is expedient to include *VLF* technique into the set instead of magnetic prospecting. A set of gravimetric prospecting, magnetic prospecting and *VLF* method has proved to be efficient for deposits of the Lesser-Caucasian type. Near-surface thermal prospecting can be employed for both types of deposits [75].

Comparing two approaches to *PGM* presentation, it should be noted that graphical *PGM* models (primarily of quantitative type) are more easy-to-grasp. However, whereas the development of quantitative graphical *PGM* using computer-aided gravitational and magnetic field computations presents no technical problem, quantitative computation of the temperature and self-potential fields using the same *PGM*, as well as fields due to distant *VLF* transmitters, leads to many mathematical and computation difficulties. This is why the joint application of these two methods supplementing each other seems rather promising [75].

## **9.3 Interpretation examples for swamp and shoal waters**

Most of the developed information-statistical and deterministic interpreting procedures have been presented for mountainous ore-bearing regions. However, as noted in Chapters 1, 4 and 6, useful information can be also obtained in case of petroleum explorations. This subsection deals with characteristic examples of investigations in difficult to traverse petroleum-bearing areas and in rift zone.

### **9.3.1 Revealing and mapping oil traps of a new type in Middle Kura depression**

The investigation in a swamp area of Kura and Araks rivers merging, where Saatly super-deep borehole SD-1 was drilled, was described in Section 8.5 (see Fig.8.7).

Many deep wells have been drilled in this area. They confirm the findings of the Kura depression deep-seated structure and hidden highs of the Mesozoic magmatic rocks (Fig.9.5). Seismic and gravimetric prospecting methods revealed Mesozoic associations with high velocities of elastic waves and densities under the Cenozoic terrigenous cover. At the same time magnetic prospecting divided the Mesozoic associations into magmatic and carbonaceous according to their composition. As a result, oil-and-gas traps of a type unknown here earlier were revealed in the zones of carbonaceous rocks pinch-out near the highs of magmatic associations and in eroded roofs of these highs [146]. A respective scheme made on the basis of Metaxa's data [114,146] is shown in Fig.9.6. The depths of magmatic rocks occurrence determined using magnetic data were confirmed by subsequent drilling with the accuracy of 10÷20%.

### 9.3.2 Mapping of area within South-Caspian depression

Gravitational and magnetic fields were separated and divided into components, and inverse and direct problems were solved for the Middle and South Caspian marine region. In particular, in this region the following results were obtained: (1) approximate distribution of disjunctive dislocations at depth, (2) data about underthrust (from south to north) Alpine geosynclinal under Epi-Hercynian platform; (3) information about the possible presence of deep-seated Mesozoic magnetic magmatic associations (as for the studied section of Middle Kura depression [146]).

For quantitative integrated interpretation of geological and geo-physical materials, the program "Integration" was used (see Sub-section 8.3.3.). The effectiveness of this program was checked on well studied Bulla-Sea area by revealing anticlinal structure, mud volcano (Fig.9.7) and disjunctive dislocations (Fig.9.8). In these computations, as a rule, residual (local) anomalies  $\Delta g$ , results of the magnetic observations and data of the sea bottom bathymetry were used. Models of the above-mentioned objects were described by Bagdatlishvili on the basis of gravitational and magnetic fields interpretation over the Bulla-Sea and Bibi-Eibat-Sea areas. Limits of the gravitational and magnetic fields variations and depths of sea bottom corresponding to the presence of the desired classes

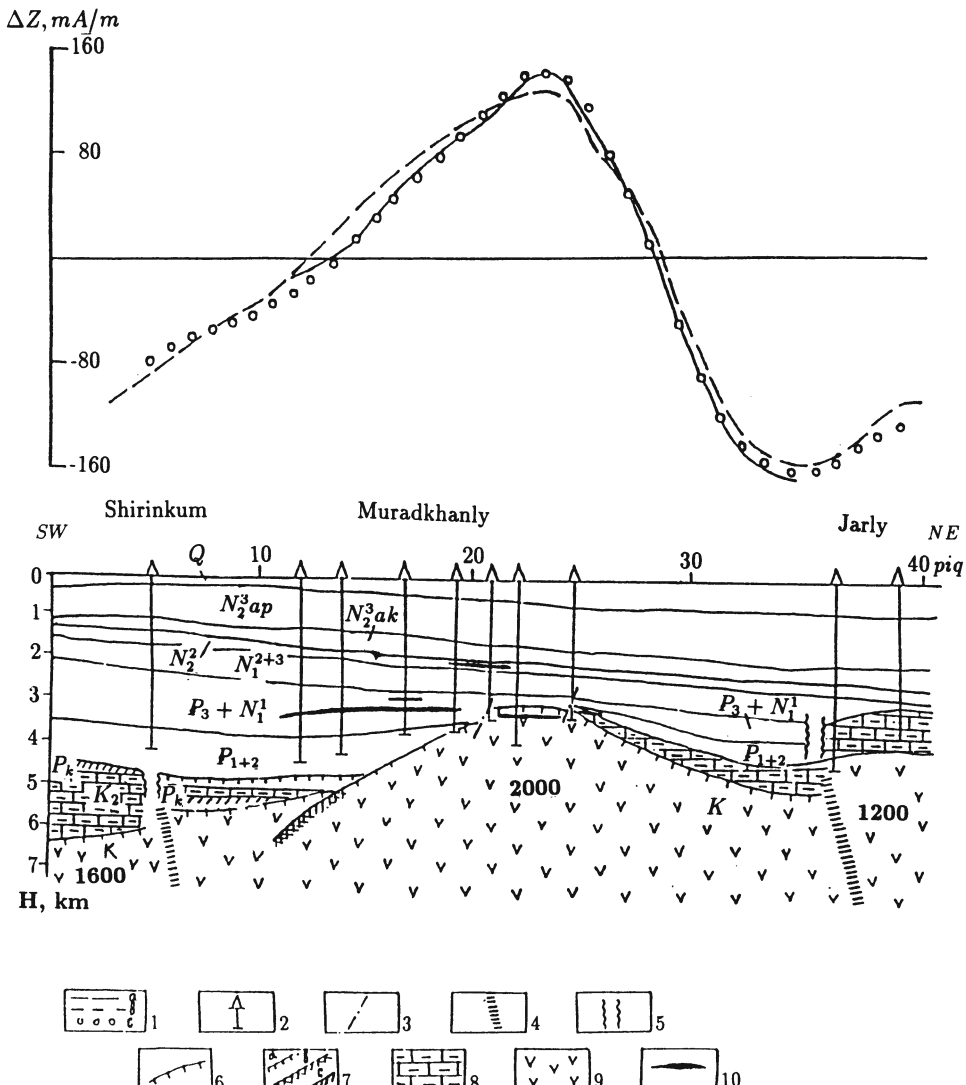
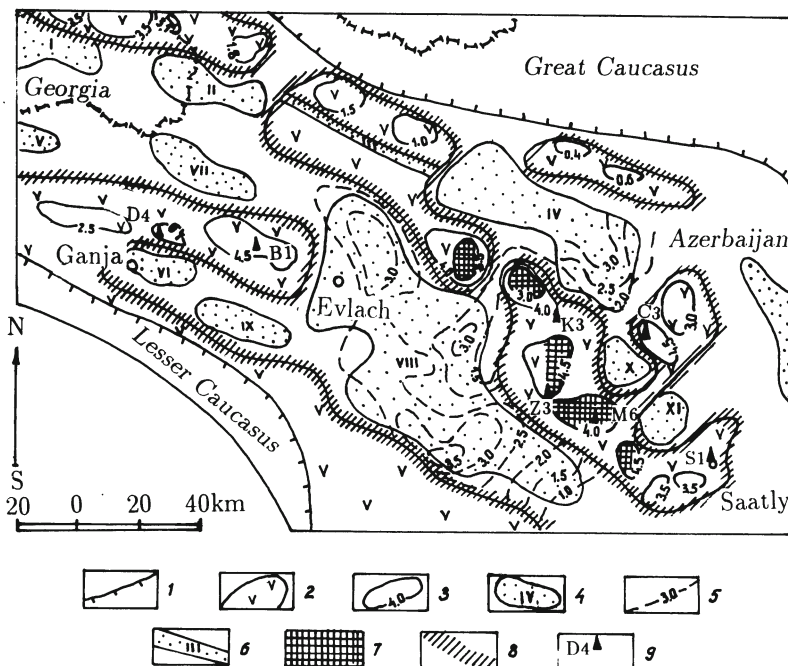


Fig. 9.5. Geological-geophysical section (Middle Kura depression) on a profile across Shirinkum – Muradkhanly – Jarly areas (according to [146], with supplement)

(1) curves  $\Delta Z_a$ : (a) and (b) observed, (c) calculated; (2) deep boreholes; faults revealed by data of: (3) drilling and seismic prospecting; (4) gravimetric and magnetic prospecting; (5) zones of complicated seismic records; (6) location of magmatic rocks roof using selection; (7) conventional seismic horizon: (a) Mz roof, (b) Mz volcanogenic rocks roof, (c) carbonaceous rocks roof; (8) carbonaceous-terrigenous rocks; (9) magnetized magmatic rocks (in the figure magnetization  $I$  is given in  $mA/m$ ); (10) oil-bearing layers



**Fig. 9.6. Schematic chart of oil-and-gas prognosis for Middle Kura depression using the interpretation of magnetic and other geophysical data**

(1) contour of mountain structures; (2) contour of Mesozoic magmatic associations of basic and intermediate composition according to magnetic prospecting data; (3) isodepths of magnetized (mainly, effusive) Mesozoic rocks according to magnetic prospecting data; (4) basins of normal sedimentary Meso-Cenozoic rocks according to a set of geological and geophysical data; (5) isopachs for Upper-Jurassic-Cretaceous complex of normal sedimentary deposits according to seismic and magnetic prospecting data; (6) part of North-Kura fault zone with most intensive movements (according to gravimetric and magnetic data); (7) most promising areas for revealing oil deposits in eroded magmatic rocks in arch structures; (8) most promising areas for revealing oil-and-gas deposits mainly in traps of non-structural type (on the pinch-out various rock associations); (9) wells of deep drilling

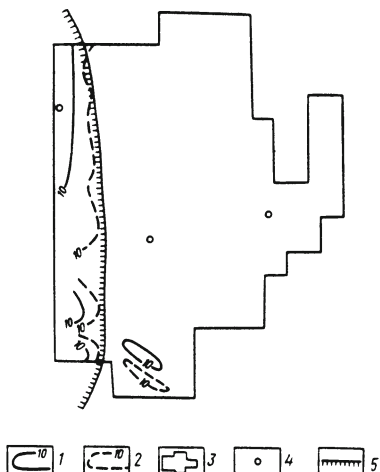


**Fig.9.7. Revealing of marine mud volcano using the parameters  $J_{compl}$  and  $\sum K$**

Isolines: (1)  $J_{compl}$ , (2)  $\sum K$ ; (3) contour of area; (4) reference point; (5) area of mud volcano breccia according to geological data

of objects, were revealed. The following values were selected for the anticlinal structure in Bulla-Sea area: variation of the residual gravity anomalies –  $(2.4 \div 0.1)$  mGal (decrease of the field), that of the observed magnetic field –  $(4 \div 1.6)$  nT (decrease of the field) and that of the depths of sea bottom –  $(20 \div 17)$  m (relative increase of the bottom level). For the mud volcano on this area the following values were selected: variation of the residual gravity anomalies –  $(0.1 \div 1.4)$  mGal (increase of the field), that of the observed magnetic field –  $(9 \div 4)$  nT (decrease of the field). For disjunctive dislocations increased values of horizontal gradients  $\Delta g$  and of the sea bottom depths and  $\Delta T$  variation from -4 to +4 nT were revealed. The limits of fields and sea depths variations on Bibi-Eibat-Sea area were selected on the same basis as those of Bulla-Sea area. They amount, respectively, to the following values: for the residual gravity anomalies –  $(0.7 \div 0.3)$  mGal, for the observed magnetic field –  $(3 \div 12)$  nT and for the depths of sea bottom –  $(14 \div 10)$  m.

Using the indices  $J_{compl}$  and  $\sum K$ , the central part of Bulla-Sea structure was singled out. The north-western block of the anticlinal raised by disjunctive dislocations, is the most marked. The disjunctive dislocations are characterized by elongated isolines

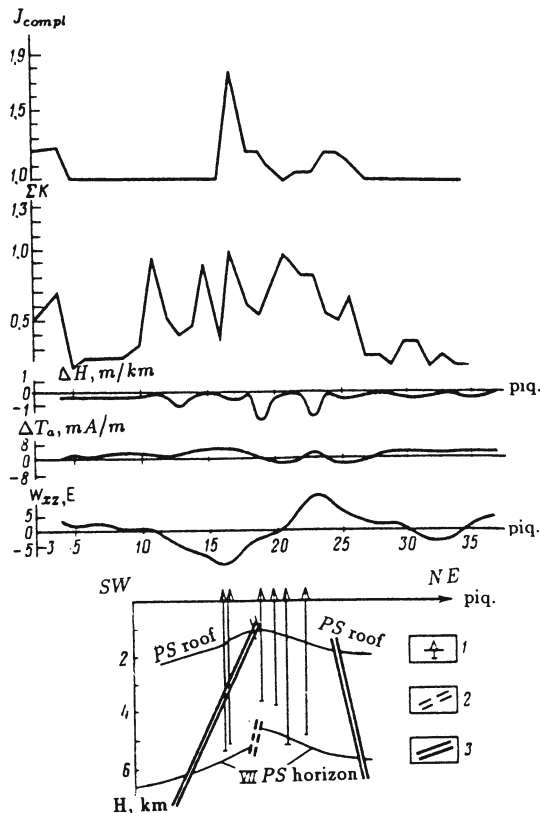


Fig.9.8. Revealing of disjunctive dislocations using the indices  $J_{compl}$  and  $\sum K$  along a profile in Bulla-Sea area

(1) wells of deep drilling; (2) disjunctive dislocations according to geological data, (3) disjunctive dislocations according to gravimetric prospecting data

Notes: 1.  $PS$  denotes the "Productive series". 2.  $W_{xz}$  is the second derivative of gravity potential (measured in Eötvös units)

of information indices. Both mentioned indices fix precisely the area of the mud volcanic breccia in the western part of the area. For revealing disjunctive dislocations (see Fig.9.8), the parameter  $J_{compl}$  is more effective. The plot of  $J_{compl}$  shows that the fault in the central part of the profile has subvertical dipping (this plot is of narrow localization). This conclusion coincides with geological data. The fault disposed in the north-eastern part is apparently, dipped to the north-east.

The structure of Bibi-Eibat-Sea is revealed by the reported indices otherwise than by preceding seismic data. Apparently, this

is connected with the fact that it is insufficiently studied by seismic prospecting. It should be noted that the zone of the complex seismic information, which can reflect the fault zone, divides the contours of isolines for these indices into two blocks. This testifies to a correlation between the seismic data and the data used for integrated interpretation.

### **9.3.3 Integrated interpretation of gravitational and magnetic fields over the Dead Sea rift in lake Kinneret area**

Lake Kinneret (Sea of Galilee) located in the northern part of the Jordan Rift Valley is one of a series of grabens within the Dead Sea rift. This shallow (till 40 m) lake is the main source of fresh water in Israel. Therefore, when studying the area, one can use only ecologically clean investigations of natural geophysical fields. Proceeding from the same considerations, kappametrical study of bottom sediments transportation was suggested and successfully fulfilled at the lake Kinneret within Jordan mouth area [152]. This river, as many others, crosses magnetite-containing basalts. Thus, the coarse fraction of the sediments of these rivers contains magnetic varieties. Their position on the lake bottom can be checked using magnetic susceptibility ( $\kappa$ ) measurements. The  $\kappa$  isolines map reflects the displacement of bottom sediments within a certain time interval (Fig.9.9). It follows from these data that young basalts outcropping around the lake Kinneret possess a high magnetization.

Gravitational and magnetic fields distributions over the area are highly complicated [25,89]. For instance, the results of the hydromagnetic survey in the eastern part of lake Kinneret show an inverse correlation between the magnetic field and depths of bottom (Fig.9.10). It is a direct proof of the presence of geological bodies with inverse magnetization in the studied area.

For integrated interpretation of gravitational and magnetic fields over lake Kinneret area, a special computation method applying GSFC program was used. The gravitational and magnetic fields were computed simultaneously along six parallel profiles with irregular distances between them. A similar scheme for 3-D modeling of gravitational and magnetic fields was applied to the Kyzylbulakh

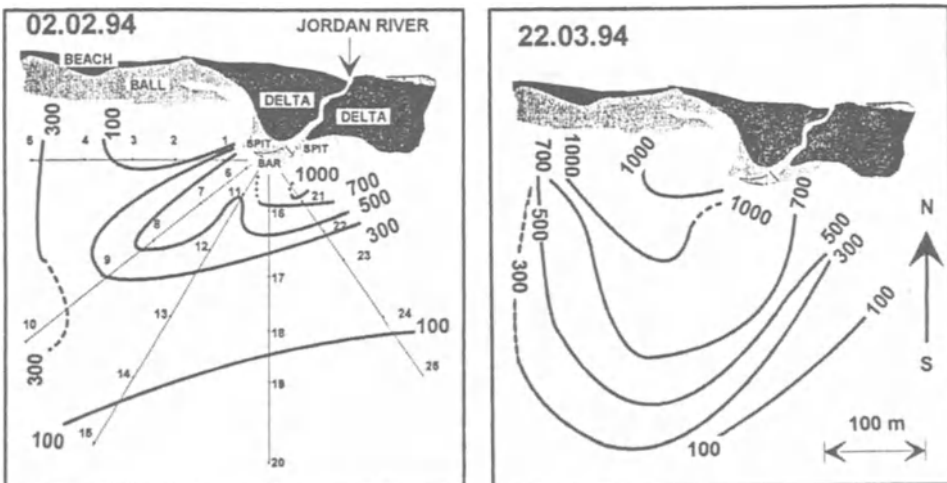


**Fig.9.9. Sediment dynamic study, Jordan river mouth**

Isolines of magnetic susceptibility of  $10^{-5}$  SI unit. 1, 2, ..., 25 are numbers of bottom probe points on radials profiles in lake Kinneret area.

gold-pyrite deposit (see Fig.5.6).

The map of the observed magnetic field over lake Kinneret area was constructed using a grid, the map of gravitational field  $\Delta g_B$  over the same area was calculated by Reznikov and Ben-Avraham [233]. The initial model (mainly, deep geological boundaries and densities) was developed on the basis of published data [25,26,88,89,etc.]. A part of one profile is shown in Fig.9.11.

The thick series of sedimentary deposits in the rift is caused by an intense negative gravity anomaly (see Fig.9.11A). After a few iterations, the quantitative parameters of the rift were refined (see Fig.9.11B). However, the magnetic field modeling was a more complicated problem. Magnetic anomaly is increasing from SW to NE (see Fig.9.11A), and at the same time the depth of deep boundaries is decreasing from SW to NE. Basalts, which are widely presented in this area can be a possible source of the magnetic anomaly [26]. The Quaternary basalts (with the density of  $2.75 \text{ g/cm}^3$  and magnetization of about  $1000 \text{ mA/m}$ ) are located on the

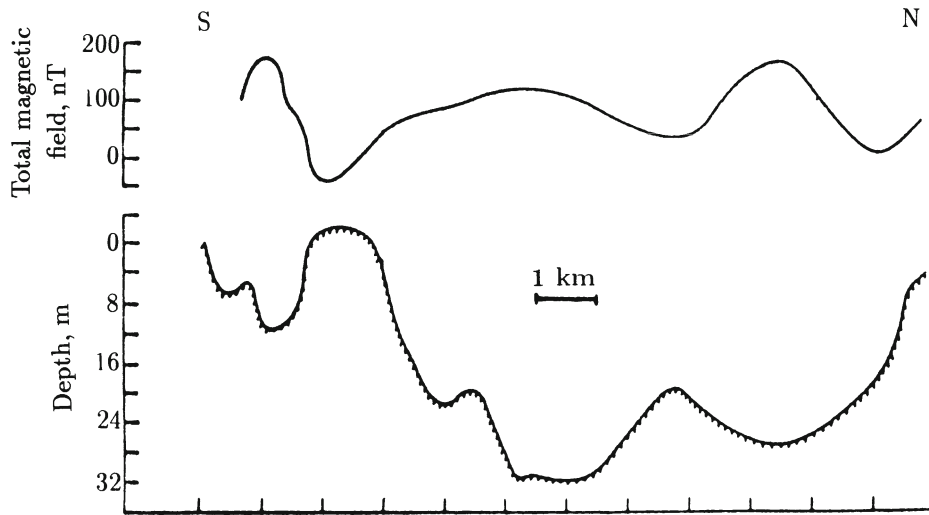
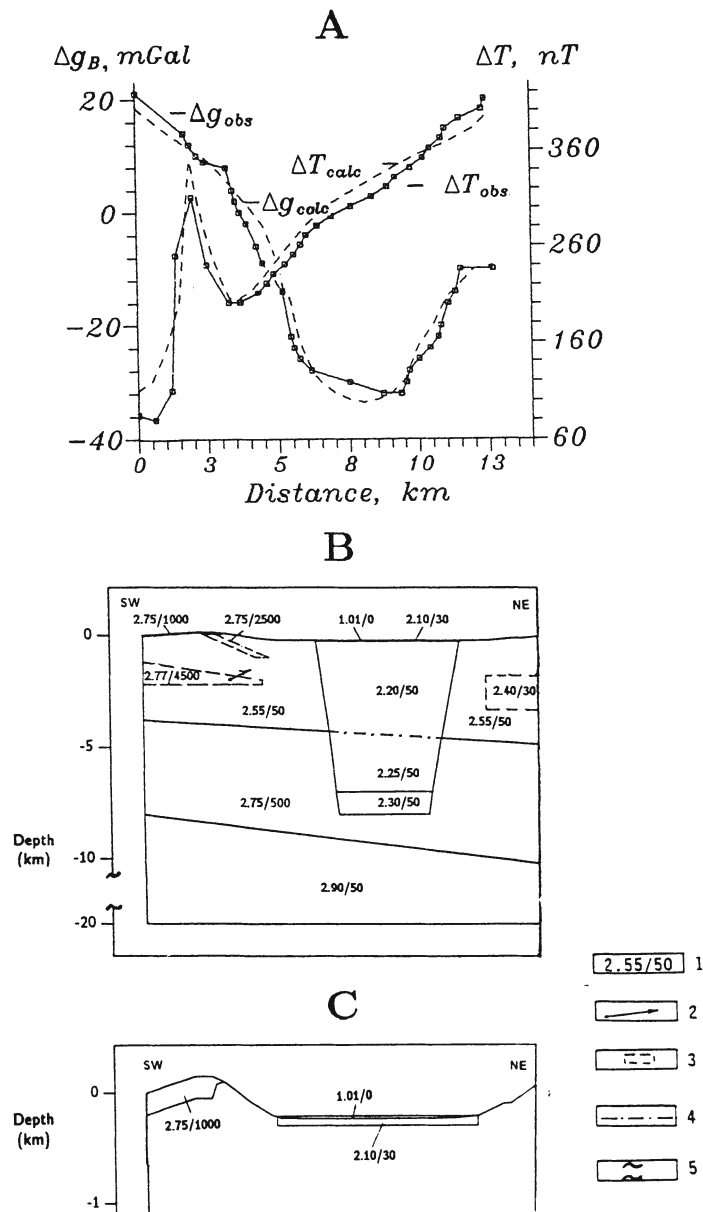


Fig.9.10. Comparison of magnetic field intensity and depth of the sea bottom for the eastern part of lake Kinneret (after [26])

earth's surface (being about 150 m thick) in the SW part of this profile (detailed description of the upper part of the profile is shown in Fig.9.11C). According to the work [26] in the upper part of the rift there are thin separate basaltic bodies. However, according to our computations, their total magnetic effect is not large. After careful analysis of the magnetic field distribution, it was suggested that the most possible source of the magnetic anomaly can be a ledge-like magmatic body with inverse magnetization in the SW part of this profile (see Fig.9.11B). This suggestion was confirmed by the results of combined 3-D modeling of magnetic and gravitational fields. The presence of this body does not contradict the available geological data.



**Fig.9.11. Results of 3-D integrated modeling of gravitational and magnetic fields over lake Kinneret area: (A) Comparison of observed and computed geophysical fields; (B) Physical-geological model; (C) Increased upper part of the model**

(1) physical properties: numerator, density ( $g/cm^3$ ), denominator, magnetization, ( $mA/m$ ); (2) direction of magnetization vector, differing from the geomagnetic field vector inclination; (3) new geological bodies selected by modeling; (4) apparent deep boundary; (5) vertical break on the section

## 9.4 Interpretation examples in detailed magnetic prospecting of archaeological objects in Israel

The territory of Israel is very attractive for archaeologists taking into account its ancient and Biblical history.

Magnetic prospecting may be successfully applied to archaeology [74], as it is a rapid, effective and non-invasive geophysical method for prospecting a broad range of various targets: buried walls, columns, foundations, water pipe systems and fire facilities (kilns, furnaces, ovens). Magnetic surveys provide a ground plan of cultural remains before excavations or may be even used instead of excavations.

Interpretation of magnetic survey in Israel is complicated by strong oblique magnetization of the Earth's magnetic field (about  $45^\circ$ ). Additional interpretation difficulties are connected with the unknown level of the normal field within the studied sites. The complicated conditions of the survey require advanced methods of quantitative interpretation and 3-D modeling (see Chapters 7–8). These methods allowed to eliminate various noises, to estimate the depth and size of archaeological remains and to conduct a precise 3-D modeling of the magnetic field. The results of geophysical investigations have been confirmed by direct archaeological excavations.

Objects of archaeological study occur at a small depth (from a few tens of centimeters to a few meters) and, consequently, the scale of magnetic survey varies from 1:50 to 1:200.

### 9.4.1 Area of ancient metallurgic works near the town of Eilat

On the site of ancient metallurgic works located near the town of Eilat, magnetic survey was conducted on a scale 1:100 (Fig.9.12A). In this figure two anomalies are clearly detected, which were recognized as furnaces used in ancient metallurgy. These anomalies were interpreted using modern methods which were described in this book. Positions of the anomalous bodies upper edges and their magnetization were determined (Fig.9.12B). The 3-D modeling

of the magnetic field was conducted for two alternative models with different magnetization values and directions of magnetization vector (Fig.9.12C,D).

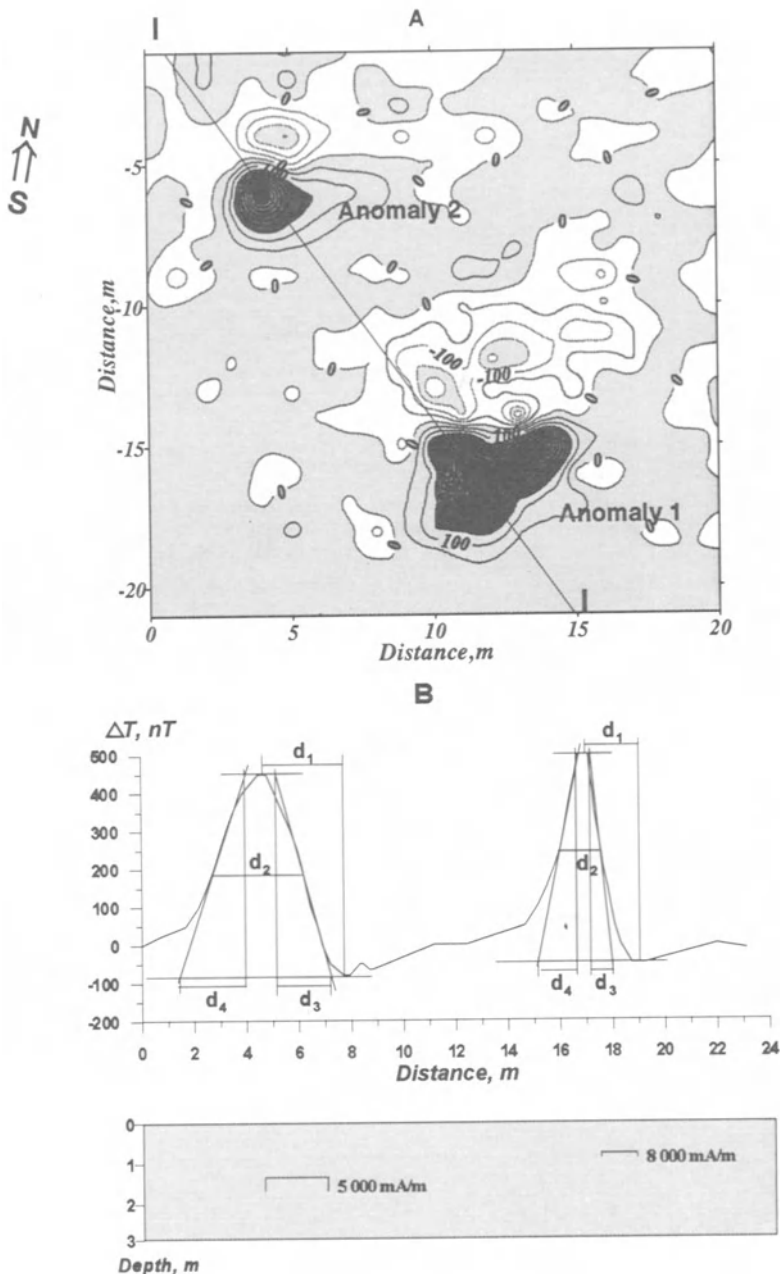
#### **9.4.2 Area of ancient Roman constructions, Yodefat site, Galilee**

The following example illustrates the interpretation of small magnetic anomalies caused by ancient (Roman) walls (mainly made of limestones and clays). This archaeological site is located in conditions of rugged terrain relief (Fig.9.13A). The terrain relief correction was calculated using correlation approach (see Section 5.2). As a result, the corrected map of  $\Delta T$  field was plotted (Fig.9.13B). Then the corrected magnetic field was transformed to informational quantity according to Subsection 8.3.3 (Fig.9.13C). The data from Fig.9.13B were used for quantitative interpretation of magnetic anomalies (Fig.9.13D). This is a confirmation of the reliability of the interpretation.

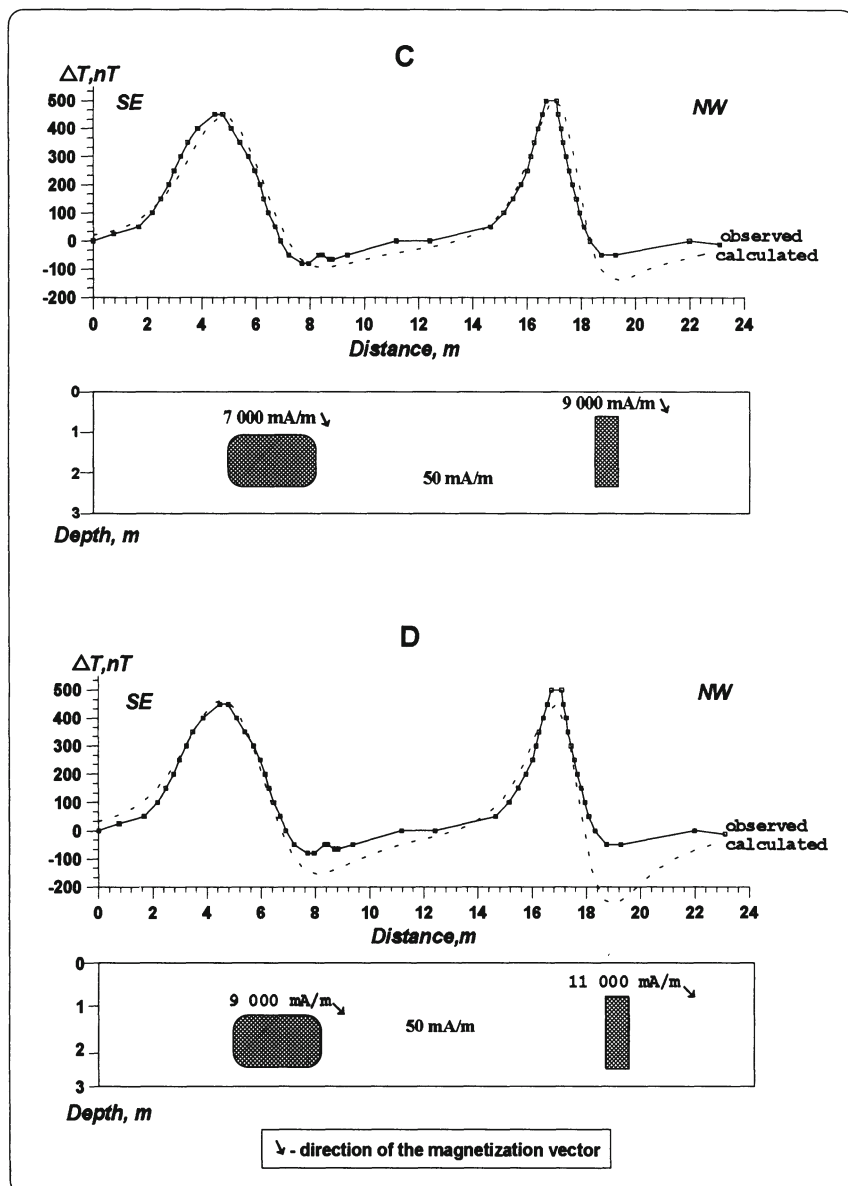
### **9.5 Estimation of the interpretation reliability and its application for optimizing a system of geophysical investigation**

The efficiency of geophysical investigations is governed in general by the reliability of the interpretation and the results obtained [78].

The reliability of geophysical interpretation is usually determined after checking it by mining and drilling, the results of the latter being compared with those obtained from the interpretation. Often retrospective estimates are of no practical use, but have a scientific and methodological value. They are used to develop recommendations for applying one or another method of interpretation. It is a good practice to estimate possible errors in the interpretation of the obtained data before completing the investigation of a certain area. This substantiates decisions concerning more expensive procedures of detailed prospecting, such as drilling, tunneling, etc. At this stage the independent (external) control is employed, as well, in



**Fig. 9.12. Rapid interpretation and 3-D modeling of  $\Delta T$  field on the site of ancient metallurgic works:** (A) Magnetic map of the studied site ( $\Delta T$  isolines in nanoTesla); (B) Rapid interpretation of magnetic anomalies using the developed procedures along the profile I-I; (C) and (D) Variants of the results of 3-D modeling of magnetic field along the profile I-I



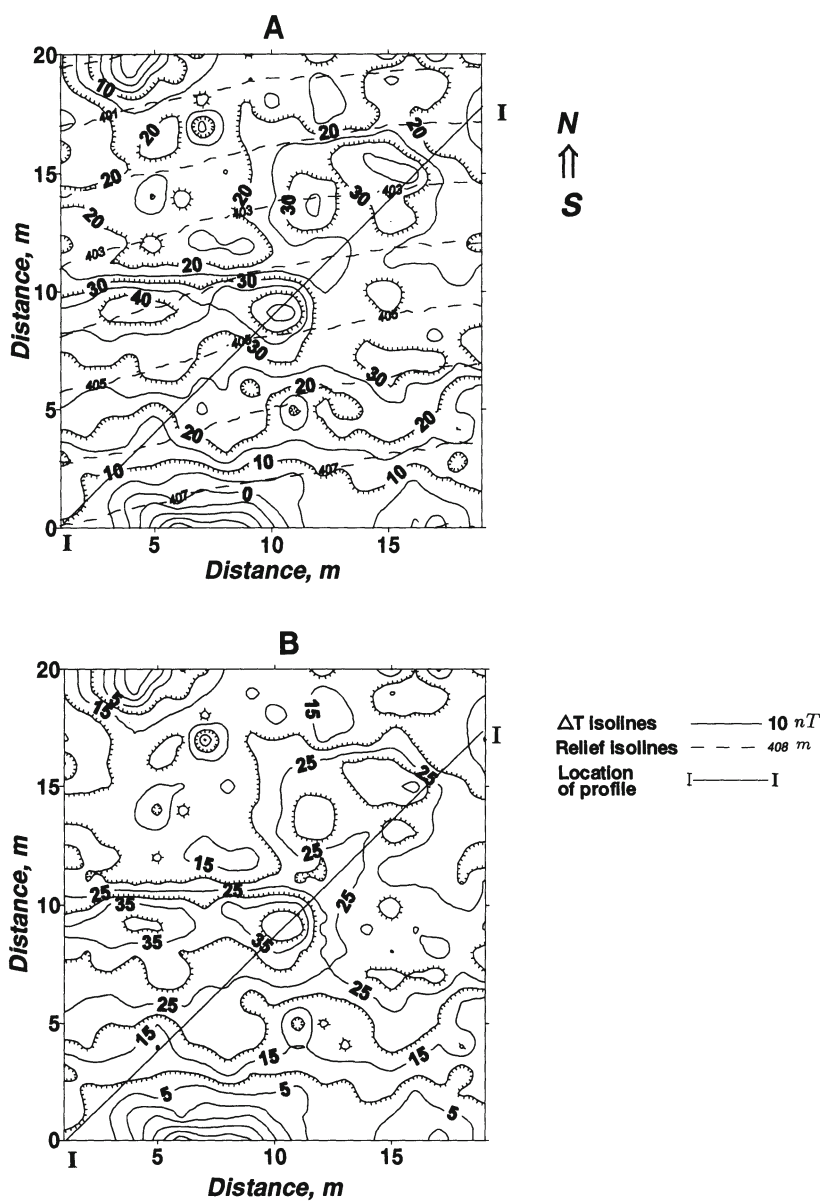
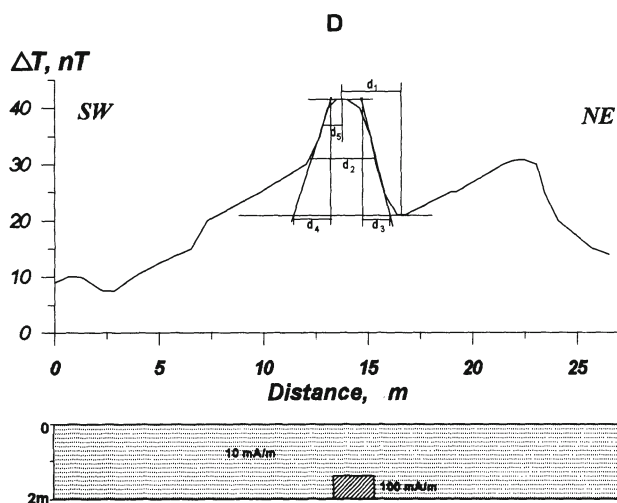
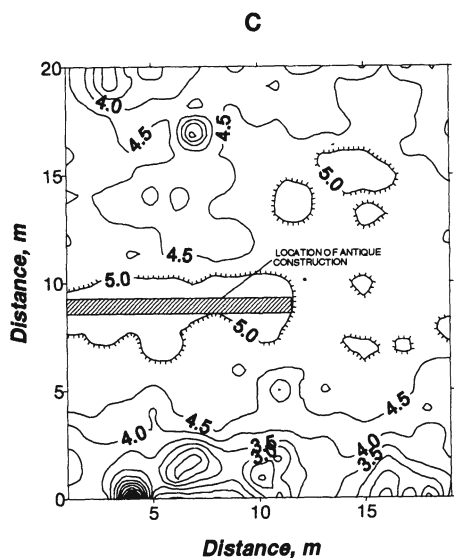


Fig. 9.13. Processing and interpretation of the magnetic field  $\Delta T$ : (A) Comparison of the observed field  $\Delta T$  and terrain relief, (B) Corrected magnetic field  $\Delta T$ ; (C) Revealing of desired object using informational criterion; (D) Results of inverse problem solution



order to reveal errors in the determination of the object's nature or its separate parameters when using independent geological evidence.

Rather frequently, independent control cannot be realized. First, it is impossible to check isolated anomalies by mining and drilling without constructing roads, power lines and other large-scale facilities. Second, such a check sometimes does not correspond to specific geophysical recommendations as to, for example, borehole and gallery locations, but follows from technical advantages or from general geological considerations. Additional geophysical explorations often bring about objective problems connected with a necessity to change respective plans. Therefore, beyond the above-mentioned approach to estimating interpretation errors, one should use estimation methods based on the materials of previous investigations and theoretical scopes of certain interpretation methods.

The inherent convergence of interpretation results can be estimated by comparing both independent data obtained by various geophysical methods and different techniques of interpretation of the same geophysical field, if these techniques have different limitations (see Section 7.4). The experience shows that though the scatter in computed parameters of anomalous bodies may amount to 10-20% and over, average estimates thus obtained are characterized by high stability and are close to external (independent) data.

The estimation of the reliability of separate parameters acquires a specific character under mountainous conditions. Whereas in flat regions, especially in oil-bearing areas, drilling data are usually sufficient for estimating the location of deep-seated geophysical boundaries, in mountainous regions it is expedient to compare depths obtained by aeromagnetic survey interpretation with the data on the earth's relief, their effect being often predominant in the observed field. Such a comparison allows to draw useful interpretation conclusions. For example, application of the improved tangent method [146] made it possible to characterize the depth distribution of magnetized masses relative to the relief in the north-eastern part of the Lesser Caucasus. It was established that the upper edges of magnetized bodies, as a rule, outcropped onto the earth's surface or were close to it. A small variance of relative depths obtained by interpretation and coinciding with terrain clearance of the aeromagnetic survey, allows us to suppose

that the magnetization  $I$  and the width  $2b$  of the upper edge of the objects approximated by a thick bed are sufficiently reliable in terms of applying them to large-scale geological mapping. This conclusion is confirmed by the closeness of corresponding parameters obtained on the basis of several profiles.

Theoretical errors in determining parameters on the basis of the regression equations, are characterized by the argument variability and measurement errors [3]. Theoretical errors can be estimated by analogy with integrated interpretation, if we check the hypothesis about classifying a parameter among a certain class (or a group of close values) of parameters. Integrated interpretation errors are the most essential, as it was shown before.

Integrated interpretation errors are determined in accord with the type of a specific algorithm. For example, in the algorithm of the “Linear solving function” program [84] with unequal covariance matrices, the classification error depends on the value of  $d$ . The latter is an analog of the generalized distance between the compared images for identical covariance matrices. The probability of correct classification is given by

$$P = 1 - \Phi(d), \quad (9.1)$$

where  $\Phi(d)$  is a normal distribution function.

When using statistical methods, certain assumptions are made concerning the distribution of probabilities or their properties, since the investigator often has no proves that the sampling is representative. Therefore, theoretical estimates of the interpretation reliability based on these assumptions should be checked by comparing them with empirical classification errors.

The empirical error or, more precisely, the probability of the error of the second kind  $\beta$  is assumed as the relative frequency of erroneous diagnosis for objects from the sampling  $B$  (geological targets), and that of the first kind  $\alpha$  – as the relative frequency of erroneous diagnosis for objects from the sampling  $\bar{B}$  (all other objects). These errors are used to determine a total unconditional error of separation ( $q$ ) of  $B$  and  $\bar{B}$  classes

$$q = \beta p(B) + \alpha p(\bar{B}), \quad (9.2)$$

where  $p(B)$  and  $p(\bar{B})$  are prior probabilities of the appearance of the objects of the first and second classes, respectively.

If  $p(B) = p(\bar{B}) = 0.5$ , then  $q$  value corresponds to the intersection area of density distributions  $p(X|B)$  and  $p(X|\bar{B})$ . Here  $X$  is the separation index. It can represent a field amplitude, information element,  $J_{compl}$ , etc. The separation reliability is

$$\gamma = 1 - q. \quad (9.3)$$

A total empirical error is comparable with a theoretical one. Their closeness testifies to the correct presumptions and a high reliability of identification.

When using logico-informational methods, the classification reliability is estimated solely by empirical errors. For example, the information obtained in the area of the Katsdag polymetallic deposit was calculated by surveying  $SP$ ,  $\Delta Z$  and secondary dispersion haloes of lead and copper on a scale of 1:5,000. This deposit was revealed in the 1960s during geophysical investigations conducted with the participation of the authors at the southern slope of the Greater Caucasus (Belokan-Zakatala ore district). Two types of integrated indices of perspectiveness were obtained: the normalized sum  $\frac{1}{4} \sum_1^4 K_i$  of the corresponding informativity coefficient and  $J_{compl}$  value. The distribution of both types of integrated indices has been compared with the contours of ore areas (Fig.9.14). The error made when assigning the observations to a certain class ("ore" or "no ore") can be determined by the number of cases of the absence of integrated index anomalies in the known ore areas (the second kind error if the target is omitted) and the number of these anomalies in the barren portion of the area (the first kind error is false alarm). These errors amount to 0 and 0.33, respectively, for the index  $\frac{1}{4} \sum_1^4 K_i$ , as shows Fig.9.14, while for the index  $J_{compl}$  – to 0 and 0.20. Thus, when prior probability for each of the two classes is assumed to be 0.5,  $q$  amounts to 0.16 for  $\frac{1}{4} \sum_1^4 K_i$  and to 0.10 for  $J_{compl}$ , according to formulas (9.2) and (9.3) while  $\gamma$  runs to 0.84 and 0.90, respectively. Therefore, the reliability of singling out ore areas by the index  $J_{compl}$  is higher than the reliability of their singling out by a sum of informant elements.

A similar computation allows to compare the efficiency of various sets in this district. With the use of a mobile set of "easy" methods ( $SP$ , magnetic prospecting, metallometric survey) dozens of anomalous areas were singled out. They were classified according

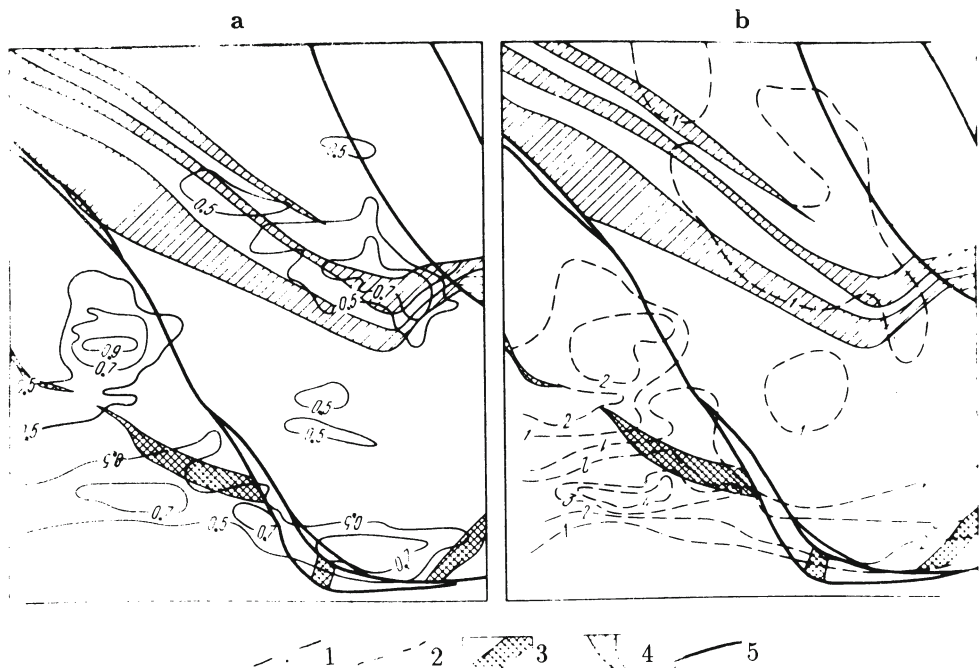


**Fig.9.14. Comparison of the indices  $\frac{1}{4} \sum_1^4 K_i$  (a) and  $J_{compl}$  (b) with ore zones location in the Katsdag deposit**

Isolines: (1) mean sums of the informativity coefficients ( $\frac{1}{4} \sum_1^4 K_i$ ); (2) values of  $J_{compl}$ ; (3) zone with known deposits; (4) a less investigated ore zone; (5) disjunctive dislocations

to the degree of their perspectiveness and to the necessity for further investigation into three classes. If the results of the subsequent control using a more complicated set (including IP, transient method and gravity prospecting) are taken as absolutely reliable, then the reliability of classification by natural fields data reaches 0.96 for the most investigated areas of the first class and about 0.7 for all the areas. A high reliability was observed in the areas with the largest pyrite-polymetallic deposits located at a shallow depth. They are top priority targets for the most efficient further exploration and usage.

The reliability of each variant of the set can be estimated by varying the number of its elements. On the basis of quantitative characteristics, this method makes it possible to select immediately a rational set, which may be also substantiated by estimating the

informativity of separate elements of the set.

It is noteworthy that special investigations for determining the reliability of the results of integration of various geological exploration techniques, for example, geophysical methods [150], have shown that not only the set of methods, but the sequence of their application, as well, is important. The formulas [150] of reliability estimation of various object's feature such as density, thickness, etc., by sets of various methods (with a given reliability of separate methods application) enable one to estimate, which combination of techniques and to what extent affects the increase in reliability of the entire set.

The interpretation reliability estimation is necessary when determining separate parameters or the nature of anomalous objects for making well-grounded decisions. This refers to the system analysis of geophysical investigations as a whole and as an element of the geological exploration process. The choice of a set is revised on the basis of the interpretation data allowing to estimate the effectiveness of its separate elements and the set on the whole, and revealing specific features of the prospective region, which have not been supposed beforehand. The feedback considerably complicates the system of geophysical prospecting and calls for the necessity of rapid interpretation of the results.

At the *first* or *initial stage* of applying a system of geophysical investigations, the field work is accomplished using a set of methods selected on the basis of prior data (with the estimation of the possibility of solving the problems stated). It is followed by the processing of the results of investigation (taking into consideration the terrain relief effect). The *second stage* involves regioning and singling out separate object indicators by the correlation analysis and transformation which have much in common. At the *third stage*, integrated indices are considered, which are constructed by the data obtained from the observed fields or by the results of their transformation, which reflect the classes of objects under study in the best possible way. At the *fourth stage* the investigator conducts the quantitative interpretation of distinct anomalies for determining the anomalous object parameters, which is controlled by selection techniques. And at the *final stage* the results of interpretation are marked on maps and sections and used along with geological and

geochemical data for solving search and exploration problems. This is a general scheme of the geophysical investigation process. During its realization, the feedback is taken into account and a procedure of sequential iterations is accomplished.

The knowledge of the error probability allows to make a well-grounded decision concerning the expediency of further exploration (or its termination) in the given area. The maximum amount of information about the area (desired object) derived at the lowest expenses (or at the earliest possible date) is taken as the criterion of the decision, since geological information is the product of all geological and geophysical investigations. The cost of investigations or time consumption are reduced to minimum depending of the importance of the task. If the task consists in accumulating the economic mineral reserves in a planned way, the cost of prospecting should be reduced to a minimum. If, however, there is a gap to be closed arising as a result of a sharp increase in the demand or with the advent of new types of raw materials, then the time of geophysical prospecting is to be minimized.

All mentioned above, as well as the experience in mining geophysics testify to the fact that the efficiency of geophysical investigations can be essential at all the stages of geophysical prospecting for ore and other deposits in mountainous conditions even under unfavorable geological-geophysical situation. The main conditions for improving the effectiveness of a system of geophysical investigation are as follows:

- consideration of the specific character of mountainous regions when setting problems, selecting methods and sequence of their solution;
- application of quantitative estimates of situations by geophysical data, combination of deterministic and probabilistic approaches to the processing and interpretation of geophysical materials;
- application of the rapid correlation method for terrain correction, requiring no special study of petrophysical characteristics and allowing to obtain the interpretation conclusions;
- deriving a large amount of information by suppressing noises in the results of separate geophysical methods, singling out the objects by a set of indicators which are less informative if taken individually, with the use of the developed information-statistical methods;
- application of a deterministic interactive system developed for

the quantitative interpretation and based on a combination of rapid methods and selection.

# **Chapter 10**

## **CHARACTERISTIC FEATURES OF THE IMIGO PACKAGE**

### **10.1 General characteristics**

Development of a package intended for interpreting materials of gravimetric and magnetic investigations (in general, this set can also include other geophysical methods) under mountainous conditions has been caused by the following considerations.

Processing and interpretation of gravimetric and magnetic survey data are the most computerized spheres in mining geophysics. There are presently over two dozens of computer-aided processing systems implementing standard operations that are basically alike. As to interpretation systems, they are far less developed yet [31,34,92,180]. Unfortunately, one can hardly choose an optimum system out of the available packages. Along with particular and general constraints due to insufficient universality and integration degree, there is still another limitation. In many cases these systems do not allow to describe the specific nature of mountainous and other hardly accessible areas. The descriptions fail to make it clear how the program parameters should be handled to attain the desired accuracy of computations under real conditions. A number of programs do not treat the topography heights at all. Therefore, they are not meant for mountainous conditions.

An ever increasing importance is currently attached to organizing programs for geological-geophysical materials processing and interpretation. These programs are supposed to employ geological-geophysical databases (*DB*) and common database management

system (*DBMS*) as an efficient means of data organization, storage, updating and access in a batch and interactive mode [56]. Of great significance is the methodology of interpreting data of a particular topic domain marked by specific features.

The interpretation methods for potential and quasi-potential fields observed in mountainous regions have been developed and discussed in the preceding Chapters. Clearly, they should be implemented in the form of a computerized system employing *DB* and *DBMS*. The principles and requirements set forth in [110, 191, 213, 278, 305] have been taken into account while developing the *IMIGO* package.

### 10.1.1 Organization principles for the *IMIGO* package

Listed below are the basic principles adhered to while designing the *IMIGO* package.

- (1) Utilization of the systematic approach presented in [146] and developed in the preceding Chapters.
- (2) Application of an interactive interpretation system.
- (3) A suitable *DBMS* (for instance, *GEOKOMPAS* [268]) controlling the operation of the package. This makes the programs independent of data, and vice versa.
- (4) Referring the package data to the *DB* structures through appropriate subsystems.
- (5) Requirements to the programs of the *IMIGO* package: modular character, structural design, adaptability and updateability, accuracy and high speed (the former having priority over the latter).

These principles are substantiated below.

The systematic approach treats interpretation as an interrelated combination of procedures united by a common objective. Chapter 3 gives a full description of the interpretation stages. The second stage (i.e. successive analysis) is fairly well formalized and susceptible to automation. As to the first (generalization of prior information) and the last stages (geological synthesis), they comprise some non-formalized procedures and practically cannot be automated. Yet the result of prior information generalization (including physical

properties of the media) is represented by a physico-geological model. It can be described in a formal language and included into a *DB* of an automated interpretation system, which is schematically presented in Fig.10.1.

In the conditions of areas with a complicated geological structure, it is usually an expert who makes comparisons with the interpretation criteria (e.g. a computed field is compared to an observed one), makes decisions concerning some necessary modifications of the model, prepares these modifications and introduces them into the model, and, probably, makes necessary changes in the interpretation techniques. All this calls for utilization of an interactive system.

There are generally five principal components in *DBMS* [213]:

- (1) System data description language (*DDL*).
- (2) Subsystem data description language.
- (3) Data manipulating language.
- (4) Resident executive module of *DBMS*.
- (5) Control language for the distribution of external carriers and storage data description language. In some cases the operators of these languages are combined with those of *DDL*.

### 10.1.2 Topic domain and conceptual model of data

The initial model of the medium gives an exhaustive representation of the topic domain and a conceptual data model (see Chapter 4). The most essential points of the given domain can be summed up as follows: geological objects (situations), terrain relief, properties of geological objects (composition, physical characteristics, etc.), observed fields and relations between fields and objects. It should be recalled that not all the objects are known *a priori*. The same applies to the relations between the fields and objects. The interpretation is just aimed at the establishment of these relations and to their use in order to reveal unknown objects. For this purpose well-known principles of the interpretation theory are employed, particularly, those of the potential theory. It is basically this somewhat vague nature of the topic domain under review that makes it different from

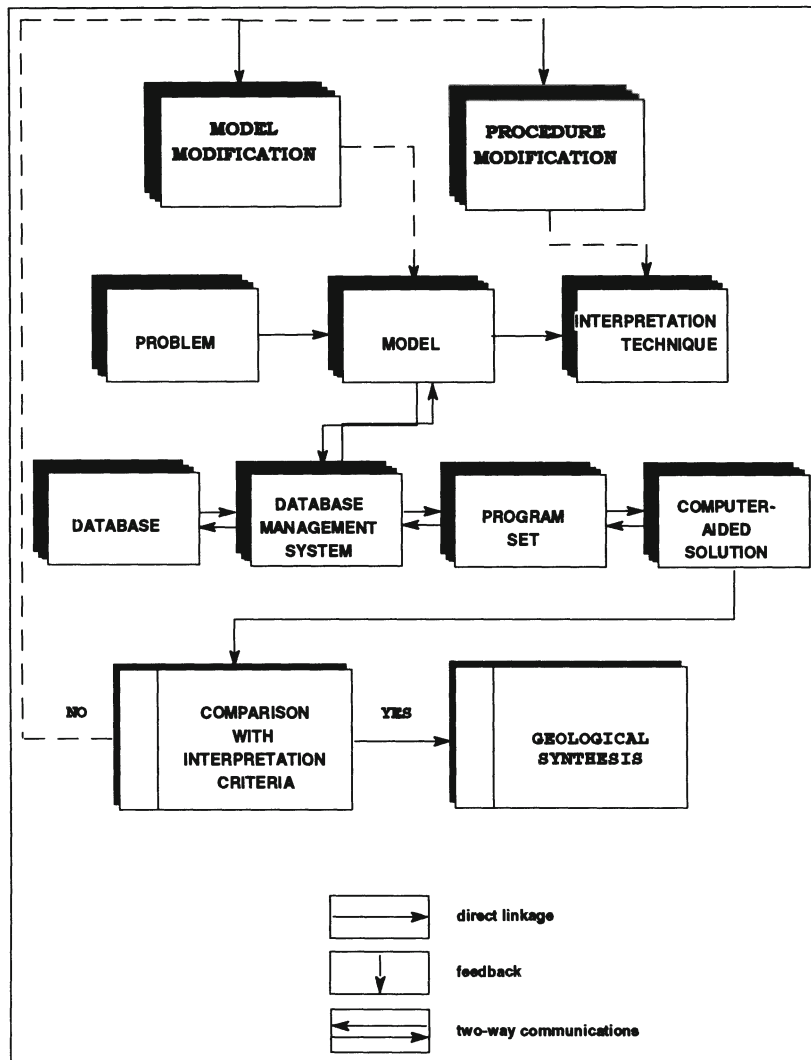


Fig.10.1. Block diagram of the automated interpretation system

other domains<sup>1</sup>.

To form the initial model of medium, the following information is necessary:

- (1) models of individual geological bodies, more generally – models of geological situations in terms of the coordinate description of the bodies contours, their physical properties and belonging to a particular association; classes of desired bodies;
- (2) indicators of desired bodies, including computed anomalous effects due to these bodies;
- (3) data obtained by geophysical methods (fields and results of their interpretation) on neighboring or similar areas (including less detailed data);
- (4) data on the intensity and shapes of anomalies over objects which resemble the desired ones;
- (5) interpretation criteria (critical levels for some quantitative features);
- (6) indirect indicators;
- (7) secondary indicators (transforms and others) and ways to obtain them (transformation parameters).

Most of the above data can be described in a quantitative form and represented in a *DB* as an implementation of the model of a medium.

Generally, the information on the observed fields includes the number of a point, its three coordinates, the values of  $\Delta g$ ,  $\Delta T$  and other fields observed.

In special cases (a rectangular or square network, a rectilinear profile) the number of elements describing the observation point coordinates may be less, but some other elements are added, namely:

- the number of profiles and points on the profile, the coordinates of the first and last points on the first profile, the distance between the profiles, the step along the profile (for an areal survey);
- the coordinates of the first and last points on the profile, the

---

<sup>1</sup> Due to of the uncertainty of the topic domain, similar problems are investigated today using a “fuzzy logic” [301]

step along the profile or the total number of points on it (for profile observations);

Both in general and special cases, the observation data should necessarily include the heights of the observations points, which can be classified as measured geophysical fields.

### 10.1.3 Data processing

Data processing involves the procedures described in Chapters 4–9. Table 10.1 presents elementary operations performed at these stages.

Fig.10.2 summarizes the structural and functional diagram of the *IMIGO* package. The presented implementation does not cover all the operations included into the diagram, but only priority operations in automating the interpretation of gravimetric and magnetic data for mountainous conditions. The next subsection gives a more detailed characterization of the *IMIGO* package application.

## 10.2 IMIGO-based interpretation: technological order of execution

The interpretation sequence is governed by the sequence of Chapters 4–9 and interpretation procedures (stages) listed in Table 10.1. As mentioned above, not all stages are equally susceptible to formalization and, as a consequence, to computer-aided processing. However, the databases used permit to store the input and output data of corresponding interpretation stages. Quite often in this case the output data of one stage are the input data for subsequent stages.

Let us give a brief review of the interpretation technology at its sequential stages using the programs of the *IMIGO* package.

### (1) Formation of the initial model of the medium

This stage basically employs non-formal methods of prior information synthesis described in Chapter 4. As a result, we get the description of a geological space of the investigated area represented by a set of geological bodies belonging to a particular association.

**Table 10.1. Automated interpretation procedures and elementary operations**

No.	INTERPRETATION PROCEDURES (STAGES)	ELEMENTARY OPERATIONS
1	Forming an initial <i>PGM</i> , modifying the <i>PGM</i>	Data preparation, primary loading and <i>DB</i> modification
2	Forming an indicator space according to the observation results:	
2.1	Eliminating complications due to the terrain relief effect and other known factors	Computation of direct effects due to the relief forms and other known bodies. Excluding the computed effects from the observed fields
2.2	Computing secondary indicators by the initial field(s)	Conversion into the upper half-space to different levels, averaging with different radii, computing gradients, calculating ruggedness measures, etc.
3	Revealing and localization	Classification (taxonomy) of the investigation area by a specified (variable) set of indicators, ruggedness included. Correlation of linear zones. Determination of axes and contours of objects
4	Determination of the anomalous bodies' quantitative parameters	Parameter determination by rapid methods. Non-formalized simulation (modeling). Formalized simulation (optimization)
5	Integrated interpretation and physico-geological modeling	Computing appropriate measures (those of probabilities, amount of information, etc.) by a set of fields of different kinds. Joint simulation by various fields
6	Graphic representation of the interpretation results	Computer graphics operations (output of charts, schemes, plots, sections)

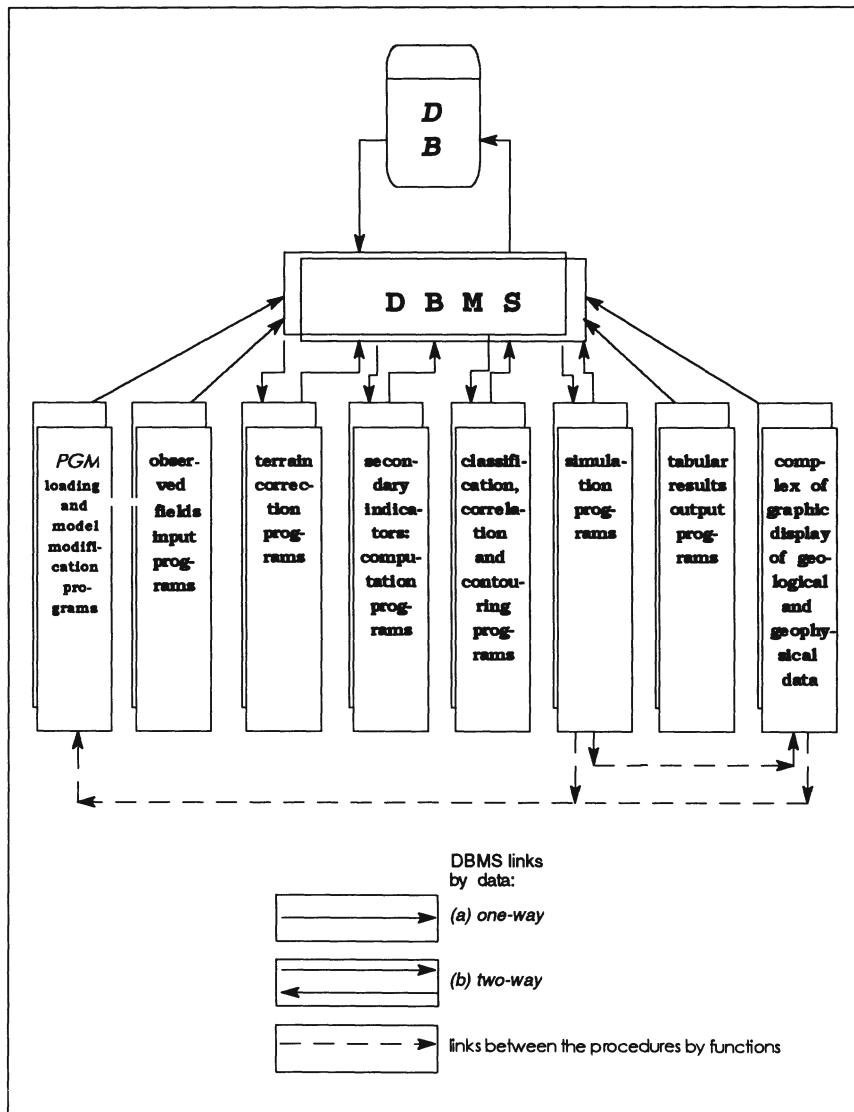


Fig.10.2. Summarized structural and functional diagram of the *IMIGO* package

These bodies may be either stretched out or localized, and characterized by certain values of physical properties (for instance, density and magnetization). The coordinate representation of these objects is obtained according to the body description rules. These data are loaded into *DB* together with the height information obtained all over the area of investigation.

Besides, observed gravitational and magnetic fields, as well as other measured fields, are also loaded into *DB*.

#### *(2) Formation of an indicator space*

Proceeding from the analysis of the observed fields and taking into account the objectives of the investigation, the interpreter makes necessary decisions regarding the type of secondary indicators, ways to obtain them and parameters of transformation. In case it is necessary to perform the terrain correction, as well as the correction of the fields due to large distant objects, appropriate data are loaded into *DB* as described above.

#### *(3) Revealing and localization of targets*

Secondary indicators computed at the preceding stage are taken out of *DB* using special programs. The isoline maps are plotted for corresponding transforms. Their analysis and the display of the analysis results are executed in accordance with the rules given in Chapter 6.

Data for initial modifications of the model of the medium are obtained at this stage. They are introduced into *DB*.

#### *(4) Determination of quantitative parameters of anomalous body (inverse problem solution)*

The substage of the choice of parameters for determination and preparation of the anomaly (numerical values or graphs) for computation precedes this stage (see Chapter 7). At the end of this stage additional data for model modification are obtained, and these data are introduced into *DB*.

#### *(5) Integrated interpretation and physico-geological modeling*

At the beginning of this stage an interpreter has a sufficiently complete idea about the majority of sources of anomaly field including deep-seated hidden sources. Therefore, the interpreter may apply the procedure of distinguishing objects (classes of objects)

with expected properties.

Physico-geological modeling on the basis of gravitational and magnetic fields is accomplished with the use of *GSFC* program, i.e. in interactive mode. At each simulation stage the fields caused by the entire model are computed over a given profile (or a group of profiles). The fields thus computed are compared with the observed ones, and decision is made regarding the necessary changes to be introduced into the model and the nature of these changes. The modifications may be relate to the physical properties of individual bodies or to the form of these bodies' surfaces (or both); certain bodies can be eliminated or, on the contrary, added. The model changes are prepared on the basis of the analysis of both fields, which determines the integrated character of physico-geological modeling. The modifications are loaded into *DB* with the help of a special subroutine. Field computations, comparison of the computed fields with the observed ones and modification of the model are repeatedly performed until the corresponding fields coincide within the observation accuracy limits.

#### (6) *Developing a final model*

Since modeling applies to geological objects rather than to physical sources, the final model selected has a geological content. The belonging of new bodies introduced during the selection to a certain association is determined by analogy with bodies with close physical properties, proceeding from general geological notions.

### **10.3 Peculiarities of interpretation technology at different stages of geophysical investigations**

Depending on the scale of geophysical surveys which is determined according to the current stage of geophysical investigation, the specific features of investigated areas manifest themselves to various extents (see Chapter 1). Accordingly, the objectives of geophysical work (as well as those of observed fields interpretation) differ for each particular case.

For example, regional and middle-scale geophysical explorations

involve investigation of sufficiently large depths. The observation network is sparse, therefore, local variability of the earth relief and near-surface geological structure is not registered. In this case a fairly schematic model of the initial medium will suffice. This model is refined at the subsequent stages of regioning (after the indicator space has been formed), interpretation of individual anomalies, and, if necessary, physico-geological modeling.

Large-scale investigations are most typical of the mountainous regions. In this case the earth's relief and near-surface objects variability stand out more sharply in the observed fields, while the signals due to the desired objects are usually low. A valid revealing of the desired objects under such conditions is only possible in the framework of integrated interpretation (see Chapter 8). Creating the initial model of medium is rather difficult and is marked by a high ambiguity. The basic procedure at this stage is the formation of an indicator space. In particular, one has to determine the type and amount of secondary indicators, which have the greatest information content regarding the targets of investigation. Rather frequently these indicators have to be determined in an empirical way. Of great value is also a correct utilization of the indicator space obtained in the recognition procedure. Information-statistical techniques (see Chapter 8) can also be applied here. The interpretation results are generally represented as a chart of an integrated criterion isolines or in the form of a chart of isoprobabilities of the presence of the desired objects.

The area under detail prospecting is not large, it can be restricted to one morphostructure. Often enough, the relief within the area can be approximated by one (or by a limited number) inclined plane. The objective of geophysical exploration at this stage consists in a detailed quantitative characterization of objects which are known by this moment, as a rule. Therefore, a sufficiently complete nature of the initial model of the medium can be explained also by a plenitude of mining data. The major technological operations at this stage are as follows: (1) thorough terrain correction in accordance with a higher accuracy of detailed surveying; (2) quantitative interpretation using rapid methods and simulation.

# CONCLUSION

A system of interpretation of gravitational and magnetic fields, anomalies of temperature field, fields of *VLF* transmitters, self-potential and induced polarization has been developed for complicated environments (rugged relief, considerable heterogeneity of media, oblique polarization and an unknown level of the normal field).

To develop this interpretation system, the authors conducted the studies aimed at solving the following problems:

- elimination of the noises (primarily of the topographic effect by correlation technique) typical of mountainous regions;
- terrain correction within the process of physico-geological modeling;
- typification of targets and summarizing their characteristics, estimating the possibilities of various sets and the role of natural geophysical fields;
- development of logico-informational methods for integrated interpretation using a set of geophysical fields and for the interpretation of individual complicated fields. Such methods, based on the accumulation of useful information and the destruction of superfluous one, can be used for revealing of important hidden objects;
- development of rapid methods (tangents and characteristic points) for solving an inverse problem under conditions of the inclined observation line, arbitrary polarization of objects and an unknown level of the normal field;
- development of interactive integrated selection on the basis of an effective algorithm of solving a direct 3-D problem of gravimetric and magnetic prospecting;

- estimation of prospecting reliability on the basis of information-statistical approach;
- development of interpretation procedures succession, which was reflected in the structure of the book;
- development of *IMIGO* program package allowing to realize formalized procedures using a computer.

The developed interpreting system and its components make it possible to solve geological problems of various types on all stages of geophysical prospecting.

Often one and the same problem is solved in contiguous stages, while during a single stage several problems can be solved. This is conditioned by the specific character of investigations carried out in mountainous and other regions, which impede repeated surveys of hardly accessible areas.

The most typical of mountainous conditions is the stage of large-scale prospecting, where the stochastic character of the medium under study and of the recorded geophysical fields manifest themselves more sharply. Therefore, the key means of interpretation at this stage are statistical techniques for processing the results and revealing certain features of geological structure from the geophysical field represented as a mixture of various noises and the target signal. This can be extended to the interpretation of geophysical data integration, which involves singling out of an object of desired class through accumulation of information contained in various fields.

When conducting regional and detailed surveying, the major focus lays on deterministic variants of interpretation. They are oriented to the investigation of marker interfaces and localized anomalous bodies.

Naturally, deterministic and probabilistic methods do not exclude but complement each other. A combination of these methods is applied in any region.

The interpretation system and its components have been successfully tested on a complicated model and in real situations in the Caucasus and other regions (primarily in Azerbaijan). The system has been used here to study deep structures, ore, oil-and-gas and underground water controls. Moreover, it helped to reveal promising

areas and new deposits, to solve other geological problems including those associated with long-term seismic activity prediction. Besides, various components of the system were successfully applied to the research of near-surface inhomogeneities, such as objects of engineering geology and archaeology. Therefore, we expect that the techniques involved and the interpretation system on the whole can be widely applied to study a number of regions and areas with complicated structure when solving various problems.

## APPENDIX A. ELIMINATION OF TIME VARIATIONS IN THE VLF METHOD AND NEAR-SURFACE THERMAL PROSPECTING

### VLF method

When applying this method for field work, one often runs into the problem of eliminating time variations of magnetic fields from distant very low frequency transmitters.

The following approaches were used to overcome this problem.

During the initial period of *VLF* method, an approximated technique was used, which was based on field intensity measurements at a control point (*CP*) before and after field work [273]. Corresponding corrections were introduced by interpolation assuming that the field intensity change was linear. However, practical application of this method brought about considerable errors.

A modification of this method is described in [70]. The difference is that the time period of supposedly linear variations is assumed to be 1 hour. The area is rejected if the level of variations for 1 hour exceeds 20%.

The above method suffers from following disadvantages. The experience in field explorations in various regions indicates that the intensity changes of the fields under study (even in an hour) often cannot be approximated by a straight line with a sufficient accuracy. Besides, the amount of variations during this period may exceed 20%. It is also note worthy that this method neglects the existing effect of variation noise intensities on useful anomalies. It is evident, however, that time variations of very low frequency field intensity affect the radiowave energy passing from the air into the ground. The intensity of the secondary field tends to increase or decrease, correspondingly (especially in the presence of anomalous objects of increased or decreased conductivity), and the variations are nonuniform. Being disregarded, this fact can distort the interpretation results.

Scintrex, a Canadian company, developed an automatic attachment to a *VLF* receiver. Variations are eliminated by obtaining a synchronous ratio of the vertical component  $H_z$  of the *VLF* magnetic field to the total horizontal component  $H_\phi$ . However,

it was found by experimental field exploration that the  $H_z/H_\phi$  ratio varies sometimes even for observations in the same point. Quantitative interpretation of the  $H_z/H_\phi$  curve presents certain difficulties. An other approach, described by Scintrex in a recent instruction for using VLF equipment, consists in the selection of frequency and time interval which is the most stable in time for the studied region. Similar method was suggested also by Villee et al. [294]. However, this approach may be improved.

The following additive model of a geophysical field is practically applicable for the investigation by VLF method:

$$F_j = \sum S_j[(n_j(x), x] + \sum n_j(x), \quad (A1)$$

where  $F_j$  is the field observed along the profile,  $\sum S_j[(n_j(x), x]$  is the sum of effects from the anomaly-forming objects and geological inhomogeneities of the section (with due account of the dependence on field variation),  $\sum n_j(x)$  represents the noises of field variations in time (time dependence is omitted in (A1) for simplicity).

The wavefront is thus assumed to be plane while the primary field intensity is taken to be constant within the area of the detailed geophysical investigation ( $25 \div 100 \text{ km}^2$ )<sup>2</sup>.

It is known that for the VLF field the conduction currents are dominant over the displacement currents [100,300], which is the major condition of quasi-stationarity [11]. The proportionality of the secondary electromagnetic fields (of both magnetic and electric type) to the primary ones has been confirmed in a number of publications [57,58,etc.]. Considering also the physical effect of the subvertical radiowave propagation in the ground [100,215] and taking into account expression (A1), the following model of VLF observations can be used in practice [76]:

$$\begin{aligned} H_o(t) &= H(t) + B_o H(t) \\ H_j(t) &= H(t) + C_j H(t) \end{aligned} \quad \}, \quad (A2)$$

where  $H_o(t)$  is observation at control point;  $H_j(t)$  is observation on the profile,  $H(t)$  is primary field intensity,  $B$  and  $C$  are certain coefficients reflecting electromagnetic properties of the medium;

---

<sup>2</sup> A large distance from VLF transmitters (2,000 to 10,000 km) is responsible for the uniformity of the primary field both at CP and in the investigated area.

indices  $j$  and  $o$  mark the observation point on the profile and  $CP$ , respectively.

Considering that  $B_o = \text{const}$ , this parameter, being a basic value for the given area, can be assumed, for convenience, equal to zero. Solving the equations (A2) in the parametric form, we obtain the values  $H_{\text{clear}}$  cleared from variations for each profile point:

$$H_{\text{clear}} = [H_j(t)/H_o(t)] \cdot \bar{H}, \quad (A3)$$

where  $\bar{H}$  is a certain averaged value of the field.

Thus, the proposed scheme of eliminating variations in the *VLF* method is based on synchronous recording of the observations along the profile and variations at  $CP$ . Automatic variation recording presents no problems and can be realized with a discretization interval of 0.05 to 0.1 minute. This method substantially eliminates observation distortions caused by field variations with time (both during a day and at different days of the survey) by reducing observation results to a common level.

### Near-surface thermal prospecting

The lag-effect of temperature waves originating from the earth surface presents the most difficult part in eliminating the seasonal temperature variations in near-surface thermal prospecting. These waves, being superimposed on deep thermal flow which is re-distributed by the anomalous object with a contrasting thermal conductivity, make the quantitative and qualitative interpretation of temperature anomalies rather difficult. In case the object with a contrasting thermal conductivity occurs above the layer of neutral temperature, the secondary effect of variations is also possible.

Various methods of geothermal survey and data processing have been developed for eliminating seasonal variations of temperature. One of the methods consists in conducting long-term geothermal investigations of the area under study and selecting a field survey period, when seasonal variations are minimal. However, this method suffers from such drawbacks as long duration, and hence inapplicability of the results, since the time of field work is frequently defined by organizational factors, etc.

Two other methods are worth mentioning: (1) synchronous measurement of temperature variations and the field survey [155] similar to the well-known method of eliminating magnetic field variations in magnetic prospecting; (2) simultaneous measurement of the temperature in all points of the profile [51]. However, the first method does not always allow to avoid the influence of the delay of temperature waves coming from the surface. Application of the second method demands simultaneous use of numerous temperature measuring devices, which technologically impedes the surveying.

Khesin [131] noted that the most difficult task is to consider atmospheric temperature variations and resulting changes in the ground temperature. He suggested a method for eliminating variations by repeated observations with subsequent statistical processing of the results.

This approach was further developed by Eppelbaum and Mishne [77]. It is known that a regional thermal field is stable in time [186], and temperature-wave propagation in a medium is linear [283]. Taking into consideration these factors, a model of the total temperature field, recorded in a heliothermal zone can be represented in the following form:

$$Q_i(t) = T_i + \sum_{j=t-t'}^t \tau(j)f(t-j), \quad (A4)$$

where  $Q_i(t)$  is observation at the  $i$ th point (borehole);  $T_i$  is the temperature conditioned by redistribution of a deep heat flow caused by an object with contrasting thermal conductivity;  $\tau(j)$  is the average temperature at a certain depth  $\Delta h$  over the region including the area under investigation (data from meteorological stations are employed) at the moment of time  $j$ ;  $f(t-j)$  is a step-wise weighting function reflecting the temperature effect at the depth  $\Delta h$  at the moment of time  $t-j$  on the temperature measured in the borehole at the depth  $h$  at the moment of time  $j$ ; and  $t'$  is the delay time of temperature waves coming from the surface.

In the described model noises at the time  $(t-j)$  are autocorrelated. Autocorrelation matrix for noises  $\mathbf{R}(t-j)$  can be written in the form:

$$\mathbf{R}(t-j) = \begin{cases} \frac{1}{1+(t-j)^2} & |t-j| \leq \psi \\ 0 & |t-j| \geq \psi \end{cases}, \quad (A5)$$

where  $\psi$  is a defined parameter.

Measurements at the points of the profile made at different moments of time  $t$  enable one to obtain a solvable set of algebraic equations. This makes it possible to distinguish the desired signal  $T_i$  with the required accuracy.

## APPENDIX B. DESCRIPTION OF THE GSFC PROGRAM

### 1. GENERAL CHARACTERISTICS

The GSFC (*Geological Space Field Calculation*) program<sup>3</sup> was developed for solving a direct 3-D gravity and magnetic prospecting problem under complicated geological conditions [144,145]. This program has been designed for computing the field of  $\Delta g$  (Bouguer, free-air or observed value anomalies),  $\Delta Z, \Delta X, \Delta Y, \Delta T$ , as well as second derivatives of the gravitational potential under conditions of rugged relief and inclined magnetization. The geological space can be approximated by (1) three-dimensional, (2) semi-infinite bodies and (3) those infinite along the strike (closed, L.H. non-closed, R.H. non-closed and open) (Fig.B1). Geological bodies are approximated

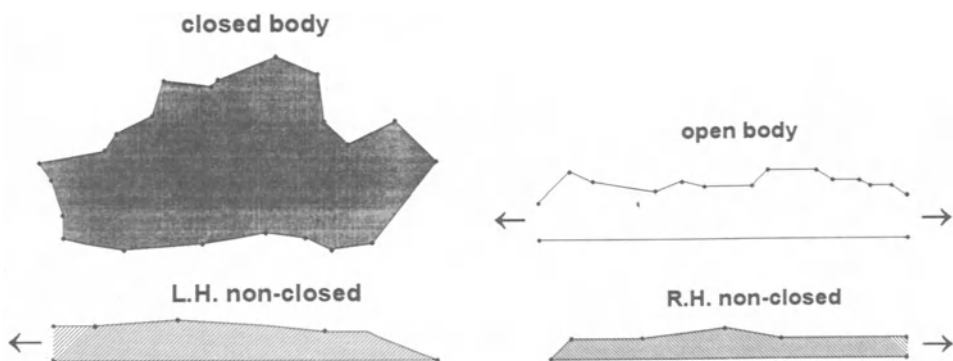


**Fig.B1. Types of geological bodies used in modeling**

by horizontal polygonal prisms. The program has the following main advantages (besides above mentioned ones):

- (1) Simultaneous computing of gravitational and magnetic fields;

---

<sup>3</sup>First version

- (2) Description of the terrain relief by irregularly placed characteristic points;
- (3) Computation of the effect of the earth-air boundary by the method of selection directly in the process of interpretation;
- (4) Modeling of the selected profiles with flowing over rugged relief or at various arbitrary levels (using characteristic points);
- (5) Simultaneous modeling of several profiles;
- (6) Description of a large number of geological bodies and fragments.

The basic algorithm realized in the GSFC program is the solution of the direct 3-D problem of gravimetric and magnetic prospecting for horizontal polygonal prism limited in the strike direction. Such an approximation is more exact than the approximation by cylinders (filling up the body's contour) or parallelepipeds which are a special case of prisms. In the well-known Talwani's [271] algorithm (where bodies are approximated by vertical polyhedron prisms), the double integration is carried out over contour and third integration is realized numerically. In the presented algorithm integration over a volume is realized on the surface limiting the anomalous body. Further, many geological objects possess a distinct strike, which is an additional reason for approximation of geological objects by horizontal prisms. According Talwani et al. [272], 3-D bodies can be approximated by thin horizontal plates. However, for exact approximation of anomalous bodies these plates must be very closely spaced. As a result, the amount of computations is drastically increased.

## 2. ANALYTICAL EXPRESSION OF THE FIRST AND THE SECOND DERIVATIVES OF GRAVITY POTENTIAL FOR 3-D BODIES

### First derivatives

Analytical expression for the first vertical derivative of gravity potential of ( $m-1$ ) angle horizontal prism (Fig.B2) has been obtained by integrating a common analytical expression:

$$U_{z'} = - \int_s \frac{z}{(R+y)R} dx dz \Big|_{y_1}^{y_2}, \quad (B1)$$

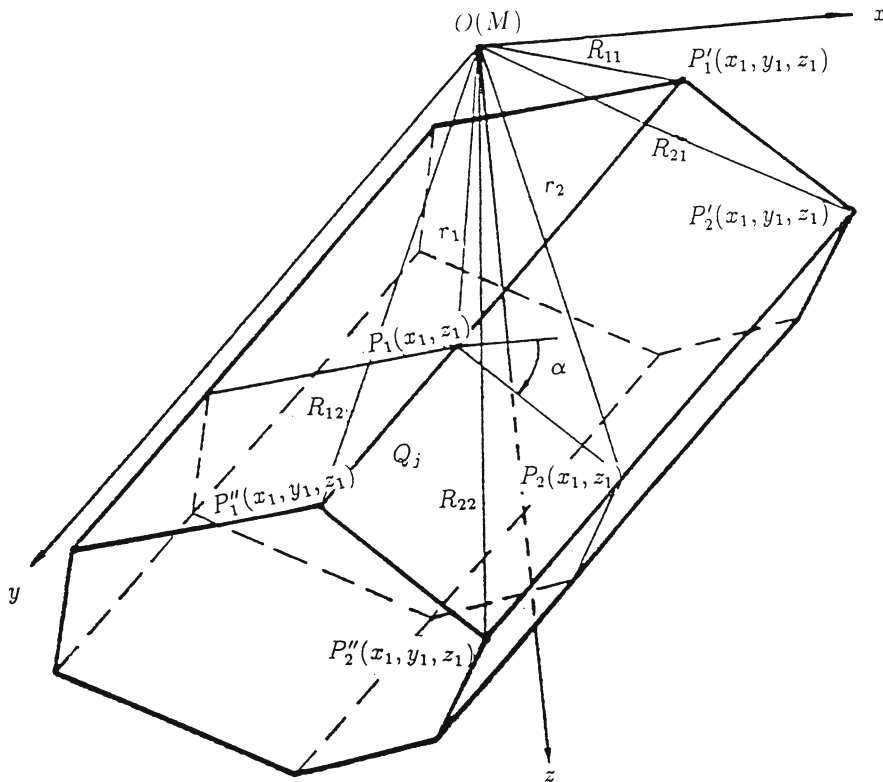


Fig.B2. A diagram for computing derivatives of gravity potential for a horizontal polygonal prism

where  $R = \sqrt{x^2 + y^2 + z^2}$ ,  $S$  is the area of normal section of the prism by the plane of  $xOz$ .

It has the following form:

$$\begin{aligned}
 U_{z',T} = & -G\sigma \sum_{j=1}^{m-1} \left[ V_j \sin \alpha_j \left( \ln \frac{R_{12j}+y_2}{R_{22j}+y_2} - \ln \frac{R_{11j}+y_1}{R_{21j}+y_1} \right) + \right. \\
 & V_j \cos \alpha_j \left( \operatorname{sgn}(y_2 V_j) \arccos \frac{\frac{V_j^2 R_{12j} R_{22j} + U_{1j} U_{2j} y_2^2}{r_{1j} r_{2j} (y_2^2 + V_j^2)} - \right. \\
 & \left. \operatorname{sgn}(y_1 V_j) \arccos \frac{\frac{V_j^2 R_{11j} R_{21j} + U_{1j} U_{2j} y_1^2}{r_{1j} r_{2j} (y_1^2 + V_j^2)} + \right. \\
 & \left. \cos \alpha_j \left( y_2 \ln \frac{R_{12j}+U_{1j}}{R_{22j}+U_{2j}} - y_1 \ln \frac{R_{11j}+U_{1j}}{R_{21j}+U_{2j}} \right) \right] \quad (B2)
 \end{aligned}$$

where  $G$  is the gravitational constant,  $\sigma$  is the density of the body,

$\alpha_j$  is the angle of the prism's side inclination;

$$\left. \begin{aligned} \cos \alpha_j &= \frac{x_{2j} - x_{1j}}{r_{12j}} \\ \sin \alpha_j &= \frac{z_{2j} - z_{1j}}{r_{12j}} \end{aligned} \right\}, \quad (B3)$$

$x_{1j}, z_{1j}$  and  $x_{2j}, z_{2j}$  are coordinates of points  $P_{1j}$  and  $P_{2j}$  (angle points of  $j$ -side of  $(m-1)$  polyhedron);  $r_{12j}$  is the length of  $j$ -side of this polyhedron:

$$r_{12j} = \sqrt{(x_{2j} - x_{1j})^2 + (z_{2j} - z_{1j})^2},$$

$r_{1j}$  and  $r_{2j}$  are distances from the selected point  $M$  to the points  $P_{1j}$  and  $P_{2j}$ , respectively:

$$\left. \begin{aligned} r_{1j} &= \sqrt{x_{1j}^2 + z_{1j}^2} \\ r_{2j} &= \sqrt{x_{2j}^2 + z_{2j}^2} \end{aligned} \right\},$$

$R_{11j}, R_{21j}, R_{12j}, R_{22j}$  are distances from the selected point  $M$  to angle points  $R_{1j'}, R_{2j'}, R_{1j''}$  and  $R_{2j''}$ , respectively, for  $j$ -side of the prism:

$$\left. \begin{aligned} R_{11j} &= \sqrt{r_{1j}^2 + y_1^2} \\ R_{21j} &= \sqrt{r_{2j}^2 + y_1^2} \\ R_{12j} &= \sqrt{r_{1j}^2 + y_2^2} \\ R_{22j} &= \sqrt{r_{2j}^2 + y_2^2} \end{aligned} \right\}. \quad (B4)$$

Here  $y_1$  and  $y_2$  are ordinates of prism end faces in the direction of the strike ( $y_2 > y_1$ );  $U_{1j}, V_j$  and  $U_{2j}, V_j$  are coordinates of points  $P_{1j}$  and  $P_{2j}$  in the inclined coordinate system  $uOv$ , respectively; the axis  $Ou$  is parallel to  $j$ -th prism's side and is directed from the point  $P_{1j}$  to the point  $P_{2j}$  ( $U_{2j} > U_{1j}$  is always valid):

$$\left. \begin{aligned} U_{1j} &= x_{1j} \cos \alpha_j + z_{1j} \sin \alpha_j \\ U_{2j} &= x_{2j} \cos \alpha_j + z_{2j} \sin \alpha_j \\ V_j &= -x_{1j} \sin \alpha_j + z_{1j} \cos \alpha_j \\ &= -x_{2j} \sin \alpha_j + z_{2j} \cos \alpha_j. \end{aligned} \right\} \quad (B5)$$

Here  $U_{1j}, U_{2j}$  and  $V_j$  are the visible solid angles of corresponding parts of the prism's  $j$ -th side.

To conduct computations in the origin of coordinates, it is sufficient to describe the coordinates of vertices of ( $m-1$ ) polyhedron formed in the normal section of the prism, and ordinates of *L.H.* and *R.H.* end faces.

The vertices are bypassed in the clockwise direction. Indices are  $x_j = x_{1j}$ ,  $x_{j+1} = x_{2j} = x_{1j+1}$ ,  $z_j = z_{1j}$ ,  $z_{j+1} = z_{2j} = z_{1j+1}$ , etc. Thus, the coordinates of the last ( $m$ -th) vertex must coincide with coordinates of the first vertex of the ( $m-1$ ) polyhedron. Respectively,  $r_j = r_{2j} = r_{1j+1}$ ,  $R_{21j} = R_{11j+1}$ ,  $R_{22j} = R_{12j+1}$ . These properties were used to decrease the amount of computations.

Let us introduce the following designations:

$$FT_{1j} = \ln \left( \frac{R_{12j} + y_2}{R_{22j} + y_2} / \frac{R_{11j} + y_1}{R_{21j} + y_1} \right), \quad (B6)$$

$$FT_{2j} = FT_{22j} - FT_{21j}, \quad (B7)$$

$$FT_{22j} = \operatorname{sgn} (y_2 V_1) \arccos \frac{V_j^2 R_{12j} R_{22j} + U_{1j} U_{2j} y_2^2}{r_{1j} r_{2j} (y_2^2 + V_j^2)}, \quad (B8)$$

$$FT_{21j} = \operatorname{sgn} (y_1 V_j) \arccos \frac{V_j^2 R_{11j} R_{21j} + U_{1j} U_{2j} y_1^2}{r_{1j} r_{2j} (y_1^2 + V_j^2)}, \quad (B9)$$

$$FT_{3j} = FT_{32j} - FT_{31j}, \quad (B10)$$

$$FT_{32j} = \ln \frac{R_{12j} + U_{1j}}{R_{22j} + U_{2j}}, \quad (B11)$$

$$FT_{31j} = \ln \frac{R_{11j} + U_{1j}}{R_{21j} + U_{2j}}. \quad (B12)$$

Thus, the expression (B2) can be written more compactly:

$$U_{z',T} = \sum_{j=1}^{m-1} \left[ V_j \left( \sin \alpha_j FT_{1j} + \cos \alpha_j FT_{2j} \right) + \right. \\ \left. \cos \alpha_j \left( y_2 FT_{32j} - y_1 FT_{31j} \right) \right]. \quad (B13)$$

The expressions for bodies outlined as *R.H.*, *L.H.* or open ones are of different form. A common equation for these types of bodies

(including formula (B13)) can be written as follows:

$$U_{z',T} = - \left[ \begin{aligned} & FK(z_1 ET_{21} + y_2 ET_{321} - y_1 ET_{311}) + \sum_{j=1}^{m-B(m-q)-1} \left( V_j (\sin \alpha_j \right. \\ & \left. FT_{1j} + \cos \alpha_j FT_{2j}) + \cos \alpha_j (y_2 FT_{32j} - y_1 FT_{31j}) \right) + B(z_q CT_{2q} + \\ & y_2 CT_{32q} - y_1 CT_{31q}) - B(z_{q+1} CT_{2q+1} + y_2 CT_{32q+1} - y_1 CT_{31q+1}) + \\ & B_{j=q+1}^{m+1} \left( V_j (\sin \alpha_j FT_{1j} + \cos \alpha_j FT_{2j}) + \cos \alpha_j (y_2 FT_{32j} - y_1 FT_{31j}) \right) - \\ & FK(z_m ET_{2m} + y_2 ET_{32m} - y_1 ET_{31m}) \end{aligned} \right], \quad (B14)$$

where  $FK = -1$  (a), 0 (b) and 1 (c) for R.H. (a), closed (b) and L.H. and open (c) contours, respectively (thus,  $FK = \text{sgn } IK$ );  $m$  is the number of contour's angle points;

$$B = \text{sgn} [\text{sgn} (IK - 2) + 1], \quad (B15)$$

$$ET_{2s} = ET_{22s} - ET_{21s}, \quad (B16)$$

$$ET_{22s} = \text{sgn} (y_2 z_s) \arccos \frac{r_s^2 - FK R_{s,2} x_s}{r_s (R_{s,2} - FK x_s)}, \quad (B17)$$

$$ET_{21s} = \text{sgn} (y_1 z_s) \arccos \frac{r_s^2 - FK R_{s,1} x_s}{r_s (R_{s,1} - FK x_s)}, \quad (B18)$$

$$ET_{3s} = ET_{32s} - ET_{31s}, \quad (B19)$$

$$ET_{32s} = \ln(R_{s,2} - FK x_s), \quad ET_{31s} = \ln(R_{s,1} - FK x_s), \quad (B20)$$

where  $s = 1$  or  $s = m$ ,

$$CT_{2t} = CT_{22t} - CT_{21t}, \quad (B21)$$

$$CT_{22t} = \text{sgn} (y_2 z_t) \arccos \frac{r_t^2 + R_{t,2} x_t}{r_t (R_{t,2} + x_t)}, \quad (B22)$$

$$CT_{21t} = \text{sgn} (y_1 z_t) \arccos \frac{r_t^2 + R_{t,1} x_t}{r_t (R_{t,1} + x_t)}, \quad (B23)$$

$$CT_{3t} = CT_{32t} - CT_{31t}, \quad (B24)$$

$$CT_{32t} = \ln(R_{t,2} + x_t), \quad CT_{31t} = \ln(R_{t,1} + x_t), \quad (B25)$$

where  $t = q$  or  $t = q + 1$ .

The analytical expression of the first horizontal (along the  $Ox'$  axis) derivative of the gravity potential of the prism under study has been obtained by integrating the expression

$$U_{x'} = - \int_s \frac{x}{(R+y)R} dx dz \Big|_{y_1}^{y_2}. \quad (B26)$$

Using expressions (B6)–(B12) the expression (B26) can be written in the following form:

$$U_{x',T} = \sum_{j=1}^{m-1} \left[ V_j \left( -\cos \alpha_j FT_{1j} + \sin \alpha_j FT_2 \right) + \right. \\ \left. \sin \alpha_j \left( y_2 FT_{32j} - y_1 FT_{31j} \right) \right]. \quad (B27)$$

### Second derivatives

Analytical expressions of the second derivatives of gravity potential  $U_{z'z''}$ ,  $U_{x'x''}$ ,  $U_{x'z'}$ ,  $U_{y'z'}$ ,  $U_{x'y'}$  have been obtained by differentiating expressions (B13) and (B27) on the  $x'$ ,  $y'$ ,  $z'$  coordinates of the observation point and finding limits in the  $x$  direction by moving the same prism's sides to the infinity.

The expression for  $U_{y'y'}$  has been obtained from Laplace's equation:

$$U_{x'x'} + U_{y'y'} + U_{z'z'} = 0.$$

The necessary components for computing a 3-D body potential with *closed*, *L.H.*, *R.H.* or *open* contour of the section are described below:

$$U_{z'z',T} = FK ET_{21} + \sum_{j=1}^{m-B(m-q)-1} \cos \alpha_j \left( FT_{1j} + \right. \\ \left. \cos \alpha_j FT_{1j} \right) + B \left[ CT_{2q} - CT_{2q+1} + \sum_{j=q+1}^{m-1} \cos \alpha_j \right. \\ \left. \left( \sin \alpha_j FT_{1j} + \cos \alpha_j FT_{2j} \right) \right] - FK ET_{2m}, \quad (B28)$$

$$U_{x'z',T} = - \sum_{j=1}^{m-B(m-q)-1} \sin \alpha_j \sin \left( FT_{1j} + \cos \alpha_j FT_{2j} \right) + \\ B \sum_{j=q+1}^{m-1} \sin \alpha_j \left( \sin \alpha_j FT_{1j} + \cos \alpha_j FT_{2j} \right) \quad (B29)$$

$$U_{y'y',T} = - \left[ \begin{array}{l} FK ET_{21} + \sum_{j=1}^{m-B(m-q)-1} FT_{2j} + CT_{2q} - \\ CT_{2q+1} + \sum_{j=1}^{m-1} FT_{2j} \end{array} \right] - FK ET_{2m}, \quad (B30)$$

$$U_{y'z',T} = FK ET_{31} + \sum_{j=1}^{m-B(m-q)-1} \cos \alpha_j FT_{3j} + \\ B \left( CT_{3q} - CT_{3q+1} + \sum_{j=1}^{m-1} \cos \alpha_j FT_{3j} \right) - FK ET_{3m}, \quad (B31)$$

$$U_{x'y',T} = - \sum_{j=1}^{m-B(m-q)-1} \sin \alpha_j FT_{3j} - B \sum_{j=q+1}^{m-1} \sin \alpha_j FT_{3j}. \quad (B32)$$

### Analytical expressions of the first and second derivatives of gravity potential for bodies unlimited along the strike

If the end faces of the selected body are outside the investigated area of geological space ( $y_2 \rightarrow \infty$ ,  $y_1 \rightarrow -\infty$ ), formulas (B14) and (B28)–(B32) become rather simple. Let us introduce the following designations:

$$\left. \begin{array}{ll} FD_{1j} = -\frac{1}{2} \lim_{\substack{y_1 \rightarrow -\infty \\ y_2 \rightarrow \infty}} FT_{1j}, & FD_2 = \frac{1}{2} \lim_{\substack{y_1 \rightarrow -\infty \\ y_2 \rightarrow \infty}} FT_{2j}, \\ ED_{2j} = \frac{1}{2} \lim_{\substack{y_1 \rightarrow -\infty \\ y_2 \rightarrow \infty}} FT_{2j}, & CD_2 = \frac{1}{2} \lim_{\substack{y_1 \rightarrow -\infty \\ y_2 \rightarrow \infty}} CT_{2j}. \end{array} \right\}. \quad (B33)$$

After computing these limits, we obtain:

$$\left. \begin{array}{ll} FD_{1j} = \ln \frac{r_{1j}}{r_{2j}}, & FD_{2j} = sgn V_j \arccos \frac{V_j^2 + U_{1j} U_{2j}}{r_{1j} r_{2j}}, \\ FD_{2s} = sgn z_s \arccos \frac{-FK x_s}{r_s}, & CD_{2t} = sgn z_t \arccos \frac{x_t}{r_t}. \end{array} \right\}. \quad (B34)$$

Using the obtained expressions ((B14) and (B28)–(B32)), we can write analytical formulas for the first and second derivatives of gravity potential for a 2-D body:

$$U_{z',g} = 2 \left[ \begin{array}{l} -FK z_1 ED_{21} + \sum_{j=1}^{m-B(m-q)-1} V_j (\sin \alpha_j FD_{1j} - \\ \cos \alpha_j FD_{2j}) + B \left[ -z_q CD_{2q} + z_{q+1} CD_{2q+1} + \right. \\ \left. \sum_{j=q+1}^{m-1} (\sin \alpha_j FD_{1j} - \cos \alpha_j FD_{2j}) \right] + FK z_m ED_{2m} \end{array} \right], \quad (B35)$$

$$U_{z'z',g} = 2 \left[ \begin{array}{l} FK ED_{21} + \sum_{j=1}^{m-B(m-q)-1} \cos \alpha_j (-\sin \alpha_j FD_{1j} + \\ \cos \alpha_j FD_{2j}) + B \left[ CD_{2q} - CD_{2q+1} + \sum_{j=q+1}^{m-1} (-\sin \alpha_j FD_{1j} + \right. \\ \left. \cos \alpha_j FD_{2j}) \right] - FK ED_{2m} \end{array} \right], \quad (B36)$$

$$U_{x'z',g} = 2 \left[ \begin{array}{l} \sum_{j=1}^{m-B(m-q)-1} \sin \alpha_j (\sin \alpha_j FD_{1j} - \cos \alpha_j FD_{2j}) + \\ B \sum_{j=q+1}^{m-1} \sin \alpha_j (\sin \alpha_j FD_{1j} - \cos \alpha_j FD_{2j}) \end{array} \right], \quad (B37)$$

$$U_{y'y',g} = -2 \left[ \begin{array}{l} FK ED_{21} + \sum_{j=1}^{m-B(m-q)-1} FD_{2j} + B(CD_{2q} - \\ CD_{2q+1} + \sum_{j=q+1}^{m-1} FD_{2j}) - FK ED_{2m} \end{array} \right] = 0, \quad (B38)$$

$$U_{y'z',g} = 0, \quad (B39)$$

$$U_{x'y',g} = 0. \quad (B40)$$

### Analytical expressions of the first and second derivatives of gravity potential for semi-infinite bodies

If one end face of a selected body is within the investigated area, while the other end face is in the infinity, we are dealing with an object termed a semi-infinite body. We will distinguish two types of these bodies: right semi-infinite body ( $y_2 \rightarrow \infty$ ) and left semi-infinite body ( $y_1 \rightarrow -\infty$ ). Let

$$\begin{aligned} FP_{1j} &= -\lim_{y_2 \rightarrow \infty} FT_{1j}, & FP_{2j} &= \lim_{y_2 \rightarrow \infty} FT_{2j}, \\ FP_{2s} &= \lim_{y_2 \rightarrow \infty} FT_{2s}, & CP_{2t} &= \lim_{y_2 \rightarrow \infty} CT_{2t}. \end{aligned} \quad \left. \right\}, \quad (B41)$$

$$FP_{3j} = -\lim_{y_2 \rightarrow \infty} FT_{3j}, \quad (B42)$$

$$EP_{31} - EP_{3m} = -\lim_{y_2 \rightarrow \infty} (ET_{31} - ET_{3m}), \quad (B43)$$

$$CP_{3q} - CP_{3q+1} = -\lim_{y_2 \rightarrow \infty} (CT_{3q} - CT_{3q+1}). \quad (B44)$$

After computing these limits, we obtain the following equations:

$$\begin{aligned} FP_{1j} &= \ln \frac{R_{11j} + y_1}{R_{21j} + y_2}, & FP_{2j} &= FD_{2j} - FT_{21j}, \\ EP_{2s} &= ED_{2s} - ET_{21s}, & CP_{2t} &= CD_{2t} - CT_{21t} \end{aligned} \quad \left. \right\}. \quad (B45)$$

$$FP_{3j} = FT_{31j}, \quad (B46)$$

$$EP_{3s} = ET_{31s}, \quad (s = 1, m), \quad (B47)$$

$$CP_{3t} = CT_{31t}, \quad (t = q, q + 1), \quad (B48)$$

We also have the following limits:

$$\lim_{y_2 \rightarrow \infty} [\cos \alpha_j (y_2 FT_{32j} - y_1 FT_{31j})] = (x_{1j} - x_{2j}) - \cos \alpha_j y_1 FP_{3j}, \quad (B49)$$

$$\lim_{y_2 \rightarrow \infty} (y_2 ET_{32s} - y_1 ET_{31s}) = -FK x_s - y_1 EP_{3s}, \quad (B50)$$

$$\lim_{y_2 \rightarrow \infty} (y_2 CT_{32t} - y_1 CT_{31t}) = x_t - y_1 CP_{3t}, \quad (B51)$$

If we determine the limits (B41)–(B44) and (B49)–(B51) by  $y_1 \rightarrow -\infty$ , and then change  $y_2$  by  $-y_1$  the expressions (B45) and (B49)–(B51) will have the same value, while in the expressions (B46)–(B48) only the sign changes. Therefore, we needn't distinguish left and right semi-infinite bodies, if a limited ordinate is determined by the expression

$$y_1 = FY \cdot y_{lim} \quad (B52)$$

(where  $FY = 1$  and  $-1$  for right and left semi-infinite bodies, respectively), and if the expressions containing equations (B42)–(B44) are computed with additional multiplication by the factor  $FY$ .

Using equations (B14), (B28)–(B32), (B41)–(B43) and (B49)–(B52), we can write the following analytical expressions of the first and second derivatives of gravity potential for bodies that are semi-infinite along the strike:

$$U_{z',l} = -FK(z_1 EP_{21} - y_1 EP_{31}) + \sum_{j=1}^{m-B(m-q)-1} \left[ V_j (\sin \alpha_j FP_{1j} - \cos \alpha_j FP_{2j}) + y_1 \cos \alpha_j FP_{3j} \right] - B(z_q CP_{2q} - y_1 CP_{3q}) + \left. B(z_{q+1} CP_{2q+1} - y_1 CP_{3q+1}) + B \sum_{j=q+1}^{m-1} \left[ V_j (\sin \alpha_j FP_{1j} - \cos \alpha_j FP_{2j}) + y_1 \cos \alpha_j FP_{3j} \right] + FK(z_m EP_{2m} - y_1 EP_{3m}) \right\}, \quad (B53)$$

$$U_{z'z',l} = FK EP_{21} - \sum_{j=1}^{m-B(m-q)-1} \cos \alpha_j (\sin \alpha_j FP_{1j} - \cos \alpha_j FP_{2j}) + B \left[ CP_{2q} - CP_{2q+1} - \sum_{j=q+1}^{m-1} \cos \alpha_j (\sin \alpha_j FP_{1j} - \cos \alpha_j FP_{2j}) \right] - FK EP_{2m} \quad (B54)$$

$$U_{x'z',l} = \left. \begin{aligned} & \sum_{j=1}^{m-B(m-q)-1} \sin \alpha_j (\sin \alpha_j F P_{1j} - \cos \alpha_j F P_{2j}) + \\ & B \sum_{j=q+1}^{m-1} \sin \alpha_j (\sin \alpha_j F P_{1j} - \cos \alpha_j F P_{2j}) \end{aligned} \right\}; \quad (B55)$$

$$U_{y'y',l} = \left. \begin{aligned} & -[F K E P_{2j} + \sum_{j=1}^{m-B(m-q)-1} F P_{2j} + \\ & B(C P_{2q} - C P_{2q+1} + \sum_{j=q+1}^{m-1} F P_{2j}) - F K E P_{2m}] \end{aligned} \right\}, \quad (B56)$$

$$U_{y'z',l} = \left. \begin{aligned} & -F Y [F K E P_{3j} + \sum_{j=1}^{m-B(m-q)-1} \cos \alpha_j F P_{3j} + \\ & B(C P_{3q} - C P_{3q+1} + \sum_{j=q+1}^{m-1} \cos \alpha_j F P_{3j}) - F K E P_{3m}] \end{aligned} \right\}, \quad (B57)$$

$$U_{x'y',l} = F Y \left[ \sum_{j=1}^{m-B(m-q)-1} \sin \alpha_j F P_{3j} + B \sum_{j=q+1}^{m-1} \sin \alpha_j F P_{3j} \right]. \quad (B58)$$

### Expressions for simultaneous computing gravitational and magnetic fields of anomalous bodies

The values of the gravitational and magnetic fields at the selected point  $M$  are determined using the following formulas:

$$\Delta g = CM f \sigma U_{z'}, \quad (B59)$$

$$\Delta Z = I_z U_{z'z'} + I_x U_{x'z'} + I_y U_{y'z'}, \quad (B60)$$

$$\Delta X = I_x U_{x'z'} - I_x (U_{z'z'} + U_{y'y'}) + I_y U_{x'y'}, \quad (B61)$$

$$\Delta Y = I_z U_{y'z'} + I_{x'y'} + I_y U_{y'y'}, \quad (B62)$$

$$\Delta T = W_{zz} U_{z'z'} + W_{zx} U_{x'z'} + W_{yy} U_{y'y'} + W_{yz} U_{y'z'} + W_{xy} U_{x'y'}, \quad (B63)$$

where  $CM$  is the scale of the chart;  $f=0.00667$  (gravitational constant is given in  $10^{-8}$  SI unit, i.e. measured in  $10^{-8} m^3 kg^{-1} s^{-2}$ );  $\sigma$  is the body's excess density determined using the formula:

$$\sigma = \sigma_d - \sigma_s.$$

Here  $\sigma_d$  and  $\sigma_s$  determine the densities of the anomalous body and of the surrounding medium, respectively. Density is given in  $10^3$  SI unit ( $10^3 kg/m^3$ ), i.e. in  $g/cm^3$ . At such dimensions of the density and gravitational constant, the computed gravity field will be obtained in  $10^{-5}$  SI unit (i.e.  $mGal$ ).  $I_x, I_y, I_z$  are the components of the excess magnetization vector determined using the formulas:

$$I_z = 0.1 [I_d \sin J_d - I_s \sin J_s], \quad (B64)$$

$$I_x = 0.1 \left[ I_d \cos J_d \cos(A_d - A_x) - I_s \cos J_s \cos(A_s - A_x) \right], \quad (B65)$$

$$I_x = 0.1 \left[ I_d \cos J_d \sin(A_d - A_x) - I_s \cos J_s \cos(A_s - A_x) \right], \quad (B66)$$

where  $I_d$  and  $I_s$  are magnetization values for the anomalous body and the surrounding medium, respectively; the coefficient 0.1 is introduced to obtain the magnetic field plots in  $nT$ ;  $I_d$  and  $J_s$  are the inclinations of the magnetization vector of the body and the medium to the horizon, respectively;  $A_d$  and  $A_s$  are azimuths of the magnetization vector horizontal projections for the body and the medium, respectively;  $A_x$  is the azimuth of the selected profile. Values  $WW_{zz}$ ,  $WW_{xz}$ ,  $WW_{yy}$ ,  $WW_{yz}$ ,  $WW_{xy}$  are connected with the vector of redundant magnetization and with components of the geomagnetic field vector:

$$\begin{aligned} W_{zz} &= W_z I_z - W_x I_x; \\ W_{xz} &= W_x I_z + W_z I_x; \\ W_{yy} &= W_y I_y - W_x I_x; \\ W_{yz} &= W_y I_z + W_z I_y; \\ W_{xy} &= W_x I_y + W_y I_x. \end{aligned} \quad (B67)$$

Orthogonal components of the geomagnetic field vector can be determined by formulas:

$$\begin{aligned} W_x &= \sin i_o; \\ W_x &= \cos i_o \cos(A_o - A_x); \\ W_y &= \cos i_o \sin(A_o - A_x), \end{aligned} \quad (B68)$$

where  $i_o$  is the geomagnetic inclination,  $A_o$  is the geomagnetic declination.

### Computation of gravitational field reductions

Computation of gravitational field with the Bouguer (*a*) and free-air (*b*) reduction and observed values (*c*) is realized using the following formulas:

$$\begin{aligned} \Delta g_B &= \Delta g_M + \Delta g_{SR}; \\ \Delta g_{f.a.} &= \Delta g_M; \\ \Delta g_{obs} &= \Delta g_M - 0.3086 H_{abs}, \end{aligned} \quad (B69)$$

where  $\Delta g_M$  is the field of the geological space model;  $\Delta g_{SR}$  is a negative effect of a homogeneous body with the density  $\sigma_R$  (the top of the body coinciding with terrain relief and the bottom being horizontal at the sea level);  $H_{abs}$  is absolute height of the selected point  $M$ ,  $\Delta g_{obs}$  is acceleration of gravity observed on the earth's surface.

These formulas have been obtained from conventional expression of Bouguer reduction:

$$\Delta g_B = g_{obs} - \gamma_o + 0.3086 H_{abs} - 0.0419 \sigma_R H_{abs} + g_{corr}, \quad (B70)$$

where  $g_{obs}$  is the observed value of gravity acceleration;  $\gamma_o$  is the normal value of gravity acceleration on the earth's spheroid;  $0.3086 H_{abs}$  is the elevation correction;  $-0.0419 \sigma_R H_{abs}$  is the correction for the attraction of intermediate plane-parallel layer with density  $\sigma_R$  and thickness  $H_{abs}$ . The value  $g_{corr}$  is the correction for the influence of the surrounding terrain relief.

From Fig.B3 it is apparent that

$$\Delta g_{SR} = -\left(0.0419 \sigma_R H_{abs} - g_{corr}\right). \quad (B71)$$

The observed anomaly of gravitational field can be designated as

$$\Delta g_{obs} = g_{obs} - \gamma_o. \quad (B72)$$

Using expressions (B71) and (B72), expression (B70) can be written in the following form:

$$\Delta g_B = \Delta g_{obs} + 0.3086 H_{abs} + \Delta g_{SR}. \quad (B73)$$

If we do not introduce the plane-parallel layer and terrain correction, we obtain the expression of free-air anomaly:

$$\Delta g_{f.a.} = \Delta g_{obs} + 0.3086 H_{abs}. \quad (B74)$$

This follows directly from equation (B69).

This expression determines the field  $\Delta g_M$  from the geological space model with the accuracy to a certain constant<sup>4</sup>, as an effect from common model is calculated at terrain relief points. This is equivalent to introducing free-air correction into the value  $\Delta g_{obs}$ .

---

<sup>4</sup>In a geological model the effects of all described bodies are computed to some deep horizontal level. Below this level, because of the absence of data, density of rocks can be assumed constant. Also, a constant effect of this deep layer can be considered as a part of the value  $\gamma_o$ .

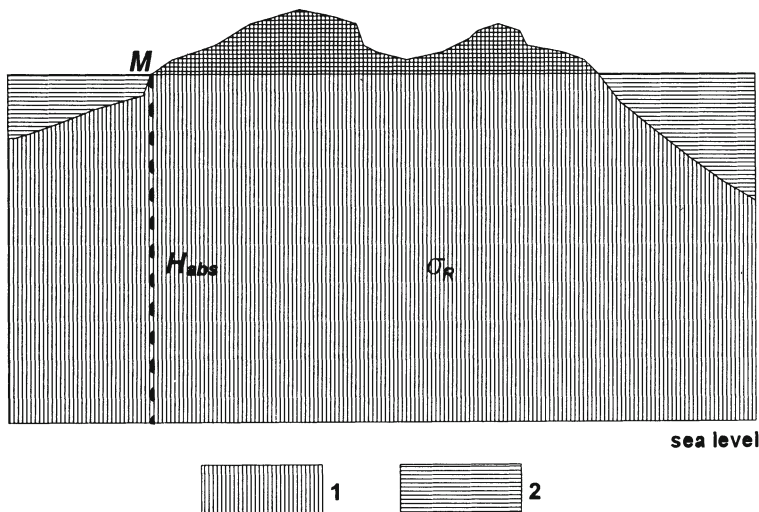


**Fig.B3. Diagram of  $\Delta g_B$  determination**

(1) area where the relief correction is computed; (2) homogeneous body with density  $\sigma_R$  (gravity effect in the point  $M$  is equal to the effect from plane-parallel layer with the account of terrain correction)

## REFERENCES

- [1] Adler, J.L.: Simplification of Tidal Corrections for Gravity Meter Surveys, *Geophysics* **7** (1942), 35–44.
- [2] Affleck, J. (Special Editor): *Special issue on magnetic methods*, *Geophysics* **29** No.4 (1964).
- [3] Akselrod, S.M. and Putkaradze, L.A.: *Integrated interpretation of logging with due account of variations in physical properties of the object under study*, Review of VIEMS, Ser. Region., Razv. i Promysl. Geofiz., Moscow, 1979 (in Russian).
- [4] Alexeyev, V.V.: Application of the self-potential method under the conditions of mountainous relief, *Razv. i Okhrana Nedr* No.9 (1971) 38–63 (in Russian).
- [5] Alexeyev, V.V.: *Development and improvement of the magnetic anomalies interpretation methods under conditions of inclined magnetization and sloping relief (a specific example of Belokan-Zakatala ore district, southern slope of the Greater Caucasus)*, Ph.D Theses. Dnepropetrovsk, Mining University, 1976 (in Russian).
- [6] Alexeyev, V.V. and Khesin, B.E.: *Interpretation of magnetic observations in orogens of the South of the USSR*, Review of VIEMS, Ser. Region., Razv. i Promysl. Geofiz., Moscow, 1971 (in Russian).
- [7] Alexeyev, V.V. and Khesin, B.E.: Processing and interpretation of gravimetric data in mountainous regions, *Prikladnaya Geofizika* No.117, (1987) 90–100 (in Russian).
- [8] Alexeyev, V.V. and Khesin, B.E.: Grouping of gravimetric observation points as a means of suppressing near-surface noises and determining the effective density, *Deposited by VINITI, USSR Academy of Sciences* No. 5721-B85 (1989) (in Russian).
- [9] Alexeyev, V.V., Khesin, B.E. and Eppelbaum, L.V.: Methods for quantitative interpretation of VLF curves in the conditions of rugged relief, *IL AzNIINTI, Baku* No.6, (1986) (in Russian).
- [10] Alexidze, M.A.: *Approximate methods for solving direct and inverse problems of gravimetry*, Nauka, Moscow, 1987, (in Russian).
- [11] Alpin, L.M., Dayev, D.S. and Karinsky, A.D.: *Theory of fields employed in geophysical prospecting*, Nedra, Moscow, 1985 (in Russian).
- [12] Andreyev, B.A. and Klushin, I.G.: *Geological interpretation of gravitational anomalies*, Gostoptekhizdat, Leningrad, 1962 (in Russian).
- [13] Antonic, S. Electromagnetic investigation by the VLF-method of the ore bearing veins in the Hornsund Fiord area, *Polish polar research* No.6 (1985), 349–356.
- [14] Appel, K., and Haken, W.: Every planar map is four colorable: Part 1, Discharging, *Ill. S. Math.* **21** 3 (1977), 424–490.
- [15] Appel, K., Haken, W., and Koch, S.: Every planar map is four colorable: Part 2,

- Reducibility, *Ill S. Math.* **21** 3 (1977), 491–567.
- [16] Aronov, V.I.: *Computer processing of gravitational anomalies under arbitrary relief of observation surface*, Nedra, Moscow, 1976 (in Russian).
- [17] Auzin, A.K.: *Electrical prospecting*, Nedra, Moscow, 1977 (in Russian).
- [18] Avdevich, M.M. and Fokin, A.F.: *Electrical modeling of potential geophysical fields*, Nedra, Leningrad, 1978 (in Russian).
- [19] Barabash, Yu.L., Barsky, B.V., Zinovyev, V.T. Kirichenko, V.S. and Sapegin, V.F.: *Items of statistical theory of recognition*, Sovetskoe Radio, Moscow, 1967 (in Russian).
- [20] Baranov, V.: A new method for interpretation of aeromagnetic maps: Pseudo-gravimeric anomalies, *Geophysics* **22** No.2 (1957), 359–383.
- [21] Bartov, Y., Eyal, M., Shimron, A.E. and Bentor, Y.K.: *Sinai Geological Map. Scale 1:500,000*, Prepared and printed by the Geological Society of Israel, 1980.
- [22] Baryshev, A.S., Vakhromeyev, G.S., Zhitkov, A.N. and Kovalevich, V.B.: *Geophysical methods of prospecting for iron ore deposits on the South of Eastern Siberia*, Nedra, Moscow, 1980 (in Russian).
- [23] Batoroyev, K.B.: *Cybernetics and analogy method*, Vysshaya Shkola, Moscow, 1974 (in Russian).
- [24] Belash, V.A.: On some methods for the interpretation of the induced polarization observations, *Geologiya i Geofizika* No.7 (1961), 90–95 (in Russian).
- [25] Ben-Avraham, Z. and Ginzburg, A.: Magnetic anomalies over the Central Levant continental margin, *Marine and Petroleum Geology* **3** (1986), 220–233.
- [26] Ben-Avraham, Z., Shoham, V., Klein, E., Michelzon, H. and Serruya, C.: Magnetic survey of Lake Kinneret – Central Jordan Valley, Israel, *Marine Geoph. Res.* **4** (1980), 257–276.
- [27] Berezhnaya, L.T. and Telepin, M.A.: Reduction of the observed potential field to the common level and a problem of its further transformation, *Razvedochnaya Geofizika* Vyp.16 (1966), 38–46 (in Russian).
- [28] Berezkin, V.M.: *Accounting for terrain relief and interlayer effects in gravity prospecting*, Nedra, Moscow, 1967 (in Russian).
- [29] Berezkin, V.M.: *Complete gradient method in geophysical prospecting*, Nedra, Moscow, 1988 (in Russian).
- [30] Berezkin, V.M., Kirichek, M.A. and Kunarev, A.A.: *Application of geophysical survey methods for direct oil and gas prospecting*, Nedra, Moscow, 1978 (in Russian).
- [31] Besprozvanny, P.A. and Chernov, A.A.: *Automated complexes (systems) of gravimetric data processing*, Review of VIEMS, Ser. Region., Razv. i Promysl. Geofiz, Moscow, 1976 (in Russian).
- [32] Bhattacharyya, B.K. and Chan, K.C.: Reduction of magnetic and gravity data on an arbitrary surface acquired in a region of high topographic relief, *Geophysics* **42** No.7 (1977), 1411–1430.
- [33] Blakely, R.J.: *Potential theory in gravity and magnetic applications*, Cambridge Univ. Press, 1995.
- [34] Boldyreva, V.A., Kanter, N.D. and Chernov, A.A.: *Automated complex for gravimetric observation processing*, Nedra, Moscow, 1976 (in Russian).

- [35] Bongard, M.M.: *Problem of recognition*, Nauka, Moscow, 1967 (in Russian).
- [36] Borisovich, V.T. and Eppelbaum, V.M.: *Optimization of ore exploration in mountainous regions*, Nedra, Moscow, 1988 (in Russian).
- [37] Borodaevskaya, M.B., Krivtsov, A.T. and Shirai, E.P.: *Types of pyrite-bearing provinces and methods for predicting pyrite mineralization*, Review of VIEMS, Ser. Geol., Metody Poiskov i Razv. Mestor. Pol. Isk., Moscow, 1977 (in Russian).
- [38] Borovko, N.N.: *Statistical analysis of spatial geological regularities*, Nedra, Leningrad, 1971 (in Russian).
- [39] Borovko, N.N.: Applicability and effectiveness of various recognition schemes for typical geological problems, *Metody Razved. Geofiziki* Vyp. 15 (1972), 5–14 (in Russian).
- [40] Borovko, N.N.: *Quantitative analysis of prospecting criteria for endogenic ore deposits*, Review of VIEMS, Ser. Geol., Metody Poiskov i Razv. Mestor. Pol. Isk., Moscow, 1973 (in Russian).
- [41] Borovko, N.N.: *Optimization of geophysical investigations in ore deposit prospecting*, Nedra, Leningrad, 1979 (in Russian).
- [42] Borovko, N.N., Mishin, L.T. and Latikainen, V.I.: *Techniques of quantitative field description for predicting stanniferous deposits on a scale of 1:50,000. Methodological Directions*, VIRG, Leningrad, 1969 (in Russian).
- [43] Brillouin, L.N.: *Science and information theory*. 2nd edition, Academic Press, N.Y., 1962.
- [44] Brodovoy, V.V. and Nikitin, A.A. (Eds.): *Integration of methods in exploration geophysics. Geophysicist's manual*, Nedra, Moscow, 1984 (in Russian).
- [45] Brodsky, M.A. and Strakhov, V.N.: On the solution of the inverse potential problem for polyhedrons with polynomial densities, *Dokl. AN SSSR* **293** No.2 (1987), 336–339.
- [46] Bugaets, A.N. and Dudenko, L.N.: *Mathematical methods for predicting economic mineral deposits*, Nedra, Leningrad, 1976 (in Russian).
- [47] Bukhnikashvili, A.V., Kebuladze, V.V., Tabagua, G.G., Dzhashi, G.G., Gugunava, G.E., Tatishvili, O.V. and Gogua, R.A.: *Geophysical exploration of Adzar group of copper-polymetallic deposits*, Metsnireba, Tbilisi, 1974 (in Russian).
- [48] Bulakh, E.G., Markova, M.N., Timoshenko, V.I. and Boiko, P.D.: *Mathematical support for automated system of gravitational anomalies interpretation (minimizing method)*, Naukova Dumka, Kiev, 1983 (in Russian).
- [49] Bulakh, E.G., Rzhanitsyn, V.A. and Markova, M.N.: *Application of minimizing method to solving structural geology problems using gravity observations*, Naukova Dumka, Kiev, 1976 (in Russian).
- [50] Carslaw, H.S. and Yaeger, J.C.: *Conduction of Heat in Solids*, 2nd edition, Oxford Univ. Press, 1959.
- [51] Chekalyuk, E.B., Fedortsev, I.M. and Osadchy, V.G.: *Geothermal field survey*, Naukova Dumka, Kiev, 1974 (in Russian).
- [52] Cheremensky, G.A.: *Geothermics*, Nedra, Leningrad, 1972 (in Russian).
- [53] Demidovich, O.A.: 1969. *Singling out weak geophysical anomalies by a statistical method*, Nedra, Moscow, 1969 (in Russian).
- [54] Demura, G.V., Nikitin A.A. and Tarkhov, A.G.: *Classification of geological objects*

- by the data obtained using a set of geophysical methods based on the principle of self-training, *Izv. VUZov, Ser. Geol. i Razv.* No.2 (1974), 133–142 (in Russian).
- [55] Detkova, N.V. and Shopin, Yu.G.: Estimation of correlation between the elastic wave velocity and the density for magmatic and metamorphic rocks in the ore-bearing regions of the Altai and Lesser Caucasus, *Voprosy Razv. Geof. Vyp.9* (1969), 160–163 (in Russian).
- [56] Dillahunt, R.C., Fash, I.L., Parsley, L.R. and Townsend, D.W.: Geophysical data base, *Geophysical Prospecting* **28** No.4 (1980), 459–512.
- [57] Dmitriyev, V.I. (Editor): *Computing mathematics and computer methods in exploration geophysics. Geophysicist's manual*, Nedra, Moscow, 1982 (in Russian).
- [58] Dmitriyev, V.I., Baryshnikova, I.A. and Zakharov, E.V.: *Anomalous electromagnetic fields of the beds*, Nedra, Leningrad, 1977 (in Russian).
- [59] Dmitriyev, V.I. and Farzan, R.Kh.: A method for calculating anomalous electromagnetic field caused by a local inhomogeneity, In: *Mathematical models of electromagnetic prospecting in geophysics* Budapest, (1980), 13–29.
- [60] Dmitriyeva, T.A., Kaner, V.V., Skornyakov, S.M. and Semenov, V.G.: Theoretical analysis of temperature fields in near-surface horizons for 2-D and 1-D ore body models, *Deposited by VINITI, USSR Academy of Sciences No.5191-85* (1985) (in Russian).
- [61] Dobrin, M.B.: *Introduction to geophysical prospecting*. 3rd ed., McGraw-Hill, N.Y., 1976.
- [62] Dobrynina, Z.K., Dmitriyeva, T.A., Pletnev, A.A. Semenov, V.G. and Skornyakov, S.M.: Shaping of seasonal thermal anomalies over ore bodies, *Izv. VUZov, Ser. Geol i Razv.* No.8 (1985), 98–101 (in Russian).
- [63] Druskin, V.L., Knizhnerman, L.A., Kosenkov, O.M., Tamarchenko, T.V. and Shchedrina, S.V.: Solution of direct and inverse problems of logging and electric prospecting in complicated models. *Transactions of the 34th international Geophysical Symposium*, Budapest, (1989) 797–800.
- [64] Dubinyuk, P.F., Kulinkovich, A.E. and Lantsman, A.Kh.: *On informational jump in integrated interpretation of logging data*, Review of VIEMS, Ser. Region., Razv. i Promysl. Geofiz., Moscow (1970), 102–106 (in Russian).
- [65] Duckworth, K. and Calvert, H.T.: An examination of the relationship between time-domain integral chargeability and the Cole-Cole impedance model, *Geophysics* **60** 4 (1995), 1249–1252.
- [66] Duda, R.O. and Hart, P.E. *Pattern classification and scene analysis*, John Wiley & Sons, N.Y., 1973.
- [67] Dukhovsky, A.A., Ilayev, M.G. and Kronidov, I.I.: *Geophysical investigations /Methodological instructions for geological survey on a 1:50,000 scale*, Nedra, Leningrad, 1970 (in Russian).
- [68] Dyadkov, P.G.: On the linearity of the geomagnetic variation secondary effects in anomalous fields by modulus measurements, *Geologiya i Geofizika* No.4 (1985), 129–136 (in Russian).
- [69] Efremova, N.A.: Peculiarities of terrain correction in detailed gravimetric survey of mountainous regions, *Metody Razv. Geof. Vyp.20* (1974), 78–84 (in Russian).
- [70] *Electrical Prospecting Instruction*, USSR Ministry of Geology, Nedra, Moscow, 1984

(in Russian).

- [71] Eppelbaum, L.V.: Multimodel approach to the study of geophysical targets, *Deposited by VINITI, USSR Academy of Sciences No.7842-87* (1987) (in Russian).
- [72] Eppelbaum, L.V.: *The development of methods for processing and interpretation of natural geophysical fields in prospecting for pyrite ores under mountainous conditions*, Ph.D Theses, Institute of Geophysics (Georgian Academy of Sciences), Tbilisi, 1989 (in Russian).
- [73] Eppelbaum, L.V.: Examples of terrain corrections in the VLF-method in the Caucasian region, USSR, *Geoexploration* **28** (1991), 67–75.
- [74] Eppelbaum, L., Itkis, S. and Khesin, B.: Modern interpretation and 3-D modeling of magnetic field by archaeological investigation *Transactions of the Conference of Israel Geological Society, Zikharon Yakov, Israel*, (1995), 25.
- [75] Eppelbaum, L.V. and Khesin, B.E.: Physico-geological models for pyrite deposits of the Filizchai and Lesser-Caucasian types, *Transactions of All-Union Meeting /Multifactor ore deposit models as the basis for developing effective methods of search, evaluation and prospecting*, Tbilisi, (1988), 126–127 (in Russian).
- [76] Eppelbaum, L.V. and Khesin, B.E.: VLF-method: elimination of noises and quantitative interpretation *Transactions of Regional Symposium on Electromagnetic Compatibility “1992 – From a Unified Region to a Unified World”, Section “LF to ULF Electromagnetics and the Earth”*, 5.2.1, Tel Aviv, (1992), 1–6.
- [77] Eppelbaum, L.V. and Mishne, L.R.: Some theoretical aspects of optimum filtration of geophysical signals with dependent noises. *Deposited by VINITI, USSR Academy of Sciences No.6034-B88* (1988) (in Russian).
- [78] Erkhov, V.A. Mishin, L.T. Stolpner, M.N. and Burde, A.I.: On the final product of geophysical prospecting for hard mineral resources, *Sovetskaya Geologiya* No.8 (1986), 24–30 (in Russian).
- [79] Erkhov, V.A., Nikitsky, V.E. and Semin, Yu.A.: Integration of methods as a necessary condition of improving the effectiveness of geophysical work, In: *Methods of Exploration Geophysics. Integration of geophysical methods for solving the prospecting problems in ore regions*, Nedra, Moscow (1984), 3–8 (in Russian).
- [80] Ernstson, K. and Scherer, V.: Self-potential variations with time and their relation to hydrogeologic and meteorological parameters, *Geophysics* **51** No.10 (1986), 1967–1977.
- [81] Erofeyev, L.Ya. and Avteneyev, G.K.: On statistical relationship between the terrain relief and magnetic field on gold deposits, *Voprosy geografii Kuzbassa i Gornogo Altaya* Vyp.4 (1971), 270–275 (in Russian).
- [82] Filippov, V.I.: A system of DB COMPAS control, *Prikladnaya Informatika* Vyp.1., Finansy i Statistika, Moscow (1982), 42–54 (in Russian).
- [83] Fitterman, D.V.: Calculation of self-potential anomalies near vertical contacts, *Geophysics* **44** No.2 (1984), 195–205.
- [84] Fotiadi, E.E. (Ed.): *Geology and Mathematics; Problems of diagnosis and identification in geology, geochemistry and geophysics*, Nauka, Novosibirsk, 1970 (in Russian).
- [85] Frazer, D.S.: Contouring of VLF-EM data, *Geophysics* **34** No.6 (1969), 958–967.
- [86] Gadjev, T.G., Karkoshkin, A.I., Khesin, B.E., Alexeyev, V.V., Potapova, E.I. and

- Salekhli, T.M.: *Petrodensity characteristics of geological associations in Azerbaijan*, Azerneshr, Baku, 1984 (in Russian).
- [87] Gadjiev, T.G., Karkoshkin, A.I., Khesin, B.E., Alexeyev, V.V., Potapova, E.I. and Salekhli, T.M.: *Petrodensity Map of the Azerbaijan SSR. Scale 1:500,000*, Map Printing Factory, Leningrad, 1985.
- [88] Garfunkel, Z.: Tectonic setting of Phanerozoic magmatism in Israel, *Isr. J. Earth Sci.* **39** No.38 (1989), 51–74.
- [89] Ginzburg, A. and Ben-Avraham, Z.: The deep structure of the central and southern Levant continental margin, *Annales Tectonicae* **1** (1987), 105–115.
- [90] Gladky, K.V.: *Gravity and magnetic prospecting*, Nedra, Moscow, 1967 (in Russian).
- [91] Goldman, M.: *Non-conventional method in geoelectric prospecting*, Ellis Horwood Ltd, Chichester, 1990.
- [92] Goldshmidt, V.I., Kuzmin, Yu.I. and Shabaldin, V.N.: An automated system of gravimetric data interpretation, In: *Theory and methods for interpreting gravity and magnetic fields*, Naukova Dumka, Kiev, (1981), 58–70 (in Russian).
- [93] Golizdra, G.Ya.: *The main methods for computer-aided solution of direct problems of gravity prospecting*, Review of VIEMS, Ser. Region., Razv. i Promysl. Geofiz., Moscow, 1977 (in Russian).
- [94] Golizdra, G.Ya.: Starting the problem of combined interpretation of gravitational fields and seismic observations, *Izv. AN SSSR, Ser. Fizika Zemli* **7** (1980), 95–100 (in Russian; in English see *Physics of the Solid Earth*).
- [95] Golovin, I.V. and Suprunenko, E.I.: Some techniques of statistical analysis of geophysical data in regional prognosis, *Metody Razv. Geofiz. Vyp. 12* (1971), 53–57 (in Russian).
- [96] Golzman, F.M.: *Statistical interpretation models*, Nauka, Moscow, 1971 (in Russian).
- [97] Golzman, F.M.: Problematic items of information-statistical theory of geophysical observation interpretation, *Izv. AN SSSR, Ser. Fizika Zemli* No.12 (1977), 75–86 (in Russian; in English see *Physics of the Solid Earth*).
- [98] Golzman, F.M. and Kalinina, T.B.: *Statistical interpretation of magnetic and gravitational anomalies*, Nedra, Leningrad, 1983 (in Russian).
- [99] Gordeyev, S.G. and Sedelnikov, E.S.: On the interpretation of the results of VLF method on the basis of the conductive bed simulation, *Trydy TSNIGRI* Vyp.116 (1974), 88–99 (in Russian).
- [100] Gordeyev, S.G., Sedelnikov, E.S. and Tarkhov, A.G.: *Electric prospecting by the radio comparing and bearing method*, Nedra, Moscow, 1981 (in Russian).
- [101] Gordin, V.M. *Methods for eliminating terrain relief effects under highly accurate gravimetric observations*, Review of VIEMS, Ser. Region., Razv. i Promysl. Geofiz., Moscow, 1974 (in Russian).
- [102] Gorzhevsky, D.I., Kurbanov, N.K., Filatov, E.I. et al.: *Methodological principles of prediction and prospecting for lead and zinc deposits*, Nedra, Moscow, 1987 (in Russian).
- [103] Griffin, W.R.: Residual Gravity in Theory and Practice, *Geophysics* **14** No.1 (January) (1949), 39–56.

- [104] Groznova, A.A. and Troshkov, G.A.: Some elements of the procedure for determining the numerical characteristic of singular points of complex potential fields in 3-D space, *Collected geophysical articles of the Academy of Sciences of the Ukraine* **69** (1979), 62–73 (in Russian).
- [105] Guberman, Sh.A.: *Non-formal analysis of data in geology and geophysics*, Nedra, Moscow, 1987 (in Russian).
- [106] Gurevich, Yu.M., Kormiltsev, V.V. and Ulitin, R.V.: On the similarity of induced polarization curves for alternating and direct currents, *Izv. AN SSSR, Ser. Fizika Zemli* No.1 (1975), 114–116 (in Russian; in English see *Physics of the Solid Earth*).
- [107] Hänl, H., Maué, A.W. and Westpfahl, K.: *Theorie der Beugung*, Springer-Verlag, Berlin, 1961.
- [108] Heinrichs, W.E. and Ludwig, C.S.: Results of an induced-polarization survey employing both time and frequency domain techniques, In: *Mining Geophysics, Society of Exploration Geophysicists* **1** (1966), 317–320.
- [109] Hughes, D.S. and Pondrom, W.S.: Computation of vertical magnetic anomalies from total magnetic field measurements, *Trans. Amer. Geophys. Union* **28** No.2 (1947), 193.
- [110] Inmon, W.N. and Friedman, L.J.: *Design Review Methodology for a Data Base Environment*, Englewood Cliffs, N.J. Prentice Hall, (1982).
- [111] Ismail-Zade, T.A., Gadzhiev, T.G., Khesin, B.E., Karkoshkin, A.I., Alexeyev, V.V. and Metaxa, Kh.P.: *Petromagnetic map of the Azerbaijan SSR. Scale 1:500,000*, Printing Map Factory, Leningrad, 1983.
- [112] Ismail-Zade, T.A., Gadzhiev, T.G., Khesin, B.E., Karkoshkin, A.I., Alexeyev, V.V. and Potapova, E.I.: *Petromagnetic characteristics of Azerbaijan*, Elm, Baku, 1983 (in Russian).
- [113] Ismail-Zade, T.A. and Khesin, B.E. (Eds.); Alexeyev, V.V., Gadzhiev, T.G., Karkoshkin, A.I. and Khesin, B.E.: *Gravity and magnetic anomalies map of Azerbaijan SSR. Scale 1:500,000*, Printing Map Factory, Leningrad, 1989.
- [114] Ismail-Zade, T.A. and Khesin, B.E. (Eds.); Alexeyev, V.V., Gadzhiev, T.G., Karkoshkin, A.I. and Khesin, B.E.: *Gravity and magnetic anomalies of Azerbaijan and their geological interpretation*, Printing Map Factory, Leningrad, 1989 (in Russian).
- [115] Johnson, I.M.: Spectral induced polarization parameters as determined through time-domain measurements, *Geophysics* **49** 11 (1984), 1993–2003.
- [116] Kalenitsky, A.I. and Smirnov, V.P.: On the selection of optimal conditions for terrain corrections in gravity prospecting, *Trudy SNIIGIMS / Sib. Nauch.-Issl. Inst. Geol., Geof. i Miner. Syria* Vyp.238 (1976), 53–63 (in Russian).
- [117] Kalinina, T.B.: Determination of the magnetized body parameters by repeated iterations on a computer, *Voprosy Razv. Geofiz.* Vyp.8 (1968), 5–11 (in Russian).
- [118] Kappelmayer, O. and Hänel, R. *Geothermics with special reference to application*, Borntraeger, 1974.
- [119] Karataev, G.I. and Pashkevich, I.K. *Geological and geophysical analysis of geological fields set*, Naukova Dumka, Kiev, 1986 (in Russian).
- [120] Karkoshkin, A.I.: *Petrophysical characteristics of the Somkhit-Agdam zone (in connection with ore prognosis from the geophysical data)*, Ph.D Theses, Leningrad University, 1979.

- [121] Karous, M. and Hjelt, S.E.: Determination of apparent current density from VLF measurements, *Dept. of Geophys., Univ. of Gulu* No.89 (1977), 1–9.
- [122] Kaufman, A.A.: *Geophysical Field Theory and Method, Volume 1: Gravitational, Electric and Magnetic Fields*, Academic Press, San Diego, 1992.
- [123] Kaufman, A.A. and Keller, G.V.: *The magnetotelluric method*, Elsevier, Amsterdam, 1981.
- [124] Kazhdan, A.B.: *Prospecting of economic minerals; Conduction of exploration operations*, Nedra, Moscow, 1985 (in Russian).
- [125] Keilis-Borok, V.I.: The lithosphere of the earth as a nonlinear system with implications for earthquake prediction, *Rev. Geophys.* **28** (1990), 19–34.
- [126] Keilis-Borok, V.I. and Levshin, A.L. (Eds.): *Mathematical modeling and interpretation of geophysical data. Computational seismology*, Issue 16, Nauka, Moscow, 1984 (in Russian).
- [127] Khain, V.E.: *Regional Geotectonics. The Alpian Mediterranean Belt*, Nedra, Moscow, 1984 (in Russian).
- [128] Khalpin, L.A.: Information theory of geophysical interpretation, *Dokl. AN SSSR* **122** No.6 (1958), 1007–1010 (in Russian).
- [129] Khesin, B.E.: A simple method of considering terrain relief effect on the magnetic survey results, *Razv. i Okhrana Nedr* No.9 (1965), 30–38 (in Russian).
- [130] Khesin, B.E.: Geophysical characteristics of tectono-magmatic zones of Azerbaijan, *Geotektonika* No.6 (1968), 61–69 (in Russian).
- [131] Khesin, B.E.: *Ore geophysics in mountainous regions*, Nedra, Moscow, 1969 (in Russian).
- [132] Khesin, B.E.: On the possibility of integrated interpretation of geological and geophysical data on the southern slope of the Greater Caucasus using the information theory, *Izv. AN Azerb. SSR, Ser. Nauki o Zemle* No.2 (1972), 141–148 (in Russian).
- [133] Khesin, B.E.: Informational technique for prognosis of geological objects in the absence of standards in the area under investigation, *Metody Razv. Geofiz. Vyp.24* (1974), 98–102 (in Russian).
- [134] Khesin, B.E.: Statistical reduction of regional gravity anomalies of Azerbaijan, In: *Geophysical Investigations in Azerbaijan* Vyp.3, Baku (1975), 125–130 (in Russian).
- [135] Khesin, B.E.: *Prognosis and localization of hidden mineralization in mountainous regions on the basis of geophysical data*, Nedra, Moscow, 1976 (in Russian).
- [136] Khesin, B.E.: Elimination of topographic effects in magnetic prospecting, *Razv. Geofizika* Vyp.83 (1978), 102–111 (in Russian).
- [137] Khesin, B.E.: On quantitative integrated interpretation of geophysical data, In: *Geophysical Prospecting of oil-and-gas and ore deposits in Azerbaijan*, Baku, (1978), 67–77 (in Russian).
- [138] Khesin, B.E.: The peculiarities of geophysical prospecting for ore deposits in the Alpine mountainous regions, *Sovetskaya Geologiya* No.12 (1978), 76–86 (in Russian).
- [139] Khesin, B.E.: *Geophysical investigations in the mountainous regions*, D.Sci. Theses, Moscow Geological Prospecting Institute, 1981 (in Russian).
- [140] Khesin, B.E.: On convergency of geophysical surveys for the prognosis of ore, oil and gas, *Prikladnaya Geofizika* Vyp.125 (1991), 110–119 (in Russian).

- [141] Khesin, B.E. and Alexeyev, V.V.: On statistical reduction and interpretation of the measured values of  $\Delta g$  in mountainous regions, In: *Methods and results of geophysical prospecting of ore deposits* Yerevan, (1986), 100–105.
- [142] Khesin, B.E. and Alexeyev, V.V.: A method for determining the magnetization of rocks in their natural occurrence, Author's Certificate No.1125578 USSR MKI 01 3/08, 1987.
- [143] Khesin, B.E., Alexeyev, V.V. and Eppelbaum, L.V.: Optimization of geophysical investigations in mountainous regions by increasing the effectiveness of interpretation, In: *Optimization of ore exploration in mountainous regions*, Nedra, Moscow (1988), 79–122 (in Russian).
- [144] Khesin, B.E., Alexeyev, V.V. and Eppelbaum, L.V.: Investigation of geophysical fields in pyrite deposits under mountainous conditions, *Journal of Applied Geophysics* **30** (1993), 187–204.
- [145] Khesin, B.E., Alexeyev, V.V. and Eppelbaum, L.V.: 3-D modeling of gravity and magnetic fields as a final stage of application of effective interpretation system of geophysical data under difficult geological conditions, In: *Recent Advances in Geomathematics and Geoinformatics. Selected Papers Presented at Section 22 in the 29th International Geological Congress (Kyoto, 1993)*, *Geoinformatics* **4** No.3 (1993), 177–188.
- [146] Khesin, B.E., Alexeyev, V.V. and Metaxa, Kh.P. (Ed. Khesin B.E.): *Interpretation of magnetic anomalies in the conditions of oblique magnetization and rugged topography*, Nedra, Moscow, 1983 (in Russian).
- [147] Khesin, B.E. and Eppelbaum, L.V.: Optimization of the set of methods in the system of geophysical prospecting of economic minerals, *Izv. AN Azerb. SSR, Ser. Nauki o Zemle* No.1 (1986), 89–93 (in Russian).
- [148] Khesin, B.E. and Eppelbaum, L.V.: Methods for quantitative interpreting the results of near-surface thermal prospecting under complicated physico-geological conditions, *Baku, IL AzNIINTI* No.109 (1988) (in Russian).
- [149] Khesin, B.E. and Eppelbaum, L.V.: Near-surface thermal prospecting: Review of processing and interpretation, *Geophysics* **59** No.5 (1994), 744–752.
- [150] Khesin, B.E., Eppelbaum, V.M., Maryakhin, Z.M. and Stepanyan, E.S.: Determination of the reliability of exploration techniques integration by the given reliabilities of the set elements, *Deposited by VINITI, USSR Academy of Sciences* No.3566–B88 (1988) (in Russian).
- [151] Khesin, B.E. and Metaxa, Kh.P.: Studies of magnetic and other fields to reveal fractures and boundaries of tectonic blocks in Azerbaijan, In: *The study of seismicity and deep structure of Azerbaijan Elm*, Baku, (1974), 92–95 (in Russian).
- [152] Khesin, B. and Steinman, B.: The mapping of magnetic susceptibility of bottom sediments as a method for studies of sedimentation in a system river-lake, *Abstracts of 2-nd Intern. Symp. on the Geology of the Eastern Mediterranean region*, Jerusalem, (1995), 22.
- [153] Khutorsky, M.D.: *Heat flow in areas of structural geological inhomogeneities*, Nauka, Moscow, 1982 (in Russian).
- [154] Khutorsky, M.D., Salnikov, V.E. and Fotogdinov, R.A.: Geothermal prospecting of ore deposits, In: *Methodological and Experimental Principles of Geothermometry* Nauka, Moscow (1983), 212–229 (in Russian).

- [155] Kilty, K.T.: On the origin and interpretation of self-potential anomalies, *Geophysical Prospecting* **32** No.1 (1984), 51–62.
- [156] Klein, J., 1971, Geophysical survey in Sinai Peninsula, Israel: Inst. Petr. Res. and Geoph. Rep. SGA/725/69.
- [157] Klichnikov, V.A. (Ed.): *Geophysical prospecting of ore deposits*, Alma-Ata, 1970 (in Russian).
- [158] Klushin, I.G. and Tolstikhin, I.N.: Singling out linear tectonic dislocations in geophysical maps, *Geologiya i Geofizika* No.6 (1961), 98–103 (in Russian).
- [159] Klushin, I.G. and Tolstikhin, I.N.: Statistical determination of occurrence depth of magnetic field sources, *Transactions of the Leningrad Mining Institute XLVI* (1963), (in Russian).
- [160] Kogan A.B.: *The theory and methods of directed summation and frequency filtration and results of the geomagnetic field investigation of the Siberian platform*, Nedra, Leningrad, 1975 (in Russian).
- [161] Komarov, V.A.: *Electric prospecting by the induced polarization method. 2nd edition, revised and supplemented*, Nedra, Leningrad, 1980 (in Russian).
- [162] Komarov V.A., Pishpareva, N.A., Semenov, M.V. and Khloponina, L.S.: *Principles of the observation interpretation in the Induced Polarization method*, Nedra, Leningrad, 1966 (in Russian).
- [163] Kondakov, N.I. *Logic Dictionary*, Nedra, Moscow, 1971 (in Russian).
- [164] Kozlovsky, E.A. and Krivtsov, A.I.: Simulation of ore deposits: Trends and targets, *Sovetskaya Geologiya* No.8 (1988), 3–8 (in Russian).
- [165] Kravtsov, G.G. and Segalovich, V.I.: Interpretation algorithms for selecting geological models from gravitational observations and their practical application, In: *Questions of mining geophysics in Kazakhstan, NPO "Geofizika"* (1976), 17–35 (in Russian).
- [166] Krivtsov, A.I. and Narseyev, V.A.: Process of geological prospecting and prediction-prospecting sets, *Sovetskaya Geologiya* No.1 (1983), 17–27 (in Russian).
- [167] Kruglyakova, G.I.: Magnetic anomalies of the Transcarpathians and their geological interpretation, *Geomagnetism i Aeronomiya* No.5 (1962), 976–994 (in Russian).
- [168] Krumbein, W.C. and Graybill, F.A.: *An introduction to statistical models in geology*, McGraw-Hill Book Company, N.Y., 1965.
- [169] Kunin, N.Ya.: Problems of singling out the observed gravity field components for structural-tectonic regioning (as applied to the Southern Kazakhstan), In: *Geophysical investigations in Kazakhstan* Alma-Ata (1968), 76–88 (in Russian).
- [170] Lachenbruch, A.N.: Rapid estimation of the topographic disturbance to superficial thermal gradients, *Rev. Geophys.* **6** No.3 (1968), 365–400.
- [171] Lakhtionov, M.O. and Tarkhov, A.G.: Experience in thermal prospecting at pyrite deposits of the Urals, *Izv. VUZov, Ser. Geol. i Razv.* No.5 (1967), 87–94 (in Russian).
- [172] Lakhtionov, M.O. and Tarkhov, A.G.: Geothermal investigations at ore deposits, *Sovetskaya Geologiya* No.3 (1970), 121–124 (in Russian).
- [173] Landau, L.D. and Lifshitz, E.M.: *Electrodynamics of Continuous Media*, Pergamon Press, Oxford, 1960.
- [174] Lapina, N.Ya.: A system of programs for transforming 2-D potential fields, De-

- posed by VINITI, USSR Academy of Sciences No.1644-70 (1970) (in Russian).
- [175] Leschak, H.A. and Lewis, J.E.: Geothermal prospecting with shallow-temperature surveys, *Geophysics* **48** No.7 (1983) 975–996.
- [176] Lines, L.R., Schultz, A.K. and Treitel, S.: Cooperative inversion of geophysical data, *Geophysics* **53** No.1 (1988), 8–20.
- [177] Logachev, A.A.: *Methodological manual on aeromagnetic survey*, Gosgeoltekhnizdat, Moscow, 1955 (in Russian).
- [178] Logachev, A.A. and Zakharov, V.P.: *Magnetic prospecting*, Nedra, Leningrad, 1973 (in Russian).
- [179] Loginov, V.E.: On the connection between methods for statistical interpretation of geophysical observations and regularization, *Geologiya i Geofizika* No.3 (1977), 135–137 (in Russian).
- [180] Lomtadze, V.V.: *Software for processing geophysical data*, Nedra, Leningrad, 1982 (in Russian).
- [181] Lukavchenko, P.I.: *Tables and nomographs for calculating terrain gravity corrections in survey with gravimeters*, Gostoptekhnizdat, Moscow, 1951 (in Russian).
- [182] Lukavchenko, P.I.: On reduction and interpretation of gravity anomalies under conditions of severely rugged relief, *Prikladnaya Geofizika* Vyp.31 (1961), 219–229 (in Russian).
- [183] Lyubavin, L.M. and Shaub, Yu.B.: Integrated interpretation of airborn electromagnetic and aeromagnetic data using correlation functions, *Razvedka i Okhrana Nedr* No.6 (1968), 40–45 (in Russian).
- [184] Lyubimov, A.A.: *Geological rapid interpretation of gravity and magnetic data*, Nedra, Moscow, 1983 (in Russian).
- [185] Lyubimov, G.A. and Lyubimov, A.A.: *Computer-aided methods of gravity and magnetic interpretation*, Nedra, Moscow, 1988 (in Russian).
- [186] Lyubimova, E.A.: *Thermometry of the Earth and the Moon* Nauka, Moscow (1968) (in Russian).
- [187] Lyubimova, E.A., Nikitina, V.N. and Tomara, G.A.: *Heat fields of the internal and marginal seas of the USSR. State of observation level and interpretation theory for 2-D inhomogeneities*, Nauka, Moscow, 1976 (in Russian).
- [188] Lyustikh, E.N.: Geological meaning of various methods for computing the gravity anomalies, *Trudy Inst. Teoret. Geof. AN USSR* No.3 (1947) 3–45 (in Russian).
- [189] Malyshev, V.P.: *Probabilistic-deterministic design of experiment*, Nauka, Alma-Ata, 1981 (in Russian).
- [190] Mamedov, A.V. (Ed.), Guseinov, A.N. and Shirinov, F.A.: *Map of geological regioning for oil of the Azerbaijan SSR. Scale 1:500,000*, Printing Map Factory, Leningrad, 1985.
- [191] Martin, J.: *Computer data-base organization* Englewood Cliffs, N.J. Prentice Hall, 1978.
- [192] Miecznik, S.: Ciala cylindryczne w polo plaskey fali elektromagnetycznej, *Techn. Poszuk. Geol.* **25** No.3 (1986), 16–22 (in Polish).
- [193] Mikov, B.D.: *Practical techniques for magnetic anomalies interpretation under conditions of complicated terrain relief*, Inst. Geol. i Geof., Novosibirsk, 1963 (in Russian).

- [194] Mikov, B.D., Pyatnitsky, V.K. and Rempel, G.G.: *The use of aeromagnetic data for investigating the basement of closed territories*, Review of VIEMS, Moscow, 1966 (in Russian).
- [195] Mironov, V.S.: *A course in gravity prospecting*. 2nd ed., revised and supplemented, Nedra, Leningrad, 1980 (in Russian).
- [196] Molchan, G.M., Dmitrieva, O.E., Rotwain, I.M. and Dewey, J.: Statistical analysis of the results of earthquake prediction, based on bursts of aftershocks, *Phys. Earth Planet. Int.* **61** (1990), 19–34.
- [197] Movshovich, E.B., Knepel, M.N. and Cherkashin, M.S.: *Formalization of geological data for mathematical processing*, Nedra, Moscow, 1987 (in Russian).
- [198] Mudretsova, E.A. (Editor): *Gravity prospecting. Geophysicist's manual*, Nedra, Moscow, 1981 (in Russian).
- [199] Muradkhanov, S.A.: Interpretation of geophysical data from the wells of Filizchai deposit using statistical methods, *Express-information of VIEMS, Ser. Region., Razv. i Promysl. Geofiz.*, Moscow, No.88, 1971 (in Russian).
- [200] Murty, B.V. and Haricharan, P.: A simple approach toward interpretation SP anomaly due to 2-D sheet model of short dipole length, *Geophys. Res. Bull.* **22** No.4 (1984), 213–218.
- [201] Nabighian, M.N.: The analytic signal of two-dimensional magnetic bodies with polygonal cross-section: its properties and use for automated anomaly interpretation, *Geophysics* **37** No.3 (1972), 507–517.
- [202] Napadensky, G.B. and Sheremet, O.G.: *Computer-aided integrated interpretation of gravitational and magnetic fields*, Review of VIEMS, Ser. Region., Razv. i Promysl. Geofiz., Moscow, 1976 (in Russian).
- [203] Naudy, H.: Automatic determination of depth on aeromagnetic profiles, *Geophysics* **36** (1971), 717–722.
- [204] Nemtsov, L.D.: High-accuracy gravity prospecting Nedra, Moscow, 1967 (in Russian).
- [205] Nepomnyashchikh, A.A.: *Interpretation of geophysical anomalies*, Nedra, Leningrad, 1964 (in Russian).
- [206] Nettleton, L.L.: *Gravity and Magnetics in Oil Prospecting*, McGraw-Hill, N.Y., 1976.
- [207] Nikitin, A.A.: Application of the statistical solution theory for classifying geological objects by the data of geophysical methods set, *Izv. VUZov, Ser. Geol. i Razv.* No.10 (1970), 135–144 (in Russian).
- [208] Nikitin, A.A.: *Theoretical principles of geophysical data processing*, Nedra, Moscow, 1986 (in Russian).
- [209] Nikitin, A.A.: 1986, Foundation of geophysical data integrated interpretation, In: (Eds. Brodovoy, V.V. and Nikitin, A.A.) *Integration of geophysical methods*, Nedra, Moscow, (1984), 45–78 (in Russian).
- [210] Nikitin, A.A., Medovsky, I.G. and Vlasova, I.I.: Analysis of simple techniques for integrated interpretation of geophysical data, *Pikladnaya Geofizika* Vyp.62 (1971), 167–174 (in Russian).
- [211] Nikitin, A.A. and Tarkhov, A.G.: Estimation of the reliability for revealing geophysical anomalies, *Razved. Geofizika* Vyp.59 (1973), 56–62 (in Russian).

- [212] Nikitsky, V.E. and Glebovsky, Yu.S. (Eds.): *Magnetic prospecting. Geophysicist's manual*, Nedra, Moscow, 1990 (in Russian).
- [213] Olle, T.W.: *The CODASIL approach to data-base management*, John Wiley & Sons, Toronto, 1978.
- [214] Olsson, O.: VLF-anomalies from a perfectly conducting half-plane below an overburden, *Geophysical Prospecting* **28** No.3 (1980), 415–434.
- [215] Olsson, O.: Computation of VLF response over half-plane and wedge models, *Geophysical Prospecting* **31** (1983), 171–191.
- [216] Orlov, V.Kh.: *Analysis and singling out the relation between Bouguer anomalies and the altitudes of relief*, Ph.D Theses, Leningrad University, 1984 (in Russian).
- [217] Paffenholz, K.A.: *Geological essay of the Caucasus*, AN Arm. SSR, Yerevan, 1959 (in Russian).
- [218] Parasnis, D.S.: *Mining Geophysics*, Elsevier, Amsterdam, 1966.
- [219] Parasnis, D.S.: *Principles of Applied Geophysics. 4th ed., revised and supplemented*, Chapman and Hall, London, 1986.
- [220] Paturet, D. and Garetta, R.: "Slalom-line" method (the layout and processing of non-straight seismic line), *Transactions of 37 Simp. of Europ. Assoc. of Explor. Geoph.*, Bergen, 17–20 June, 1975.
- [221] Paul, M.: Über Messingew der erdbodentemperatur und salzodomen, *Z. Geophys.* **11**, 7/8 (1935), 388–392.
- [222] Peresada, V.P.: *Automated pattern recognition*, Energiya, Leningrad, 1970 (in Russian).
- [223] Peters, L.J.: The Direct Approach to Magnetic Interpretation and its Practical Applications, *Geophysics* **14** (1949), 290–320.
- [224] Poddar, M.: Very low-frequency electromagnetic response of a perfectly conducting half-plane in a layered half-space, *Geophysics* **41** (1982), 1059–1067.
- [225] Poley, J.P. and Steveninck, J.V.: Delineation of shallow salt domes and surface faults by temperature measurements at a depth of approximately 2 meters, *Geophys. Prosp.* **18**, 666–700.
- [226] Polyakov, A.S.: *Methodological manual on electric profiling*, Nedra, Leningrad, 1969 (in Russian).
- [227] Quick, D.H.: The interpretation of gradient array chargeability anomalies, *Geophysical Prospecting* **22** No.4 (1974), 736–746.
- [228] Raiffa, H.: *Decision analysis. Introductory lectures on choices under uncertainty*, Addison-Wesley, London, 1968.
- [229] Rao, D.A. and Babu, H.V.: On the half-slope and straight-slope methods of basement depth determination, *Geophysics* **49** No.8 (1984), 1365–1368.
- [230] Reford, M.S. and Sumner, I.S.: Aeromagnetics, *Geophysics* **29** No.4 (1964), 482–516.
- [231] Rempel, G.G. and Parshukov, N.P.: Experience in coordinated computer simulation of gravity anomalies and vertical electric sounding, *Trudy SNIIGIMS Vyp.* 238 (1976), 5–8 (in Russian).
- [232] Report of the CODASIL DDLG, *Inform. Syst.* **3** No.4 (1980), 247–320.
- [233] Reznikov, M. and Ben-Avraham, Z.: Structure of Lake Kinneret region from gravity analysis, *Israel Geological Society, Annual Meeting. Nof Ginossar* (1994), 88.

- [234] Riznichenko, Yu.V., Khesin, B.E. and Metaxa, Kh.P.: Relation between seismicity and magnetic field according to observations in Azerbaijan, *Izv. AN SSSR, Ser. Fizika Zemli* No.1 (1983) 3–14 (in Russian; in English see *Physics of the Solid Earth*).
- [235] Rodionov, P.F. and Sofronov, N.I.: On the possibility of thermometry application to prospecting sulphide deposits, *Problemy Sovetskoy Geologii* Vyp.8 (1935), 257–268.
- [236] Roy, A.: 1970. Gravity and magnetic interpretation on uneven topography by  $\sin x/x$  method of continuation, *Geoexploration* 8 No.1 (1970), 37–40.
- [237] Ruderman, E.N. and Golubkov, V.V.: *Some algorithms for processing and interpreting the results of electromagnetic survey by Induction, VLF and IP methods*, Review of VIEMS, Ser. Razv. Geofiz., Moscow, 1985 (in Russian).
- [238] Scott, W.R. and Geyer, R.A.: An integrated multidisciplinary method as applied to Appalachia, *Oil & Gas Journal* 7 (1982), 286–302.
- [239] Seigel, H.O.: Mathematical formulation and type curves for induced polarization, *Geophysics* 24 No.3 (1959), 547–565.
- [240] Semenov, A.S.: *Electric prospecting by self-potential method*. 3rd ed., revised and supplemented, Nedra, Leningrad, 1974 (in Russian).
- [241] Semenov, M.V.: *Principles of prospecting and investigating pyrite-polymetallic ore fields by geophysical methods*, Leningrad, Nedra, Leningrad, (1975) (in Russian).
- [242] Sercombe, W.J., Stratton, M.A., Albertin, M., Wilson, W.P., Roth, B.L., Van Nieuwenhuise, R.E., Pivnik, D.A. and Beck, R.A.: Wrench faulting in the northern Pakistan foreland region, *The Leading Edge* 13 11 (1994), 1007–1110.
- [243] Shakhnazaryan, A.L., Agamaliev, G.N. and Elenbogen, A.M.: Peculiarities of geophysical prospecting of fresh underground water in mountainous region of the Lesser Caucasus (Azerbaijan part), *Razved. Geofizika* Vyp. 103 (1986), 89–97 (in Russian).
- [244] Shalayev, S.V.: *Geological interpretation of geophysical anomalies with the help of linear programming*, Nedra, Leningrad, 1972 (in Russian).
- [245] Shannon, C.: A Mathematical Theory of Communication, *Bell Syst. Techn. J.* 27, 3–4 (1948), 379–423, 623–656.
- [246] Sharma, P.V. *Geophysical methods in Geology*. 2nd ed., Elsevier, N.Y., 1986.
- [247] Shatrov, B.B. and Dun Tsun-in.: *Determination of ore body parameters by the data from geophysical methods*, Review of VIEMS, Ser. Razv. Geofiz., Moscow, 1984 (in Russian).
- [248] Shaub, Yu.B.: Application of correlation analysis to geophysical data processing, *Izv. AN SSSR, Ser. Geofiz.* No.4 (1963), 578–589 (in Russian).
- [249] Shraibman, V.I., Zhdanov, M.S. and Vitvitsky, O.V.: *Correlation methods for transformation and interpretation of geophysical anomalies*, Nedra, Moscow, 1977 (in Russian).
- [250] Sidorenko, A.V. (Chief Editor): *Geology of the USSR* 17, Azerbaijan SSR (Geological Description), Nedra, Moscow, 1972 (in Russian).
- [251] Simmons, G.: Interpretation of heat flow anomalies, *Rev. of Geophys.* 5 2 (1967), 42–52.
- [252] Smirnov, A.A.: *Introduction to theory of electromagnetic field*, Nedra, Moscow, 1975 (in Russian).

- [253] Sokolov, B.A. and Khain, V.E.: Presence of oil and gas in overthrusting margins of folded mountainous structures, *Sovetskaya Geologiya* No.12 (1982), 53–58 (in Russian).
- [254] Starostenko, V.I.: *Stable numerical methods in gravimetry problems*, Naukova Dumka, Kiev, 1978 (in Russian).
- [255] Starostenko, V.I., Kostyukevich, A.S. and Kozlenko, V.G.: Comprehensive interpretation of seismometric and gravimetric data. I. Principles and methods. II. Application, *Physics of the Solid Earth* **24** (1988) 4, 371–282, 6, 456–462 (translated from Russian).
- [256] Stolpnier, M.N.: Simulation of pyrite deposits in geophysical prospecting, *Sovetskaya Geologiya* No.6 (1979), 90–95 (in Russian).
- [257] Strakhov, V.N.: Experience in magnetic anomaly interpretation by plotting of  $\Delta Z$  isolines in the vertical plane, *Prikl. Geofizika* Vyp.27 (1960), 116–130 (in Russian).
- [258] Strakhov, V.N.: On the state and problems of geological interpretation of gravimetric and magnetic observations, In: *Exploration geophysics of the USSR in the beginning of the 70-s* Nedra, (1974) (in Russian).
- [259] Strakhov, V.N.: *Main ideas and methods for deriving information from gravitational and magnetic observations*, Nedra, Moscow, 1976 (in Russian).
- [260] Strakhov, V.N.: On the theory of filtration and transformation of potential fields under conditions of different prior information on noises in input data, *Izv. AN SSSR, Ser. Fizika Zemli* No.3 (1976), 60–68 (in Russian; in English see *Physics of the Solid Earth*).
- [261] Strakhov, V.N.: A novel stage in the development of the theory of interpreting gravitational and magnetic anomalies, *Izv. AN SSSR, Ser. Fizika Zemli* No.12 (1977), 20–41 (in Russian; in English see *Physics of the Solid Earth*).
- [262] Strakhov, V.N. and Lapina, M.I.: Some results of interpreting aeromagnetic survey data by analytical continuation into the lower semispace, In: *Theoretical substantiation and practice of transformation of potential geophysical fields for solving regional geological problems*, Nedra, Moscow (1969), 311–339 (in Russian).
- [263] Strakhov, V.N., Lapina, M.I. and Efimov, A.B.: Solving direct problems of gravimetry and magnetometry on the basis of novel analytical concepts for field elements from standard approximating bodies, 1-2. *Izv. AN SSSR, Ser. Fizika Zemli* No.6 (1986) 55–69 and No.7 (1986), 66–78 (in Russian; in English see *Physics of the Solid Earth*).
- [264] Strakhov, V.N., Lapina, M.I. and Zhavoronkin, I.A.: Modern methods for interpreting magnetic and gravitational anomalies of KMA type, *Izv. AN SSSR, Ser. Fizika Zemli* No.3 (1971), 49–66 (in Russian; in English see *Physics of the Solid Earth*).
- [265] Suggestion to authors of the reports of the United States Geological Survey, Washington, US Government Publishing Office, 1978.
- [266] Suryaninov, E.Yu., Vishnevsky, P.V. and Vasserman, V.A.: Investigation of geothermal anomaly behavior over geological objects with contrasting thermal conductivity, *Izv. AN SSSR, Ser. Fizika Zemli* No.12 (1983) 96–102 (in Russian; in English see *Physics of the Solid Earth*).
- [267] Svetov, B.S.: *Information Theory Basis of Geophysics*, Electromagnetic Research Centre, Moscow, 1992.

- [268] System of database “GEOKOMPAS” management, geophysical variant of database management system “KOMPAS”, *VNIIGeofizika and Calculation Center of AN USSR Moscow*, 1985 (in Russian).
- [269] Tafeyev, Yu.P.: Calculation of the  $\Delta T$  magnetic field, In: *Geophysical prospecting for ore deposits*, Gosgeolizdat, Moscow (1953), 3–42 (in Russian).
- [270] Tafeyev, Yu.P. and Sokolov, K.P.: *Geological interpretation of magnetic anomalies*, Nedra, Leningrad, 1981 (in Russian).
- [271] Talwani, M.: Computation with the help of a digital computer of magnetic anomalies caused by bodies of arbitrary shape, *Geophysics* **30** No.5 (1965), 797–817.
- [272] Talwani, M., Windisch, C.C. and Langseth Jr., M.G.: Reykjanes Ridge Crest: a detailed geophysical study, *J. Geoph. Res.* **76** (1971), 473–517.
- [273] Tarkhov, A.G.: *Principles of geophysical prospecting by radio comparing and bearing method*, Gosgeoltekhnizdat, Leningrad, 1961 (in Russian).
- [274] Tarkhov, A.G. (Editor): *Electrical prospecting. Geophysicist’s manual*, Nedra, Moscow, 1980 (in Russian).
- [275] Tarkhov, A.G., Bondarenko, V.M. and Nikitin, A.A.: *Principles of integration in exploration geophysics*, Nedra, Moscow, 1977 (in Russian).
- [276] Tarkhov, A.G. and Sidorov, A.A.: On mathematical processing of geophysical data, *Izv. AN SSSR, Ser. Geofiz.* No.10 (1960), 1450–1457 (in Russian).
- [277] Telford, W.M., Geldart, L.R., Sheriff, R.E. and Keys, D.A.: *Applied Geophysics*, Cambridge University Press, 1976.
- [278] Teorey, T.J. and Fry, J.P.: *Design of Database structures*, Englewood Cliffs, N.J. Prentice Hall, 1988.
- [279] Terekhova, R.V.: Determination of the magnetic anomaly nature by daily geomagnetic variations In: *Geology, rock magnetism and paleomagnetism of the Southern Urals*, Ufa, Ural Scientific Center (1977), 85–95 (in Russian).
- [280] Tesmull, F.A. and Crossley, D.I.: Inversion of VLF-data for simple lateral inhomogeneities, *Geological Survey of Canada No.81-15* (1981) 79–86.
- [281] Tikhonov, A.N. and Bulanzhe, Yu.D.: On averaging gravity fields, *Izv. AN SSSR, Ser. Geof.* No 2 (1945) (in Russian).
- [282] Tikhonov, A.N. and Goncharsky, A.V. (Eds.): *Ill-posed problems in the natural sciences*, Mir publisher, Moscow, 1987.
- [283] Tikhonov, A.N. and Samarsky, A.A.: *Equations of Mathematical Physics*, Pergamon Press, Oxford, 1963.
- [284] Troshkov, G.A. and Groznova, A.A.: *Mathematical methods of magnetic anomaly interpretation*, Nedra, Moscow, 1985 (in Russian).
- [285] Turcotte, D.L.: *Fractals and chaos in geology and geophysics*, Cambridge Univ. Press, 1995.
- [286] Tvalchrelidze, G.A.: On types of pyrite deposits and provinces, *Izv. AN SSSR, Ser. Geolog.* No.10 (1978), 5–16 (in Russian).
- [287] Tyapkin, K.F.: *Interpretation of magnetic anomalies due to sheet-like beds and contacts*, Nedra, Moscow, 1973 (in Russian).
- [288] Vakhromeyev, G.S. and Davydenko, A.Yu.: *Modeling in exploration geophysics*, Nedra, Moscow, 1987 (in Russian).

- [289] van den Bouwhuysen, J.N.A.: The thermocouple proves useful on a geophysical survey, *Eng. and Min. J.* **135**, 342–344.
- [290] Varlamov, A.S. and Filatov, V.G.: *Determination of the density of rocks and geological objects*, Nedra, Moscow, 1983 (in Russian).
- [291] Vekilov, R.G. and Khesin, B.E.: On the application of information theory for the comparison of economical efficiency of prospecting methods, *Za Technich. Progress* No.4 (1970), 29–31 (in Russian).
- [292] Ventsel, E.S.: *The probability theory. 3rd ed., revised*, Nauka, Moscow, 1969 (in Russian).
- [293] Veselov, K.E.: *Gravimetric survey*, Nedra, Moscow, 1986 (in Russian).
- [294] Villee, M.A., Chouteau, M. and Palacky, G.J.: Effect of temporal and spatial variations of the primary signal on VLF total-field surveys, *Geophysics* **57** No.1 (1992) 97–105.
- [295] Voskoboinikov, G.M. and Nachapkin, N.A.: *Methodological recommendations on the application of the singular point method for interpreting potential fields*, Izd. Ural. Nauchnogo Tsentrana AN SSSR, Sverdlovsk, 1980 (in Russian).
- [296] Vysokostrovskaya, E.B. and Zelenetsky, D.S.: On quantitative evaluation of the prospects of a territory when searching for ore mineral deposits, *Sovetskaya Geologiya* No.8, (1968), 58–71 (in Russian).
- [297] Ward, S.H. (Ed.): *Geotechnical and Environmental Geophysics I–III*, SEG Book Mart, Academic Series, 1990.
- [298] Yaglom, A.M. and Yaglom, I.M.: *The probability and information. 2nd ed., revised and supplemented*, Nauka, Moscow, 1973 (in Russian).
- [299] Yanovsky, B.M.: *Earth's magnetism*, Leningrad Univ. Publ., 1978 (in Russian).
- [300] Zaborovsky, A.I.: *Electric prospecting*, Gostoptekhizdat, Moscow, 1963 (in Russian).
- [301] Zadeh, L.A.: The role of fuzzy logic in the management of uncertainty in expert systems, *Fuzzy Sets and Systems* **11** (1983), 199–227.
- [302] Zhdanov, M.S.: *The analogues of the Cauchy type integral for the theory of geophysical fields*, Nauka, Moscow, 1984 (in Russian).
- [303] Zhdanov, M.S. and Keller, G.V.: *The Geoelectrical Methods in Geophysical Exploration*, Elsevier, 1994.
- [304] Zhogolev, L.P. and Gran, B.B.: *Problems of micromagnetic survey*, Trudy VIRG, Vyp.16, 1959 (in Russian).
- [305] Ziegler, C.A.: *Programming System Methodologies*, Englewood Cliffs, N.J. Prentice-Hall, 1983.
- [306] Zonge, K.L., Sauck, W.A. and Sumner, J.S.: Comparison of time, frequency, and phase measurements in induced polarization, *Geophysical Prospecting* **20** No.3 (1972), 626–648.
- [307] Zorin, Yu.A. and Lysak, S.V.: Quantitative interpretation of geothermal anomalies, *Izv. AN SSSR, Ser. Fizika Zemli* No.9 (1972), 68–73 (in Russian; in English see *Physics of the Solid Earth*).

- [308] Zverev, V.P., Dolnikov, V.A., Khutorsky, M.D. and Fotogdinov, R.A.: Thermal effect and sulphide oxidation rate in the Katekh deposit (as applied to the southern slope of the Greater Caucasus), *Dokl. AN SSSR* **265** No.4 (1982), 960–962 (in Russian).

# Index

- E-polarization**, 37, 208, 209  
**H-polarization**, 208  
3-D modeling, 96, 224, 281, 287  
3-D models, 96, 268
- absolute permeability, 39  
aeromagnetic survey, 2, 108, 144, 291  
Alpine epoch, 7  
alpinotype structures, 10  
Altai, 3, 271  
Altai-Sayan, 62  
alternative models, 286  
Aniezie curl, 80  
Appalachians, 3, 232  
Araks zone, 13  
autocorrelation function, 191, 221, 223  
autocorrelation radius, 85, 132, 222  
automatic classification, 240
- Baikalian basement, 250  
Baikalian complex, 260  
Bayes' criterion, 196  
Bongard's algorithm, 237  
Bouguer anomalies, 64, 94, 103  
Bouguer reduction, 103, 330  
breaking down effect, 129
- Carpathians, 3, 12  
Cauchy-type integral, 37  
characteristic points, 154, 163, 187, 204  
classification error, 292  
classification reliability, 293  
closed currents, 36  
coefficient of informativity, 243  
complete normalized gradient, 164, 241  
conduction currents, 313  
conductive half-plane, 208  
conductive minerals, 38  
cone, 62, 83  
conical hollow, 83  
control point, 76, 312
- cooperative interpretation, 260  
cooperative inversion, 232  
covariance matrices, 292  
cross-correlation, 120, 135
- database management system, 299  
Dead Sea rift, 281  
decision making, 235  
decision-making, 29, 51, 195  
delineation, 159  
deterministic-statistical model, 164  
dielectric constant, 38  
difference anomalies, 149  
digital field models, 139  
digital terrain model, 88, 116, 117  
dipole moment, 38  
dipping thin bed, 34, 202  
Dirichlet's problem, 122  
displacement currents, 313  
downward continuation, 122, 129, 168, 169  
drilling site pattern, 118  
DTB, 34, 38, 42
- effective density, 64, 84  
effective magnetization, 65, 158, 168  
Eilat, 141, 285  
electric double layer, 34  
electric prospecting, 19, 76, 104, 208, 209
- electromagnetic sounding, 28  
elliptical cylinder, 41  
emanation survey, 152  
endogenic deposits, 23, 117  
entropy, 117, 137, 238  
Epi-Hercynian platform, 276  
epicenter, 43, 159, 173, 179, 186
- fictitious body, 46, 47, 122, 167, 170  
fictitious center, 204  
fictitious vector, 167  
field transformations, 68, 74, 122

- field transforms, 67  
 filtration-correlation techniques, 240  
 finite differences method, 207  
 first kind error, 293  
 four color problem, 31  
 Fourier's law, 33  
 free-air, 88, 94, 317, 329  
 frequency domain, 38, 208  
 fuzzy logic, 302  
 generalized angle, 153, 169, 209  
 geoelectric horizons, 231  
 geomagnetic declination, 153  
 geomagnetic inclination, 329  
 geothermal investigations, 213, 266, 314  
 gold-pyrite deposit, 93, 210, 246  
 gradient array, 204, 206  
 gradient principle, 152  
 gravimetric data, 4  
 gravimetric prospecting, 20, 275  
 gravity steps, 150  
 Greater Caucasus, 3, 22, 149, 232, 260  
 Green's function, 201  
 Green's solution, 37  
 ground-air interface, 42  
 grounding, 19  
 grouping the points, 93  
 GSFC, 96, 224, 249, 254, 307  
 Hankel function, 37  
 harmonic functions, 163  
 HCC, 34, 42, 199, 204, 233, 249  
 heat transfer, 33  
 heights field, 85  
 heights spectrum, 101  
 heliothermal zone, 315  
 Helmholtz equation, 37  
 homogeneous slope, 103  
 horizontal circular cylinder, 34, 170, 179, 214  
 horizontal gravity component, 46  
 hyperbolic approximation, 84  
 inclined circular cylinder, 130  
 inclined coordinate system, 44  
 inclined magnetization effect, 178  
 inclined polarization effect, 21  
 inclined relief, 44, 179, 201  
 inclined semispace, 49  
 incomplete Bouguer reduction, 10, 141  
 induced magnetization, 59, 114, 209  
 information-statistical integrated interpretation, 235, 245  
 informational jump, 51  
 integral method, 164, 187  
 integrated criterion, 237, 242, 308  
 integrated interpretation, 25, 119, 292  
 integrated interpretation reliability, 241  
 integrated quantitative interpretation, 233  
 interactive interpretation system, 299  
 interactive selection, 220  
 interactive system, 300  
 intermediate layer, 64, 88, 103  
 interval velocity, 73  
 inverse magnetization, 154, 283  
 inverse probability method, 120, 133, 134  
 inverse problem, 162  
 inverse problem solution, 114, 165, 214  
 IP, 2, 104, 204, 219, 294  
 IPM, 133  
 isometric anomalies, 121, 124, 204  
 ITB, 42  
 Jordan Rift Valley, 281  
 Karatau, 104  
 Kotelnikov's criterion, 230  
 Kotelnikov's theorem, 12  
 Krivoy Rog, 10  
 Kura depression, 187, 257, 266, 276  
 Kursk Magnetic Anomaly, 10  
 Lake Baikal, 214  
 lake Kinneret, 281  
 Laplace's equation, 33, 34, 36, 122, 163  
 layer of neutral temperature, 314  
 learning "with a teacher", 240  
 Lesser Caucasus, 4, 10, 22, 60, 85, 93, 99, 149, 187, 246, 266, 291  
 level of the normal field, 190, 250, 309  
 linear discriminant functions, 237  
 linear programming, 195, 231  
 local anomalies, 120, 127, 159, 255  
 localization principle, 193  
 logico-informational methods, 293  
 macroseismic evidence, 128

- macroseismic evidence, 128  
magnetic declination, 227  
magnetic induction, 201  
magnetic moment, 172  
magnetic prospecting, 4, 20, 29, 32, 37, 43, 76, 93, 196, 222, 275, 309  
magnetic steps, 150  
magnetic susceptibility, 33, 59, 62, 92, 99, 209  
magnetotelluric sounding, 208, 260  
mathematical logic, 235  
metallometric survey, 293  
modern geomagnetic field, 60  
mountainous conditions, 7, 19, 32, 64, 77, 271, 291, 303, 310  
multiplication method, 65
- Nagorny Karabakh, 117  
natural polarization vector, 201  
near-surface thermal prospecting, 76, 314  
noise dispersion, 230  
noise distribution, 22  
noise tolerance, 190  
non-stationary anomalies, 78  
normal background level, 154, 173, 186  
normal distribution function, 292  
normal field, 207
- oblique magnetization, 59, 99, 122, 129, 145, 148, 152, 171, 187, 219, 246  
oblique polarization, 47, 122, 129, 218, 226, 309  
oil-and-gas controls, 3, 127  
oil-and-gas pool, 73  
oil-and-gas prognosis, 278  
oil-and-gas traps, 276  
ore controls, 3, 51, 241
- paleomagnetic investigation, 60  
paleomagnetic zone, 59  
parabolic approximation, 99  
parallel interpretation, 232  
pattern recognition, 52  
PGM, 3, 246, 270  
physico-geological model, 66, 246, 272, 300  
Poisson's equation, 33
- Poisson's integral, 126  
Poisson's ratio, 231  
potential array, 204  
Pre-Alpine basement, 12, 257  
probabilistic-deterministic interpretation, 235  
profile inclination, 46  
pseudogravimetric anomalies, 194  
pyrite-polymetallic deposit, 133, 215, 232
- Rexford's rule, 158  
regional background, 22, 120, 134  
regional component, 124, 191  
regional field, 190, 255  
relief digital description, 96  
remanent magnetization, 4, 59, 60  
residual gravity anomalies, 279  
Rocky Mountains, 3  
Roman constructions, 286  
rose-diagram, 139  
Rudny Altai, 202  
ruggedness, 85, 119, 137
- Saatly super-deep borehole, 257, 275  
scalar potential, 34  
Sea of Galilee, 281  
seasonal temperature variations, 314  
second kind error, 293  
secondary dispersion halo, 29, 293  
secondary electromagnetic field, 313  
seismic activity, 126, 137  
seismic activity prediction, 311  
seismic boundaries, 235  
seismic prospecting, 28, 83  
self-setting filter, 132, 240  
series interpretation, 231  
Shannon's information unit, 51  
Shaw's algorithms, 237  
sign-correlation function, 136  
signal/noise ratio, 70  
Sinai, 18, 114, 141  
singular points, 129, 153, 163, 187, 192, 219  
slalom-profile, 29  
South Caspian depression, 260  
SP, 2, 29, 35, 78, 102, 197  
space-charge polarization, 40  
spectrometallometry, 29

- standard deviation, 66, 84, 94  
statics, 80  
statistic game techniques, 237  
statistical approach, 21, 221  
statistical reduction, 101, 104  
stereoproduction, 60  
strike-limited bed, 170  
Suez, 141  
symmetrical model dikes, 194  
synthetic magnetic field, 139  
system of quantitative interpretation,  
    226
- Talysh, 13  
tangent method, 218, 291  
tare, 22  
tectono-magmatic chart, 269  
temperature variations, 315  
terrain correction, 4, 80  
terrain relief effect, 93, 104, 108, 210,  
    295  
thermal conductivity, 272, 314  
thermal prospecting, 21, 34, 272  
thermomagnetic cleaning, 60  
thick bed, 42, 168, 175  
thin bed, 37, 99, 170  
time domain, 38  
time variations, 20  
topographic complexity, 108  
topographic effect, 21, 74, 85, 97, 101,  
    117, 309  
topographic mass attraction, 84  
total elliptic integral, 83  
total magnetization, 60  
transient method, 294  
transverse dislocations, 24, 262  
trapps, 66  
trial-and-error method, 200  
triaxial ellipsoid, 59  
Turgay, 10  
  
underground water, 15, 137  
upward continuation, 90, 120, 124, 168  
Urals, 3, 213  
useful signal, 28, 130, 135  
  
variation effects, 75  
VES, 231  
VLF, 2, 35, 207, 246, 272, 312

## MODERN APPROACHES IN GEOPHYSICS

---

1. E.I. Galperin: *Vertical Seismic Profiling and Its Exploration Potential*. 1985 ISBN 90-277-1450-9
2. E.I. Galperin, I.L. Nersesov and R.M. Galperina: *Borehole Seismology*. 1986 ISBN 90-277-1967-5
3. Jean-Pierre Cordier: *Velocities in Reflection Seismology*. 1985 ISBN 90-277-2024-X
4. Gregg Parkes and Les Hatton: *The Marine Seismic Source*. 1986 ISBN 90-277-2228-5
5. Guust Nolet (ed.): *Seismic Tomography*. 1987 ISBN 90-277-2521-7
6. N.J. Vlaar, G. Nolet, M.J.R. Wortel and S.A.P.L. Cloetingh (eds.): *Mathematical Geophysics*. 1988 ISBN 90-277-2620-5
7. J. Bonnin, M. Cara, A. Cisternas and R. Fantechi (eds.): *Seismic Hazard in Mediterranean Regions*. 1988 ISBN 90-277-2779-1
8. Paul L. Stoffa (ed.): *Tau-p: A Plane Wave Approach to the Analysis of Seismic Data*. 1989 ISBN 0-7923-0038-6
9. V.I. Keilis-Borok (ed.): *Seismic Surface Waves in a Laterally Inhomogeneous Earth*. 1989 ISBN 0-7923-0044-0
10. V. Babuska and M. Cara: *Seismic Anisotropy in the Earth*. 1991 ISBN 0-7923-1321-6
11. A.I. Shemenda: *Subduction. Insights from Physical Modeling*. 1994 ISBN 0-7923-3042-0
12. O. Diachok, A. Caiti, P. Gerstoft and H. Schmidt (eds.): *Full Field Inversion Methods in Ocean and Seismo-Acoustics*. 1995 ISBN 0-7923-3459-0
13. M. Kelbert and I. Sazonov: *Pulses and Other Wave Processes in Fluids. An Asymptotical Approach to Initial Problems*. 1996 ISBN 0-7923-3928-2
14. B.E. Khesin, V.V. Alexeyev and L.V. Eppelbaum: *Interpretation of Geophysical Fields in Complicated Environments*. 1996 ISBN 0-7923-3964-9